

27
1482
750.

GENESIS OF THE LEAD-ZINC MINERALIZATION AT
GAYS RIVER, NOVA SCOTIA, CANADA: A GEOLOGIC,
FLUID INCLUSION AND STABLE ISOTOPIC STUDY

by

Samuel Olusegun Akande

Submitted in partial fulfillment
of the requirements for the degree of Doctor of Philosophy at
Dalhousie University, Halifax, Nova Scotia, Canada, on
November 26th 1982

DALHOUSIE UNIVERSITY
FACULTY OF GRADUATE STUDIES

The undersigned hereby certify that they have read and recommended to the Faculty of Graduate Studies for acceptance a thesis entitled "Genesis of the Lead-Zinc Mineralization at Gays River, Nova Scotia, Canada: A Geologic, Fluid Inclusion, and Stable Isotopic Study

"

by Samuel O. Akande

in partial fulfillment of the requirements for the degree of Doctor of Philosophy.

Dated November 26, 1982

External examiner

Research Supervisor

Examining Committee

Date November 26th 1982

Author Samuel Olusegun Akande

Title "Genesis of the Lead-Zinc Mineralization at Gays River, Nova Scotia,

Canada: A Geologic, Fluid Inclusion, and Stable Isotopic Study"

Department or School Department of Geology, Dalhousie University

Degree Ph.D. Convocation February Year 1983

Permission is herewith granted to Dalhousie University to circulate and to have copied for non-commercial purposes, at its discretion, the above title upon the request of individuals or institutions.

Signature of Author

THE AUTHOR RESERVES OTHER PUBLICATION RIGHTS, AND NEITHER THE THESIS NOR EXTENSIVE EXTRACTS FROM IT MAY BE PRINTED OR OTHERWISE REPRODUCED WITHOUT THE AUTHOR'S WRITTEN PERMISSION.

TABLE OF CONTENTS

	Page
ABSTRACT	1
ACKNOWLEDGEMENTS	3
TABLE OF CONTENTS	iv
LIST OF FIGURES	x
LIST OF TABLES	xvii
CHAPTER 1. INTRODUCTION	5
1.1 General Statement	5
1.2 Location	5
1.3 History	5
1.4 Objectives of This Thesis	7
1.5 Methods	8
a. Materials for Study	8
b. Laboratory Work	9
1.6 Previous Work	10
1.7 Organization of the Thesis	11
CHAPTER 2. REGIONAL GEOLOGY	12
2.1 Tectonic Setting	12
2.2 Stratigraphy	14
2.3 Mine Geology	18
a. Basement Structure and Paleogeography	18
b. Structures in the Carbonate Rocks	20
c. The Gays River "Trench"	25

	Page
CHAPTER 3. DESCRIPTION OF THE CARBONATE LITHOLOGY	30
3.1 General Statement	30
3.2 Terminology	30
3.3 Rock Descriptions	32
3.3.1 Group One Rock Types	33
a. Basal Conglomerate	33
b. Carbonaceous Skeletal Grainstone.	36
c. Stromatolitic Packstone	37
d. Algal Skeletal Packstone-Bindstone.	38
e. Skeletal Grainstone	40
f. Gypsiferous Wackestone-Packstone	45
3.3.2 Group Two Rock Types	46
a. Algal Bindstone	47
b. Coralgal Bafflestone.	50
c. Algal Fenestral Wackestone-Packstone.	51
d. Lime Packstone and Breccia	55
3.4 Discussion	58
CHAPTER 4. DESCRIPTION OF THE STRATIFORM AND VEIN ORES AND THEIR HOST ROCKS	63
4.1 General Statement	63
4.2 Stratiform Ores, Geological Setting	66
a. Form	66
i. Laminated sulfide mineralization	67
ii. Mineralized stylolites	71
iii. Geopetal structures and stromatactis	74
iv. Disseminations	75
v. Sulfide lenses.	75

- b. Mineralogy 75
- c. Porosity 79
- d. Host Rock Relationship 79
- 4.3 Vein Ores, Geological Setting 82
 - a. Mineralogy 82
 - b. Host Rock Relationship 91
- 4.4 Marcasite and Pyrite Not Associated with Ore Minerals 94
- 4.5 Chemical Constituents of the Stratiform and Vein Sulfide Minerals 96
- 4.6 Mineralogy and Composition of the Host Rock to Ores 98
- 4.7 Dedolomitization and the Limestone Texture . . . 101
- 4.8 Vuggy and Vein Calcite 102
- 4.9 Discussion 104
- CHAPTER 5. FLUID INCLUSION MICROTHERMOMETRY 108
 - 5.1 Introduction 108
 - 5.2 Terminology 109
 - 5.3 Classification and Assumptions 110
 - a. Origin of Inclusions 110
 - b. Criteria 111
 - c. Assumptions in the Present Study 111
 - 5.4 Thermometry 112
 - a. The Vapour Bubble 112
 - b. Sample Selection 113
 - c. Degree of Fill and Density 118
 - d. Homogenization Experiments 119
 - e. Observations and Results 119

f. Freezing Experiments	134
g. Method	134
h. Observations and Results	135
5.5 Pressure Corrections	140
5.6 Discussion	145
CHAPTER 6. STABLE ISOTOPE GEOCHEMISTRY	148
6.1 Introduction	148
6.2 Sulfur Isotopic Composition	149
a. Principle and Assumption	149
b. Sample Selection	152
c. Sample Preparation	153
d. Sulfur Isotope Ratios	154
i. Sulfate minerals	154
ii. Sulfide minerals	154
e. Interpretation of the Sulfur Isotope Ratios .	157
i. Sulfate minerals	157
ii. Sulfide minerals	160
6.3 Lead Isotopes	168
a. Principle and Assumptions	168
b. Procedure	170
c. Results	172
d. Interpretations	172
6.4 Oxygen and Carbon Isotopic Composition	176
a. Principle and Assumptions	176
b. Sample Selection and Preparation	179
c. Experimental Procedure	180
d. Oxygen and Carbon Isotope Relations	180

	Page
i. Unmineralized limestone	180
ii. Mineralized dolomite and limestone	181
iii. Ore stage calcite	181
iv. Post ore calcite	181
e. Interpretation of the oxygen and carbon iso- topic relations	182
i. Unmineralized limestone	182
ii. Mineralized dolomite and limestone	183
iii. Ore stage calcite	189
iv. Post ore calcite	190
6.5 The Ore forming Environment	193
6.6 Discussion.	197
CHAPTER 7. BASEMENT ALTERATION	204
7.1 General Statement	204
7.2 Occurrence.	204
7.3 Method of Study	205
7.4 a. General Characteristics of the Quartz Meta- wacke	205
b. Petrography	206
i. Fresh quartz metawacke	206
ii. Altered quartz metawacke.	206
7.5 Petrochemistry.	207
7.6 Discussion.	210
CHAPTER 8. GENETIC MODELS	215
8.1 Introduction.	215
8.2 Jackson and Beales' Hypotheses.	216

	ix Page
8.3 The Sabkha Model	219
8.4 Downward Excavating Hydrothermal Cells	221
8.5 Boyle's Epigenetic Model	224
8.6 Gays River Model	227
a. General.	227
b. Dewatering and Brine Release	230
c. Mineralization	233
d. Preservation	235
8.7 Evidence on the Type of Deposit.	237
CHAPTER 9. COMPARISON OF THE GAYS RIVER DEPOSIT WITH SELECTED SEDIMENT HOSTED AND MISSISSIPPI VALLEY TYPE LEAD-ZINC ± COPPER MINERALIZATION	240
9.1 General Statement.	240
9.2 a. Irish Base Metal Deposit: The Tynagh Example	240
b. The Pine Point Lead-Zinc District.	242
c. South East Missouri District: Buick Mine. .	242
9.3 Summation.	248
CHAPTER 10. CONCLUSIONS	249
REFERENCES	252
APPENDICES	277
VITA	348

LIST OF FIGURES

Figure	Description	Page
1.1	Location of the Gays River Deposit.	6
2.1	Location map of the Fundy Basin	13
2.2	The Shubenacadie and Musquodoboit Basins.	15
2.3	Stratigraphic setting of the Windsor Group in the Shubenacadie and Musquodoboit Basins.	16
2.4	Geology of the Gays River area.	19
2.5	Structural contours of the basement topography.	21
2.6	Schematic representation of basement structures	22
2.7	Fault and tension gashes in the quartz-metawacke basement.	23
2.8	Poles to joint planes in the carbonate rocks.	24
2.9	Gypsum veins in parallel and conformable orientation to carbonate bedding.	27
2.10	Semiconsolidated "trench" sediments in a fault gouge adjacent to massive sulfide vein.	27
3.1	Basal conglomerate in the 119 drift	35
3.2	Carbonaceous skeletal grainstone	35
3.3	Stromatolitic packstone	40
3.4a	Algal skeletal packstone-bindstone.	40
3.4b	Algal skeletal packstone-bindstone with encrusting algal structures.	42
3.5a	Algal bindstone with digitate laminated columns of stromatolites	42
3.5b	Algal bindstone with irregular hemispherical forms of algal stromatolites	49

Figure	Description	Page
3.6	Coralgal bafflestone with good intraskeletal porosity . . .	49
3.7	Algal fenestral wackestone-packstone	54
3.8	Limestone breccia with angular limestone fragments	54
3.9	Limestone breccia (solution collapse type) with good vuggy, interparticle and breccia porosity	57
3.10	Distribution of the carbonate lithozones in section AA ¹ . . .	60
3.11	Paleoenvironmental reconstruction of the carbonate reef . . .	61
4.1a	Plan of the vein ores	64
4.1b	Cross section AA ¹ through the central part of the Gays River mine	65
4.2	Styles of stratiform mineralization	68
4.3	Laminated sulfide mineralization	70
4.4	Mineralized stylolite, concordant to carbonate bedding . . .	73
4.5	Unmineralized stylolite	73
4.6	Geopetal structures filled with sphalerite and calcite . . .	77
4.7	Subhedral grains of marcasite in chalcopyrite	77
4.8	Scalenohedral calcite overgrowths on coarse crystalline galena	81
4.9	Fault bounded, vertically dipping massive sulfide vein in the 104 drift	84
4.10	Coarse crystalline galena traversing massive sphalerite . . .	87
4.11	Massive sphalerite and galena encrustations in a veinlet . .	87
4.12	Crystals of coarse crystalline galena within vein calcite	90
4.13	Finely crystalline marcasite on scalenohedral calcite . . .	90

Figure	Description	Page
4.14	Brecciated limestone (dedolomite) adjacent to a sulfide vein.	93
4.15	Cross section of fault bounded sulfide veins in drift 104.. . . .	95
4.16	Concentration of cadmium and manganese in sphalerite and galena.	97
4.17	Concentration of manganese and iron in the dolomite host for ore.	100
4.18	Concentration of manganese and iron in calcite.	103
5.1a	Morphologies and composition of fluid inclusions in sphalerite, calcite, fluorite and barite.	115
5.1b	Photomicrographs of fluid inclusions in sphalerite, calcite and fluorite.	117
5.2	Histogram for the frequency distribution of fluid inclusions temperature in ore-stage calcite	123
5.3	Histogram for the frequency distribution of post-ore calcite fluid inclusion temperature	123
5.4	Histogram for the frequency distribution of fluorite fluid inclusion temperature	127
5.5	Schematic diagram of high temperature phase equilibria in NaCl saturated brines.	128
5.6	Composition of the liquid phase of saturated NaCl brines.	129
5.7	Histogram for the frequency distribution of barite fluid inclusion temperature	131

Figure	Description	Page
5.8	Histogram for the frequency distribution of quartz fluid inclusion temperature.	133
5.9	Diagrammatic representation of the freezing behaviour of post-ore calcite	137
5.10	Plot of the concentrative properties of aqueous NaCl solution	138
5.11	Relationship between the degree of filling at 25°C and the total density of the inclusion for different NaCl brines	139
5.12	Boiling-point curves for H ₂ O liquid (0 wt %) and for brines of constant composition given in wt % of NaCl . . .	142
5.13	Temperature correction for a 20% NaCl solution as a function of homogenization temperature and pressure. . . .	144
5.14	Summary comparison of homogenization temperatures in sphalerite, calcite, fluorite and barite	146
6.1	Histogram of all sulfur isotope ratios in the stratiform and vein sphalerite and galena	155
6.2	Sulfur isotope ratios of sulfate and sulfide minerals at Gays River.	156
6.3a	Variation in the sulfur isotopic composition of sphalerite and galena in a N/S vein	161
6.3b	Variation in the sulfur isotopic composition of sphalerite and galena across a massive sulfide vein	162

Figure	Description	Page
6.4	$^{207}\text{Pb}/^{204}\text{Pb}$ and $^{208}\text{Pb}/^{204}\text{Pb}$ versus $^{206}\text{Pb}/^{204}\text{Pb}$ for Gays River, carbonate hosted deposits and selected ore environments.	173
6.5	$^{207}\text{Pb}/^{204}\text{Pb}$ versus $^{206}\text{Pb}/^{204}\text{Pb}$ in galenas hosted in Lower Carboniferous sedimentary rocks in Nova Scotia and Newfoundland.	174
6.6	Oxygen and carbon isotopic composition of host rock to ore and carbonate gangue at Gays River	184
6.7	Oxygen and carbon isotopic composition of host rock to ore and carbonate gangue at Gays River; mean values and range	185
6.8	Variation in oxygen and carbon isotopic composition in the carbonate host versus distance to massive sulfide veins	186
6.9	Sulfur isotope ratios at Gays River compared to selected lead-zinc deposits.	198
6.10	Oxygen isotopic composition and temperature relations of calcite.	201
6.11	Carbon isotopic composition and temperature relations of calcite.	202
7.1	Element gain and losses in the altered quartz metawacke basement.	209
7.2	Sulfide bearing calcite veinlet in the quartz metawacke basement.	213
8.1	Brine release from the compaction of shale and the Mississippi Valley Type deposits.	217

Figure	Description	Page
8.2	The sabkha model, schematic representation.	220
8.3	Downward excavating convective cells.	223
8.4	Schematic mode of emplacement of the barite, manganese, lead, zinc, copper, silver deposits of the Walton- Cheverie area, Nova Scotia	225
8.5	Pressure-temperature conditions for gypsum-anhydrite conversion.	232
8.6	Gays River genetic model; dewatering and release of saline brines	234
8.7	Gays River genetic model; mineralization and preserv- ation	236
9.1	Location map of the Tynagh deposit.	241
9.2	Location of the Pine Point lead-zinc district and the geologic setting of the Great Slave Lake region	243
9.3	Location of the Pine Point barrier complex.	243
9.4	Location of the south east Missouri lead district.. . . .	244
9.5	Location of the Buick mine and the major subdistricts and mines within the south east Missouri district	244
I-1	Location of drift plans, basement paleogeography and the areas mapped in the Gays River decline.	278
II-1	Estimation of dolomite percentage in carbonate sample . . .	280
II-2	Histogram of the frequency distribution of vitrinite reflectivity on coaly materials from the "trench"	283
VI-1	Regional and local stratigraphy at Tynagh.	335
VI-2	Geologic map of the Tynagh deposit.	336

Figure	Description	Page
VI-3	Stratigraphic column of Paleozoic Formations, southern Great Slave Lake area.	340
VI-4	Middle Devonian stratigraphic relationships, Pine Point mining district.	341
VI-5	Cross section of the Pine Point barrier complex.	341
VI-6	Stratigraphic column of Upper Cambrian in southeastern Missouri	344
VI-7	Distribution of ore bodies in the Buick deposit.	345

LIST OF TABLES

Table	Description	Page
3.1	Classification of carbonate rocks	31
4.1	Gays River diagenetic sequence; after Macleod (1975).	105
4.2	Generalized summary of mineral paragenesis.	106
5.1	List of homogenization temperatures in sphalerite fluid inclusions.	122
6.1	Model age of lead in galenas.	171
9.1	Summary comparison of the geological features of Gays River, Tynagh, Pine Point and Buick Mine.	245
(In Appendix)		
II-1	Reflectance readings (Ro) on lignite.	282
II-2	Palynological analysis of semi-consolidated "trench" samples	284
II-3	Microprobe analysis of sphalerite and galena.	287
II-4	Microprobe analysis of marcasite, pyrite and chalcopyrite .	288
II-5a	Minor and trace element content of sphalerite and galena. .	290
II-5b	Minor and trace element content of marcasite and pyrite . .	291
II-6	Microprobe analysis of carbonates	292
II-7	Microprobe analysis of barite	300
IV-1	Sulfur isotopic composition of sulfate and sulfide minerals.	314
IV-2	Sulfur isotopic composition of coexisting sulfide mineral pairs	320
IV-3	Summary comparison of the sulfur isotope results.	321

Table	Description	Page
IV-4	Isotopic composition of carbon and oxygen in the unmineralized limestone fossils of Mississippian age.	322
IV-5a	Isotopic composition of carbon and oxygen in host rock, ore-stage and post-ore carbonate	323
IV-5b	Summary comparison of the $\delta^{18}\text{O}$ and $\delta^{13}\text{C}$ values in the host rock, ore stage, post ore carbonate, and unmineralized limestone.	326
V-1	Whole rock analysis of altered and unaltered quartz metawacke basement rocks	328
V-2	Element gain and losses in the altered quartz metawacke. . .	333

ABSTRACT

The Gays River lead-zinc deposit consists of stratiform bodies and discordant fault controlled vein systems within a Mississippian dolomitic reef that overlies unconformably a Cambro-Ordovician metasedimentary basement and is overlain by Mississippian evaporites.

Detailed underground mapping and laboratory studies suggest 3 main stages of evolution: 1) pre-ore evaporite deposition, pervasive reef dolomitization and growth of marcasite, 2) precipitation of ore sphalerite, galena, chalcopyrite and calcite, and 3) post-ore deposition of calcite, fluorite, barite, marcasite, pyrite and selenite. Fluid inclusions homogenize at the following temperatures: sphalerite, 215°C; ore-stage calcite, 172°C; post-ore calcite, 142°C; fluorite, 143°C, and barite, 137°C. Salinity of the hydrothermal fluids was approximately 20.4 equivalent weight percent NaCl during deposition of post-ore calcite and fluorite.

Gypsum and anhydrite in the overlying evaporites and barite within the ore, are enriched in heavy sulfur ($\delta^{34}\text{S}$ +13.1 to +16.5‰); ore-stage sphalerite, galena and chalcopyrite show a limited spread of $\delta^{34}\text{S}$ (+8.0 to +13.65‰); whereas post-ore marcasite and pyrite give widely scattered light $\delta^{34}\text{S}$ values (-9.7 to -46.0‰). The similarities of the $\delta^{34}\text{S}$ values of gypsum, anhydrite and barite with that of Mississippian seawater confirm this as the dominant sulfur source for the sulfates. The heavy sulfur of the ore-stage sulfide minerals is either directly contributed from seawater or from a solution in equilibrium with evaporites. A biogenic source is preferred for the sulfur in post-ore marcasite and pyrite. Mineralized carbonates are significantly depleted in the heavier

isotopes of carbon and oxygen with respect to their unmineralized equivalents. Preliminary lead isotope data for galena suggest that the source of the lead is in the Cambro-Ordovician metasedimentary basement.

The present evidence eliminates the possibility that the lead-zinc ores are an early low-temperature diagenetic cement of the dolomitic reef as previously envisaged. Contact relationships and remarkable similarities between the stratiform and vein ores suggest that the discordant veins acted as feeders for the epigenetic conformable mineralization. A model involving deeply circulating brines released during gypsum dehydration best explains the metal leaching, transportation and subsequent deposition of lead and zinc ores as replacements and open-space fillings within the dolomitic reef.

ACKNOWLEDGEMENTS

The present thesis has been completed with the generous help, guidance and understanding of a number of people, companies, and government departments to which the author is greatly indebted. I would like to express my gratitude to the members of my supervisory committee, Dr. Marcos Zentilli, Dr. Peter Reynolds, Dr. Paul Schenk and Mr. William Palmer for their help and useful suggestions in the preparation of this thesis.

I am extremely grateful to Dr. Marcos Zentilli who introduced me to the geology and metallogeny of Nova Scotia and whose supervision, guidance, criticism and suggestions have contributed to the completion of this thesis. A great deal of thanks is owed to Dr. Paul Schenk for acquainting me with the carbonate geology in Nova Scotia and also in the classic carbonate localities at Bermuda. I wish to thank Dr. Peter Reynolds and Mr. Keith Taylor for their help and advice in the use of the mass spectrometer for oxygen and carbon isotopic measurements. I am greatly indebted to Mr. William Palmer, chief geologist at the Gays River mine for his assistance and suggestions during my field work. The help rendered by Mr. R.M. MacKay in the use of the electron microprobe and Mr. Doug Meggison in drafting some of the figures are gratefully appreciated.

My sincere thanks also go to Canada Wide Mines Limited and Esso Minerals of Canada Limited for the access to the drill cores and for giving me the opportunity to study the rocks in the underground working areas of the mine. The summer employment provided me by Canada Wide Mines in 1980 is gratefully appreciated. My appreciation goes to the

staff of the Gays River mine particularly Mr. John Horton and Mr. Chris Cavannah who provided able geological assistance during my underground mapping. I would also like to thank Mr. Pat Hannon and Mr. John Macleod of Esso Minerals. Special thanks go to Dr. Martin Gibling and Dr. Michael Russell (University of Strathclyde) for critically reading the manuscript.

I wish to thank Dr. Peter Hacquebard of the Bedford Institute of Oceanography for the use of his laboratory for the analysis of the coaly materials from the Gays River semi-consolidated "trench" sediments. I am grateful to Dr. Ed Davies of the same Institute for the identification of the species of pollen and spore contained in the semi-consolidated "trench" sediments studied. Special thanks go to Dr. Peter Giles of the Department of Mines and Energy, for stimulating discussions on the Carboniferous stratigraphy of Nova Scotia. My thanks also go to Mr. Reginald Morrison of the Department of Mines and Energy for his help and advice in photography.

I am grateful to the Federal Government Scholarship Board of Nigeria for financial support throughout my stay in Canada. Funds for laboratory work have been provided by the National Science and Engineering Council of Canada through grants to Dr. Marcos Zentilli; to this I express my sincere gratitude. I am extremely thankful to Mrs. Barbara Cossar for her excellent typing of the manuscript and to all members of the Department of Geology for their hospitality.

Finally, I would like to give many thanks to my father, Deacon J.O. Akande and my mother Felicia Folorunso Akande for giving me the parental support, courage and advice throughout my stay in school.

CHAPTER 1

INTRODUCTION

1.1 General Statement

The genesis of carbonate-hosted lead-zinc deposits has been the subject of controversy. It is becoming evident, that their formation must be considered as an integral part of sedimentary basin evolution. However, the evaluation of genetic models is fruitless without an adequate description of the distribution and field relationships of mineralization obtained from geological mapping at various scales. Mineralogical and geochemical tools can then be effectively utilized to establish boundary conditions and test multiple working hypothesis.

1.2 Location

The Gays River lead-zinc deposit is 65 kilometres north east of Halifax and 10 kilometres south east of the village of Shubenacadie on Latitude 45°02' North, Longitude 63°22' West in central mainland Nova Scotia (Fig. 1.1). It is accessible by road through highway 102 and highway 224, and is only 9 kilometres from the Canadian National rail line which passes through the village of Shubenacadie.

1.3 History

The occurrence of lead and zinc in the Gays River area was known to French soldiers as early as the 1700's when lead was used for ammunition. The first attempt to explore the occurrence was made in 1952 by the Gays River lead mines. A deposit containing 900,000 tonnes of 3% combined lead and zinc was established over a total of 2,830 metres of closely spaced drilling.

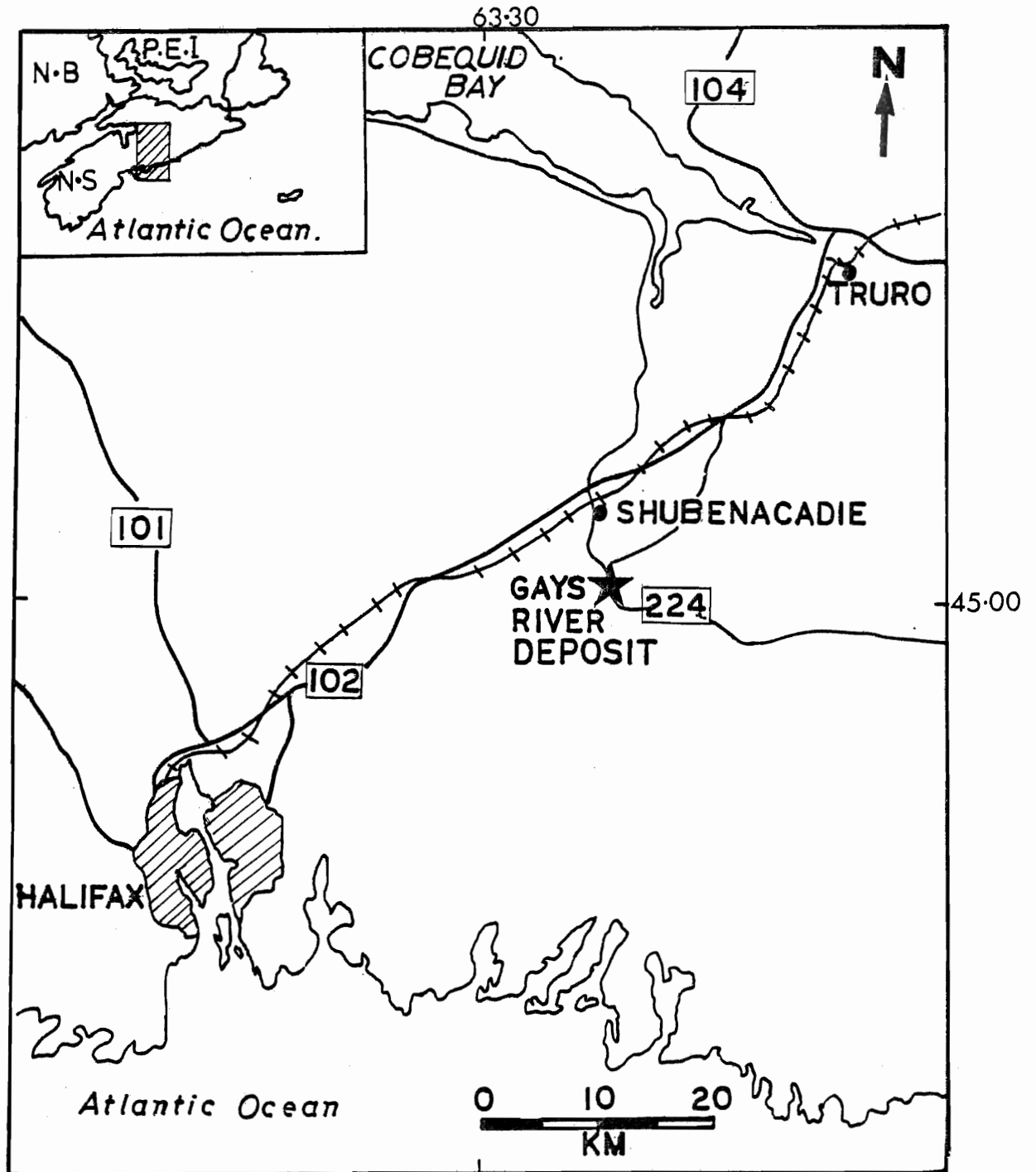


Figure 1.1 Location of the Gays River deposit in central mainland Nova Scotia.

From 1972 to 1977 fence type drilling was carried out on a joint venture by Imperial Oil and Cuvier Mines Limited. These led to the discovery of significant ore grade intersections over an area of 4 kilometres by 0.6 kilometre. An estimated total of 12,000,000 tonnes proven ore with 7% combined lead and zinc was established.

In 1977, Imperial Oil Limited bought out Cuvier's interest and turned over its ownership of the mining and concentration to Esso Minerals Canada Limited, a division of Imperial's Calgary based subsidiary, Esso Resources Limited. Development and mining began in 1978 through a decline, with Canada Wide Mines, a subsidiary of Esso Minerals, as the sole operator. The mining activities encountered problems of unsafe roof conditions and excessive water in areas adjacent to faults controlling massive sulfide veins. This led to what was supposed to be a temporary shut down of the mining operation in August 1981. Unfortunately, at the time of writing this thesis (October 1982) the mine has been shut down and the workings flooded. Total production during the operation amounts to approximately 550,000 tonnes of 3.3% combined lead and zinc (unpublished Gays River mining records 1982).

1.4 Objectives of the thesis

This thesis was undertaken as part of a long term project initiated at Dalhousie University, to gain a clearer understanding of the metallogenic development of the basinal and upland areas of Nova Scotia.

The Lower Carboniferous (Windsor) basin, represents a unique metallogenic domain because of its significant deposits of gypsum, anhydrite, barite and celestite, associated with the base metal sulfides of Pb, Zn ± Cu ± Ag mineralization. The Gays River deposit is of particular interest

because it provides a "window" into the complex interrelationships of a part of this basin.

The Gays River lead-zinc mineralization had been described as a stratiform, low temperature, early diagenetic cement of a carbonate reef complex (MacEachern and Hannon 1974, Macleod 1975). The present work had as its main objective to test this hypothesis using field work and modern analytical methods, and to propose a working model for the genesis of the deposit. The definition of geological controls should aid in the exploration and development of new reserves, and the study should provide a better understanding of the evolution of base metal mineralization in the Carboniferous basin with regards to the source, transport mechanism, concentration and preservation.

1.5 Methods

a. Materials for Study

Field work leading to this thesis began in February 1980 and was continued to the end of the summer of the same year while the author was in the employ of Canada Wide Mines Limited. The field work was completed at the end of the summer of 1981.

The field work involved a detailed geological mapping underground in the decline areas where the central part of the Gays River orebody was exposed for mining. Mapping was carried out on scales 1:200, 1:100, 1:50, 1:25 on several mine levels. Oriented, representative and systematic samples were gathered during the author's mapping and also from the sampling of selected diamond drill cores from exploratory holes drilled by Imperial Oil. A total of 350 carefully located samples were collected at the end of the mapping period.

b. Laboratory Work

Most of the samples collected were slabbed and polished in the Department of Geology of Dalhousie University during the preliminary stage of study. Polished, polished thin and thin sections were made and the thin sections of the carbonates were stained with Alizarin Red S to distinguish calcite from dolomite. Polished sections of the sulfide minerals were etched for detailed ore microscopy.

The percentage of dolomitization in selected carbonate rocks was determined by the use of the X-ray diffractometer technique by the methods of Hutchison (1974, pp. 214-218). Major and minor elemental compositions of the carbonates were determined by the use of the electron microprobe technique.

The main laboratory work consisted of:

1. Fluid inclusion homogenization and freezing temperature determinations.
2. Determination of trace element abundance in the sulfide minerals.
3. Analysis for the stable isotopes of sulfur in the sulfates and sulfides.
4. Analysis for the carbon and oxygen isotopic composition in selected carbonates.
5. Whole rock analysis of the altered footwall quartz metawacke basement and their unaltered equivalents.
6. Mica K-Ar ages determination in the altered quartz metawacke basement.

All the laboratory work was performed at Dalhousie University with the exception of the analysis of the stable isotopes of sulfur in the sulfide and sulfate minerals which was performed at the Geochron Laboratory, Cambridge, U.S.A. and McMaster University, Hamilton, Canada. The reader is referred to the appendix for a detailed description and results of each

of the methods used.

1.6 Previous Work

The Gays River deposit offers a unique opportunity for the study of carbonate petrology and stratigraphy as well as base metal sulfide mineralization. This has attracted several geologists interested in carbonate stratigraphy and carbonate hosted ore deposits. Indeed these interests led to the discovery of the deposit by Imperial Oil geologists in 1974.

The first comprehensive account of the geology of the Gays River deposit was that of MacEachern and Hannon (1974) who recognized the lead-zinc deposit as a Mississippi Valley type in a carbonate reef complex.

Macleod (1975) described in detail the diagenesis of the carbonate rocks and the associated mineralization from cores taken from 3 vertical holes spaced at 60 metre intervals along a single line. Macleod concluded that the sulfide mineralization represents an early diagenetic cement of the carbonate reef. He interpreted the high grade massive sphalerite and galena as products of secondary reconcentration of the sulfide minerals during the process of karsting.

Hartling (1977) and Osborne (1977) described the carbonate lithofacies, biofacies and depositional environments of the carbonate rocks from drill cores adjacent to Macleod's area.

Hatt (1978) interpreted the depositional environment of the carbonate rocks exposed in parts of the Gays River decline.

Giles, Boehner and Ryan (1979) described the biofacies and lithofacies encountered in the carbonate banks of the Gays River formation.

Schenk and Hatt (1981), Schenk (1981) described the carbonate environments of the Gays River mound and the carbonate-sulfate relations in the

Windsor Group.

A great amount of underground development in the decline area of the Gays River deposit exposed continuous outcrops of the lead-zinc ores and the carbonate host over about 15 kilometres length. This has made possible the present re-assessment of the ore-host relationships.

1.7 Organization of the Thesis

This thesis first describes the geological setting of the Fundy Basin and the Gays River in particular in order to clarify the geological development and stratigraphy of this basinal region.

A description of the carbonate rocks in the mine area is presented in Chapter 3 and the lead and zinc ore types are described in Chapter 4. Chapter 5 discusses the results of the fluid inclusion microthermometric determinations and Chapter 6 describes the isotope geochemistry of the carbonates, sulfate and sulfide minerals.

The alteration of the basement is discussed in Chapter 7 and the hypothesized model is tested by comparison with selected known deposits in similar geological settings in Chapter 9. A summary of the conclusions is presented in Chapter 10.

CHAPTER 2

REGIONAL AND LOCAL GEOLOGY

2.1 Tectonic Setting

After the mid Devonian Acadian orogeny, a complex rift valley system, the Fundy Basin (Belt, 1965) was formed in Atlantic Canada as a result of basement subsidence, fragmentation, and block faulting (Bell 1958, Belt 1965, Howie and Cumming 1963, Howie and Barss 1975, Schenk 1967). This tectonic activity perhaps resulted from shearing during the gradual tangential collision of North America and Africa which culminated at this latitude during the Late Carboniferous Maritime Disturbance (Schenk, 1975). The NE trending, spindle shaped basin (Fig. 2.1), consists of horsts and deep linear basins extending at least from the Gulf of Maine to Western Newfoundland. The rift system is bordered by the New Brunswick Platform to the north west and the Meguma Platform to the south.

Fluvial erosion of horsts and uplifts dominated the Carboniferous, Permian and Triassic periods with occasional floodings of hypersaline seas into the interbasinal grabens (Schenk, 1969). Sediments deposited during this period consist of red, non marine terrigenous detritus overlain and intertongued with cyclic offlap sequences of carbonate and evaporite (Ami 1900; Bell 1929; Belt 1965; Mamet 1970; Schenk 1969). According to Howie and Barss (1975) the Fundy Basin was filled by up to 9,100 metres of Lower Carboniferous to Permian sediments.

At least a dozen inundations of hypersaline seas produced the cyclic offlap sequences of carbonate, sulfate and siliclastic red beds which constitute the Windsor Group within the Fundy Basin (Bell 1958; Schenk 1971). The carbonate hosts for the Gays River deposit were probably deposited

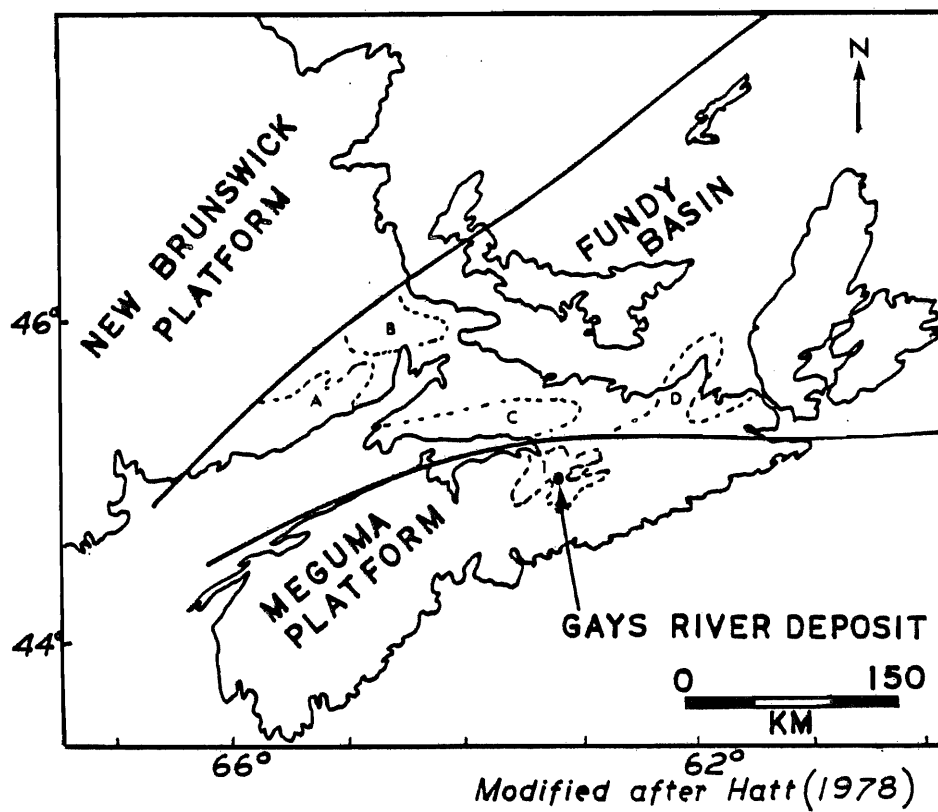


Figure 2.1 Location map of the Fundy Basin showing the largest tectonic elements. Letters indicate horsts, numbers indicate basins. 1 - Shubenacadie Basin, A - Caledonian, B - Un-named, C - Cobequid, D - Antigonish-Pictou.

during the first of these inundations on the Pre-Carboniferous Meguma Platform about 30 kilometres south of the Fundy Basin - Meguma Platform Margin (Hatt, 1978).

2.2 Stratigraphy

The Gays River deposit lies within a sequence of carbonate and evaporite which form a part of the Lower Carboniferous Windsor Group in the southern part of the Fundy Basin. The deposit lies more specifically between two sub-basins, the Shubenacadie Basin to the north west and the Musquodoboit Basin to the south east (Fig. 2.2).

The Windsor Group

The Lower Carboniferous Windsor Group is a succession of cyclic marine carbonate and evaporite within red terrigenous clastics that were deposited in arid to semi arid conditions within the Fundy Basin (Schenk, 1969). Paleomagnetic evidence of Irving (1964), Roy and Robertson (1968) showed that the Carboniferous paleoequator passed north of Nova Scotia, thus placing the Fundy Basin within 10°S latitude at this period.

Bell (1929) made the first description and detailed correlation of the Windsor Group from a type section of more than 470 metres thick. He divided the Windsor into a Lower and Upper unit and 5 subzones based on brachiopods and coral distribution. These subzones were designated A, B, C, D, E in ascending stratigraphic order. Bell (1958) assigned a Middle to Late Visean age to the Windsor Group after recognizing a sixth subzone F. Mamet (1970) assigned a Late Visean to Early Namurian age to the Windsor Group on the basis of foraminiferal assemblage.

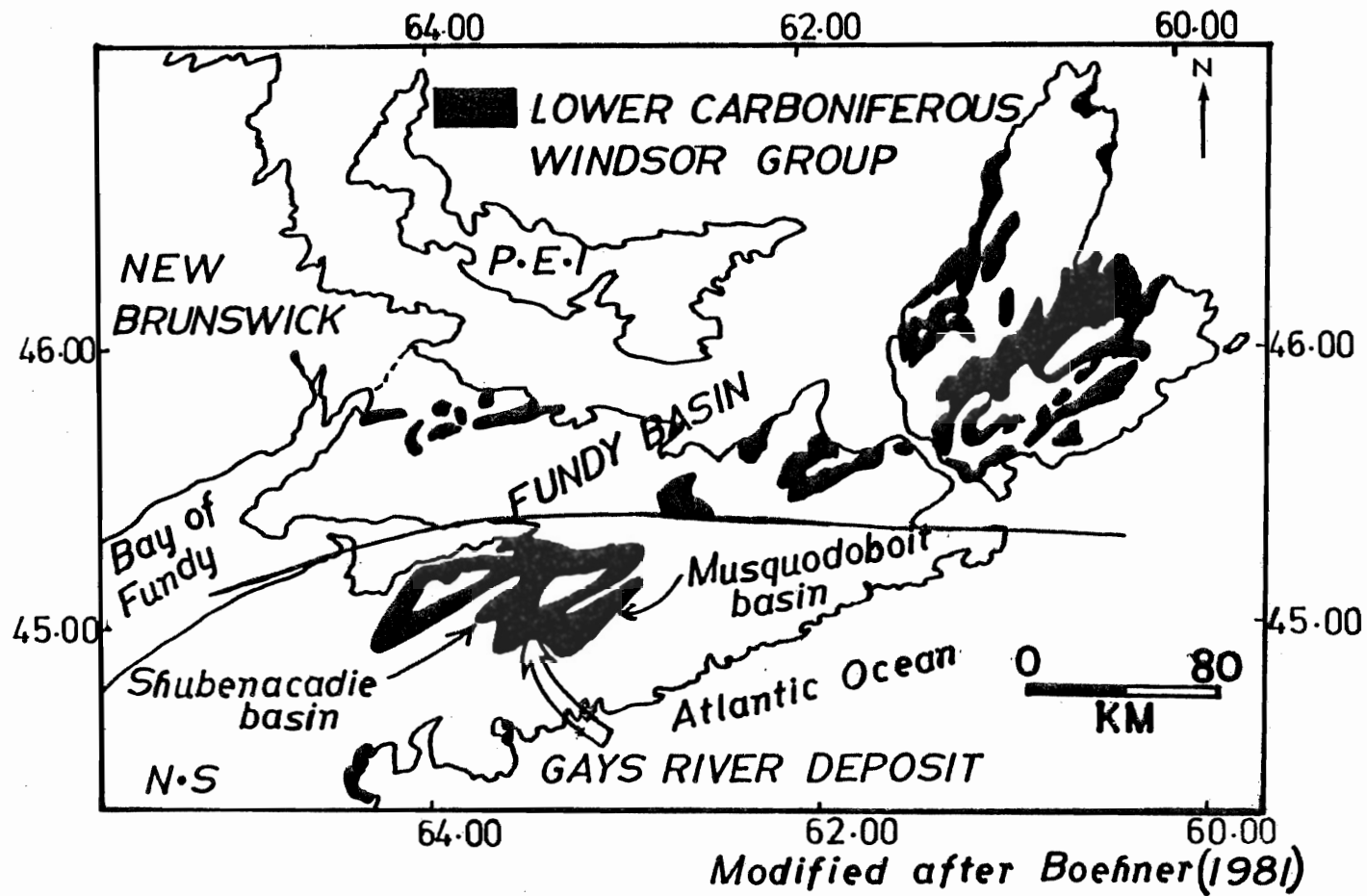


Figure 2.2 Location of the Shubenacadie and the Musquodoboit Basins, central Nova Scotia.

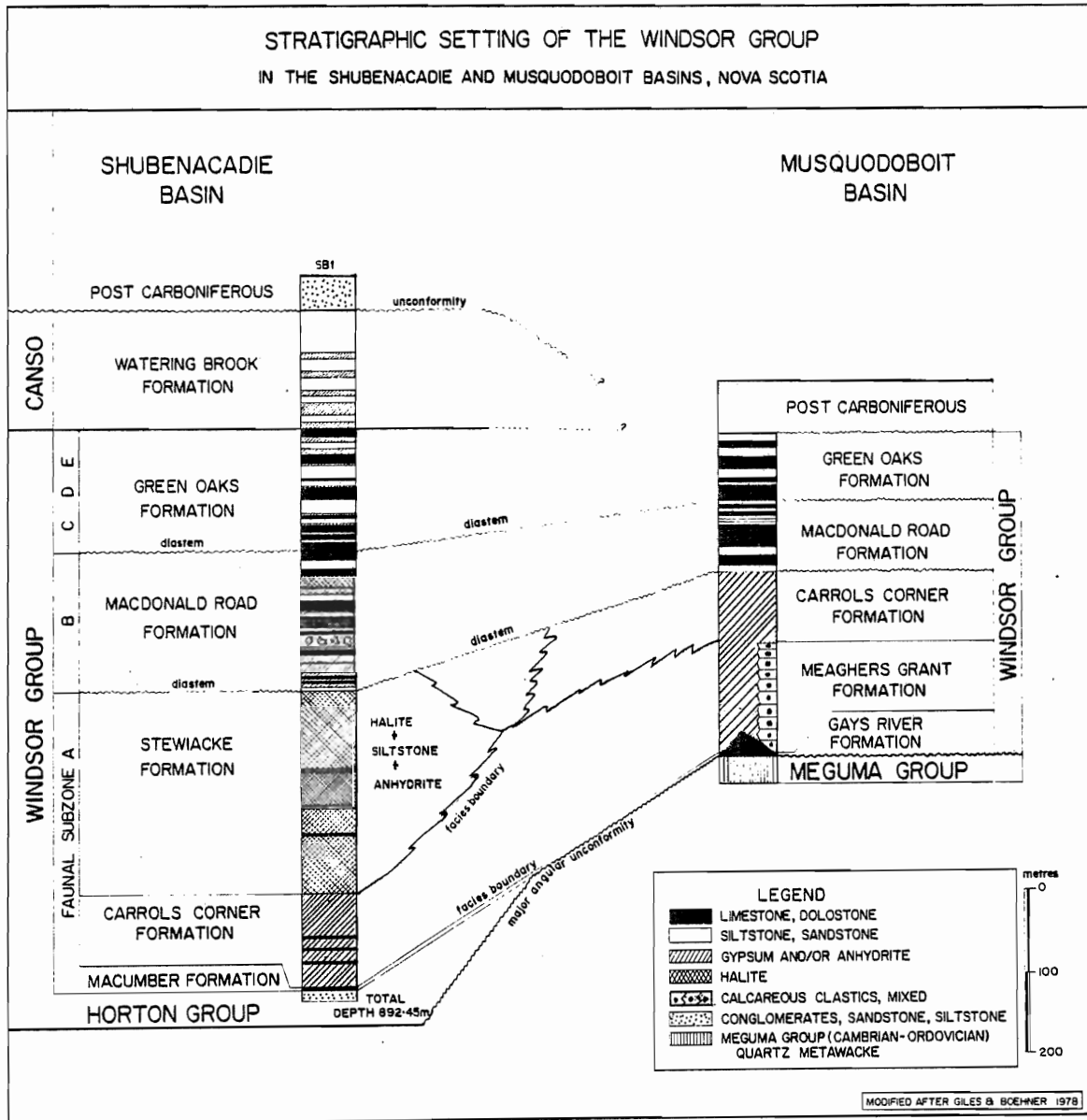


Figure 2.3 Stratigraphic setting of the Windsor Group in the Shubenacadie and Musquodoboit Basins, Nova Scotia.

The Gays River Formation.

Boehner (1977) described the Gays River Formation (new name) in his study of the Carboniferous stratigraphy of the Musquodoboit Valley to the south of the Gays River deposit. He concluded that the Gays River Formation represents the initial sediments of the Mid-Visean marine transgression which deposited the Windsor Group. Giles, Boehner and Ryan (1979), described the Gays River Formation as a lateral equivalent of the Macumber Formation of Weeks (1948) with a facies boundary within the Shubenacadie Basin (Fig. 2.3). These authors reported that although the Gays River Formation overlies the Pre-Carboniferous Meguma Group with a pronounced angular unconformity, the Macumber Formation lies concordantly upon the sandstone, shales, and conglomerates of the Lower Carboniferous Horton Group.

The Gays River Formation is overlain by gypsum and anhydrite of the Carrols Corner or Gleason Brook Formation (Giles et al., 1979) except on the southern parts of the Musquodoboit Basin where sandstone, siltstone and shale of the Meaghers Grant Formation (Giles et al., 1979) rests directly on the Gays River Formation (Fig. 2.3). The Meaghers Grant Formation is inferred to be a facies equivalent of the Gleason Brook and Carrols Corner Formation (Giles et al., 1979). The Carrols Corner Formation is overlain by a thickness of rock salt of c.a. 300 metres in the Shubenacadie Basin (Giles et al., 1979).

On the basis of stratigraphic correlation with Bell's subzones for the Windsor Group, Giles and Ryan (1976) and Hatt (1978) concluded that the gypsum and anhydrite overlying the Gays River Formation is part of the thick basal anhydrite of Bell subzone A. Hence, the carbonate of the Gays River Formation may be classified as part of the "A" sub-

zone of Bell (1929) on stratigraphic grounds (Giles and Ryan, 1976, Hatt 1978). Macrofauna in the Gays River formation, however, belongs to Bell's "B" subzone (Hatt 1978).

The complex stratigraphic relationships made the correlation of the Gays River carbonate uncertain and reflect the lithostratigraphic and chronostratigraphic problems encountered in the Windsor Group in general. Schenk (1969) concluded that rapid changes in environments affected the distribution of fauna in the Windsor and indeed the fauna are strongly controlled by environments rather than evolution. This conclusion points to the extreme difficulty in the stratigraphic correlation of the Gays River Formation to the Windsor Group in general.

2.3 Mine Geology

a. Basement Structure and Paleogeography

The Cambro-Ordovician quartz metawacke Goldenville Formation of the Meguma Group forms the basement for the Gays River deposit. In the vicinity of the mine, this basement rock has been folded into a N/E trending anticline (Fig. 2.4). The anticline resulted from the folding which accompanied the Middle Devonian Acadian Orogeny during which southern Nova Scotia was metamorphosed, folded, faulted and intruded by granitic plutons (Fyson 1966; Poole 1967; Poole et al., 1970). Major folds produced during this major tectonic event are generally NE trending, low plunging and upright (Fyson 1966). The folds tend to be tight to open, with steep axial planes. A regional slaty cleavage is generally parallel or subparallel to the axial planes.

In the mine area, the carbonate rocks rest with a pronounced angular unconformity on the north west limb of the north east trending anticlinal ridge of the basement. The basement has been eroded into several knobs

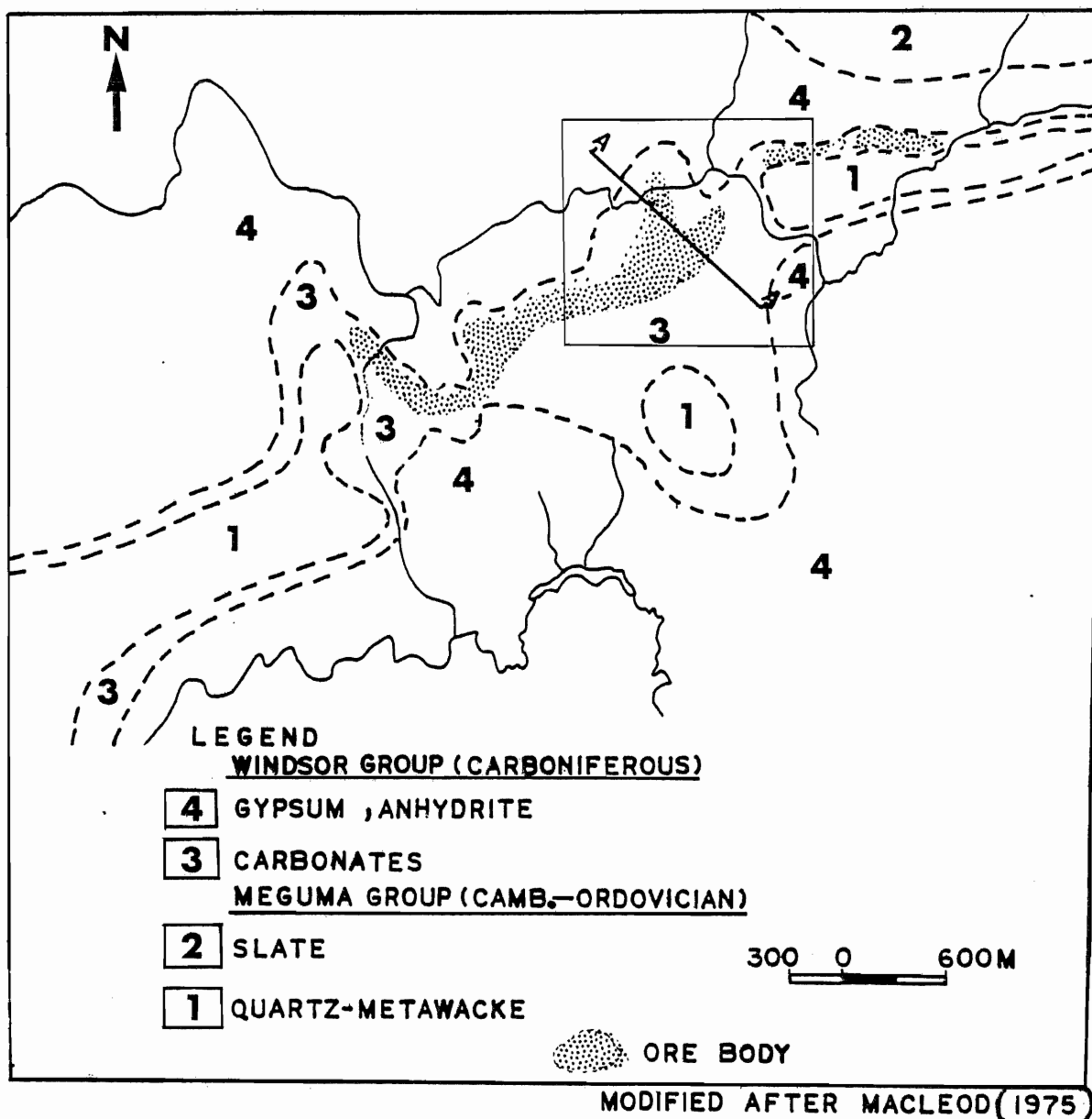


Figure 2.4 Geology of the Gays River area. Boxed area is shown in Figure 2.5. Section AA¹ as in figures 3.10, 3.11, 4.1a and 4.1b.

and ridges prior to the deposition of the Gays River carbonates. Structural contours over the basement paleoerosional surface illustrate a relief between 100 and 200 metres (Figs. 2.5 and 2.6).

Fault and joint systems in the quartz metawacke basement played a major role in the shape and style of the slopes and controlled the subsequent carbonate buildup. Faults with N/S, E/W and N60W orientations were mapped in the basement. The fault systems are locally associated with slickensides and quartz-filled tension gashes. The quartz-filled tension gashes suggest an E-W sinistral shear (Fig. 2.7a, 2.7b). Intersecting joint systems cut the basement rock in a N/S and E/W orientation. Prominent intersecting sets are 330/70W and 085/50N. These two sets control the basement slopes in the north/south and east/west directions respectively. Less prominent sets are 310/75W, 355/80E, 015/30W, 090/85S, 040/40S and 060/15S. Steepening of the basement slopes and the linearity in the adjacent valleys are the results of weathering and erosion emphasized along the main fault and joint systems.

b. Structures in the Carbonate Rocks

The carbonate rocks exposed in the decline area are cut by intersecting sets of faults and joints. Faults with principal N/S and E/W orientations are consistent with the basement fault system. The faults in the carbonates are associated with steeply plunging slickensides between 60 to 80°SE suggesting dip slip motions. Brecciation and clay gouge are commonly associated with the fault zone. The clay is predominantly montmorillonite. Joint sets in the carbonate are 085/80S, 75/80S, 355/70W and 015/80E. A stereographic plot of the joint planes shows their cross-cutting relationship (Fig. 2.8).

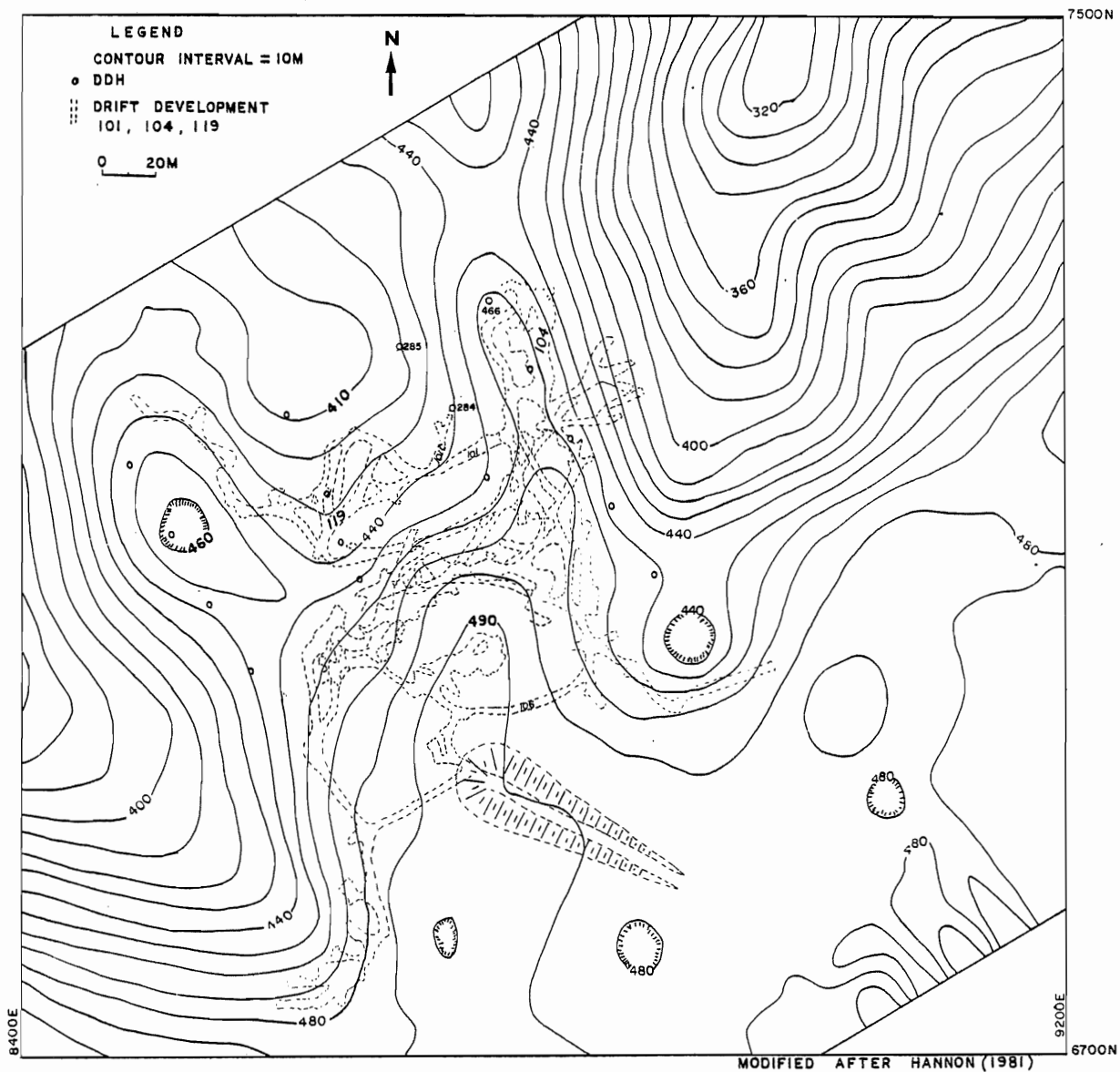


Figure 2.5 Structural contours of the basement topography, Gays River mine. Contours cover the boxed area on Figure 2.4.

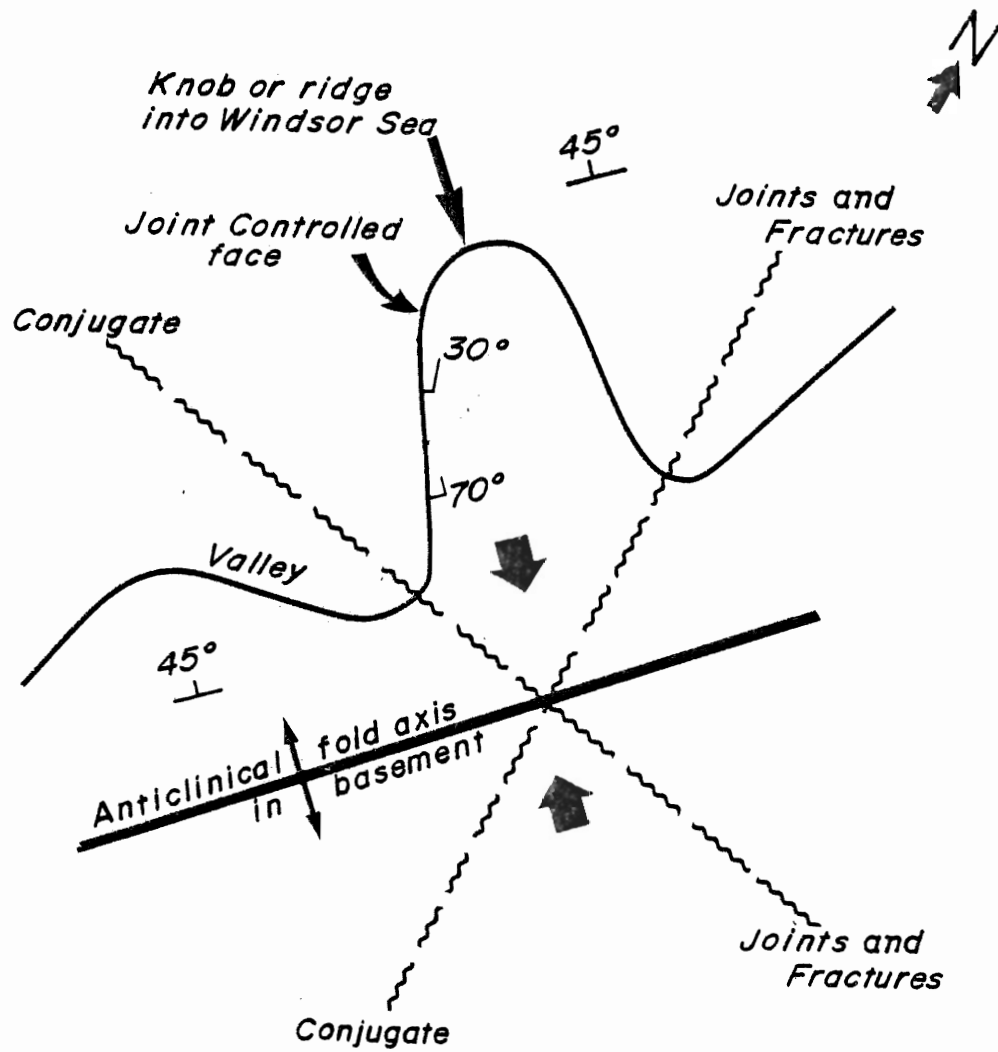


Figure 2.6 Schematic representation of basement structures, Gays River mine.

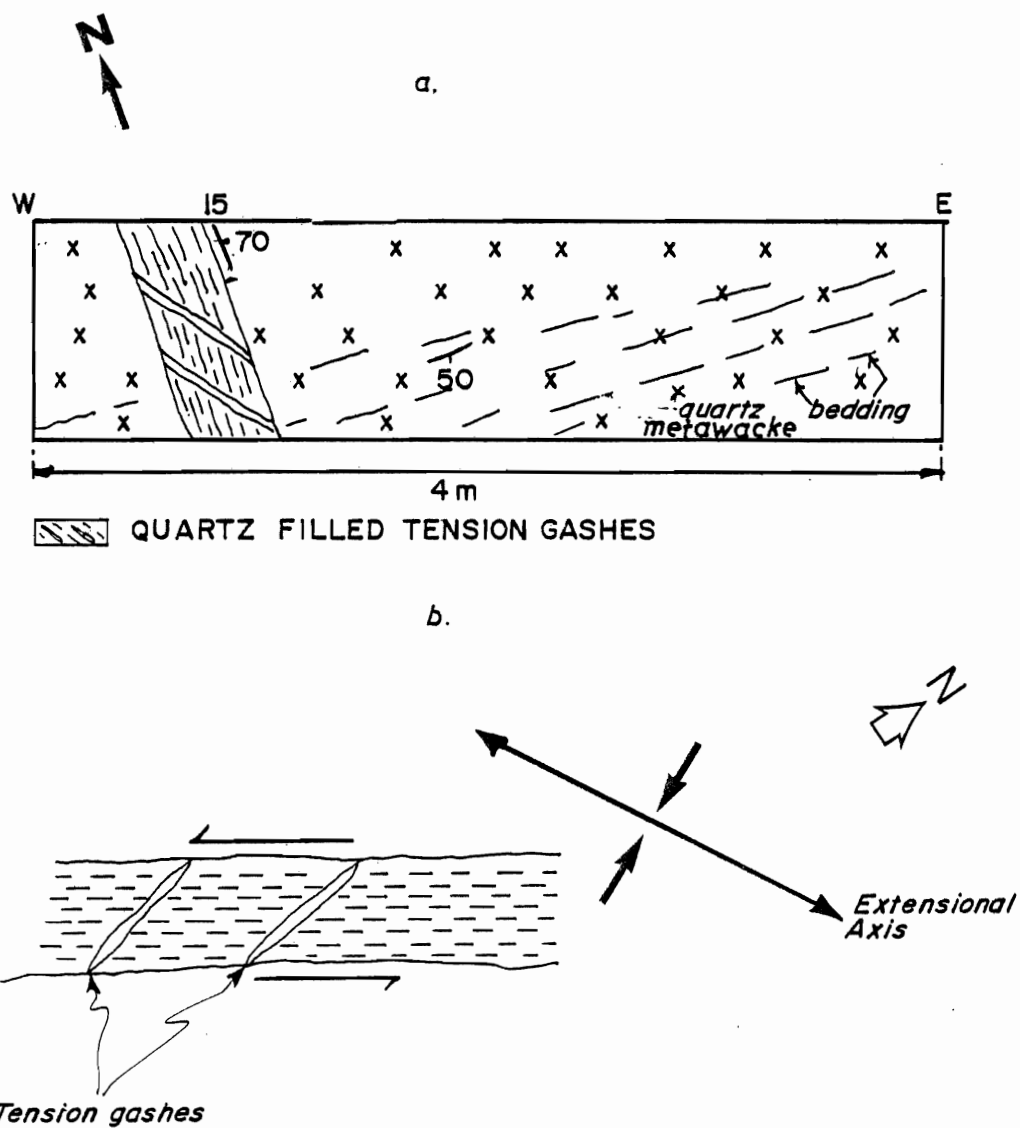


Figure 2.7 Fault and tension gashes in the quartz metawacke basement.

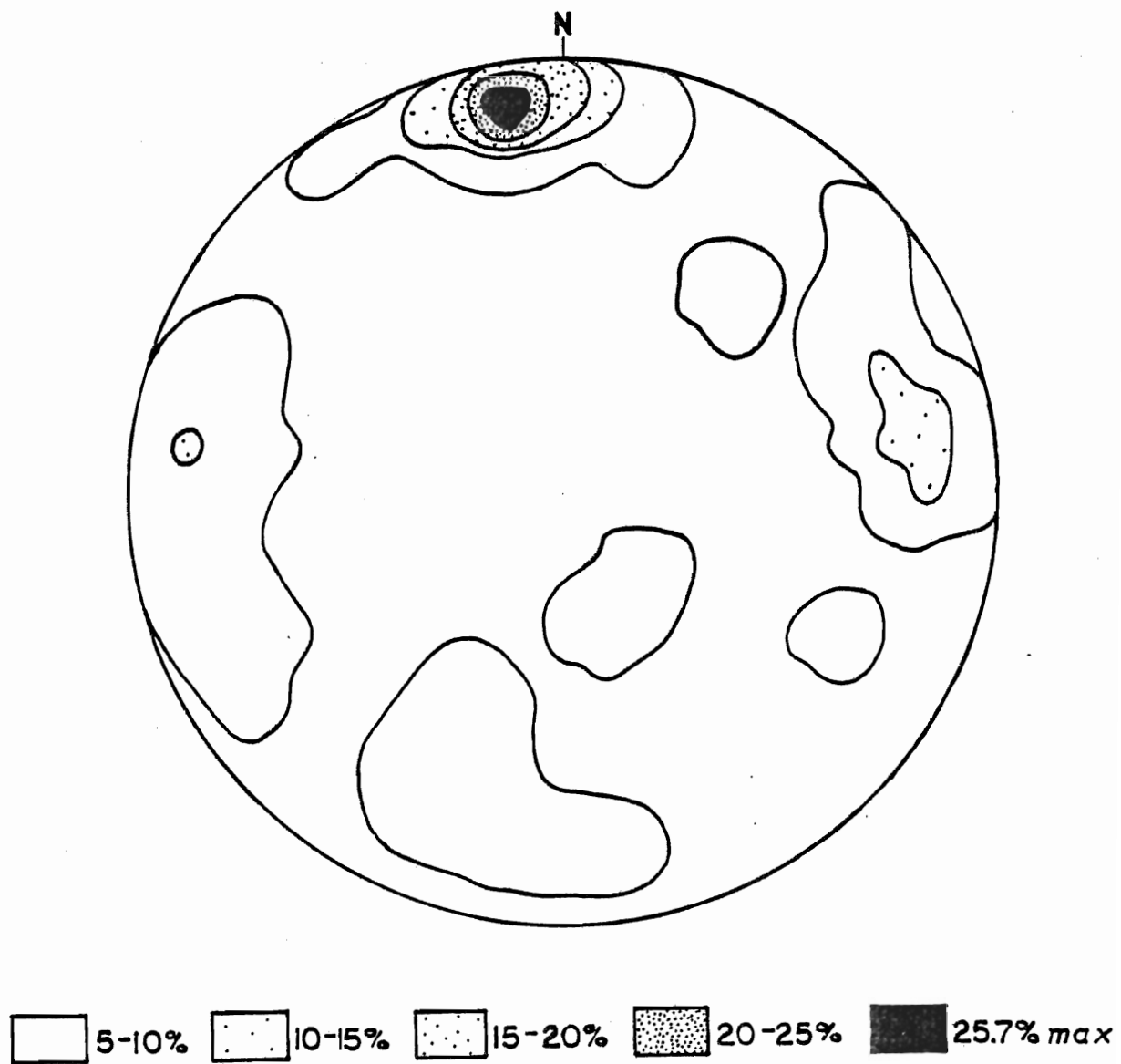


Figure 2.8 Joint planes in the carbonate rocks, 104 drift: Equal area net, lower hemisphere (101 poles).

At the evaporite/carbonate interface, shearing is defined by near horizontal slickensides, plunging between 10° to 15° to the north east. In the drifts 101C and 119, secondary gypsum veins (Fig. 2.9) occur within the first 2 metres below the evaporite/carbonate contact. The veins are concordant to the carbonate bedding, although the gypsum fibres normal to bedding indicate that the extension perpendicular to these bedding planes represents a distinct phase from the shear movements at the carbonate/evaporite contact. The extension of the carbonate bedding planes could result from hydraulic overpressure during anhydrite-gypsum conversion with the formation of gypsum veins by hydraulic injection of the fluid released. Shearman et al. (1972) indicated that where gypsum veins are present in association with secondary gypsum rocks, the gypsum of the veins represents (at least in part) the additional volume of gypsum resulting from the hydration of the former anhydrite. This explanation is compatible with the author's observation. Intense brecciation of the carbonate, probably of solution collapse origin is common at this contact.

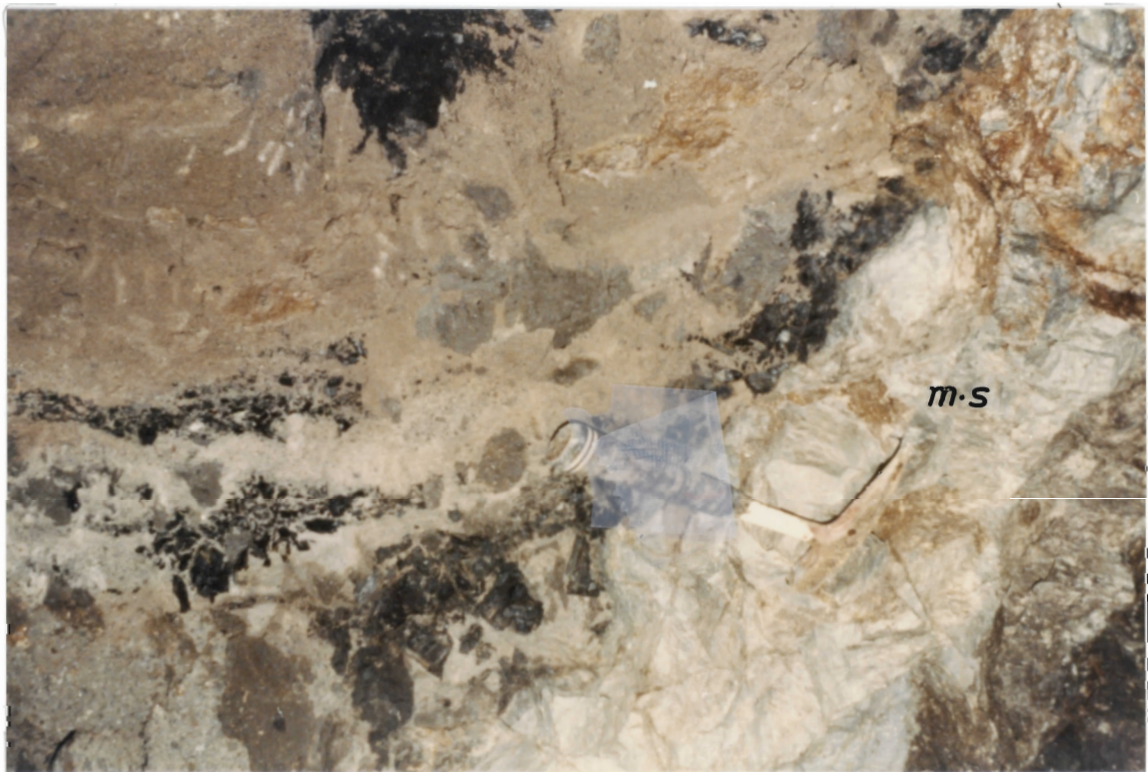
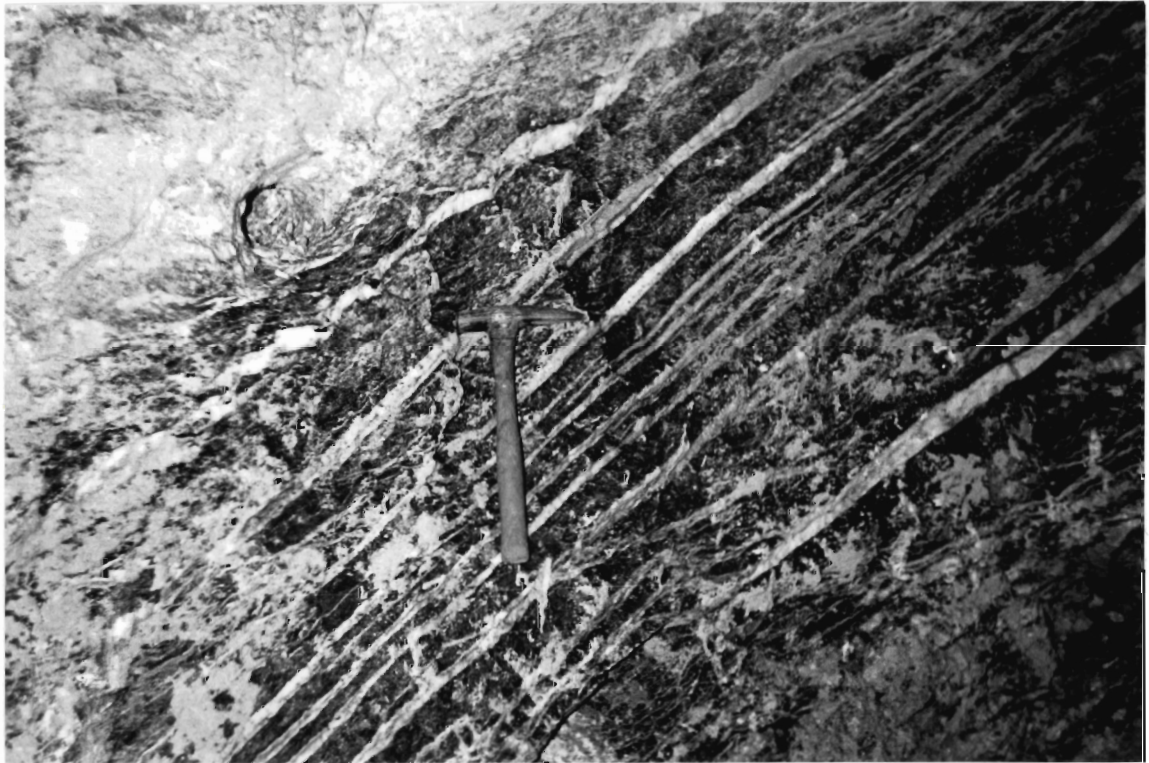
c. The Gays River "Trench"

The term "trench" has been used by Imperial Oil geologists to describe the long narrow sinuous ditch at the carbonate/evaporite interface at Gays River. They argued that the "trench" was formed in recent times as a result of the dissolution of the evaporite by fresh water in streams flowing in a karst topography. Imperial Oil geologists supposed that sediments stratigraphically above the evaporite have ultimately been washed down into this "trench" and the associated "sinkholes". This study shows that the "trench" corresponds to a much older (Mesozoic) erosional event.

Gravels, sand, silt and clay form the major in-fill in the trench with

Figure 2.9 Gypsum veins in parallel and conformable orientation to carbonate bedding. Note the minor offsets and boudinage of some of the gypsum veins. Drift 119.

Figure 2.10 Semiconsolidated "trench" sediments (ts) in a fault gouge adjacent to a massive sulfide vein (ms) in drift 104. Note the chips of coaly material (lignite) adjacent to the vein and the clayey and sandy texture of the "trench" sediments.



coaly materials as a minor constituent (Fig. 2.10). These sediments are unconsolidated, water saturated and have created a major mining problem.

A palynological analysis of five samples of the trench sediments was performed on request by Dr. E.H. Davies of the Bedford Institute of Oceanography, Dartmouth, Nova Scotia. A detailed list of the species reported are given in Table II-2.

The results of this analysis show that the "trench" sediments contain abundant Late Aptian-Early Albian pollen and spores. No Tertiary and Quaternary pollen was found in this sediment. This strongly suggests that the "trench" sediments are of Early Cretaceous age. The sediments were probably deposited after the uplift and erosion known for this period in the Appalachian tectonic belt (Rodgers 1967).

An examination of two samples of the coaly materials associated with the "trench" sediments was carried out in the laboratory of Dr. P. Hacquebard at the Bedford Institute of Oceanography, Dartmouth, Nova Scotia. Over 50 determinations of vitrinite reflectance on the two coaly materials was performed to assess the rank of the coal and its possible age. These determinations gave an average value of R_o of 0.44 (see appendix) which suggests a lignite rank for the coal and a possible Cretaceous age (Dr. P. Hacquebard, personal communication, 1981). The lignite is completely barren of palynomorphs although it contained abundant resinous material (Dr. E. Davies, written communication, 1982). This lignite has attained a higher degree of maturation than lignite reported in the Cretaceous Shubenacadie clay pit (R_o 0.28) about 10 km north of the mine property (Hill 1976). If the coalification process to form this lignite occurred in the "trench", this could be interpreted as having been buried to about 1 to 2 kilometres depth to attain the rank of vitrinite established

(Hacquebard 1973, p. 234) although vitrinite reflectance may not be a very accurate indicator of temperature in lignites of this rank.

Slickensides with near horizontal plunges (between 10-15°) to the north are commonly present at the carbonate/evaporite contact in the 101 and 119 drifts. Plastic deformation structures of N/S orientation occur locally in the "trench" sediments. These indicate that the "trench" was affected by shearing. Although the "trench" outline commonly follows the faults controlling massive sulfide veins as in the 104, 107 and 4470 drifts, the "trench" sediments are not mineralized. This clearly indicates that the "trench" sediments post date the lead-zinc mineralization. Furthermore, the "trench" sediments probably represent a filling of a Cretaceous landscape into structurally controlled channels. This Cretaceous drainage system has been emphasized in glacial and post glacial times with the localization of sinkholes.

CHAPTER 3

DESCRIPTION OF THE CARBONATE LITHOLOGY

3.1 General Statement

It is not the intention of this author to give a detailed diagenetic history or to construct a paleoenvironmental model for the carbonate lithofacies in the Gays River complex. This objective was dealt with in some detail in the previous theses by Macleod (1975), Osborne (1977), Hartling (1977) Hatt (1978) and Hancock (1982). The reader is referred to these works for detailed paleoenvironmental reconstructions.

The terminology used to describe the rocks in the mapped areas follows. Unless otherwise stated, the term porosity is used to indicate open spaces available for mineralization.

3.2 Terminology

The carbonate rock types will be described using the terminology of Dunham (1962) revised by Embry and Klovan (1971). This terminology seems adequate for the dolomite and limestone mapped because it identifies the proportions of constituents of each rock (Table 3.1).

Briefly, Dunham recognized 2 broad categories of carbonate rocks: allochthonous and autochthonous. The autochthonous group comprises those rocks in which organic binding of grains during sedimentation could be recognized. Dunham classified this as boundstones. In the allochthonous group, sediment binding is unimportant, but they can be grouped according to the relative proportions of lime mud matrix in the rock, e.g.

- Mudstone : Mud supported, less than 10% grains
- Wackestone : mud supported, greater than 10% grains
- Packstone : mud present but grain supported

ALLOCHTHONOUS LIMESTONES ORIGINAL COMPONENTS NOT ORGANICALLY BOUND DURING DEPOSITION				AUTOCHTHONOUS LIMESTONES ORIGINAL COMPONENTS ORGANICALLY BOUND DURING DEPOSITION		
				BY	BY	BY
				ORGANISMS	ORGANISMS	ORGANISMS
CONTAINS LIME MUD (<0.03 mm)			NO LIME MUD	WHICH	WHICH	WHICH
MUD SUPPORTED		GRAIN SUPPORTED		ACT	ENCRUST	BUILD
LESS THAN 10% GRAINS <0.03 mm	GREATER THAN 10% GRAINS			AS	AND	A RIGID
				BAFFLES	BIND	FRAMEWORK
MUD- STONE	WACKE- STONE	PACK- STONE	GRAIN- STONE	BAFFLE- STONE	BIND- STONE	FRAME- STONE

Table 3.1 Classification of carbonate rocks. (After Dunham, 1962, modified by Embry and Klovan 1971).

Grainstone : no mud present, grain supported.

Dunham only differentiated between rocks with grains less than 0.03 mm in size (mud) and those greater than 0.03 mm (grains) in this allochthonous group. This lack of size differentiation led Embry and Klovan (1971) to propose three size divisions: mud (less than 0.03 mm), grains (0.03 mm to 2 mm), and a new division of grains larger than 2 mm. The new grain division consists of floatstone, a mud supported rock with more than 10% grains larger than 2.0 mm, and rudstone, a grain supported rock with more than 10% grains larger than 2 mm.

Embry and Klovan (1971) modified Dunham's autochthonous group (boundstone) to include the following rock types:

Bafflestone : sediments in which baffling by organic component results in grain or mud accumulation

Bindstone : sediments organically bound by encrusting or agglutinating organisms

Framestone : sediments comprised mainly of rigid framework of organisms.

The carbonate rock types exposed in the area mapped will be described by using these terms where applicable.

3.3 Rock Descriptions

The carbonate rocks can be divided into two main groups: (group one and group two). Group one rocks were deposited in the valley reentrants between basement knobs and ridges. The group two rock types occur directly on the tops of these basement ridges and their leeward slopes. The two groups of rocks illustrate complex interrelationships which bear on their paleotopographic settings, depositional environments and diagenetic modifications.

3.3.1 Group One Rock Types

The carbonate succession in the reentrant area ranges from 3 to 5.5 metres in thickness with thicker successions on gentle basement slopes. The succession thins out with increasing slope. It rests with an angular unconformity on the quartz metawacke basement and is overlain by a thick sequence (50 m) of gypsum and anhydrite of the Carrols Corner or Gleason Brook formations (Giles and Boehner 1976).

Six main rock types were recognized in this group. These include:

- a. Basal conglomerate
- b. Carbonaceous skeletal grainstone
- c. Stromatolitic packstone
- d. Algal skeletal packstone-bindstone
- e. Skeletal grainstone
- f. Gypsiferous wackestone-packstone.

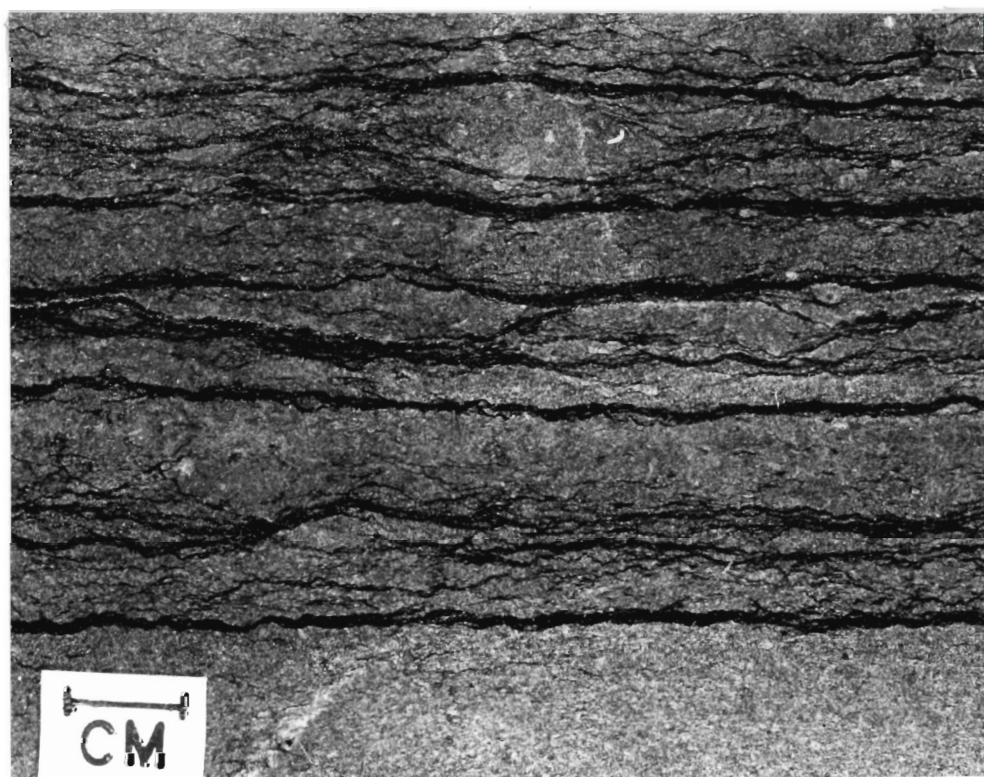
a. Basal Conglomerate

A basal conglomerate rests directly on the quartz metawacke basement at the bottom of the carbonate succession in the reentrant areas. This conglomerate varies in thickness from 1 to 3 metres with an average thickness of 1.5 metres. It consists of angular to subangular lithoclasts of the basement all cemented by detrital grains of carbonate. The lithoclasts vary in size from pebbles, cobbles to boulder size blocks of approximately 1 metre across. Sorting in the rock is poor with respect to size and shape and bedding is poorly developed except in localities where the axes of elongate clasts are parallel to the general bedding (Fig. 3.1).

The conglomerate is moderately graded into a lower boulder conglomerate where boulders predominate and an upper pebble conglomerate where finer fragments are common. The upper pebble conglomerate locally contains badly worn fragments of skeletal carbonate grains.

Figure 3.1 Basal conglomerate in the 119 drift area. Note the variable sizes of fragments. Hammer points to a boulder size fragment of the quartz metawacke basement.

Figure 3.2 Carbonaceous skeletal grainstone. Note the parallel conformable orientation of the carbonaceous laminae to carbonate bedding. Porosity is dominantly intraparticle and interparticle.



Porosity in this basal conglomerate is generally tight because of the lack of pore spaces in the angular siliclastic fragments. Pore space is restricted to the carbonate cement and is dominantly interparticle and fracture porosity. Matrix carbonate cement is locally replaced by sphalerite and galena.

Environment: The position of this rock type in the valley areas between basement highs, and the accumulation of angular fragments of basement composition suggests that the constituents are locally derived from the adjacent paleotopographic highs. This implies that scree accumulation on the basement slopes supplied the fragments that were subsequently cemented by an added carbonate matrix during the initial transgression. Erosion along basement fractures led to the deposition of joint bounded blocks of the lower boulder conglomerate. The deposition of a conglomerate bed suggests a high energy condition during the initial stages of transgression.

b. Carbonaceous Skeletal Grainstone

This is a dark brown, highly bituminous rock type in the reentrant area. The rock consists of skeletal grainstone alternating with carbonaceous laminae. It attains a thickness of approximately 1.5 metres with thin uniform continuous bedding over a distance of 10 metres. Dip varies from 25° to 35° and is generally basinward to the north or north west. Basinward dipping cross beds at a low angle of 12° were mapped in drift 101C. The rock consists of diverse varieties of fragmented bioclasts and lithoclasts within a matrix of quartz sands and sandy dolomite (Fig. 3.2). Skeletal grains include algae and frequently broken shells of gastropods, bivalves, encrusting bryozoa, ostracods and corals in a decreasing order

of abundance. Lithoclasts consist of pebbles of basement clasts. Siliclastic constituents constitute an average of 20% of the rock by volume. The carbonaceous laminae in the rock attain an average thickness of 2 mm and consist of approximately 10% quartz grains. Chemical analysis of this carbonaceous laminae revealed that they contain an average of 80% carbon by weight (P. Hannon, personal communication) with a composition of gilsonite (an asphaltite).

Porosity is generally very good in the grainstone. Filled pore spaces include interskeletal, intraskeletal, moldic and sheltered pores. Most of the pore spaces are filled by sphalerite, galena, calcite and fluorite.

Environment: The abundance of carbonaceous laminae which constitute about 15% of this rock is indicative of plant forms which are probably algal colonies in an initial shallow water environment. Other features as cross bedding, fragmental remains of skeletal types, and the presence of encrusting forms of bryozoa point to high energy stormy conditions. Encrusting bryozoa are more adapted to high energy stormy conditions than the erect stem like forms which are adapted to deeper water (Schopf 1969). These features suggest a high energy subtidal environment for the skeletal grainstone.

c. Stromatolitic Packstone

In the upper parts of the reentrant, where the basement slope increases, a stromatolite dominated carbonate rock was mapped. The rock consists of columnar algal stromatolites with fairly distinct convex laminae resting on the basal conglomerate. The laminae are very thin with an average thickness of 0.5 mm. The stromatolites occur as isolated

cylindrical columns and club shapes. Columns are steep walled and they attain heights of approximately 3 centimetres over a width of 1 centimetre (Fig. 3.3). The matrix of this rock is dolomite microspar with silt and quartz sand grains. Infrequent basement pebbles occur in few instances within the matrix. The siliceous component of the matrix is approximately 10%. Bioclasts are less than 2% and include encrusting bryozoa and gastropods. Bedding is poorly developed except where the axes of elongated pebbles of the basement are aligned.

Pore spaces in this rock type are interstitial to columns and interparticle and fracture porosity are the dominant types.

Environment: Although algal stromatolites are widespread in environments ranging from supratidal to subtidal, most authors attribute their presence to intertidal environments. Playford and Cockbain (1976) have shown that intertidal forms of algae may extend to the subtidal zones without any significant change in morphology. Hence the presence of columnar stromatolites in this rock type does not conclusively point to an intertidal environment. The position of the rock on the reentrant slope and the presence of encrusting forms of bryozoan and pebbles of basement composition suggest a moderate energy subtidal environment.

d. Algal Skeletal Packstone-Bindstone

These admixtures of packstone and bindstone overlie and intertongue with the skeletal grainstone in the reentrant area. The rock consists of fragmental grains of diverse organisms in a matrix of silt and quartz grains and recrystallized dolomite microspar. The rock is grain supported and the skeletal types include encrusting and erect bryozoa, gastropods, brachiopods, ostracods, bivalves and coral fragments in a decreasing order

Figure 3.3 Stromatolitic packstone. Note the excellent fracture and interparticle porosity in this lithology. The porosity has been filled by sphalerite (sph) and calcite (ca).

Figure 3.4a Algal skeletal packstone-bindstone. Skeletal components include bryozoans (by), brachiopods (bp), bivalve (bi), gastropods (ga), and algal encrustations (alg). Intra-skeletal and fracture porosities are common.

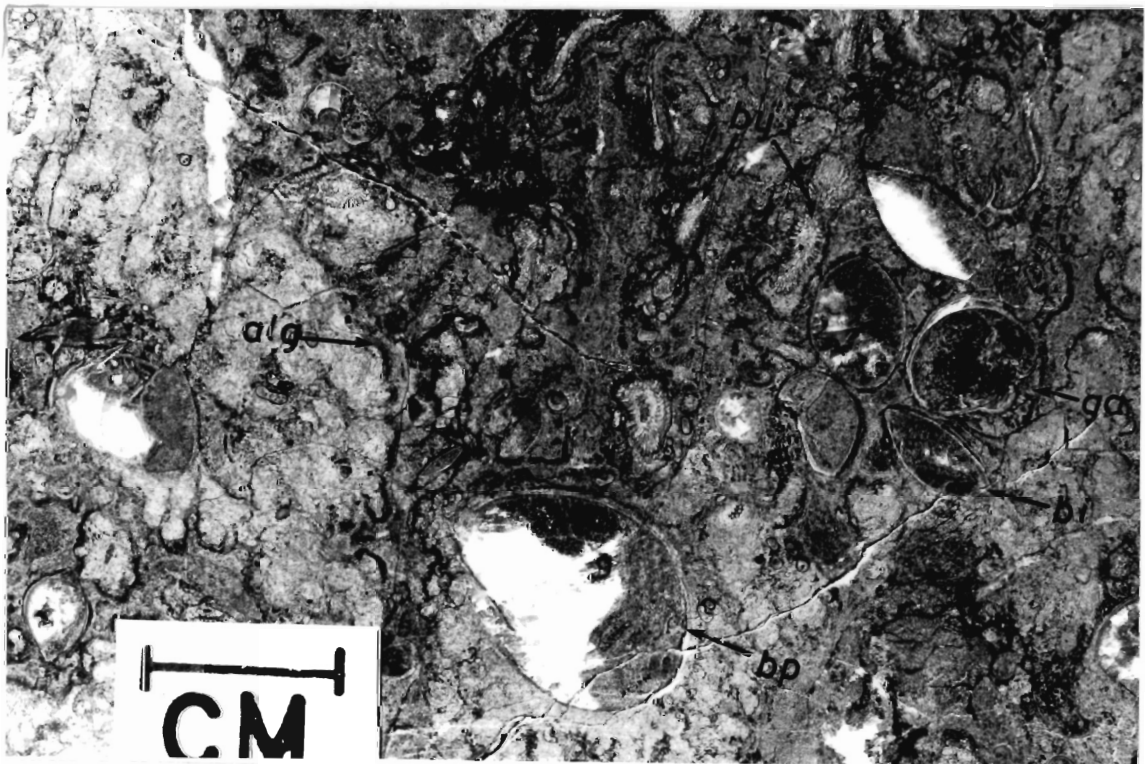
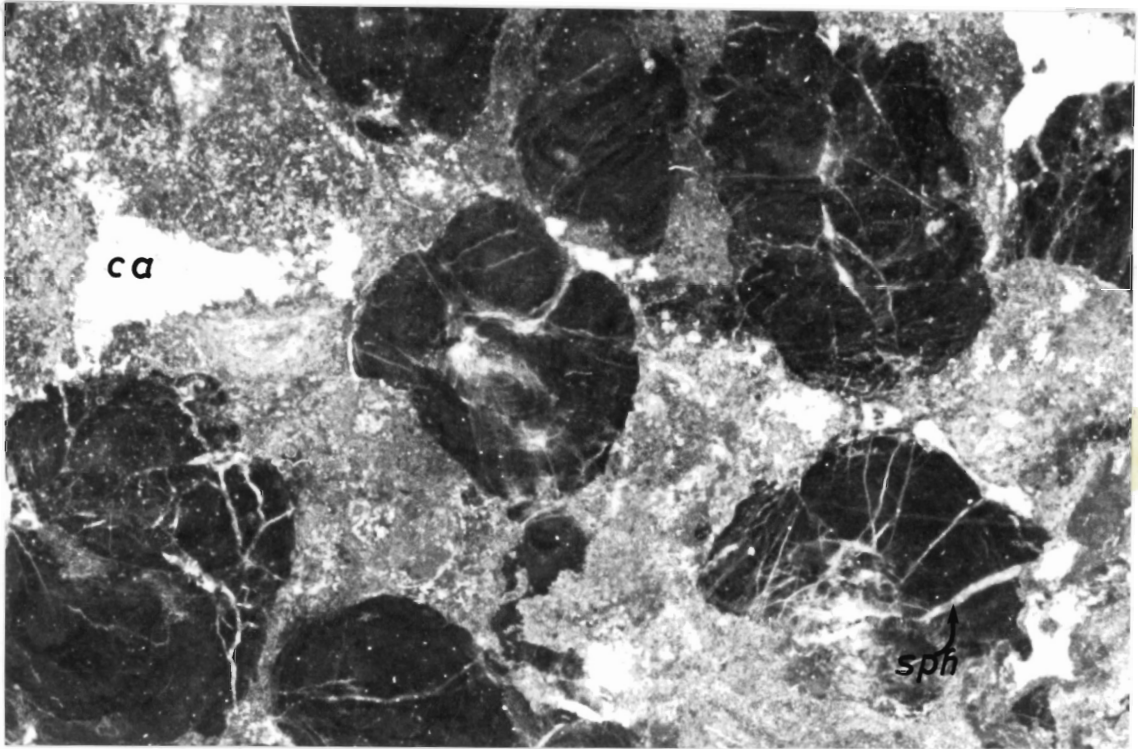
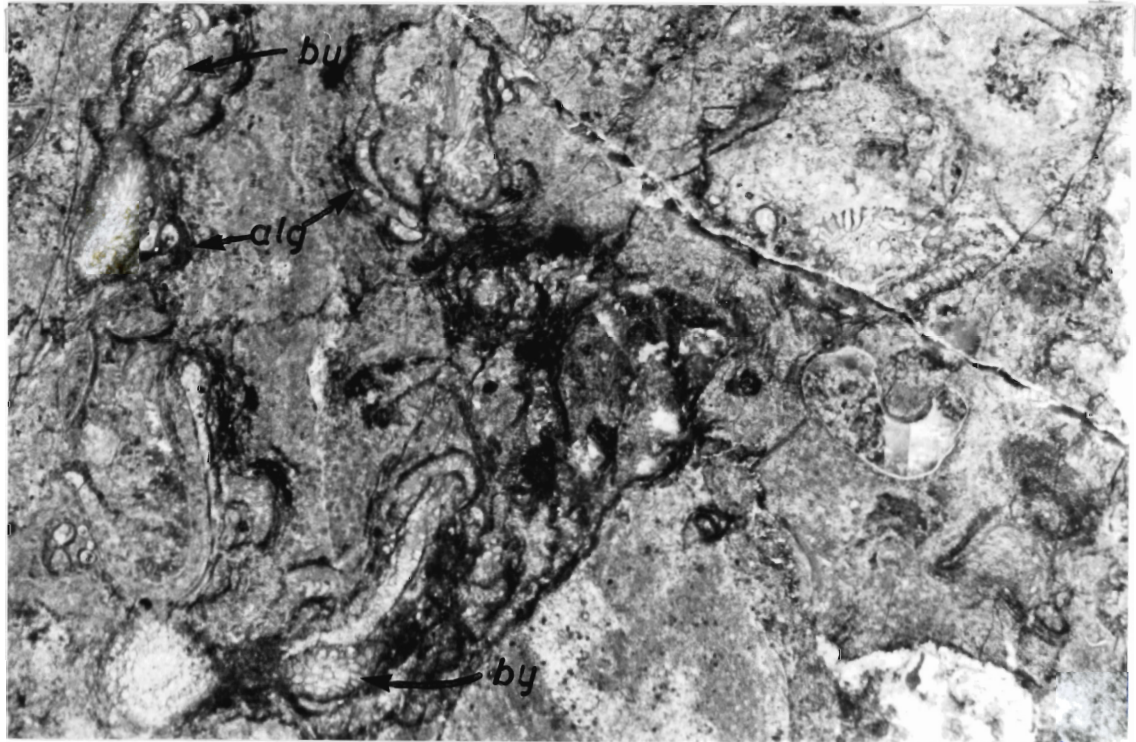
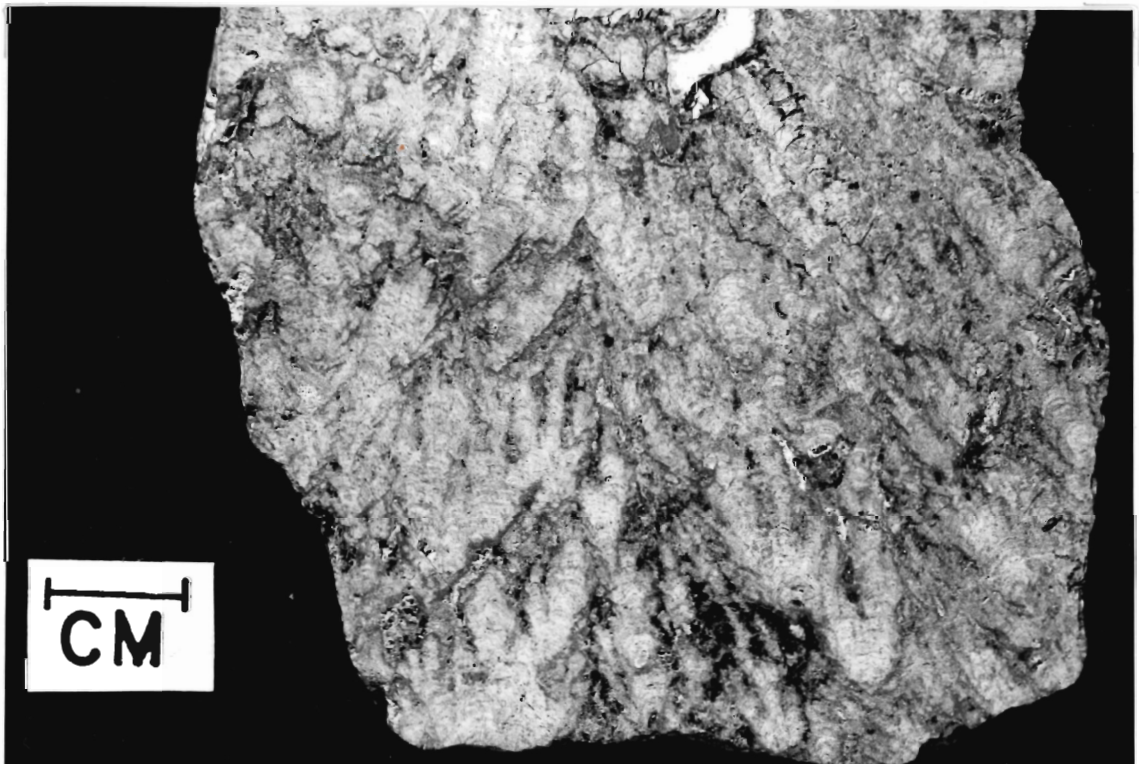


Figure 3.4b Algal skeletal packstone-bindstone. Note the algal encrustations (alg) on bryozoan fronds (by). The algal structures produce umbrella effects on the bryozoans.

Figure 3.5a Algal bindstone. Note the digitate laminated columns of the stromatolites. Laminations are gently convex. Fabric selective porosity include interparticle and moldic types.



CM



of abundance. Siliclastic grains in the matrix constitute about 5% of the rock. Although most of the skeletal grains are fragmented, bryozoans, gastropods and brachiopods are well preserved. Algal textures are poorly preserved and algae only occur as indistinct laminae and clumps. The largest skeletal grain types are the brachiopod shells with approximate length of 10 to 15 mm and the spiralled gastropod shells with 5 to 10 mm diameter (Fig. 3.4a). Bedding in this rock is poorly developed and sorting is fair with respect to size and shape.

In the bindstone parts, encrusting bryozoans and algae are intimately associated. This gives the rock an organic bindstone texture. The algal laminae are very thin, averaging 0.2 mm in thickness and generally envelope the encrusting bryozoa fronds (Fig. 3.4b). Locally, the algal texture is lump shaped with rims of carbonaceous laminae. The algal lumps may be described as thrombolite forms as illustrated by Aitken (1967) in his classification of algae forms. Stylolitized carbonaceous laminae frequently produce umbrella effects on stemlike and encrusting bryozoan fronds (Fig. 3.4b). The stemlike bryozoa appear to be in life consistent positions.

Porosity and permeability in this rock type is generally good. Pore spaces include intraparticle, interparticle and sheltered. Sheltered pores are frequently developed below the umbrella texture produced by stylolitized carbonaceous laminae over erect bryozoans. Non fabric selective porosity is common in this rock along crosscutting microfractures. Porosity in the packstone is approximately 10% but decreases to 4% in the bindstone.

Environment: The deposition of this rock type in the reentrant area overlying and interfingering the skeletal grainstone suggest a deposition in deeper quiet water where finer matrix can be added. The presence of stemlike bryozoans support a moderate energy condition. The fragmental nature of some of the skeletal grains point to occasional storm activities and shell destructions.

e. Skeletal Grainstone

This rock type overlies the packstone-bindstone lithology and intersects the bindstone in few localities. It is carbonaceous in part and nearly identical to the carbonaceous skeletal grainstone in the lower part of the sequence. It differs from this because of the reduction in the number and size of the carbonaceous bands, reduction in the siliclastic component and a better preservation of bioclasts. Thicknesses of carbonaceous laminae in this rock rarely exceeds 100 μm but they consist of 10% quartz grains, 5% calcite and 2% gypsum by volume. Siliclastic component to the rock is generally less than 10% and consists of silt and sand size grains in the matrix. Whole shell bioclasts include stemlike and encrusting bryozoans, gastropods, ostracods and bivalves in a decreasing order of abundance. The rock is bedded and grains are well sorted with respect to size and shape.

Discrete grains of gypsum 0.5 to 2 mm with an average of 0.8 mm across are contained in the groundmass. These grains are ovoid or rounded in shape. Gypsum also occur as in fillings in the intraskeletal pores and as replacements of the matrix material. Celestite blades occur locally in the intraskeletal pores.

Porosity in this rock is dominantly interparticle with lesser development of intraparticle, sheltered and fracture porosity.

Environment: The abundance of well preserved whole shell bioclasts in this rock type with lesser amount of fragmental shells suggests a minimum transportation of these organisms from their flourishing sites. The presence of encrusting and stemlike bryozoans are indicative of high to moderate energy conditions. Encrusting forms of bryozoans can withstand high energy stormy conditions better than the erect forms (Schopf 1969). Since this grainstone cuts across the bindstone lithology, the rock probably represents channel deposits in a shallow subtidal environment.

f. Gypsiferous Wackestone-Packstone

This rock type is restricted to the top of the carbonate succession and lies at the contact with the overlying gypsum and anhydrite. Recognizable skeletal grains are absent in the rock except for few degenerated bivalve shells. Lithic grains include oval and discoid forms of gypsum 0.5 to 2 mm in diameter and gypsum porphyroblasts with an average diameter of 1 centimetre. Peloids frequently occur in parallel alignment with bedding. The gypsum crystals are well sorted with respect to size and shape. The matrix consists of sand size dolomite cement, and gypsum peloids. The gypsum content of this rock represents an average of 20% by volume. Both gypsum and dolomite grains have been replaced to a large extent by sphalerite and galena.

Leaching by calcium rich waters has converted a large part of the rock from dolomite to a dedolomitized limestone. This effect is quite profound at the contact with gypsum and is probably related to the

secondary hydration and dissolution of anhydrite.

Pore spaces in this rock have been completely filled by gypsum, sphalerite and galena. These minerals form the matrix to the rock in areas adjacent to massive sulfide lenses.

Environment: The lack of fauna in this rock type is indicative of a hypersaline environment of deposition. Schenk (1981)

described the structural forms and textures of anhydrites in the Windsor basin under 3 groupings: nodular and displacive in the upper Windsor, laminated and bladed in the middle, and macrocrystalline and microcrystalline forms with dolomite relics in the lower parts. The occupancy of the carbonate matrix of the gypsiferous wackestone-packstone by gypsum suggests that a partial replacement of this rock has taken place by the overlying gypsum. The presence of carbonaceous films in the lower grainstone and packstone lithology probably prevented the replacement of these, compared to the gypsiferous wackestones above them. Post depositional changes in the rock include dedolomitization, celestite precipitation and gypsum veining.

3.3.2 Group Two Rock Types

This group of rocks were deposited on the tops of the fault bounded basement crests and on their leeward slopes. Unlike the group one rock types, they are clearly marked by the absence of the basal conglomerate which were deposited as "screes" or talus in the reentrant areas. Diverse types of organisms are less abundant in the group two rocks. The four rock types in group two are (a) algal bindstone, (b) corallgal bafflestone, (c) algal fenestral wackestone-packstone and (d) lime packstone and breccia.

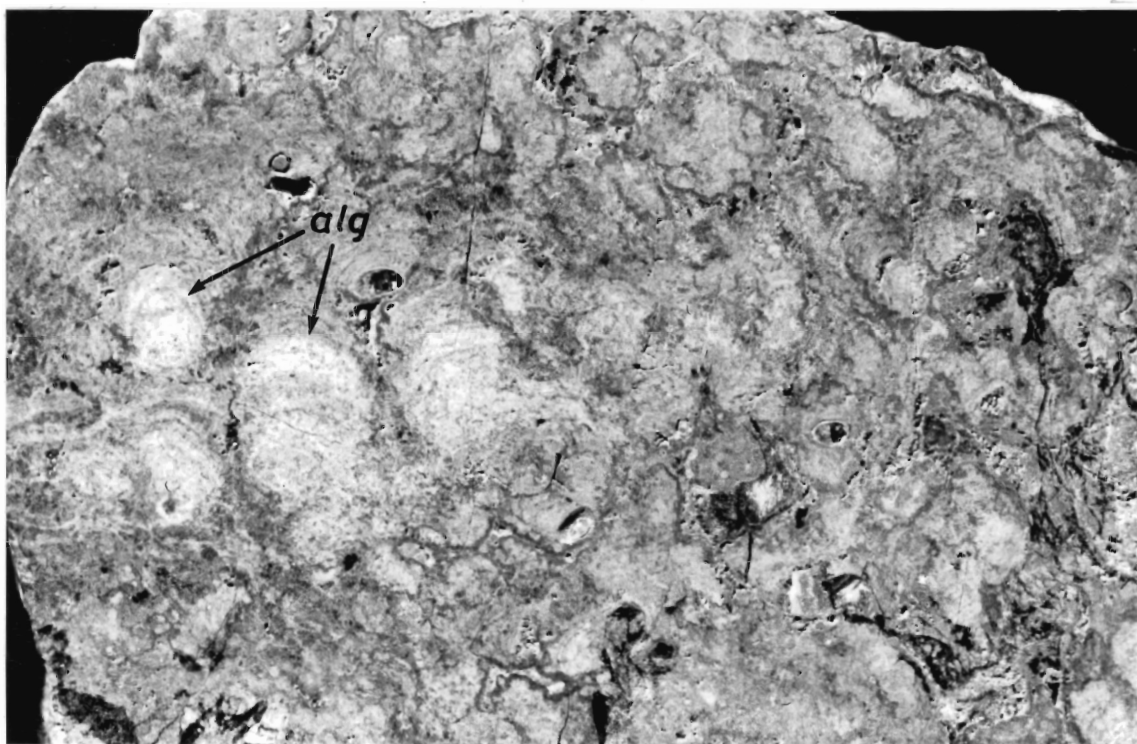
a. Algal Bindstone

This rock type was deposited on the crest of the basement paleotopographic high which stands as an upfaulted ridge in the decline area. It is a light to dark brown rock with encrusting forms of algae as the dominant organism representing approximately 70% of the rock by volume. Skeletal grains in the rock include encrusting bryozoans, corals and ostracods in decreasing order of abundance. The skeletal grains represent approximately 2% of the rock by volume. The matrix consists of a mosaic of sand size dolomite. Where shells of corals or ostracods occur, they are frequently encrusted by algae and bryozoans. The rock is termed a bindstone (Embry and Klovan 1971) because of the organic binding texture preserved by encrusting algae.

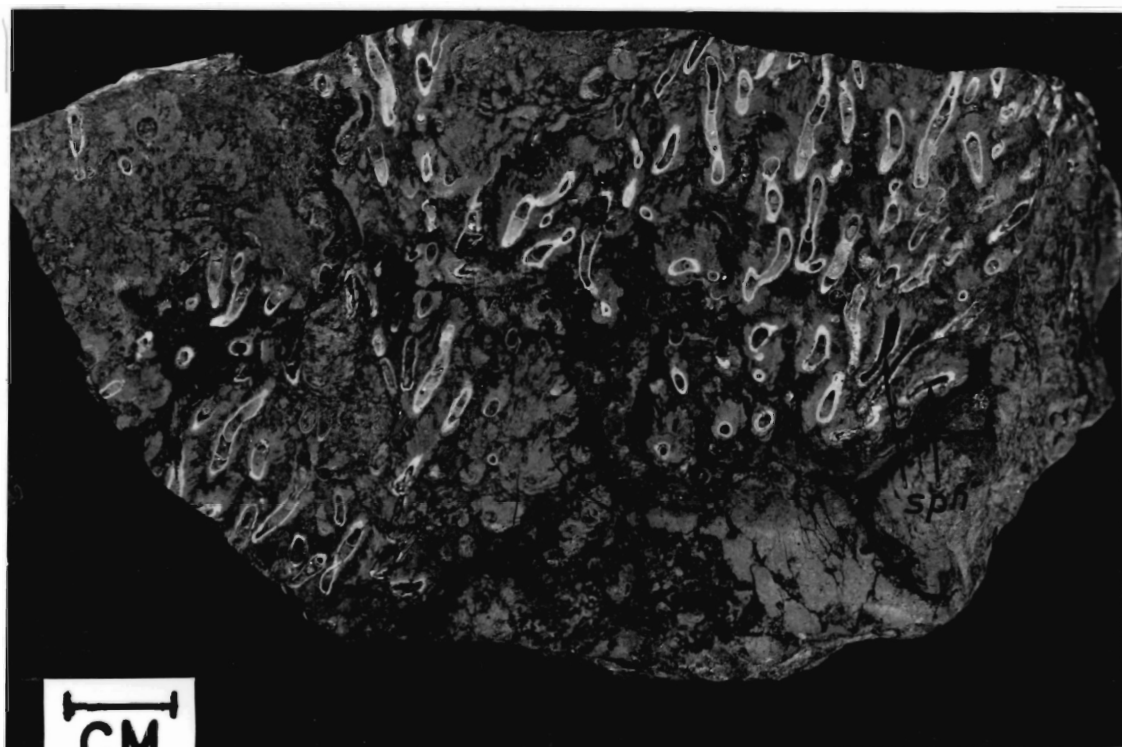
The encrusting algae occur in two forms; (1) as digitate stromatolites with columns of well laminated hemispheroids branching upwards (Fig. 3.5a) and (2) as irregular hemicylindrical forms with indistinct laminations (Fig. 3.5b). In the first form, the branches of columns are nearly parallel, with axes of new columns almost parallel to the axis of the original column. The columns attain heights ranging between 5-15 mm. The columns are erect and consist of mottled dolomite cement. Interstitial spaces between columns are filled with sand size grains. The second form of encrusting algae lack distinct laminations and attain an average height of 12 mm over a width of 2 mm. They are identical to the cryptalgal forms described as thrombolites (Aitkens 1967). Bedding is poorly developed and sorting is fair with respect to size and shape.

Figure 3.5b Algal bindstone. Note the irregular hemicylindrical forms of algal stromatolites (alg) with indistinct laminations.

Figure 3.6 Coralgall bafflestone. Note the good intraskeletal porosity in the coral molds. Growth framework porosity is common. Most of the intraskeletal pores in this sample are filled with sphalerite (sph).



CM



Porosity in this rock is fabric selective and is dominantly interparticle, moldic and growth framework. Interstitial pores between algal columns are infrequently filled with sphalerite, galena, calcite and marcasite. Coral fragments that are incorporated within lumps and nodules of algae enhance moldic porosity.

Environment: The distribution of this rock type on the crests of basement paleotopographic highs and the presence of encrusting algae and encrusting bryozoans suggest a moderate to high energy environment that was stabilized by algae. The lack of abundant fauna is indicative of a restricted shallow hypersaline environment.

b. Coralgal Bafflestone

This rock type lies stratigraphically above the algal bindstone on the crest of the basement paleotopographic high. The rock is buff coloured to dark brown and consists of corals and algae as the main baffling agents associated with stemlike bryozoa and rare ostracods. The skeletal types represent an average of 15% of the rock by volume. Grains of corals range in dimensions from 3 mm to 8 mm high with an average of 4 mm and are typified by steep walls. The disposition of coral fragments in near vertical orientations in the slabs cut perpendicular to beddings suggest that they are in life consistent positions (Fig. 3.6). Algal encrustations are frequently rimming coral fragments and the rock can be called a bindstone in part. Encrusting algae on coral substrate mimic the shape of the coral fragments. In few cases, stem like bryozoans are also

encrusted by algae. Matrix to this rock consists of fine grained silt to sand size grains of dolomite. Bedding in the cut slabs is obscure but is fairly distinct on outcrop scale. Sorting is fairly good with respect to the size and shape of grains.

Porosity in this rock is fabric selective except where fracture porosity is locally developed. Moldic, sheltered, interparticle, intraparticle and growth framework porosity are common. Coral molds are commonly filled with sphalerite, galena and calcite in areas adjacent to sulfide veins. In other areas, the pore spaces in the rock are empty due to the dissolution of preexisting gypsum.

Environment: The intimate association of corals and stemlike bryozoa coated by encrusting algae suggest deposition in a subtidal environment. Stemlike bryozoa can flourish better in deep and quiet water conditions (Schopf 1969). The rigid stemlike bryozoa were probably deposited in quiet water below the wave base. A low energy environment on basement niches can provide an adequate water depth for corals, algal and bryozoan colonies. The gradation from an algal bindstone lithology lower in the sequence to coralgall biotopes suggest that the original colonizers were algal.

c. Algal Fenestral Wackestone-Packstone

This rock type occurs as a cap for the algal bindstones and bafflestone on the basement paleotopographic high. It attains a thickness ranging from 5 to 20 metres with an average of 8 metres. The rock is an admixture of wackestone and packstone. It is light brown to dark brown in colour and consists of peloids, algal lumps and less than 2% skeletal components in a matrix of micrite and sandy dolomite. Infrequent

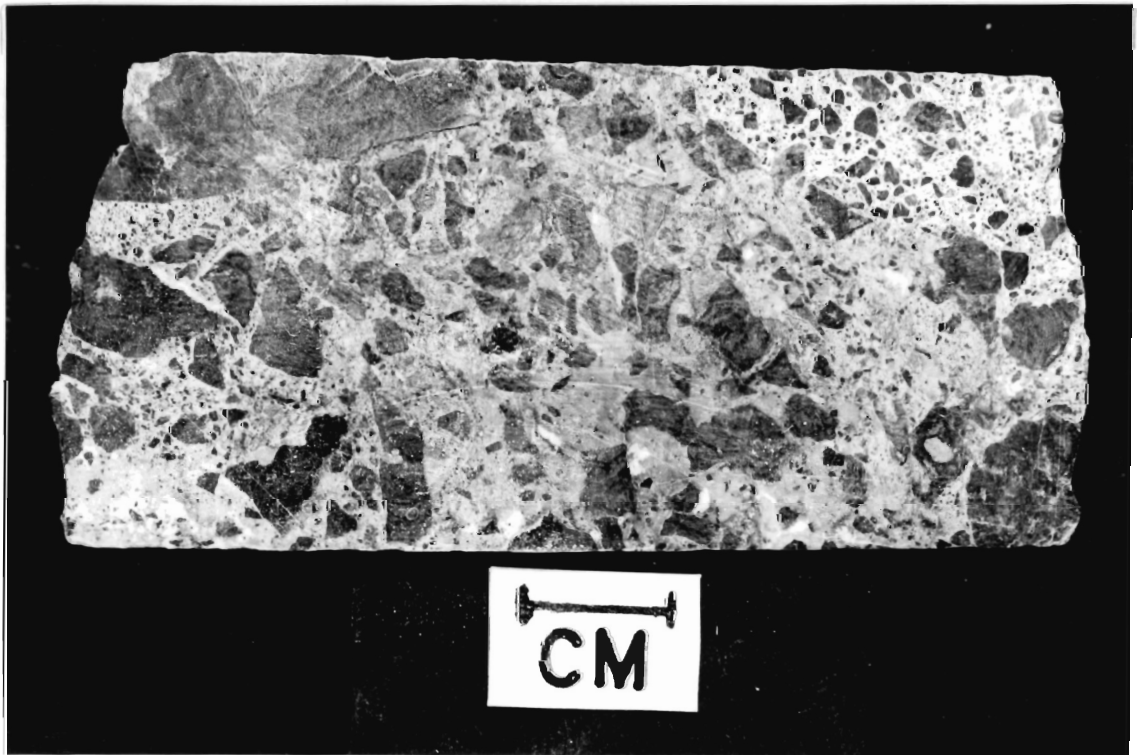
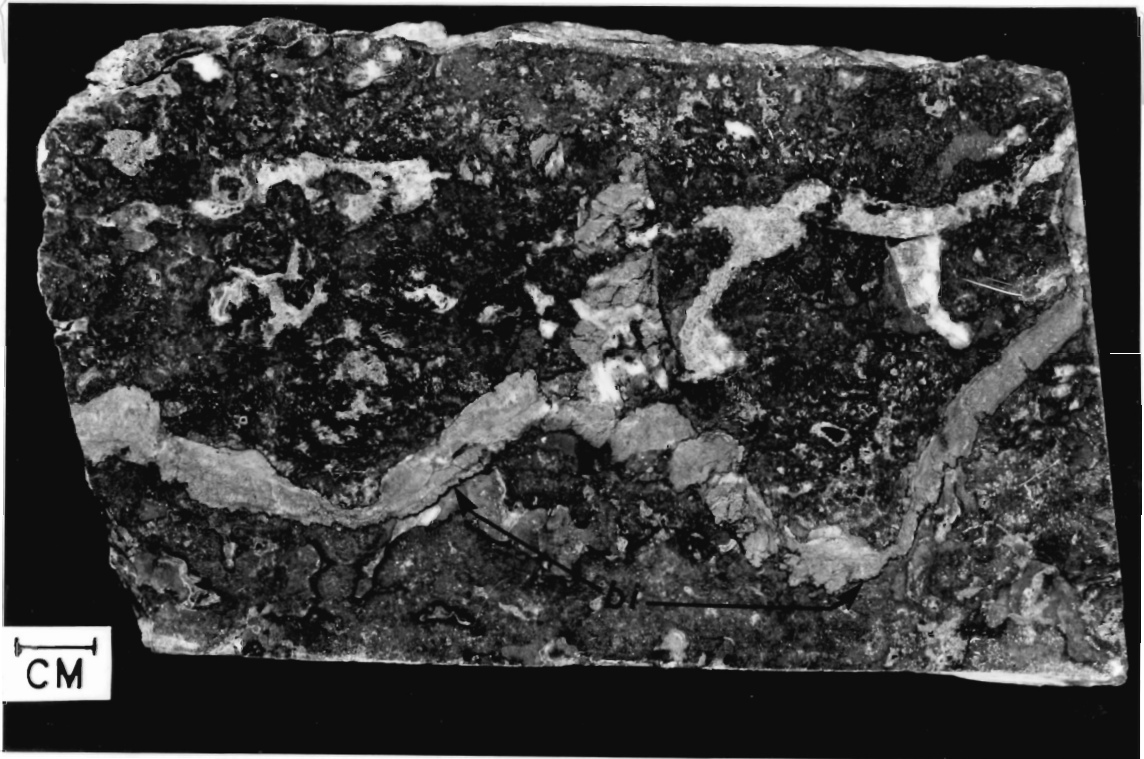
skeletal grains consist of scattered ostracods, disarticulated bivalves and small gastropods. Algal lumps and peloids are the most abundant constituents of the rock. Peloids are generally oval shaped, 0.5 to 1 mm across and constitute an average of 20% of the rock by volume. Siliclastic grains constitute an average of 5% of the rock. Bedding is generally obscure and the rock has a mottled texture. Laminar and irregular fenestrae are common. These fenestrae give the rock a highly porous fabric (Fig. 3.7):

Porosity in this rock type is dominantly fenestral type. This type of porosity is approximately 10% in the rock. Other types include intergranular, intragranular, moldic and fracture porosity. The total porosity in the rock is approximately 15%.

Environment: The presence of abundant peloids, algal peloids, algal lumps and fenestral fabric in this rock suggest deposition in a restricted shallow water environment. The extreme lack of fauna is indicative of a hypersaline environment. Fenestrae structures are better formed in middle intertidal environment due to shrinkage of pustular algal mats during wet and dry periods (Logan et al., 1974). Hatt (1978) indicated that the irregular fenestrae recognized in this rock type are probably pustular algal mats. The present author could not confirm this conclusion because no evidence for an algal mat colony was observed. However, these features are consistent with deposition in a shallow water environment with alternating dry and wet periods. Micritization by boring endolithic algae in the environment can explain the degeneration of the bioclasts present into indeterminate peloids although subsequent dolomitization has also masked

Figure 3.7 Algal fenestral wackestone-packstone. Note the irregular fenestral fabric in the rock. The fenestral pores have been filled by sphalerite and calcite. Sphalerite veinlet on the bottom part of the slab has a rim of bituminous material (bi).

Figure 3.8 Limestone breccia. Note the angular limestone fragments within a matrix of finely crystalline sphalerite and calcite. Some of the fragments have indistinct laminations suggesting an algal origin.



their texture.

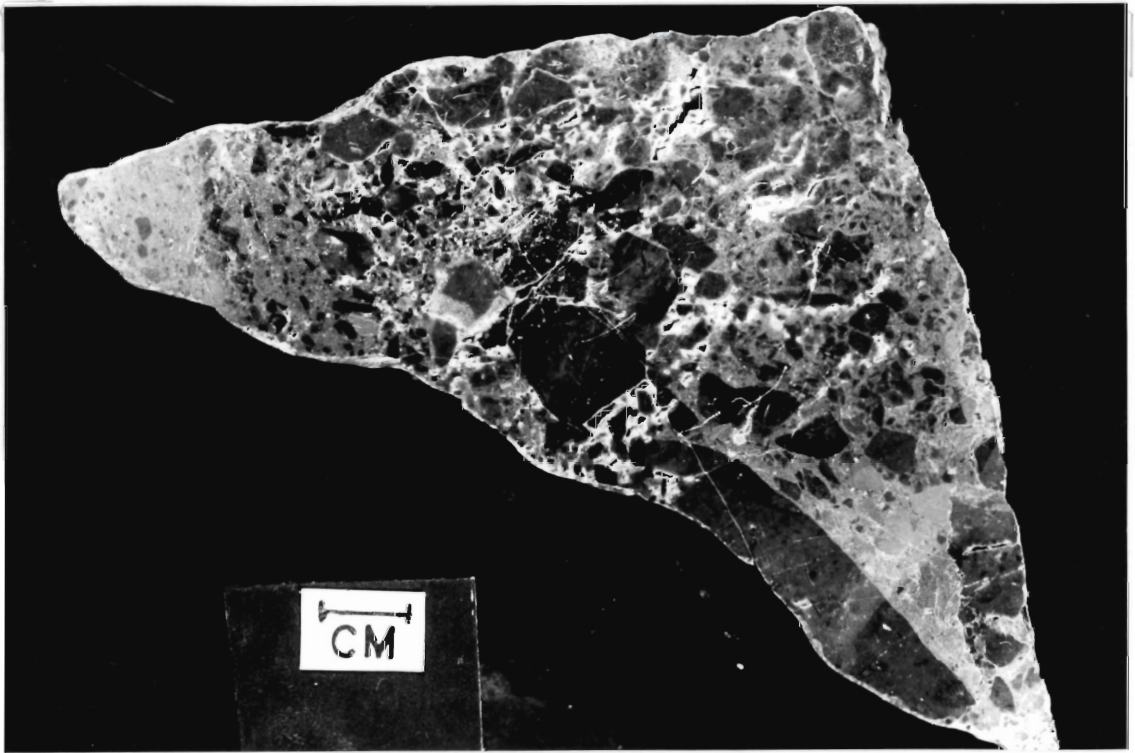
d. Lime Packstone and Breccia

This rock type is mainly restricted to areas adjacent to faults in the carbonate rock and at the evaporite-carbonate contact. It consists of angular fragments of limestone ranging in size from 2 mm to 2.8 centimetres with an average of 5 mm in a matrix of finely crystalline silt to sand size limestone, sphalerite, galena and sparry calcite (Fig. 3.8). The angular fragments represent an average of 30% of the rock by volume. They are frequently laminated and partially replaced by sphalerite and galena. This laminated texture suggests an algal origin for the clasts although the primary textures are almost completely masked by dolomitization and dedolomitization. Unmineralized limestone breccia occur on the footwall of the sulfide veins in few cases. The pore spaces in this unmineralized limestone breccia include vuggy, interparticle and breccia types. These pores are completely filled with sparry calcite in few samples (Fig. 3.9).

Environment: The occurrence of this rock type adjacent to faults, fractures and sulfide veins is indicative of a tectonic origin although the possibility of a solution collapse origin cannot be ruled out. Laminated angular clasts in a matrix of finely crystalline limestone, suggest an original deposition in a quiet shallow hypersaline environment before breccia formation.

Finely crystalline sphalerite and galena form a matrix for some of the angular limestone clasts as observed in drift 104. This suggests that the brecciation of the adjacent carbonate rock occurred before the mineralization. A process involving chemical brecciation was advocated by Saw-

Figure 3.9 Unmineralized limestone breccia probably of solution collapse origin, with good vuggy, interparticle and breccia porosity.



kins (1969) to account for the intimately broken and veined materials in the breccias associated with zinc deposits of the Mascot-Jefferson city. Sawkins (1969) explained that such breccia could be formed by a process involving an often invoked mechanism of solution collapse and chemical brecciation. Although the restricted position of the limestone breccia to faults and sulfide veins suggests a tectonic origin, the present author suggests that this breccia may be of solution collapse origin.

3.4 Discussion

Many authors have described the complex carbonate lithologies and their depositional environment in the Gays River area with widely varied conclusions. MacEachern and Hannon (1974) concluded that the carbonate lithologies can be termed a reefal complex with four physiographic zones: a fore reef, reef crest, reef proper and back reef each distinguished by a unique lithology.

Macleod (1975) suggested that the Gays River carbonates record a subtidal to supratidal condition as a result of a single transgression and regression cycle. He formulated an environment within a tidal bank model accompanied by localized wave resistant structures. Hartling (1977) and Osborne (1977) both agreed with Macleod's postulation that the carbonate lithology they studied in drill hole cores represent deposition in a protected tidal flat environment. Osborne further emphasized that the carbonate lithotypes represent a mudbank with similarities to the Rodrigues Bank, a Holocene mudbank situated in the Florida reef tract. Water depths increase from 1 m on the bank to about 4 m in the surrounding area (Turmel and Swanson 1976).

Hatt (1978) in his study of the depositional environment of a part of the Gays River decline concluded that the carbonate lithologies constitute a

wave resistant organic-framework reef according to the definition of Heckel (1974).

Giles et al. (1979) in their study of the Gays River Formation applied the term organic bank in a regional sense to describe the carbonate build up with recognition of the prevailing association with rocks accumulated by trapping or baffling of sediments by organisms.

Although it is not within the scope of the present thesis to reconstruct the paleodepositional history of the lithofacies in the deposit, the distribution of the varieties of rock types described in the preceding section permit these conclusions.

1. Pre-carbonate basement faults and joints had a strong control on the carbonate deposition. Erosion along these basement structures produced sets of N-S and N-W trending knobs and ridges prior to carbonate deposition.
2. The reentrant areas separating the basement knobs and ridges consist of channel fill conglomerates and grainstones which are commonly separated by bindstone and packstone. The author agrees with Hatt (1978) in the use of the term flank deposits to describe these channel deposits between basement knobs and ridges. At least six different rock types are recognized in this flank deposits compared to four rock types recognized by Hatt (1978).
3. The carbonate rock types on the paleotopographic highs are predominantly bindstones and bafflestones capped by algal fenestral wackestone-packstone. These rock types are locally brecciated in areas adjacent to faults. They represent deposits on the crest of the ridges and adjacent lagoon on the leeward slope of the paleotopographic high (Fig. 3.10).
4. The erratic distribution of rock types and their admixtures is indicative of abrupt changes in environments or shifting environments even

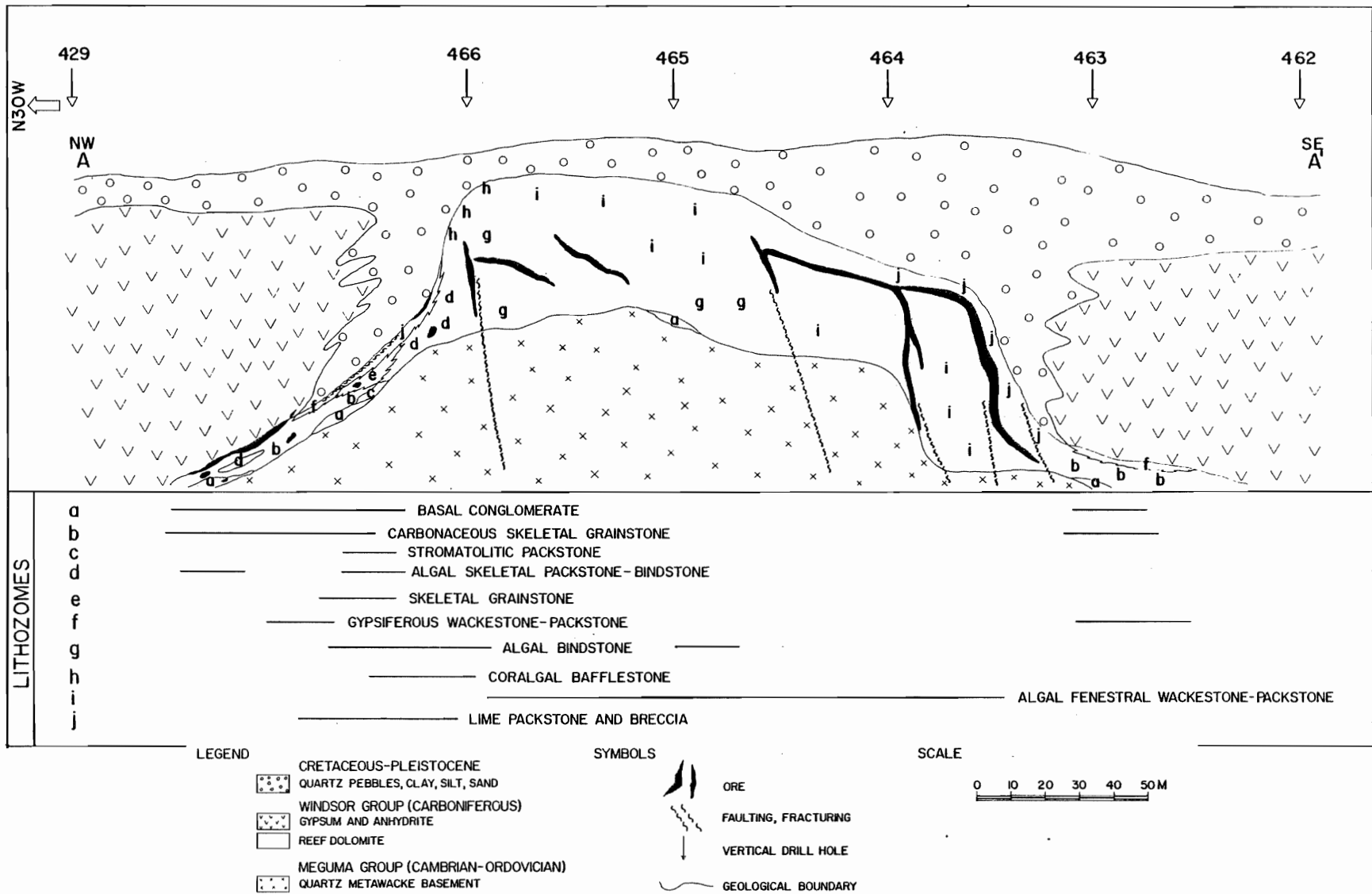


Figure 3.10 Distribution of the Carbonate lithosomes along the cross section AA¹.

* No vertical exaggeration

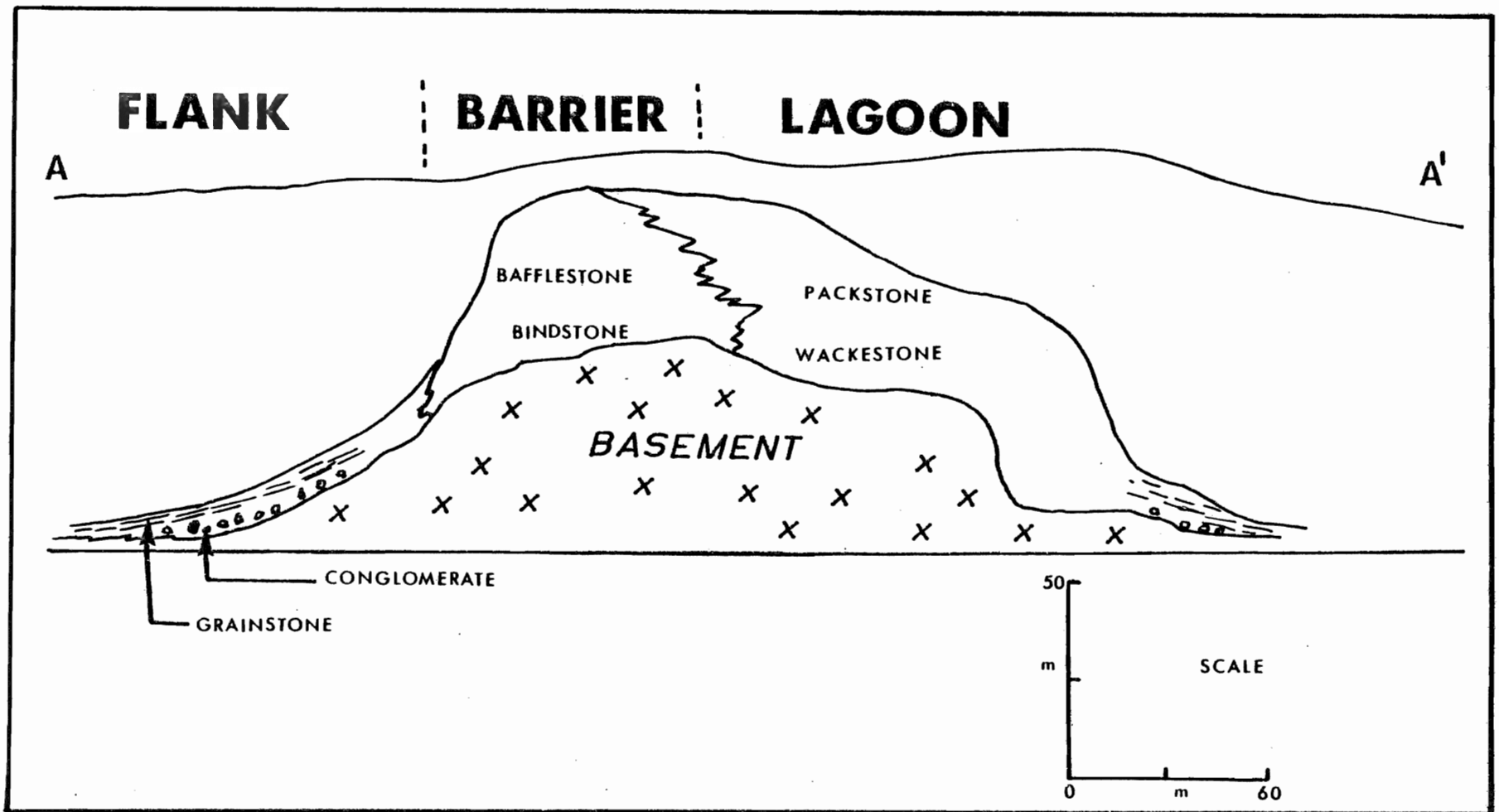


Figure 3.11 Paleoenvironmental reconstruction of the Gays River carbonate reef in section AA¹ interpreted as in Hatt (1978).

on a centimetre scale.

5. Although the rapidly changing lithologies and environments may apply to either a reefal or mudbank model of deposition, a gross lithologic grouping of rock types across the general strike of the carbonate build up support an organic framework reef as described by Hatt (1978). The author agrees with MacEachern and Hannon (1974) and Hatt (1978) hypotheses of a reefal complex.
6. A division of the carbonate build up into a reef flank, reef crest and lagoon environment may explain the gross relationships of fauna distribution across the general strike of the complex.
7. Subsequent tectonic movements and diagenetic alterations participate in the ground preparations for the sulfide mineralization.

CHAPTER 4
DESCRIPTION OF THE STRATIFORM AND VEIN ORES
AND THEIR HOST ROCKS

4.1 General Statement

The economically important lead and zinc mineralization at the Gays River deposit is divisible into 2 major groups: 1) stratiform ores and 2) vein ores. These two groups of mineralization have different forms, texture, distribution and host rock relationships which bear on their genesis.

The stratiform ores are concordant masses of open space fillings of sphalerite and galena (which made up 99.5% of the sulfide minerals) with minor marcasite, fluorite, and calcite contained in a dolomite host. The stratiform ores contain an average grade of 5% combined lead and zinc. This grade increases to approximately 20% combined lead and zinc in the conformable lenses of massive sphalerite and galena along the evaporite/carbonate contact.

The vein ores are discordant fault controlled massive sphalerite and galena bodies that are distributed in a pattern of N-S, NNE and E-W orientations within the carbonate host (Fig. 4.1a). These fissure veins form the highest grade areas of the mine averaging 60% zinc and 10% lead. Massive sphalerite and coarse crystalline galena constitute an average of 90% of the fissure veins by volume. Pyrite, chalcopyrite, calcite, barite and bitumen are minor constituents.

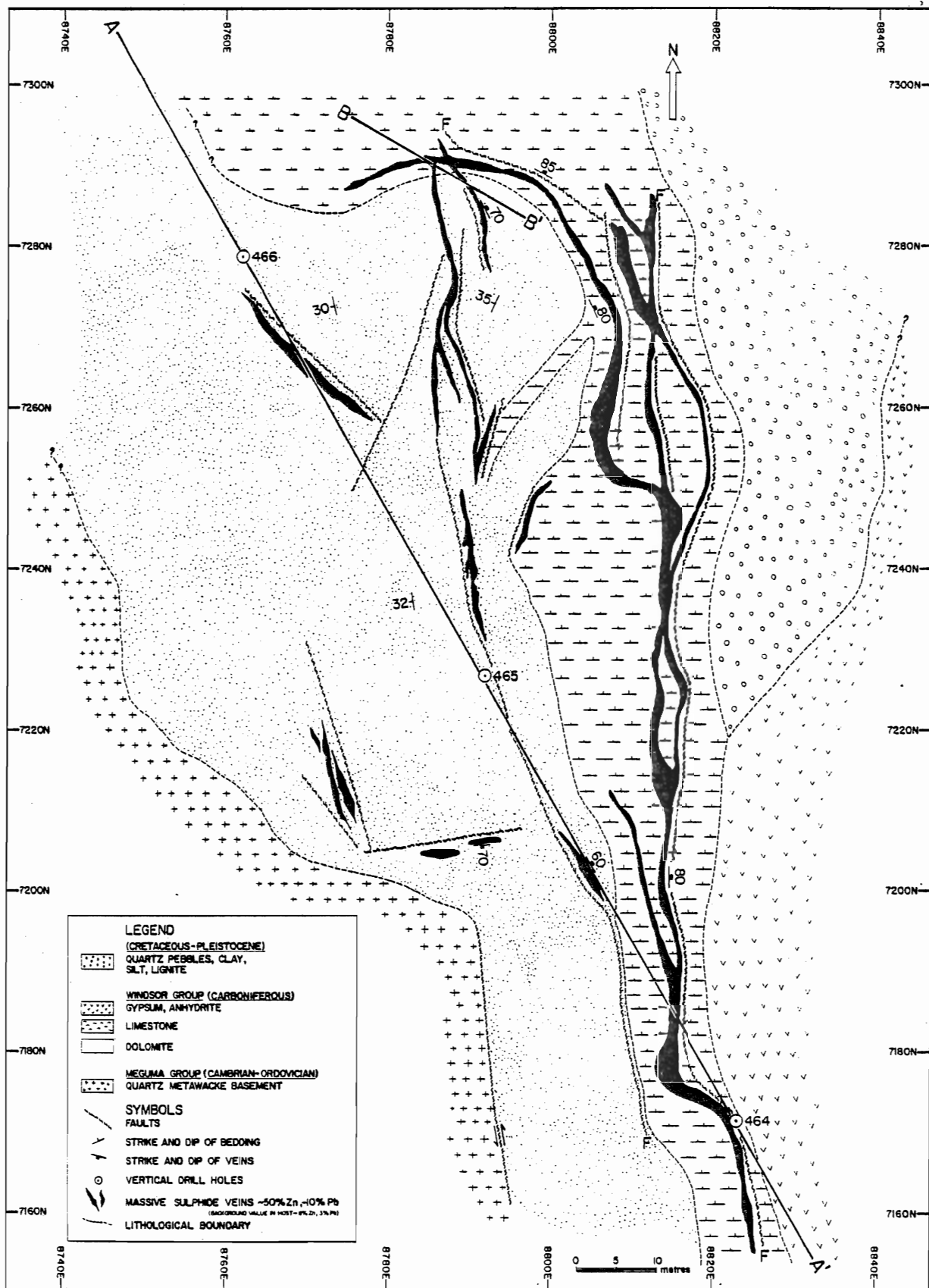


Figure 4.1a Plan of vein ores in the central part of the Gays River mine. Section AA¹ as in Figure 2.4 and BB¹ as in Figure 4.15.

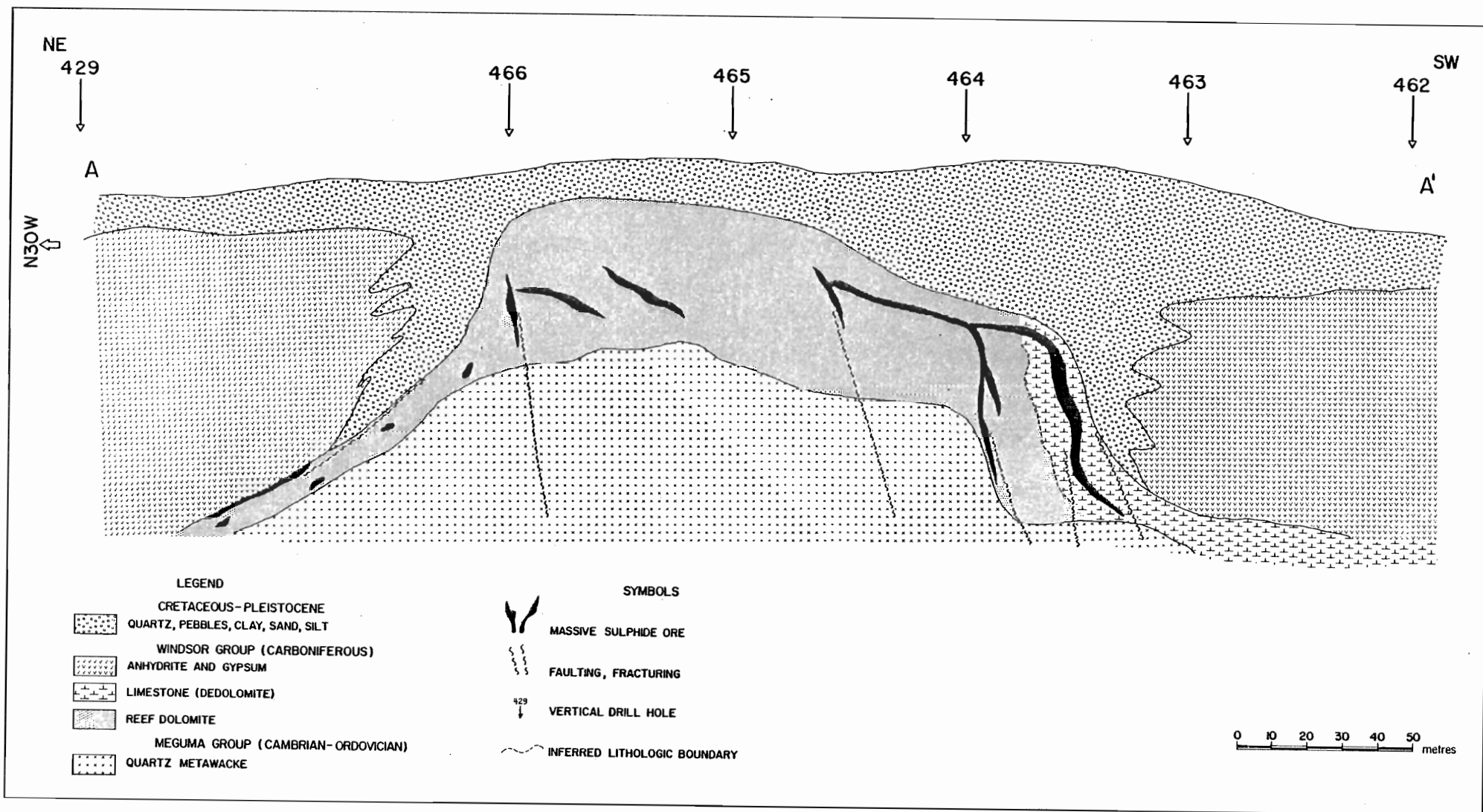


Figure 4.1b CROSS SECTION A-A' THROUGH THE CENTRAL PART OF THE GAYS RIVER MINE. LINE 400E

4.2 Stratiform Ores

Geological Setting

This group of lead-zinc ore constitutes an average of 75% of the mineable ore in the decline areas studied. They are distributed on the flanks of the carbonate build up and also in areas adjacent to mineralized fissure veins where post lithification and diagenetic features are most common. Sphalerite and galena are distributed in pore spaces contained in the carbonate host. In few drill cores, e.g. DDH 506, sulfide minerals occur in the gypsum and anhydrite stratigraphically above the carbonate where they have been concentrated through sets of joints and fracture systems. Such fractures have been healed in the evaporite but are traceable in the carbonate host and the basement rocks (Figs. 4.1a, 4.1b).

Pores within the carbonate rock types in the erosional channels separating several basement knobs and ridges are good sites for the distribution of the sulfide minerals. Areas with good porosity and permeability are consistently highly mineralized. Hence the grade of stratiform mineralization is directly proportional to the porosity and permeability of the carbonate host except in areas like the 119 drift where stratiform sulfide lenses occur at the evaporite/carbonate contact.

a. Form

The form of the stratiform mineralization is primarily related to the carbonate lithology. The mineralization is commonly characterized by several post lithification and diagenetic features. Imprints of these features dictate the form of mineralization and also reflect the continuous diagenetic and tectonic alterations which the carbonates went through.

From the diversities of the carbonate fabric, the forms of stratiform

mineralization include;

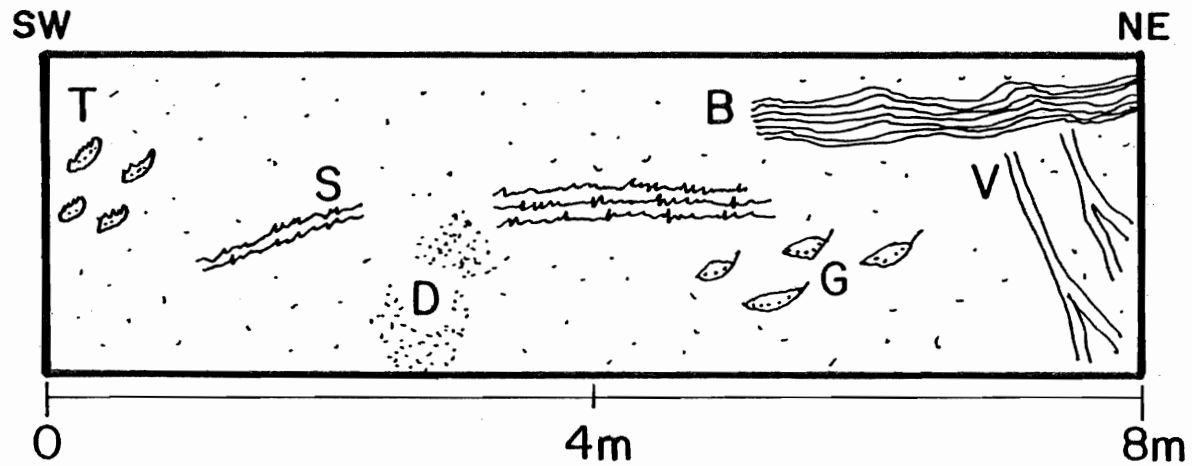
- i) concordant rhythmically laminated sulfide mineralization
- ii) mineralized stylolites
- iii) geopetal structures and stromatactis
- iv) disseminations
- v) sulfide lenses.

These textural forms are maximally developed in the carbonate paleo-erosional channels that are located in the flank areas of the carbonate build up. An illustration of these features is observed on the drift wall 101C in the flank area (Fig. 4.2).

i. Laminated Sulfide Mineralization

Finely crystalline laminated microdolomite in the flank areas of the carbonate build up are commonly filled with sphalerite and galena along single layers (Fig. 4.3). Each layer ranges from 0.8 mm to 4 mm in thickness and is commonly bounded by stylolitized carbonaceous material. The layers are commonly interconnected by minute fine fractures that are filled with similar sulfide minerals. Linear vugs and fenestral cavities averaging 2.5 mm across are common along the layers. The consistent parallel fabric of the laminated rock and the presence of carbonaceous constituent indicate a stromatolitic origin for the rock. Each layer can be described as a stromatolite bedding. Each stromatolite bed consists of sphalerite and galena at the centre within intra and interpore spaces of the light brown dolomite grains. The dolomite grains have been replaced locally by fine grained sphalerite. Marginal to each stromatolite bed are dark brownish grains of dedolomite. This indicates the conversion of dolomite grains to calcite at the bed margins.

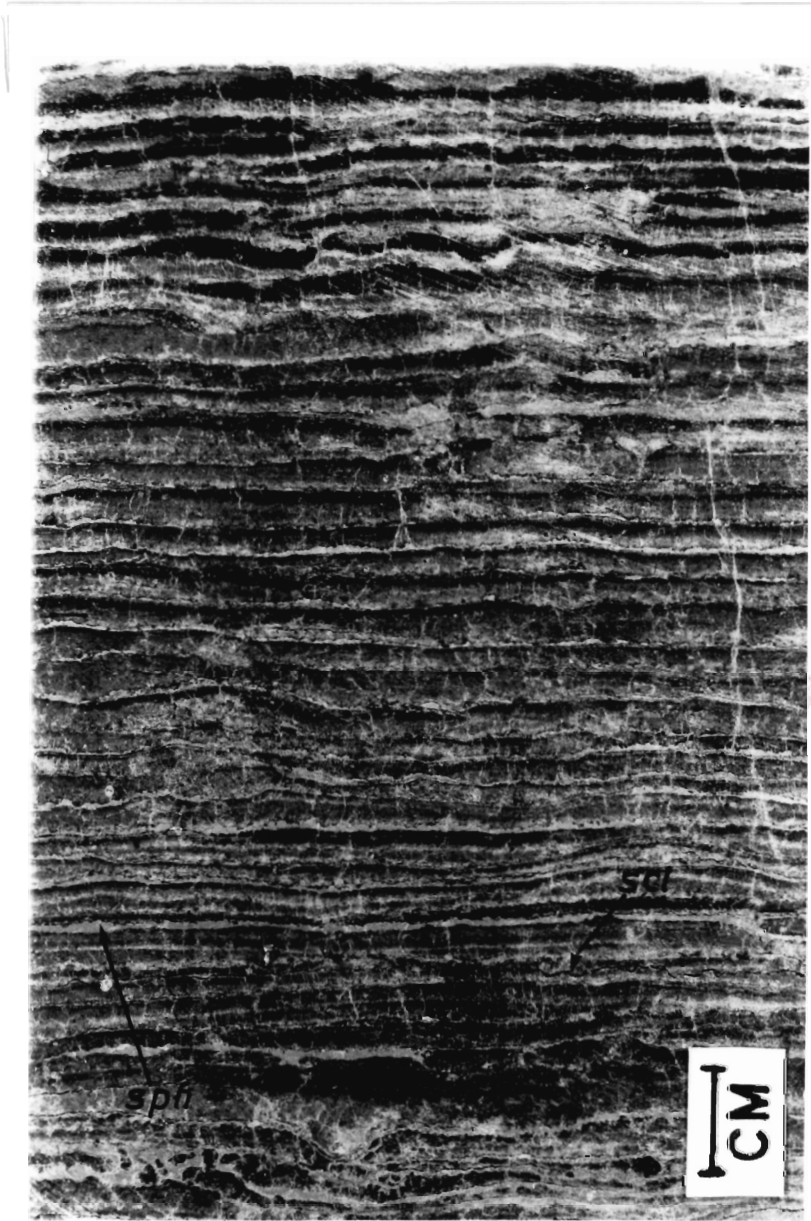
Although the distribution of sphalerite and galena within the stroma-



- B = Banded sulphide mineralization
- S = Mineralization in stylolites (chiefly Galena)
- V = Massive sulphide veinlets along fractures
- G = Geopetal structures (Sphalerite base - Calcite top)
- D = Disseminated sulphides (filling Porosity)
- T = Void filling *Stromatolites*

Figure 4.2 Styles of stratiform mineralization.
(drift 101c).

Figure 4.3 Laminated sulfide mineralization. Note the prevalence of sphalerite (sph) along each layer. Each layer is bounded by stylolitized carbonaceous laminae (scl).



tolite bed may be indicative of a rhythmic precipitation phenomenon through bacteria activity, (Helgeson 1964; Bubela et al., 1969), the presence of filled linear vugs and fenestrae structures along the stromatolite bedding favours an open space filling phenomenon for sphalerite and galena precipitation. Metal carrying fluids can flow with considerable ease along the stromatolitic bedding planes and their associated pore spaces. Precipitation of the sulfide minerals in the pores and as replacements of the host can therefore occur along the bedding planes (Riedel, 1980).

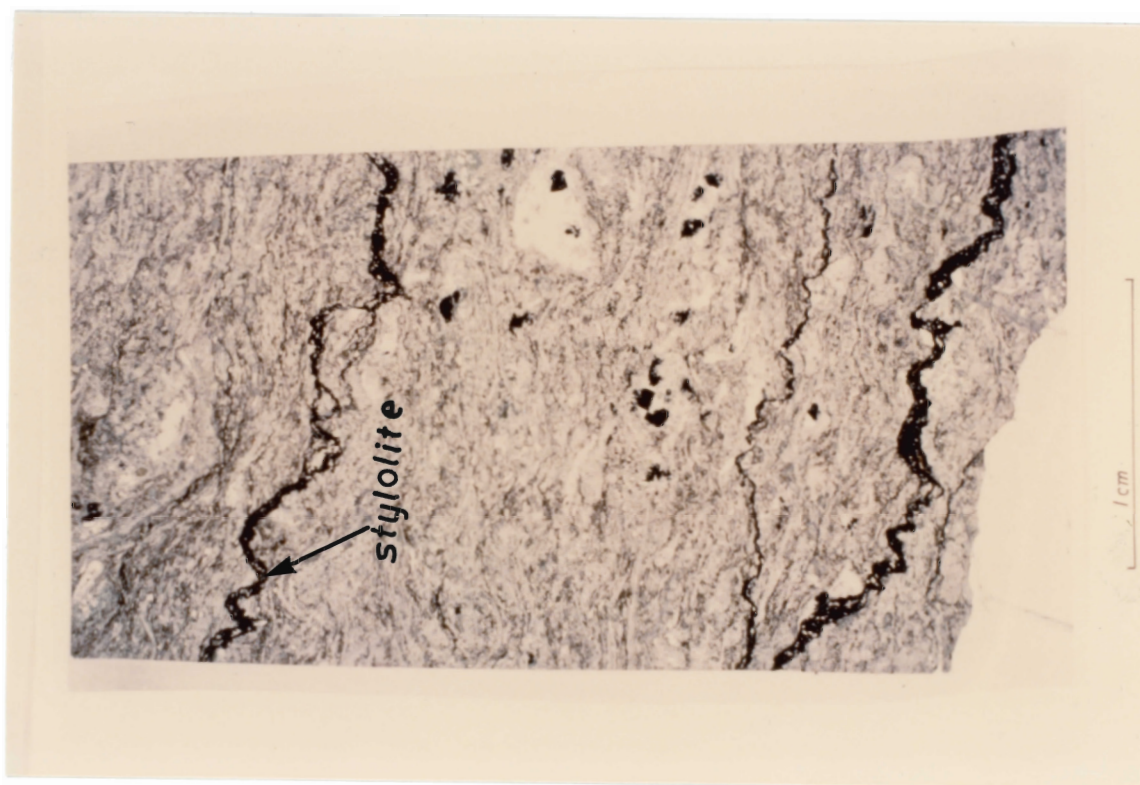
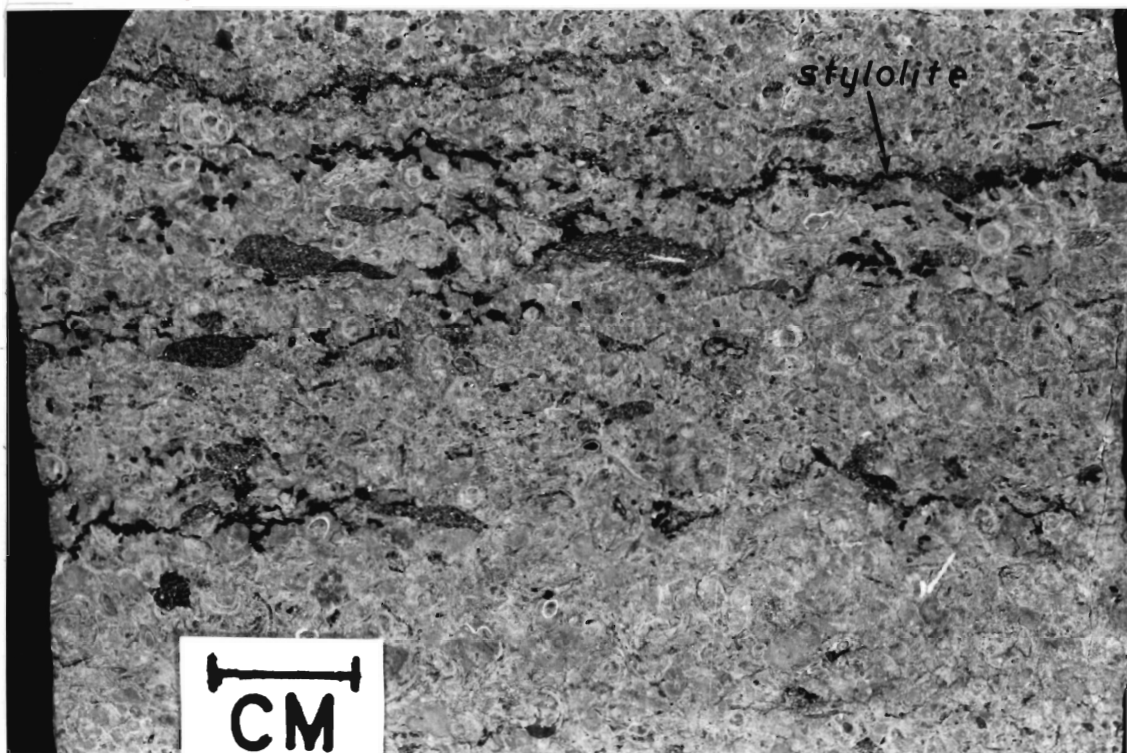
ii. Mineralized Stylolites

Stylolites in the carbonate host range from microns to millimeter thicknesses with an average thickness of 2.5 millimetres. They have low amplitudes and are in conformable orientations with the bedding planes as in cut samples from drift 101C (Fig. 4.4). The stylolites occur locally as disoriented structures at approximately 70° to bedding. They generally contain the insoluble residue that is distributed in the carbonate host. Significant proportions of sphalerite and galena are generally contained in the stylolites. Quartz, sandy dolomite, gypsum and bitumen are the chief constituents that are commonly intergrown with the sulfide minerals in the stylolites. Quartz content may be as much as 20% whereas sphalerite and galena comprise less than 10%. Bituminous materials commonly represent the remaining proportion and may constitute up to 80% of the stylolites.

Although the stylolites are good sites for sulfide concentration, they are only mineralized in areas adjacent to high grade stratiform mineralization. In other instances, stylolites are completely barren of sulfide minerals and only contain bituminous substance (Fig. 4.5).

Figure 4.4 Mineralized stylolite, concordant to carbonate bedding.

Figure 4.5 Unmineralized stylolite. These near-horizontal stylolites consist of bituminous substance and detrital quartz.



Stylolites represent surfaces between two rock masses where dissolution of the rock has taken place as a result of pressure solution phenomenon (Bathurst 1975). Bathurst illustrates that the controlling factor is the orientation of the axis of linear stress which is presumably vertical as a consequence of the overburden. Hence the concentration of the sulfide minerals in stylolites could be due to a pressure solution phenomenon accompanying a compressive deformation event or compaction of the carbonate host after the sulfide mineralization. The present author suggests that loading after sulfide mineralization could explain the re-concentration of the sulfide minerals in stylolites.

iii. Geopetal Structures and Stromatactis

This is one of the most common forms of stratiform mineralization in highly porous carbonate rocks where skeletal grains are present. Geopetal fabric is defined by the molds of gastropods and brachiopods that have been filled completely or incompletely by sulfide and the associated gangue. The geopetal molds can be as large as 3 centimetres. They are approximately 5 mm across. The cavities are locally filled with sphalerite at the base and the remaining pore space is frequently sealed by calcite. Walls of geopetal structures are commonly lined with sphalerite. In general, pale yellow microcrystalline sphalerite lines the bottom of a geopetal structure and galena overgrows the sphalerite with the remaining pore space being filled by sparry calcite. This relationship suggests an earlier precipitation of sphalerite that was succeeded by galena and later calcite. An up-direction is easily recognized where the geopetal structures are in situ.

The geopetal structures are commonly connected by small sulfide bearing veinlets and therefore have acted as "sinks" for sulfide precipitation. Stromatactis in the carbonate rock occurs in the form of irregular cavities. They commonly have digitate tops and flat bottoms. These are commonly mineralized in areas adjacent to sulfide bearing veinlets and mineralized stylolites (Fig. 4.6).

iv. Disseminated Sulfides

Finely crystalline sphalerite and galena averaging 100 μm in size form a part of the matrix for the carbonate rock. This consists of equigranular and xenomorphic grains of sphalerite, galena, marcasite and pyrite. They occur generally as pore in-fillings and minor replacements of host carbonate.

v. Sulfide Lenses

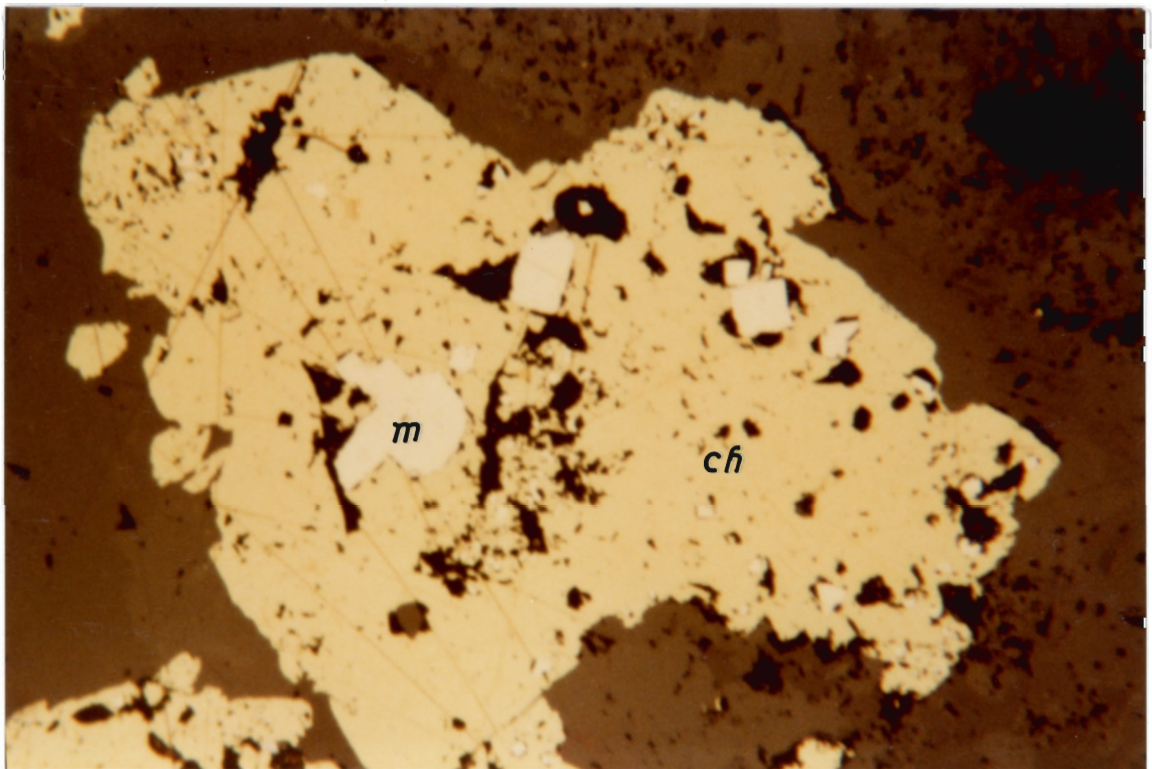
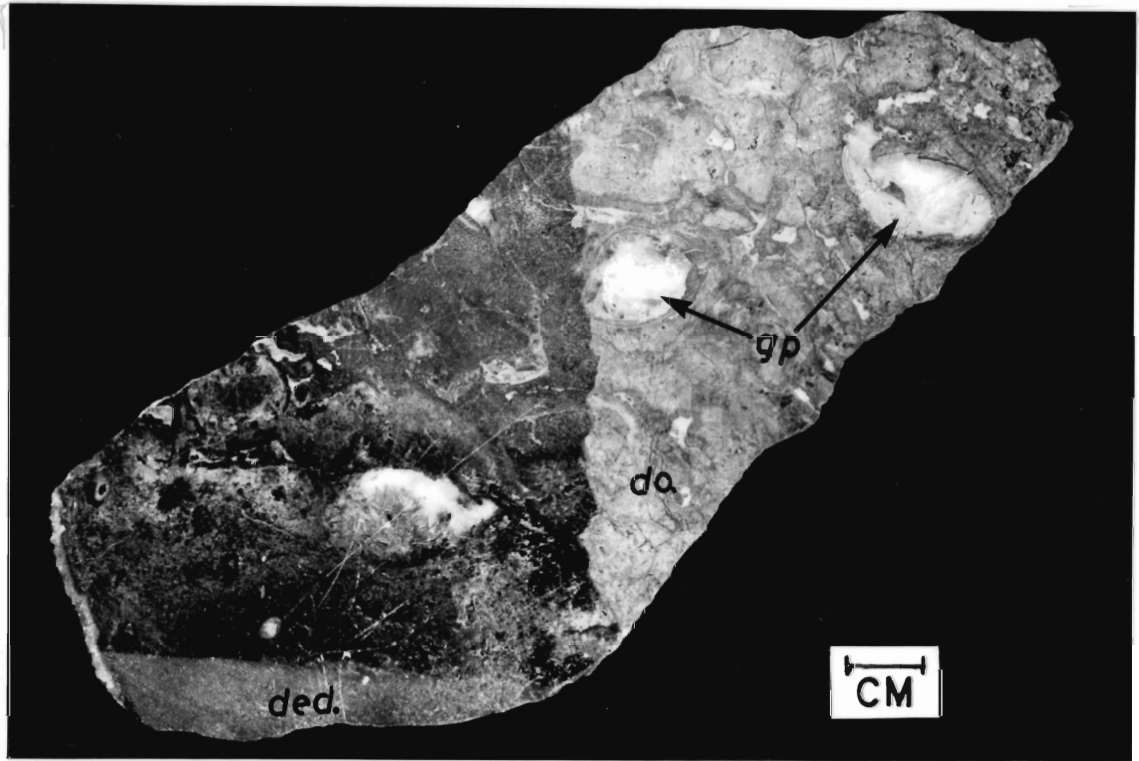
Lenses of massive sphalerite and galena 7 cm to 75 cm thick occur locally at the carbonate-evaporite contact. These lenses are known over an average strike length of 6 metres. They commonly consist of relics of fine-grained bituminous substance streaked out in the finely crystalline sulfide mineral matrix. The presence of limestone relics and bituminous substance in the matrix of the sulfide lenses suggest that they are of replacement origin.

b. Mineralogy

Sphalerite and galena are the main constituents contained in the pore spaces and as host replacements within the concordant stratiform mineralization. Other associated minor sulfide minerals include marcasite, pyrite and chalcopyrite. The gangue minerals include calcite, fluorite and gypsum.

Figure 4.6 Geopetal structure (gp) filled with sphalerite at the base and along the rims and calcite at the centre. Note that the half portion of this slab is dolomite (do) and the second half is limestone (dedolomite). Both portions consist of sphalerite filled geopetal structures.

Figure 4.7 Subhedral grains of marcasite (m) in chalcopyrite (ch). Note the passive replacement of marcasite by chalcopyrite.



50um

Sphalerite in the stratiform ores is pale yellow and finely crystalline with an average size of 50 μm . The sphalerite is locally associated with inclusions of the carbonate host. It is commonly intergrown with equigranular crystals of galena. Microscopic examination of the sulfide minerals reveals that sphalerite and galena have scalloped contacts with galena overgrowths on sphalerite. This agrees with the common occurrence of sphalerite at the bottom of geopetal structures overgrown by galena. Both minerals are commonly intergrown and it is difficult to establish a contact or textural equilibrium relationship. Isolated grains of sphalerite are commonly present within galena. This suggests that galena precipitation post dated sphalerite. Indeed the presence of sphalerite at the base of most of the pore spaces suggests that most of the original primary porosity in the carbonate host were filled with sphalerite before the precipitation of galena. The pale yellow sphalerite is very low in iron content and iron only constitutes an average of 1.0 mole percent FeS .

Marcasite and pyrite occur as equigranular grains in the stratiform ores. Grain sizes range from 50 μm to 1.2 mm across. They are commonly found within intragranular and intergranular pores in the carbonate host. Massive streaks of chalcopyrite averaging 1.5 centimeters thick extends for approximately 7 centimetres. These contain inclusions of marcasite, pyrite and relics of calcite. Euhedral to subhedral grains of marcasite and pyrite with no obvious corrosion are completely enclosed in the chalcopyrite streaks (Fig. 4.7). These suggest that chalcopyrite succeeded iron sulfide formation.

Calcite is the dominant gangue mineral associated with the stratiform ores. It occurs as open-space fillings in two main forms: a) rhombohedral well twinned crystals with good optical continuity and basal pinacoidal 001 cleavages and b) as dog tooth scalenohedrons encrusting on void spaces and

on pebbles of host rock (Fig. 4.8). Calcite is frequently associated with fluorite. The fluorite is of 3 colour varieties; purple, white and green. They are frequently intergrown with calcite. In few instances, where carbonate hosts are very thin and have been dedolomitized, gypsum crystals as selenite occupy the carbonate pore spaces and fracture-related cavities. Such association suggests that the dedolomitization process is directly related to anhydrite hydration and dissolution. The selenite is therefore a crystallite from a supersaturated solution of the evaporite.

c. Porosity

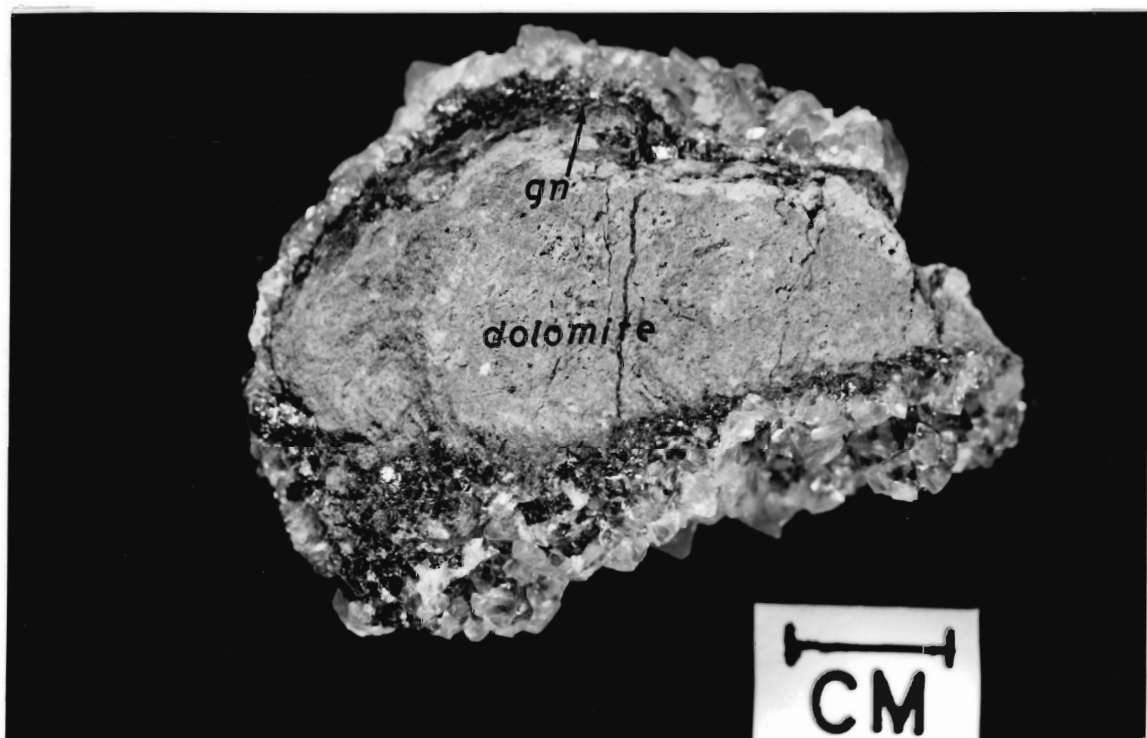
Porosity in the carbonate host rocks for the stratiform mineralization include a fabric selective and non fabric selective types. Pore spaces occupied by the sulfide minerals and gangue include interparticle, intraparticle, sheltered, moldic, and fenestral, which are dominantly fabric-selective, whereas growth framework and fracture porosities represent the non fabric selective types.

d. Host Rock Relationships

The stratiform ore distribution has no obvious relationship to the type of carbonate lithology or any particular strata. The predominant control on the mineralization is the availability of pore space leading to permeability of the rock and the proximity to solution pathways. The proximity of high grade sphalerite and galena in-fillings to the stratiform massive sulfide lenses at the contact with the evaporite suggest a genetic relationship between these forms of mineralization.

Ghost relics of the carbonate host in the stratiform ore lenses suggest at least a replacive mechanism for the massive sulfide lenses. It

Figure 4.8 Scalenohedral calcite overgrowths on coarse crystalline galena (gn). Note that the galena occur along the rims of the centrally located dolomite pebble.



is interesting to note that pore spaces in the carbonate host adjacent to these sulfide lenses are frequently mineralized with similar sulfide minerals.

4.3 Vein Ores

Geological Setting

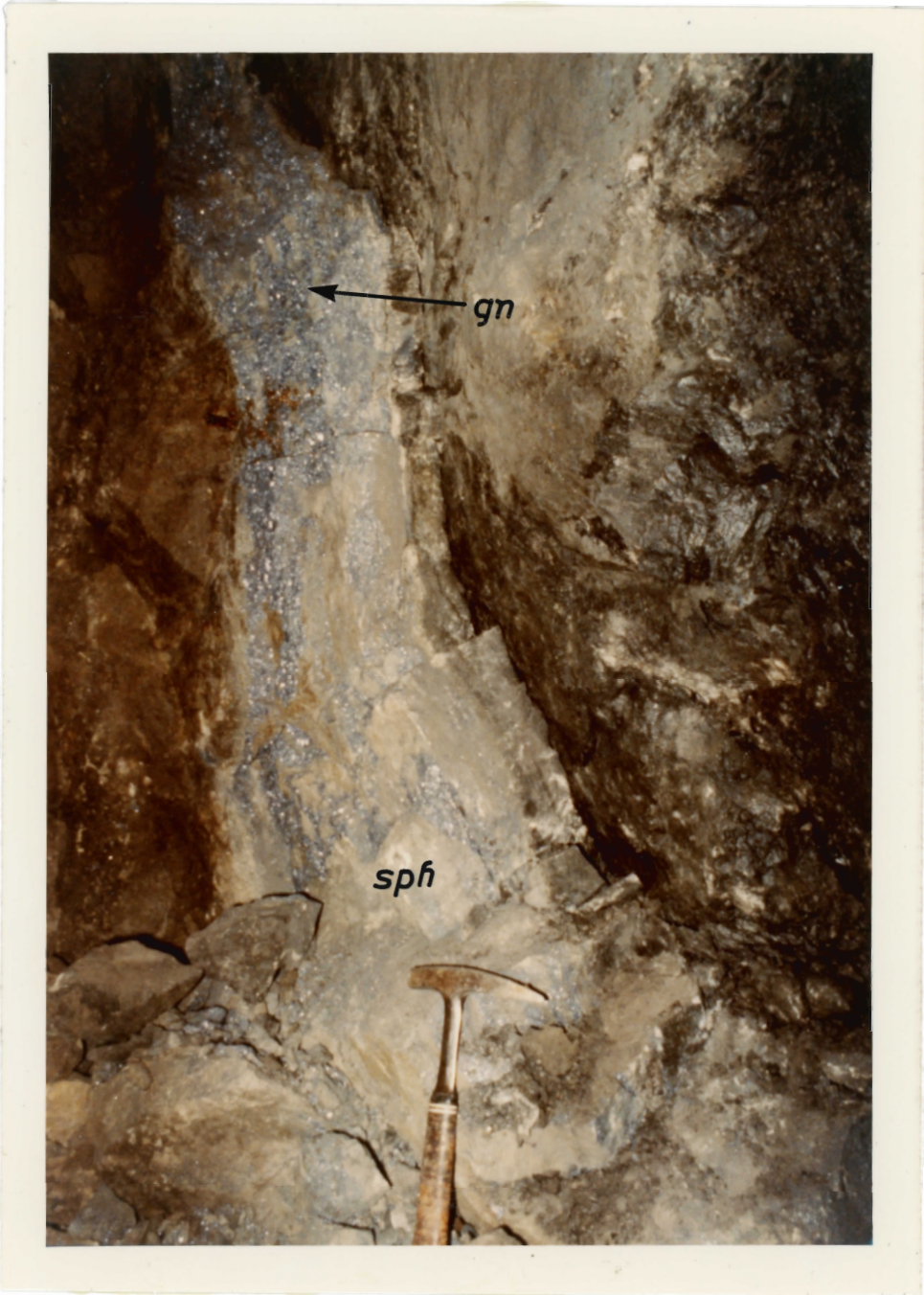
This group of lead-zinc ores constitute an approximated average of 25% of the mineable ore in the decline area of the Gays River deposit. They represent the highest grade areas in the mine with assay grades averaging 60% zinc and 10% lead (Fig. 4.9).

The massive sulfide veins are localized within a pattern of N-S, NNE and E-W faults in the carbonate host. They are enclosed in fault planes which commonly extend downward into the basement. In the 4490 raise, the veins are located at the intersections of a N-S and E-W trending faults. The veins are generally discordant, dipping between 60° to 80° to the east and range in thickness from 5 cm to 4 metres with an average thickness of 2.5 metres. Some of the vein systems are known over an approximate strike length of 150 metres. Vein offshoots are commonly 5 to 50 cm thick and these frequently thin out along the strike. Fine splays 1 to 2 centimetres thick commonly terminate the vein offshoots. The offshoots and splays are traceable at least to a depth of 5 metres below the basement-carbonate unconformity. This is common along the basement extensions of the faults and complementary fractures.

a. Mineralogy

The massive sulfide veins consist of sphalerite, galena, pyrite, chalcopyrite, calcite, barite and bitumen. Sphalerite is the most abundant sulfide mineral and this constitutes an average of 70% of the vein by

Figure 4.9 Fault bounded, vertically dipping massive sulfide vein in the 104 drift, Gays River mine. Vein constituents are chiefly massive sphalerite (sph) and coarse crystalline galena (gn).



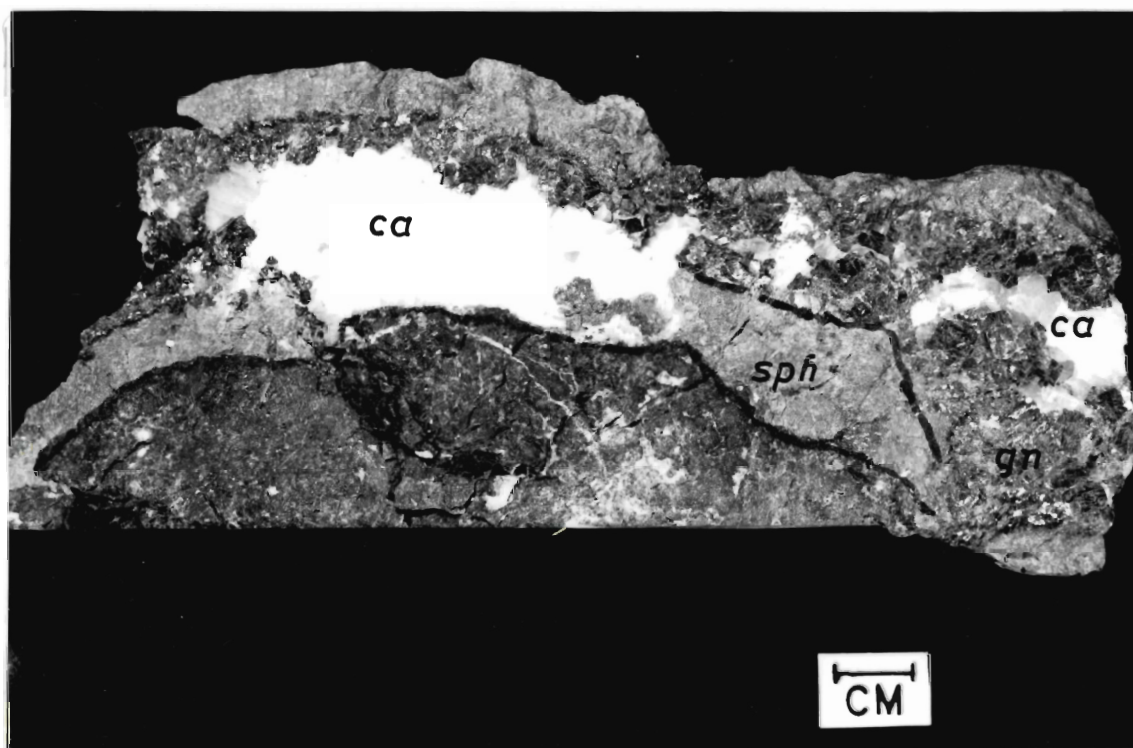
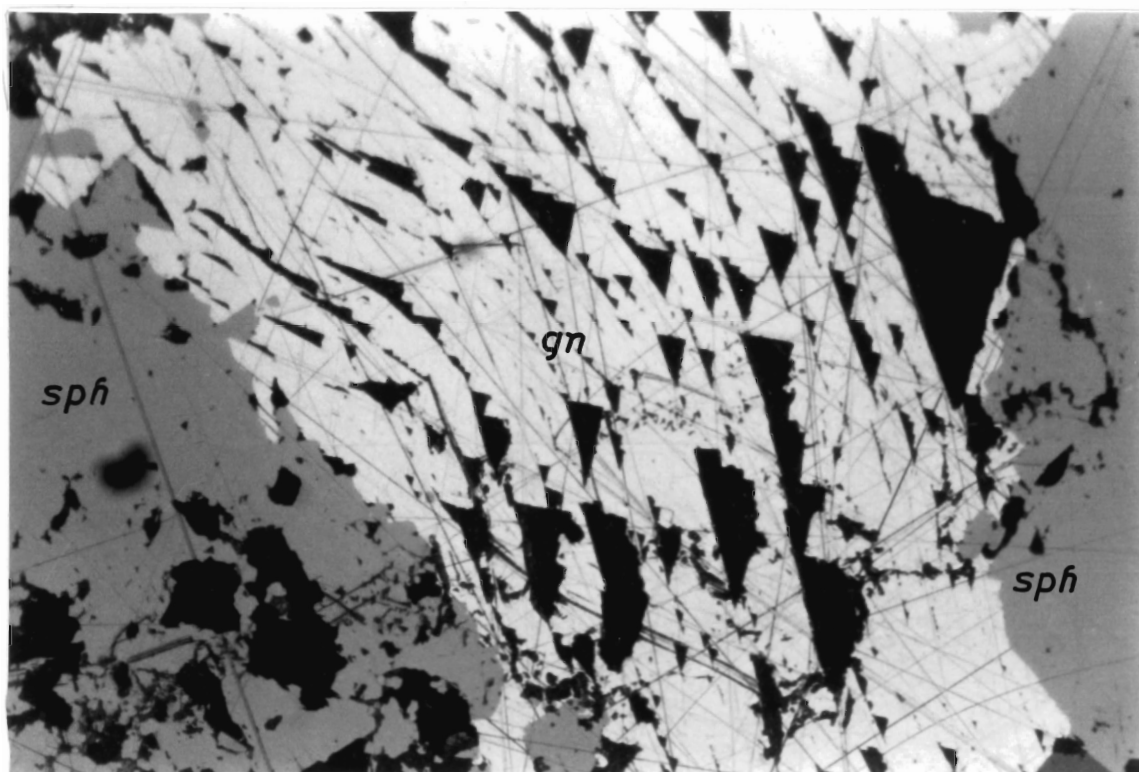
volume. Galena represents 2 to 10% and pyrite, chalcopyrite, calcite, barite and bitumen are minor accessories.

Sphalerite in the veins is a massive pale yellow to reddish brown variety. The massive sphalerite consists of finely crystalline aggregates and also euhedral to subhedral crystal forms. Subhedral grains range in size between 20-60 μm across. Etching of the sphalerite with permanganate-sulphuric acid reveals polysynthetic twins and zoned textures. The polysynthetic twinning in sphalerite may be due to shearing forces caused by post-ore tectonic deformation or have resulted from the interference of equigranular grains during growth. The polysynthetic twinning is commonly disoriented and this probably reflects the lack of preferred orientation of the sphalerite during growth as explained by Ramdohr (1980). Growth zoning in the sphalerite suggests that equilibrium was not attained during precipitation. Etching reveals the recrystallization of sphalerite into fine microcrystalline grains at the grain boundary positions. The sphalerite grains are commonly intergrown with galena, pyrite, chalcopyrite, calcite and barite.

Galena occurs in two textural varieties: 1) as finely crystalline irregular masses averaging 50 μm in diameter and 2) as coarse crystalline idiomorphic cubes ranging between 0.25 to 5 millimetres across. Both varieties are commonly intergrown with finely crystalline sphalerite. The coarsely crystalline variety commonly occurs along the boundaries of the veins and wall rock (Fig. 4.9). Finely crystalline galena is completely devoid of the characteristic triangular cleavage pits whereas the coarsely crystalline variety has well developed triangular cleavage pits. These cleavage planes are consistently bent in many samples (Fig. 4.10). Such bending

Figure 4.10 Coarse crystalline galena (gn) traversing massive sphalerite (sph). Note the bent triangular cleavage pits in the galena crystal.

Figure 4.11 Massive sphalerite (sph) and galena (gn) encrustations in a veinlet. Note the calcite (ca) intergrowths.



illustrates slipping along a preferred plane as a consequence of translation. Translation gliding along the widest interplanar spacing in the galena lattice can result from shearing after crystallization. The widely spaced 001 plane of galena renders it as the most preferred plane for movement (Ramdohr, 1980).

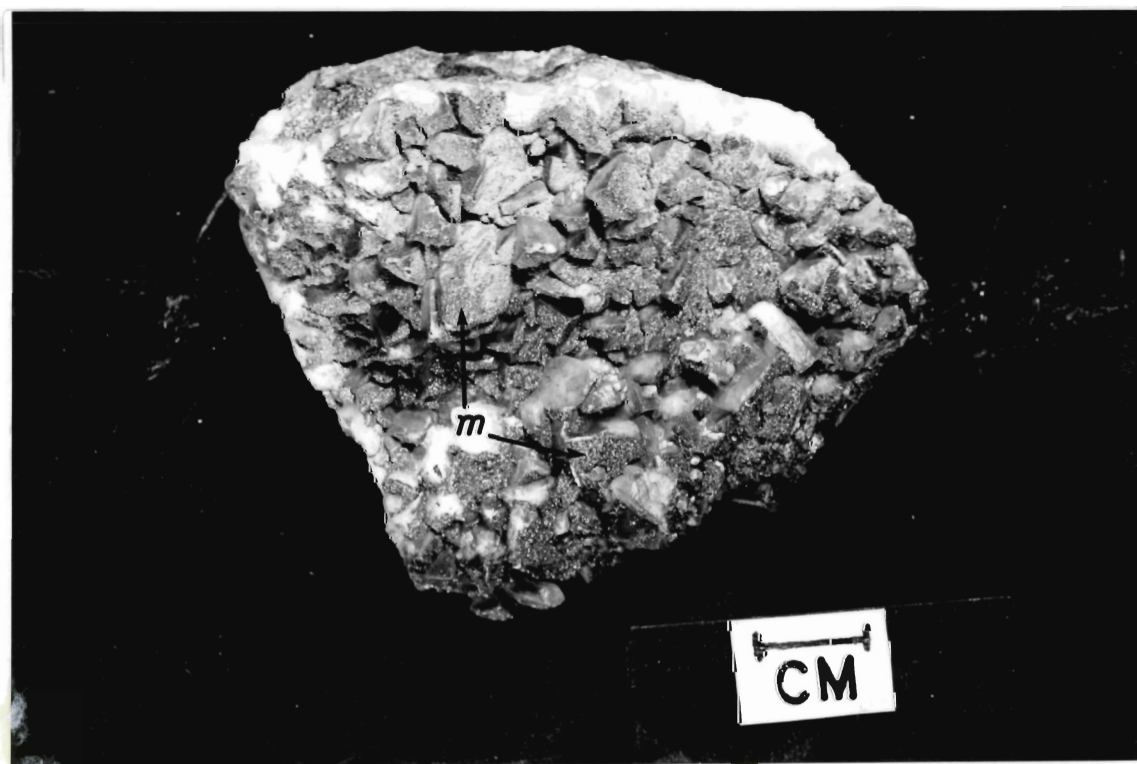
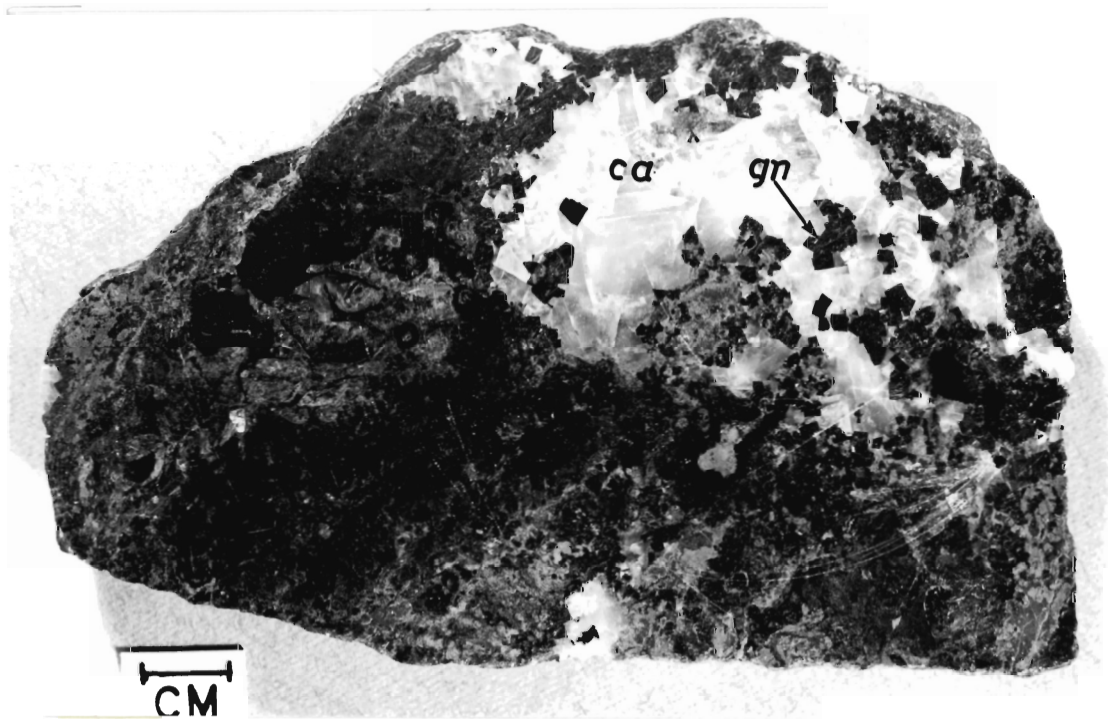
Pyrite, marcasite and chalcopyrite represent minor constituent approximating up to 1% of the veins by volume in some areas. Pyrite and marcasite are commonly found as irregular aggregates and as blebs in a matrix of sphalerite. Separate euhedral to subhedral grains of marcasite averaging 30 μm across occur as inclusions within chalcopyrite crystals in few samples. Chalcopyrite commonly contain inclusions of sphalerite, galena, marcasite, and carbonate.

Calcite is the most abundant gangue mineral in the vein systems. At least 2 forms of calcite can be distinguished. These include 1) whitish to pinkish rhombohedral forms and, 2) simple amber coloured and transparent to milky complex scalenohedrons. The rhombohedral forms of calcite are the most abundant form within the veins and in the adjacent wall rock. They are generally euhedral with sizes averaging 3 centimetres in long dimension.

This rhombohedral form occurs together with sphalerite and galena as crustifications (Fig. 4.11). In many samples veinlets averaging 5 centimeters across are filled with sphalerite and galena on the walls and rhombohedral calcite occupies the center. This suggests that the rhombohedral forms of calcite post date sulfide mineralization. In other sites, coarse crystalline galena, occupies the center of the rhombohedral calcite suggesting an intergrowth phenomenon (Fig. 4.12).

Figure 4.12 Crystals of coarse crystalline galena (gn) within vein calcite.

Figure 4.13 Finely crystalline marcasite (m) on scalenohedral calcite.



The simple amber coloured scalenohedra occur generally as overgrowths in the vugs within the veins. This form is generally translucent and the crystals are of varying sizes averaging 1 mm to centimetres across.

The transparent complex scalenohedra form is locally associated with the amber coloured types. They are commonly found in areas adjacent to faults, and also as coatings on joint planes. These complex scalenohedra have tiny "pin head" shapes and an average diameter of 5 millimetres. They sometimes occur as overgrowths in fault related cavities. In few samples, scalenohedra calcite are coated with finely crystalline marcasite (Fig. 4.13).

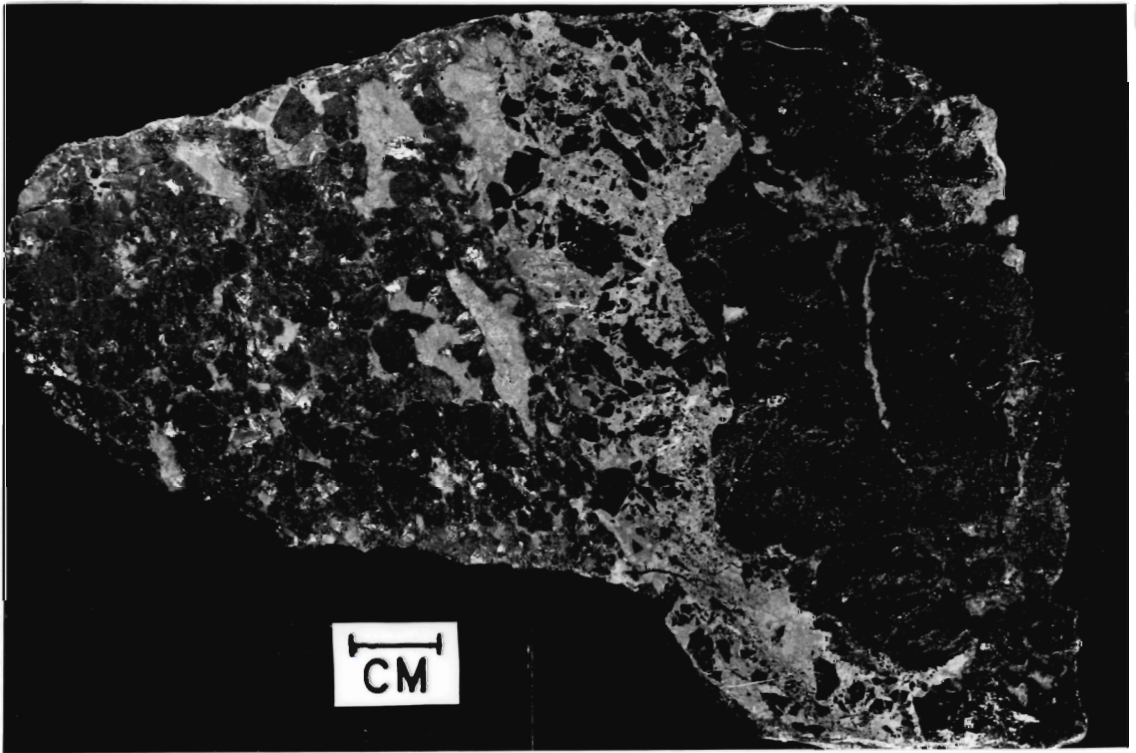
Barite in the veins occurs in 2 forms: 1) as irregular, dendritic or spindle shaped grains averaging 50 μm in diameter within the sphalerite matrix and 2) as bladed and platy crystal intergrowths with calcite. The platy crystals average 1 mm across and are commonly associated with scalenohedra calcite. As evidenced by microprobe analyses, barite is strontium rich and strontium concentrations average 4.2 weight percent.

Bitumen occurs as streaks or lenses in the sphalerite matrix. This indicates the presence of organic carbon during the precipitation of the sulfide minerals and suggests that hydrocarbons might have played a significant role in the precipitation of the sulfide minerals.

b. Host Rock Relationships

The vein systems commonly have sharp well defined contact with the dolomite wall rock. In many samples, thin veinlets averaging 2 cm thick are rimmed by bitumen at the contact with the wall rock (Fig. 3.7). Localized brecciation at the vein margins is common (Fig. 4.14). This frequently extends for at least 10 centimetres in the adjacent carbonate. In few

Figure 4.14 Brecciated limestone (dedolomite) adjacent to a sulfide vein. Note the intergrowths of sphalerite (light grey) within dark grey galena. Angular fragments of limestone (black) occur within sphalerite.



instances, an intense zone of brecciation on the vein footwall extends for approximately 3 metres. The footwall is completely dedolomitized in these brecciated areas (Fig. 4.15). The hanging wall to the veins have significant proportions of sphalerite and galena in these instances. The lack of significant mineralization in the footwall suggests that the dedolomitization of the footwall is probably not related to the mineralization event, but post-dates it.

4.4 Marcasite and Pyrite Not Associated with Ore Minerals

Apart from the minor grains of marcasite and pyrite occurring as inclusions within the stratiform and vein ores, these two sulfide minerals occur with no obvious association with the ore minerals in few instances. Two textural forms of marcasite are present: a) idiomorphic crystals averaging 300 μm across b) xenomorphic cryptocrystalline forms averaging 100 μm across.

The idiomorphic crystal forms are interstratified on the bedding planes of the dolomite host. This type shows no evidence of corrosion and they commonly occur as isolated grains in the dolomite matrix. The fine-grained xenomorphic marcasite occur as coatings on fault gouge, in fault related cavities and as overgrowths on vuggy calcite. They are commonly associated with fine grained pyrite.

The vuggy calcite substrate for the marcasite and pyrite are identical to calcite overgrowths on sphalerite in geopetal structures. The marcasite and pyrite are therefore post ore precipitates in this instance, whereas those as inclusions in the ore stage sulfide minerals are early generations.

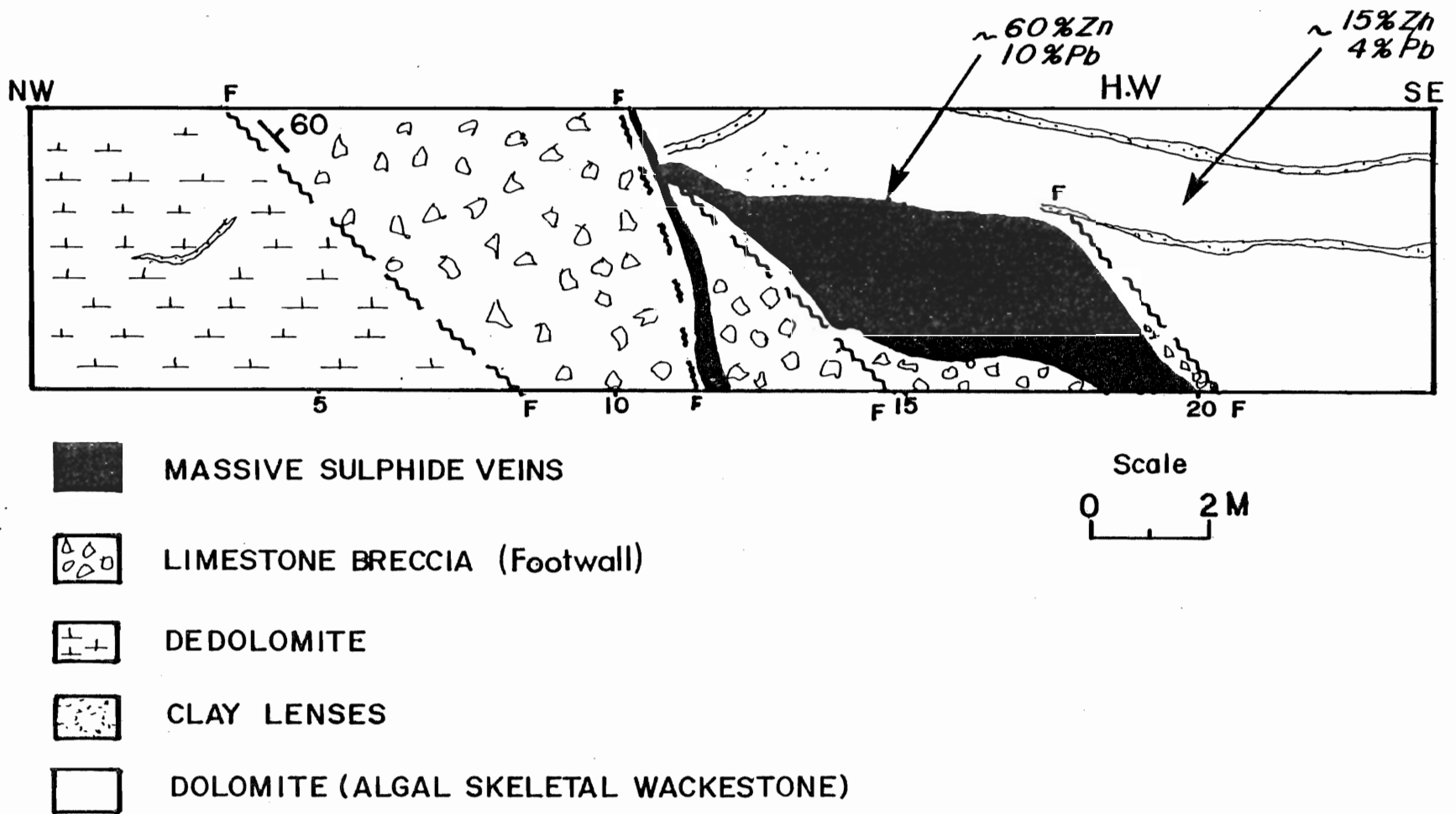


Figure 4.15 Cross section of fault bounded sulfide veins in the 104 drift.

4.5 Chemical Constituents of the Stratiform and Vein Sulfide Minerals

The stratiform and vein sulfide minerals were analyzed for their major elements by the use of the electron microprobe. Selected minor and trace elements were analyzed for by the atomic absorption spectrometric technique after a total "aqua regia" digestion of clean sulfide separates.

These analyses show that the major elements in the stratiform and vein sphalerite and galena are identical (Table II-3). Constituents include Zn, S and low Fe content in sphalerite and Pb and S in galena. The low iron contents in sphalerite range from 0.4 mole percent FeS in the vein sphalerite and up to 1.1 mole percent FeS in the stratiform pale yellow sphalerite (Table II-3). Marcasite, pyrite and chalcopyrite are close to stoichiometry and consist of varied Fe, Cu and S Contents (Table II-4). Minor and trace element analysis in the sulfide minerals indicate that sphalerite contain trace amounts of Cd, Mn, Cu, Co, Ni, V and Sn (Table II-5). Similar elements are present in galena in lesser quantities (Table II-5). A slight positive correlation exists between Cd and Mn values in sphalerite and galena (Fig. 4.16). Silver values in galena are slightly higher than sphalerite. This value ranges from less than 1 ppm to 121 ppm in galena whereas silver in sphalerite is not more than 2 ppm (Table II-5). It is useful to note the greatest silver value of 121 ppm in a vein galena sample AGR 91 (Table II-5).

Marcasite intergrown with dolomite and as fracture overgrowths contain significant amounts of Mn, Cu, Co and Ni although these elements are quite low in the associated pyrite. Manganese values in marcasite range from 0.074 wt percent to 0.21 wt percent while the copper values range from

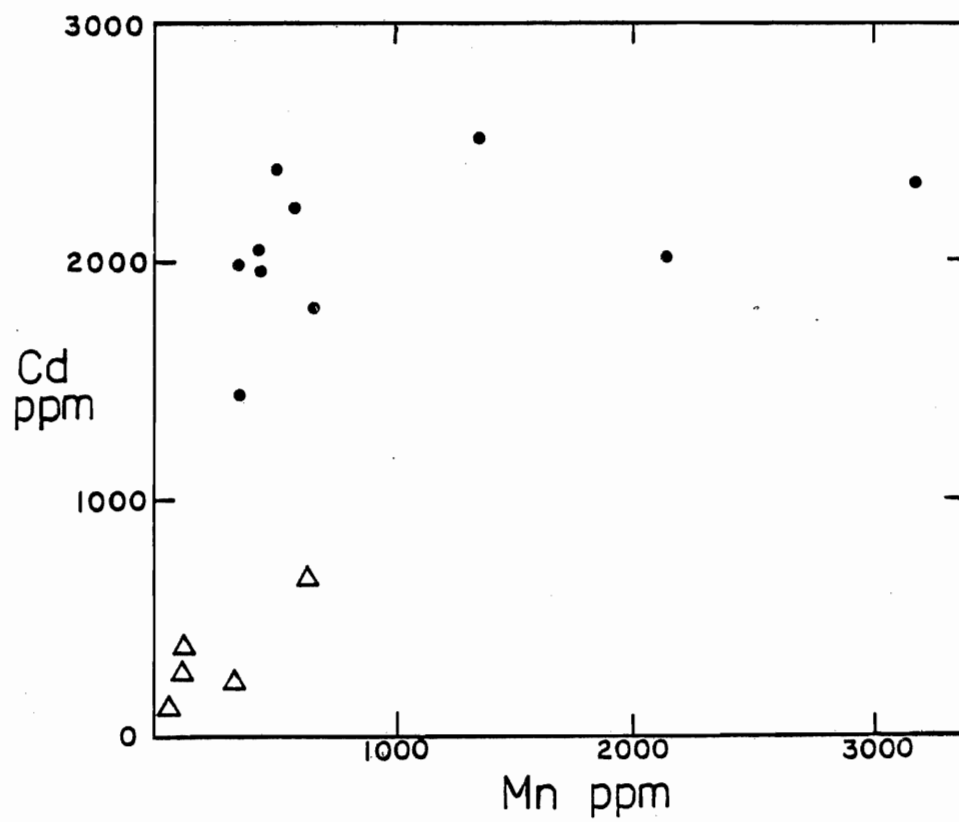


Figure 4.16 Concentration of cadmium and manganese in sphalerite and galena.

• sphalerite

△ galena

6 ppm to 583 ppm. A Co/Ni ratio of approximately 0.53 calculated for the marcasite is compatible with a sedimentary diagenetic origin (Loftus-Hills and Solomon, 1967). These authors proposed that Co/Ni ratios less than 1 are indicative of sedimentary and/or diagenetic origin for pyrite; whereas values greater than 1 do indicate a volcanic origin. The present author believes that such evidence although not conclusive suggests that the marcasite clots in dolomite and in fracture overgrowths are of sedimentary or diagenetic origin.

4.6 Mineralogy and Composition of the Host Rocks to Ores

The host rocks for the stratiform and vein ores are commonly dolomite and limestone. Rare occurrences of ore minerals are found in the gypsum and anhydrite stratigraphically above the ore.

Dolomite is the most abundant host for the stratiform and vein ores. This dolomite is a light brown to buff finely crystalline type. Three main matrix components of dolomite can be distinguished on the basis of their textures and fabric: 1) Pelmicrites, 2) recrystallized micrite and 3) fringe cement. These three textural varieties commonly occur as intergrowths and are not distinctly separated from one another. Fringe cements are most abundant in grainstone with large amounts of bioclasts.

The pelmicrite is made up of pellets of grain-sizes between 5-10 μm . Such aggregates form a grapestone matrix. The fabric of the rock is well preserved when pellets are abundant.

The recrystallized micrite is a sucrosic dolomite matrix with grain size greater than 10 μm , but less than 40 μm . This texture is of microspar range. The rock has large interparticle porosity compared to the dense pelmicrite and it frequently consists of interlocking grains of

sphalerite and galena.

The dolomite fringe cement consists of two types: 1) fibrous cement and 2) blocky euhedral cement. The fibrous cement is generally cloudy, full of carbonaceous particles and the grains average 30 μm across. The blocky euhedral cement has dolomite crystals ranging from 100-150 μm across and some dolomite rhombs are as much as 500 μm across. These blocky dolomite crystals are generally clearer than the cloudy fibrous cement. In many samples the blocky cement is seen to overgrow on the fibrous cement.

The different matrix components of dolomite were analyzed by the use of the electron microprobe. This facilitates the distinction and analysis of individual grains that would otherwise have been impossible by bulk chemical analysis. The microprobe analyses of the dolomite (Table II-6), reveal that they are impure, non stoichiometric grains with varying proportions of magnesium, calcium, manganese, iron and minor quantities of sodium and sulfur.

Dolomite pelmicrite has an average of 50 mole % CaCO_3 whereas the recrystallized micrite and fringe cements have an average of 54.5 mole % CaCO_3 . The dolomite grains are rich in manganese and iron, with manganese values averaging 1.3 wt % and iron 1.2 %. A good positive correlation of manganese and iron exists in the dolomite (Fig. 4.17). The lowest Mn/Fe ratio was found in the dense pelmicrite. Higher Mn/Fe ratios were found in the recrystallized micrite and fringe cements (Fig. 4.17). This suggests that the proportion of manganese and iron contents of the dolomites depends on the degree of recrystallization. This is commonly associated with an increase in porosity of the rock and a corresponding increase in the

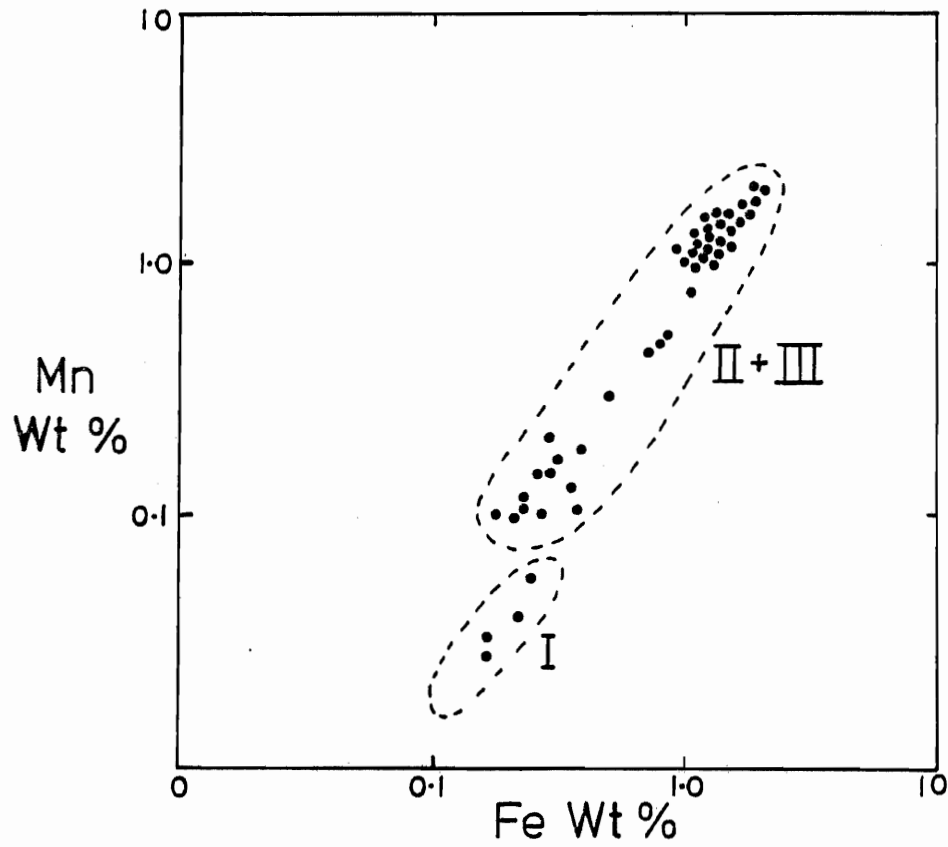


Figure 4.17 Concentrations of manganese and iron in the dolomite host for ore.

- I Dolomite pelmicrite
- II Recrystallized micrite
- III Fringe cement

sphalerite and galena content. Sodium values are largest in the recrystallized micrite and can be as much as 0.23 wt %. Sulfur concentration of approximately 0.32 wt % was measured in the recrystallized micrite.

The dispersion of manganese, iron, sodium and sulfur in the dolomitic host reflect on the diagenetic alterations of the carbonate prior to and after the mineralization event. The intimate association of the recrystallized micrite with high manganese and iron, and significant contents of sphalerite and galena suggest a genetic relationship with the ore solutions. If the ore solutions were responsible for the dolomite recrystallization, the trace contents of sodium and sulfur in the dolomite are probably remnants of the saline brines in the dolomite lattice.

4.7 Dedolomitization and the Limestone Texture

In areas adjacent to faults, joints and at the dolomite-evaporite contacts, the host dolomite for ore has been converted to a dedolomitized limestone. The faults and joints served as channels for the dedolomitizing fluid. The spatial relationship of the dedolomitized rock to gypsum and anhydrite suggest that the dedolomitizing fluid was derived from the dissolution of evaporites.

The rock is a dark brown, coarsely crystalline secondary limestone. Primary textures have been partially or completely masked by the dedolomitizing process in many instances. In few instances, relics of the primary depositional features of dolomite are present where only partial dedolomitization has taken place. The rock locally consists of pellets, recrystallized limestone micrite, fringe cements and breccia textures. These textures are identical to the dolomite precursor. Breccia textures with angular clasts are developed adjacent to faults.

The secondary limestone is non stoichiometric, manganese rich, iron

poor and has lower impurities of sodium and sulfur compared to the dolomite precursor. Manganese values in the limestone averages 8000 ppm and iron averages 3000 ppm. There is a lack of correlation in the M_n/Fe ratios and this relationship suggests the separation of iron from manganese during the dedolomitization process (Fig. 4.18).

4.8 Vuggy and Vein Calcite

The vuggy calcite aggregates are generally overgrowths on sulfide minerals and therefore post ore. Vein calcite occurs as intergrowth with the sulfide minerals quite commonly and is probably precipitated contemporaneously with ore, or subsequent to the sulfide mineral precipitation. The vein calcites are classified as ore-stage calcites where obvious intergrowth phenomenon is recognized.

The chemical composition of the vein and vuggy calcite is identical. Vein calcite intergrown with sulfide minerals is closest to stoichiometry. Significant concentrations of manganese averaging 0.8 wt % but may be as large as 2.0 wt %. They are depleted in iron, sodium and sulfur with respect to dolomite.

Vuggy calcite overgrowths on sulfide minerals and calcite veinlets not associated with sulfide minerals are non stoichiometric, have manganese content averaging 0.7 wt % and contain an average of 0.25 wt % iron. Sodium and sulfur concentrations are quite erratic in this group of calcite but one crystal analyzed contained as much as 0.25 wt % sodium. Sulfur values of 0.42 % were measured in a calcite crystal in one sample. The composition of these calcite compare closely with the dedolomitized rock. This suggests a genetic relationship with the dedolomitized rock and further distinctions will be made in the subsequent chapters. The

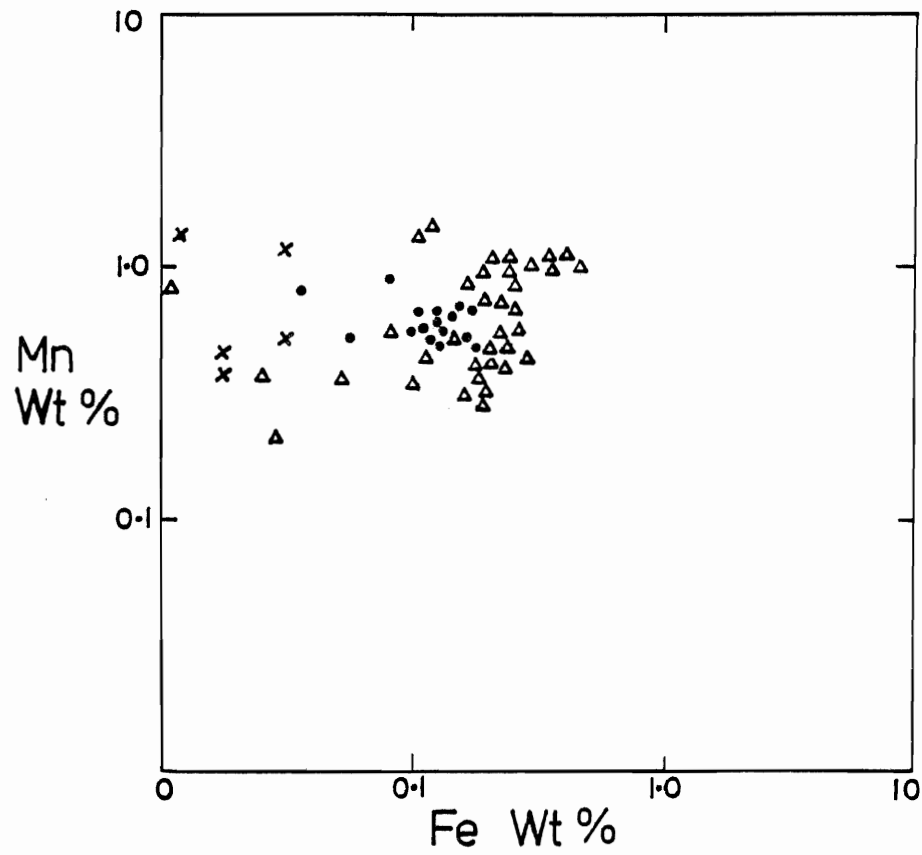


Figure 4.18 Concentrations of manganese and iron in calcite.

x Ore stage calcite

• Post ore calcite

Δ Dedolomite

dedolomitized rock has contents of magnesium varying from 0.1 wt % to as much as 6 wt %. It is the least stoichiometric of the forms of calcite.

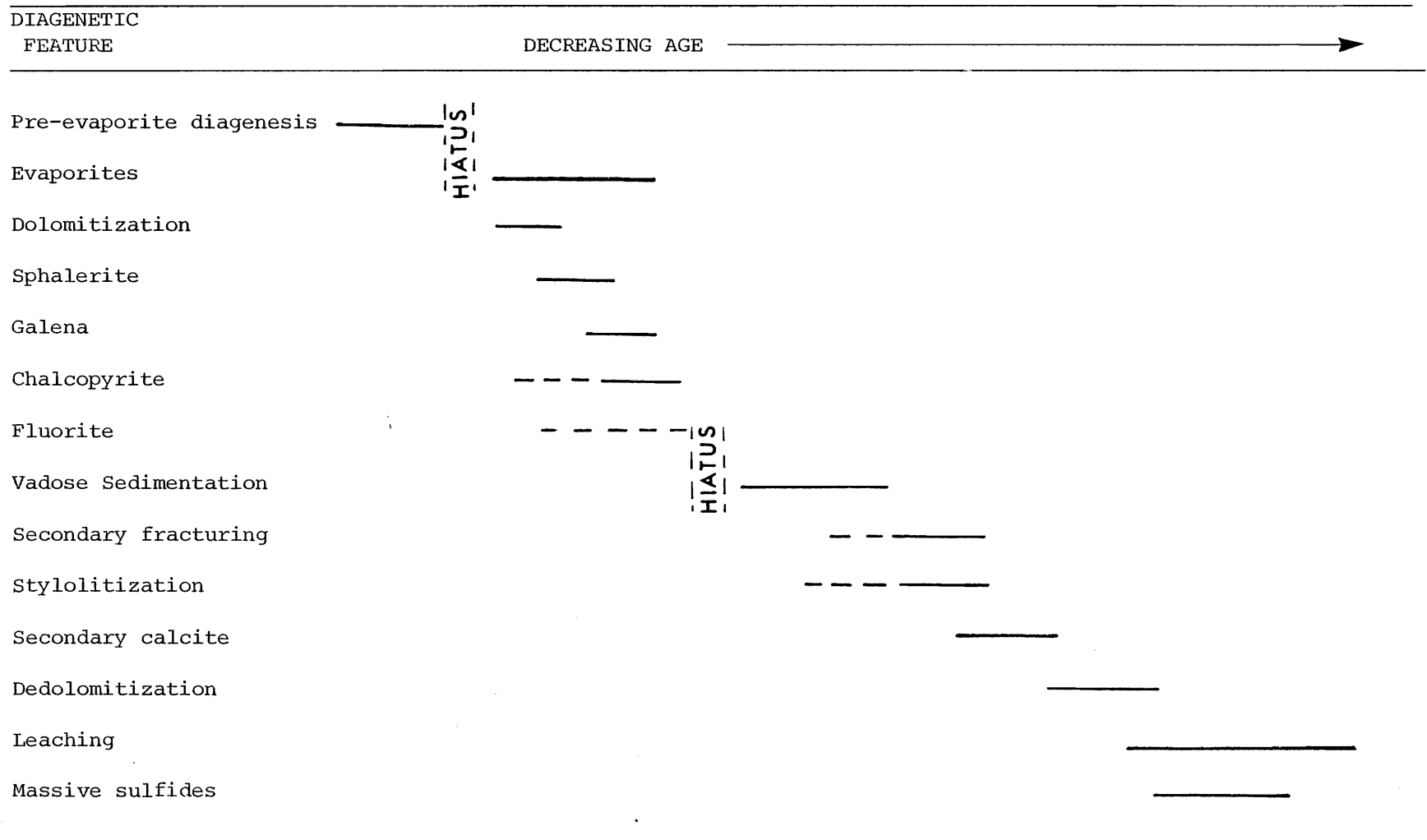
4.9 Discussion

Earlier workers on the Gays River deposit described two groups of lead-zinc ores: 1) primary low grade ore and 2) secondary high grade ore (Mac Eachern and Hannon, 1974; Macleod 1975). These authors described the primary ore as sphalerite and galena in-fillings of the pore spaces contained in the dolomitic host rock. The secondary ore was described as products of secondary leaching of the primary sphalerite and galena cement of the dolomitic host during karst processes (MacEachern and Hannon, 1974). These authors concluded that the sphalerite had been leached by groundwater from the reef proper and redeposited on the reef slope. They explained that the secondary ore in the form of massive sulfide minerals has a direct relationship with the sinkholes on the flanks of the reef.

Macleod (1975) concurred with MacEachern and Hannon (1974) and concluded that primary sphalerite and galena precipitation closely followed the dolomitization of the carbonate build up and this was subsequently followed by groundwater erosion of the carbonates and the secondary re-concentration of the earlier primary sulfide minerals (Table 4.1). Macleod emphasized that the leaching process is related to the diagenesis in the vadose zone where sphalerite, galena and carbonate silt were eroded and mechanically reprecipitated as high grade secondary ores.

Detailed underground mapping in the mine and petrographic studies of the ore and host reveal that the lead-zinc ores are structurally controlled and are divisible into low grade stratiform ores and the high

Table 4.1 Diagenetic Sequence from Macleod (1975)



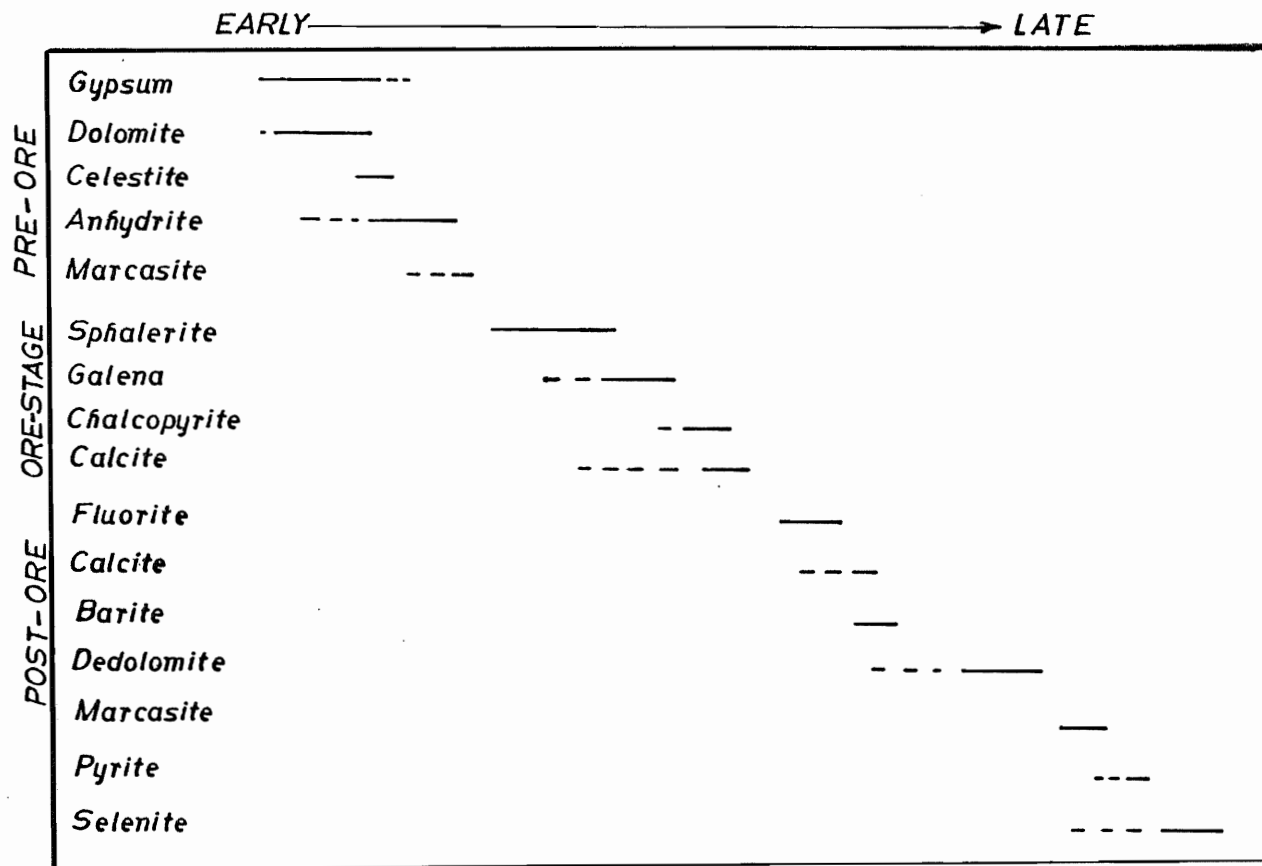


Table 4.2 A generalized summary of mineral paragenesis at Gays River.

grade vein ores on the basis of their geological setting and textures.

The persistent distribution of the massive sphalerite and galena veins along faults and related fissures within the carbonate host, and the complete fillings of the pore spaces of the carbonate host by sphalerite and galena in areas adjacent to the veins discount the possibility that these veins are products of leaching and the mechanical weathering of a primary mineralization.

Both fabric and non fabric selective porosities of the carbonate host are filled with sulfide minerals in areas adjacent to the massive sulfide veins. Petrographic examination of cut slabs and polished sections confirms that the stratiform and vein ores have similar mineralogy with differences in the proportions of sulfide minerals. Thin and polished section studies also reveal the presence of sulfide veinlets terminating in the pore spaces of the dolomite host. Such veinlets are traceable to the contacts of the sulfide veins. Indeed the major and trace element composition of the stratiform and vein sphalerite and galena are identical (Tables II-3 and II-5). These relationships indicate that the veins are feeders into the pore spaces of the carbonate host.

The previous interpretation of the lead-zinc ores as primary and secondary ores is therefore untenable and the author believes that the terms stratiform and veins can better describe the two groups of ores. A paragenetic sequence of deposition for the associated minerals in ore and host is summarized from the deductions made from their textural and crosscutting relationships (Table 4.2). Three main stages of mineral paragenesis can be distinguished; a pre ore stage, an ore stage and a post ore stage. This can be compared with the diagenetic features summarized by Macleod (1975).

CHAPTER 5

FLUID INCLUSION MICROTHERMOMETRY

5.1 Introduction

The determination of the physical and chemical parameters of ore deposition has become a major concern in metallogenic research. Although many techniques could be used in this regard, the studies of fluid inclusions in ore minerals and their associated gangue has proved very informative. The temperature, pressure and the composition of the geological environments in which several ore deposits are formed have been well documented from fluid inclusion studies. Of particular interest is the determination of the temperature of formation of Mississippi Valley Type deposits where a range of temperatures from 80 - 150°C and occasionally up to 200°C have been documented. Salinity measurements from inclusions in this group of deposits reveal that the ores were deposited by highly saline brines up to ten times the salinity of sea water (Roedder, 1976).

In general, fluid inclusions are commonly dominated by a composition of several ions. These commonly include Na^+ and Cl^- ions (Roedder, 1972). Other components may include $\text{SO}_4^{=}$, $\text{CO}_3^{=}$, HCO_3^- , K^+ , Mg^{2+} , Ca^{2+} and CH_4 in some inclusions (Konnerup-Madsen, 1979; Roedder, 1972; Hanor, 1980). A liquid and gas phase are common in fluid inclusions, but solid phases in the form of daughter minerals occur in some deposits. The liquid phase is frequently dominated by H_2O or CO_2 while the gas phase which is represented by a bubble may contain CO_2 , H_2O or CH_4 . Although the liquid phase is predominantly H_2O rich, other ions as Na^+ , Cl^- , $\text{SO}_4^{=}$, $\text{CO}_3^{=}$ and HCO_3^- , may be present.

The relative abundance of ions in the inclusions of Mississippi Valley Type deposits are $(Cl > Na > K > Mg > B)$ (Roedder, 1979). Roedder (1972) indicated that heavy metal ions as Pb^{++} and Zn^{++} in parts per million levels may be present in this group of inclusions. The experimentally determined equilibria in the $NaCl-H_2O$ systems especially have been often used in the interpretation of homogenization and freezing phenomena in Mississippi Valley Type inclusions. Fluid inclusions homogenization and freezing experiments were used in this thesis as a tool to clarify the temperature of ore deposition at Gays River and to examine the identity of the mineralizing fluid.

5.2 Terminology

A considerable amount of literature on fluid inclusions have adopted the usage of certain terms and abbreviations to describe the temperatures at which specific phase change occurred in inclusions. For the purpose of this thesis, the following terms and abbreviations will be used to describe the observations made during the homogenization and freezing experiments:

Th: This represents the temperature of total homogenization of the phases present in the inclusion, i.e. the temperature at which the liquid and vapour phases become one. This does not take into account the independent behaviour of daughter minerals which are present in some inclusions.

Tm: This is used to describe the melting temperature of specific solid phases that are present in the inclusion either as daughter mineral during homogenization experiments or ice melting temperatures during the freezing experiments.

Td: This represents the temperature of decrepitation of the inclusion due to rupture at or beyond the normal homogenization temperature of the

particular inclusion.

T_n : This is the temperature of nucleation. This is equivalent to the temperature at which a phase first freezes on lowering the temperature of the inclusion. Nucleation in an inclusion generally occurs only after a considerable supercooling and depends on many factors such as (i) the presence of foreign nuclei, (ii) size of the inclusion and the cooling rate.

L, V, S: These refer to the liquid, vapour and solid phases respectively in an inclusion.

SST: This is the saturated solution temperature of the solid phases in the inclusion (e.g. melting of NaCl daughter mineral).

Immiscibility: This is used to describe the existence at equilibrium of two liquid phases that are probably different in physical properties and composition.

5.3 Classification and Assumptions

a. Origin of Inclusions

Fluid inclusions are gross defects in crystals and result from a number of complex processes. Those formed as the crystal is growing are called primary inclusions (P). Any process interfering with the growth of perfect crystals may cause the trapping of primary inclusions. These include (i) variation in growth rate, (ii) variation in the chemistry of the precipitating fluid, and (iii) the proximity and interaction of other crystals and stress. Secondary inclusions (S) may form from the rehealing of cracks within the crystals and can trap fluids that bathed the crystal at an earlier period. Such inclusions occur within planes containing similar inclusions. Since the time period between the trapping of primary and

secondary inclusions in a crystal can be quite short in geological terms, evidence abounds in favour of the formation of secondary inclusions in fractures which occurred while the crystal was still growing. These groups of inclusions are called pseudosecondary (PS).

b. Criteria

It is important to distinguish the primary (P), pseudosecondary (PS) and secondary inclusions (S) in order to make a meaningful interpretation of the microthermometric observation. Several criteria that are useful for these distinctions are given by Roedder (1976), p. 74-75 and Roedder (1979), p. 689-691. A summary of these criteria are given in the appendix.

These criteria were applied to distinguish the varieties of inclusions seen in the present study. Most primary inclusions studied have the following characteristics; (i) large well developed regular shape and size relative to the others (e.g. negative crystal shape in fluorite), (ii) isolated geometrically regular inclusion separated away from the other inclusions and (iii) non planar isolated forms.

c. Assumptions in the Present Study

The use of the fluid inclusion tool in this thesis is based on the following assumptions which is an expansion of a summary of assumptions presented by Roedder (1967).

1. That the minerals examined have grown in a fluid medium.
2. During the growth of the minerals, some of the liquid in which the crystals were growing was trapped as fluid inclusions.
3. In most cases, only the liquid was trapped when the inclusions formed.

4. There has been no significant gain or loss of material from the inclusions since their formation.
5. Primary fluid inclusions can in most cases be differentiated from secondary fluid inclusions.

The possibility of loss or gain of material in an inclusion represents the greatest concern in the application of fluid inclusions techniques. Leakage of inclusions has been a problem of considerable concern. Kennedy (1950) and Skinner (1953) indicate that fracturing during mechanical deformation may cause leakage even during sawing and abrasive grinding of the thin samples. A careful polishing, grinding and microscopic examination of fluid inclusions is therefore necessary before the selection of usable inclusions. Although some inclusions do leak under certain adverse conditions, most inclusions in natural situations do not (Roedder, 1963). The greatest evidence against large scale leakage of inclusions is found in the evidence of systematic variation in the filling temperature and composition of inclusions in zoned minerals (Roedder, 1963; 1965). Systematic variations in the homogenization temperatures most commonly follow a reasonable paragenetic order in well studied ore deposits.

5.4 Thermometry

a. The Vapour Bubble

Empirical evidence shows that the gas phase of an inclusion (vapour bubble) forms as the inclusion cools from its trapping temperature to room temperature because of the differential thermal contraction of the host crystal and the inclusion fluid. Thus as soon as the internal pressure of the inclusion drops below the total vapour pressure of the fluid,

the vapour bubble nucleates and grows.

In microthermometric determinations, the relative size of the vapour bubble provides a visual estimate of the temperature of trapping. In general, low temperature products produce characteristically small vapour bubbles or none at all in comparison to large bubbles that are formed at high temperatures (Roedder, 1962). The apparent gas/fluid ratio is greatly affected by the inclusion shape even though the inclusions that appear different may have the same temperature of homogenization (Roedder, 1976). During homogenization, the temperature of disappearance of the bubble will indicate the homogenization temperature T_h . This is not the true trapping temperature but it may be corrected to a trapping temperature if an independent estimate of pressure can be made.

b. Sample Selection

More than 70 doubly polished plates (1-1.5 mm thick) of the representative specimens of honey yellow sphalerite, ore stage calcite, post ore calcite, fluorite and barite were studied under the microscope. Detailed notes on the individual specimens are given in the appendix. Of these mineral specimens, post ore calcite and post ore fluorite contain large numbers of good size usable inclusions within 5-20 μm range whereas the inclusions in sphalerite are very small with a size range of 5-10 μm across. Samples of the post ore calcite and fluorite contain many inclusions as much as 0.5% by volume.

The fluid inclusions studied display a wide variety of morphology (Fig. 5.1). Some are regular in outline with spherical, ovoid, rectangular, negative crystal, multifaceted and tubular shapes, while others are highly irregular. Those used for the heating and freezing experiments are gener-

Fig. 5.1a Morphologies and composition of fluid inclusions in sphalerite, ore stage calcite, post ore calcite, fluorite and barite.

Sphalerite; 1. Primary two phase spherical inclusion.

2. Primary rectangular inclusion with an immiscible liquid which became miscible during heating runs.
3. Primary inclusion with a cubic daughter NaCl crystal (h) in the liquid phase.
4. Secondary two phase inclusion with tapered ends and a larger vapour bubble approximately 20% by volume.

Ore stage calcite; 1, 2, 3, are primary two phase inclusions. The inclusion (2) commonly occur as multiples in planar orientation across the cleavage plane of calcite.

Post ore calcite; 1, 2, are primary or pseudosecondary two phase inclusions. Vapour bubbles are commonly identical in size.

3. Secondary two phase inclusion with long tails along calcite cleavage plane. This inclusion shows strong evidence of necking down and have probably leaked.

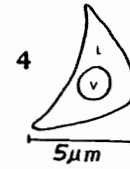
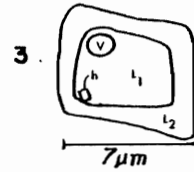
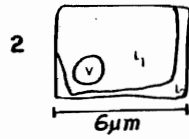
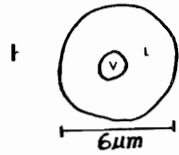
Fluorite; 1. Primary two phase inclusion.

2. Primary multiphase negative crystals in fluorite. Note the oil globule (ol) with a centrally located vapour bubble (v) and an outer ring suspected to be methane (m?). This ring disappears on heating.
3. Tubular multiphase pseudosecondary inclusion.
4. Primary multiphase inclusion with a cubic daughter NaCl crystal. Note the oil globule adhering to the inclusion wall.

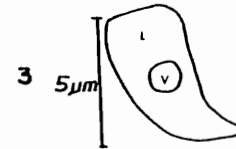
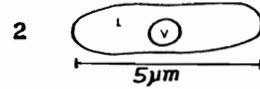
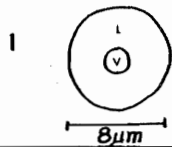
Barite; 1, 2, are primary two phase inclusions.

3. Secondary large size inclusion with tapered ends. Such inclusions occur along the cleavage plane of barite and yield higher homogenization temperature.

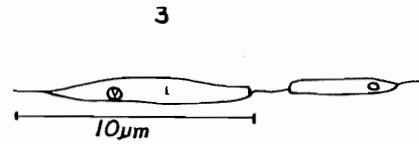
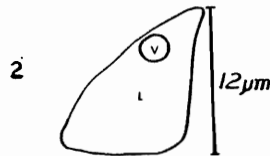
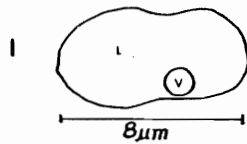
SPHALERITE



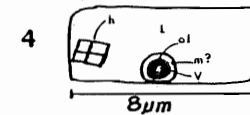
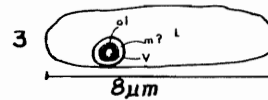
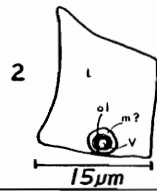
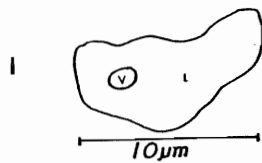
ORE STAGE CALCITE



POST ORE CALCITE



FLUORITE



BARITE

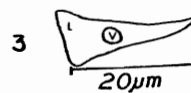
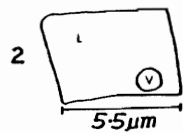
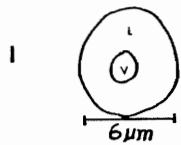
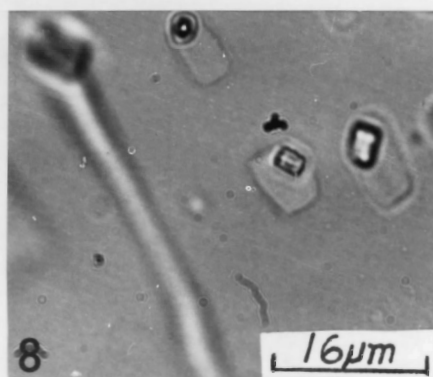
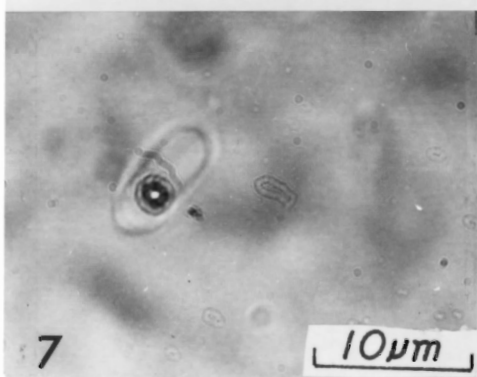
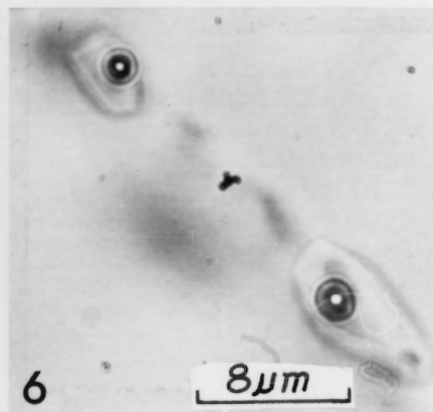
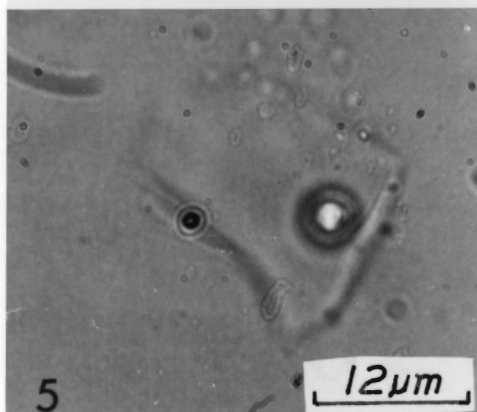
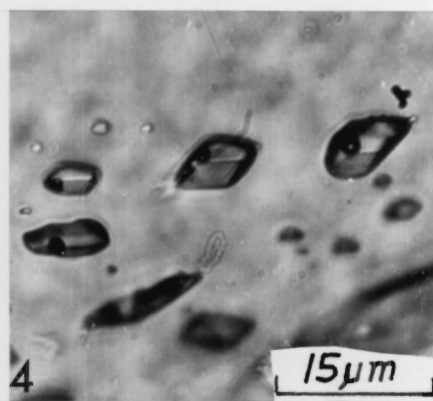
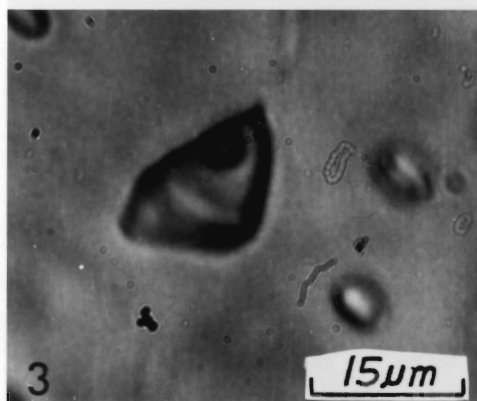
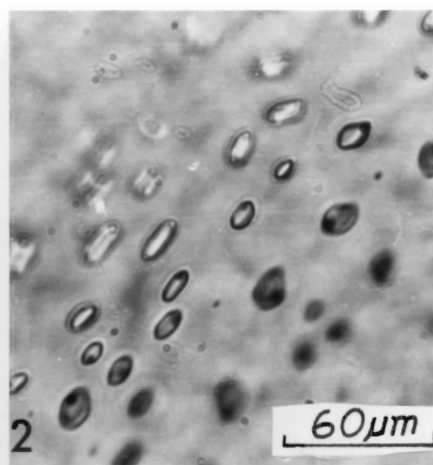
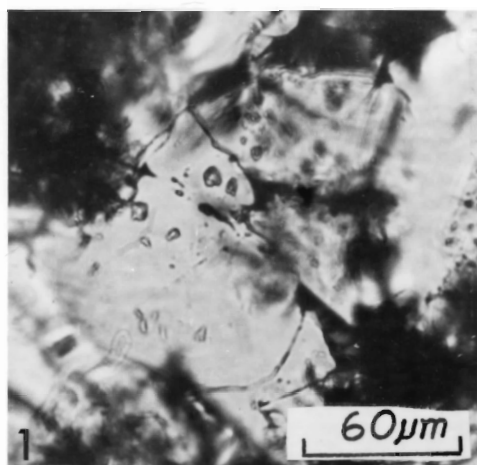


Figure 5.1b

1. Photomicrograph of primary two phase (l + v inclusions in vein sphalerite.
2. Photomicrograph of a plane of primary? or pseudosecondary two phase inclusions in the ore stage calcite.
3. A single primary two phase inclusion in post ore calcite.
4. A plane of probably pseudosecondary two phase inclusions in post ore calcite.
5. A primary negative crystal shaped hydrocarbon inclusion in fluorite. Note that the oil globule with a centrally located vapour bubble adheres to the inclusion wall.
6. A plane of probably pseudosecondary hydrocarbon inclusions in fluorite.
7. A single primary tubular hydrocarbon inclusion in fluorite.
8. A plane of pseudosecondary inclusions containing daughter minerals in fluorite. The lack of vapour bubble in some of the inclusions and the long tail of one of the inclusions indicates leakage as a result of necking down.



ally regular in shape and greater than 5 μm in diameter. Smaller ones <5 μm are common in the sphalerite and ore stage calcite but were not used. It becomes quite difficult to see the phase changes in them with the resolution used.

In selecting inclusions for analysis, care was taken to avoid those which showed features that are indicative of modification after trapping. These include, trails of minute inclusions between large ones, variable vapour liquid ratios between spatially associated inclusions, and some obvious signs of leakage such as cracks and anomalous gas rich inclusions. All of the inclusions which show clear evidence of necking down were also discarded. Over 170 heating and freezing experiments were performed on usable inclusions.

c. Degree of Fill

In geological thermometry, it is more convenient to use the degree of filling (F) at room temperature than the specific volume (V). These two magnitudes are uniquely related to each other by the densities of the liquid and gas phases coexisting at room temperature, Lemmlin and Klevstov (1961).

$$\text{Degree of fill (F)} = \frac{\text{volume liquid}}{\text{volume total}}$$

At room temperature

$$\text{the density of inclusion in gm/cm}^{-3} \equiv F$$

F can be related to density:

$$dt = d_L F + dg (1-F) + \dots\dots\dots$$

Where dt = total density of the inclusion

dL = density of the aqueous phase

dg = density of the gas phase.

At room temperature, the density of the gas phase is zero,
 hence, $dt = D_L F$

$$dt = F = \frac{\text{volume liquid}}{\text{volume total.}}$$

Since the temperature of homogenization of the inclusions depends on the degree of fill, i.e. density, an approximate temperature can be determined by using only the ordinary microscope. The density of the inclusion can be more accurately determined if the salinity of the inclusion is known (Rankin, 1978).

d. Homogenization Experiments

The homogenization experiments were performed on a heating stage that was built by Graves (1976) and has been modified by Dr. M. Zentilli of Dalhousie University. The stage was attached to a thermocouple which consists of nickel-chromium versus nickel-aluminum. Calibration of the nickel-chromium thermocouple was achieved with the melting temperatures of organic compounds (tempilstiks) of known melting points. Reproducibility was better than 1.5% up to temperatures of 300°C. In order to minimize the effects of temperature gradients within the heating stage, the final stages of heating were always carried very slowly and many duplicate runs were performed. The filling temperatures in most cases were reproducible to within 1-2°C or better. Where the vapour bubble visibility is poor, the uncertainty in the measurements was about 3°C.

e. Observations and Results

Microscopic examination of the inclusions showed that both aqueous and hydrocarbon inclusions are present in the doubly polished plates studied. They all homogenized to the liquid phase during the heating experi-

ments. This confirms that the original fluid in the inclusions was liquid. Hydrocarbon inclusions were seen only in the green fluorite. They can be distinguished by their wetting characteristics and the presence of oil globules with a centrally located vapour bubble (Fig. 5.1). A thin ring of immiscible liquid probably containing methane? surrounds the outer wall of the oil globule. The immiscible fluid homogenized during the heating runs into the liquid phase. The characteristic behaviour of the inclusions in each of the mineral phases studied and their homogenization temperatures are described as follows:

Sphalerite

Although sphalerite occurs as massive finely crystalline and coarse crystalline grains, fluid inclusions are rare in them. Out of the 24 doubly polished sphalerite specimens examined, only 9 of these plates contain usable inclusions. The few inclusions in sphalerite are contained in the honey yellow subhedral grains that are embedded in the massive pale yellow sphalerite. Primary inclusions in sphalerite occur as isolated spherical, rectangular, oval or equant cubes (Fig. 5.1). They are generally small 2 phase inclusions with an average diameter of 6 μm . There is a liquid and a vapour phase and the degree of filling (F) is approximately 90%. In one instance, the liquid phase exhibited immiscibility at room temperature and a cubic crystal daughter mineral that was suspected to be NaCl. These phases disappeared on heating and failed to renucleate. The vapour bubble in the primary inclusions frequently exhibit "brownian motion" during heating runs; a phenomenon that is characteristic of very saline fluids (Roedder, 1962).

Homogenization temperatures in the primary inclusions in sphalerite range from 205-219°C for the 9 usable inclusions with a mean value of

214.3°C (Table 5.1). The obvious secondary inclusions that are found along fractures in the subhedral sphalerite grains have lower degrees of fill of approximately 75%. These sets of inclusions are larger in number compared to the rare primary inclusions and were discarded during the heating experiments. Although an internal consistency within a reasonable range of temperatures occurred in the primary inclusions, few scattered values were recorded in 2 instances where a temperature as high as 274°C was recorded. Such values are believed to be due to leaking or stretching of the inclusions probably during the sample preparation or heating and they are not considered accurate.

Ore Stage Calcite

The ore stage calcite intergrowths within sphalerite are generally poor in usable inclusions although they look quite suitable in hand specimen. Primary inclusions in this group of calcite occur as rectangular or ovoid isolated forms, averaging 8 μm in diameter with liquid and vapour phases and a degree of fill of approximately 90%. The secondary inclusions are generally smaller, averaging 5 μm in length and have characteristic tapered ends. Apart from the secondary inclusions, a group of tubular planar inclusions intersecting the calcite cleavages are present. These are believed to be pseudosecondary in origin and are confined to a plane in different levels of calcite.

Homogenization temperatures (T_h) from 25 primary inclusions in this group of calcite range from 167°C to 178°C with a mean at $172.2 \pm 3^\circ\text{C}$ (one standard deviation) (Fig. 5.2). No run was performed on secondary and pseudosecondary inclusions.

Sphalerite

HOMOGENIZATION TEMPERATURES

214°C

215.5°C

215°C

218°C

219°C

215°C

215.5°C

205°C

214°C

MEAN $214.3 \pm 3.9^\circ\text{C}$

Table 5.1 List of homogenization temperatures in sphalerite fluid inclusions.

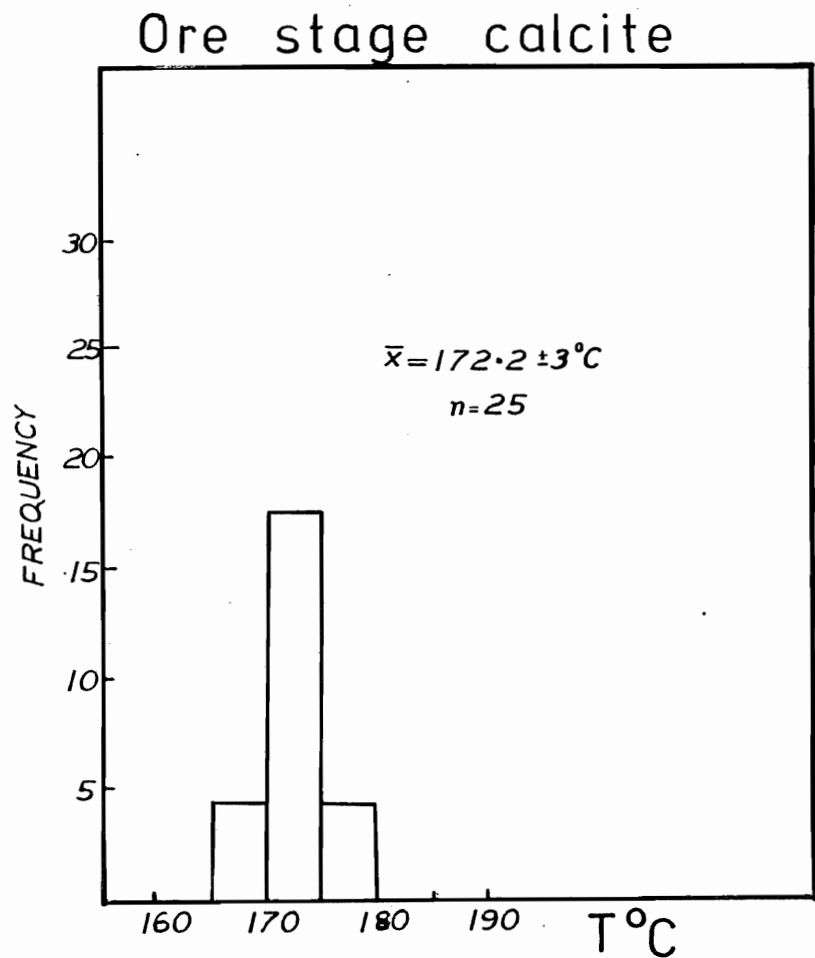


Figure 5.2 Histogram for the frequency distribution of ore stage calcite fluid inclusion temperature.

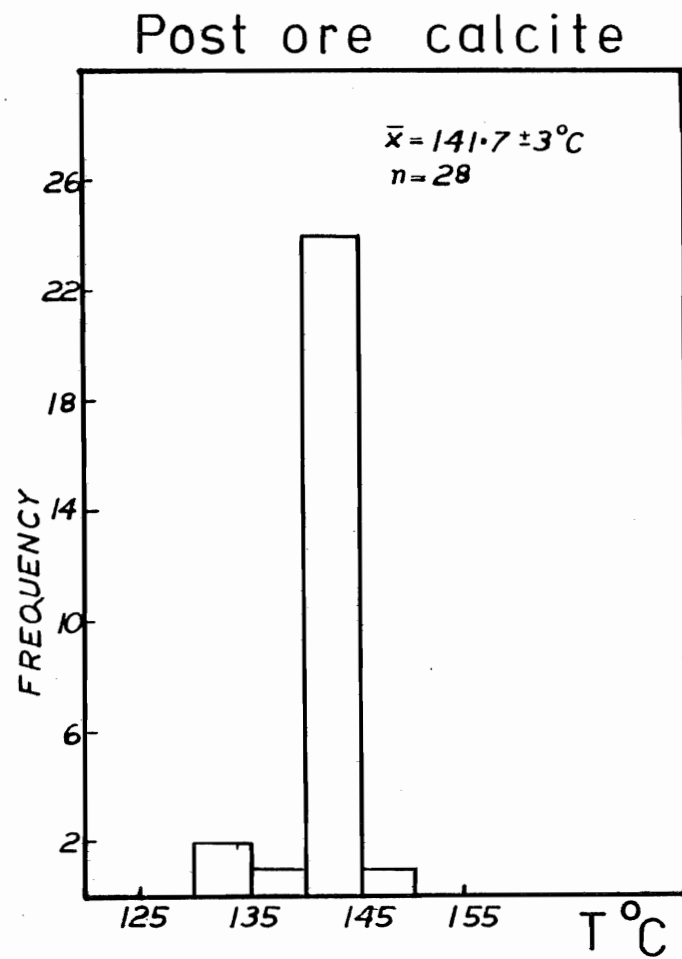


Figure 5.3 Histogram for the frequency distribution of post ore calcite fluid inclusion temperature.

Post Ore Calcite

The post ore calcite in vugs and as overgrowths on sphalerite contain more usable inclusions than the sphalerite and ore stage calcite. Primary inclusions in this calcite are generally spherical, ovoid or irregular in shape. They have an average diameter of 8 μm and a degree of fill of approximately 95%. Pseudosecondary inclusions are generally regular in shape and flattened, while the secondary inclusions have elongated, tubular shapes. Necking effects are commonly demonstrated by the secondary inclusions and they are frequently characterized by long trails (Fig. 5.1). Homogenization experiments were not performed on the secondary inclusions.

During the heating experiments, the vapour bubbles frequently exhibit brownian movements. Homogenization temperatures (T_h) for 28 inclusions in this group of calcite range from 132°C to 147°C with a mean at $141.72 \pm 3^\circ\text{C}$ one standard deviation (Fig. 5.3). The internal consistency in the primary and pseudosecondary inclusions confirm the assumption that these two types of inclusions were contemporaneous. In one instance a higher homogenization temperature of 168°C was recorded for one inclusion. This was interpreted to have resulted from the effects of necking down.

Other Calcite

Late stage calcite that encrusts on dolomite pebbles and as crustiform rings in cavities contain no usable fluid inclusions. Single phase inclusions $< 5 \mu\text{m}$ were present in few samples. These are believed to have either leaked completely or more likely have formed in cooler water and did not develop vapour bubbles (Yermakov, 1965). This group of calcite are not directly related to the lead-zinc mineralization.

Fluorite

About 20 specimens of purple, whitish and green colour varieties of fluorite were examined under the microscope. Aqueous inclusions are common in the purple and white varieties and hydrocarbon inclusions are most common in the green fluorite. The aqueous inclusions consist of the liquid and vapour phase with the infrequent presence of birefringent daughter mineral that are believed to be NaCl. Both primary and secondary types are present. The primary inclusions are generally ovoid, irregular, or tubular in shape, averaging 7 μm in diameter with a degree of fill of approximately 94%. The hydrocarbon inclusions are generally 2 phase (L + V) but the vapour phase is centrally located in the immiscible oil globule. These hydrocarbon inclusions average 8 μm across and can be as large as 17 μm in diameter. Volume shrinkage of the oil globule have produced a centrally located vapour bubble in the hydrocarbon-inclusion. Their refractive indices are identical to the host fluorite. Primary (P), pseudosecondary (PS), and secondary (S) inclusions are present. The P types occur as negative crystals and as irregular and tubular shapes. Pseudosecondary types are frequently arranged in planes and the secondary types are found along the fluorite cleavage (Fig. 5.1). Highly birefringent NaCl daughter minerals are present in the primary and pseudosecondary inclusions in some polished thin plates. These daughter minerals are identified as NaCl crystals because of their strong relief, high birefringence and crystallography.

Homogenization experiments were performed only on the primary and pseudosecondary aqueous and hydrocarbon inclusions. On heating the hydrocarbon inclusions, the immiscible ring of liquid surrounding the oil

globules disappeared at an approximate temperature of 100°C before the final homogenization of the vapour bubble at 143°C. The homogenization experiments on both the aqueous and hydrocarbon inclusions gave identical results with a range between 135 and 149°C and a mean of $143.3 \pm 2^\circ\text{C}$ (Fig. 5.4). In few instances, decrepitation phenomena were observed as series of explosions in the inclusions at a temperature of 2-3°C above the inclusions homogenization temperature. Most inclusions examined ruptured at this stage and had to be completely discarded.

The daughter minerals in the inclusions did not homogenize at the T_h of the fluorite inclusions. This phenomenon also confirms that the inclusions consist of very dense solutions. Melting of the NaCl daughter mineral took place at 166°C. Since the disappearance of the solid daughter mineral will depend on the composition and volume of the liquid, this difference in the temperatures T_{h1} and T_{h2} (Fig. 5.5) is directly related to the pressure at the time of formation of the inclusion (Crawford, 1981), and also the salinity of the hydrothermal fluid (Rankin, 1978). Therefore if the liquid phase of the inclusion was trapped from a solid saturated solution, the homogenization of the solid phase T_{h2} will give the temperature of trapping as well as the salinity at the time of trapping. This may provide an estimated value of the temperature correction needed i.e. $T_{h1} - T_{h2}$. This assumption has to be applied with caution since only few of the inclusions studied (<2%) contain solid daughter minerals it is difficult to generalize that all the inclusions formed from a solid saturated hydrothermal solution. An extrapolation of Rankin's (1978) curve of salinity versus T_h to lower temperatures (Fig. 5.6) gave a measurement of 24.8 equivalent weight percent NaCl for the melting temperature

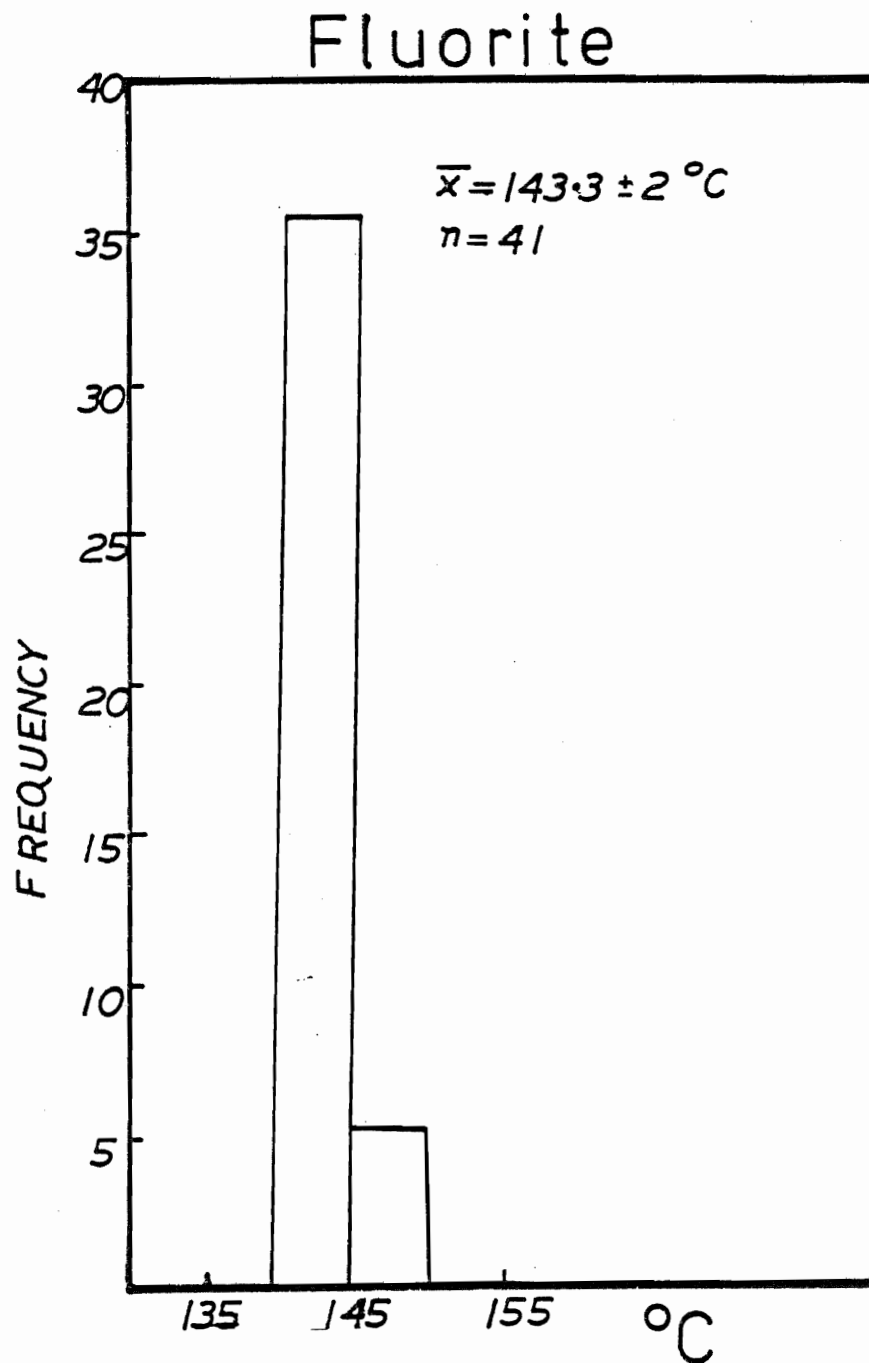


Figure 5.4 Histogram for the frequency distribution of fluorite fluid inclusion temperature.

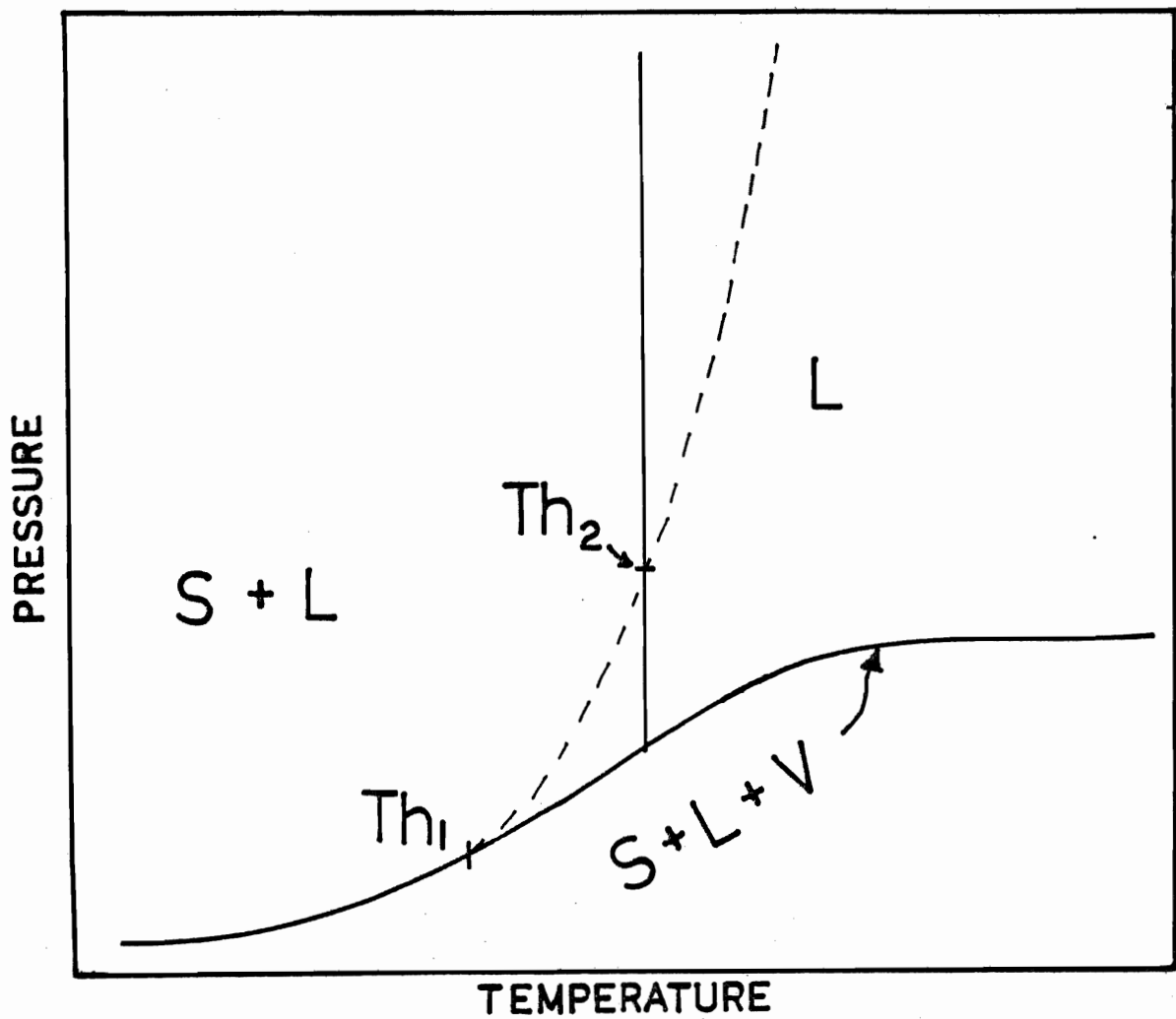
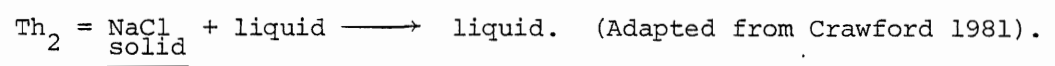
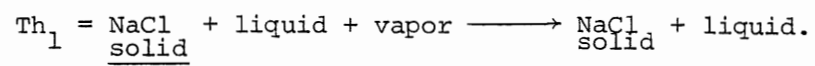


Fig. 5.5 Schematic diagram of high temperature phase equilibria in NaCl saturated dense brines. Homogenization temperatures:



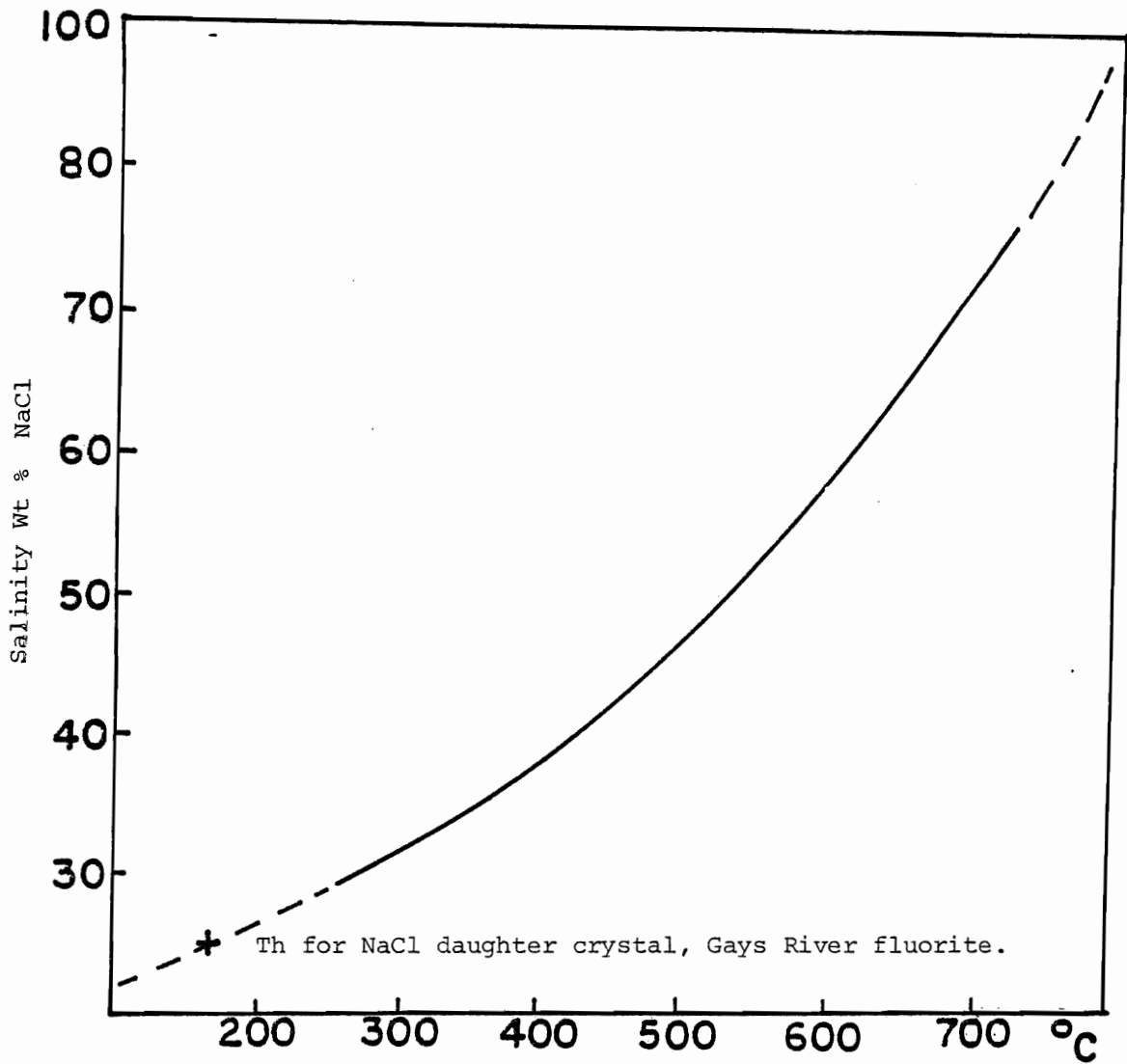


Figure 5.6 Composition of the liquid phase of saturated NaCl brines
(Data from Souririjan and Kennedy, 1962; figure, modified
from Rankin 1978).

of the daughter NaCl crystals at 166°C.

This salinity is slightly higher than values of 20.4 wt % estimated from the ice melting temperatures of fluorite inclusions and may be attributed to the uncertainty of Rankin's curve at lower temperatures. An approximate density of 1.1 gm/cm³ was estimated from the degree of fill and salinity of fluorite (Rankin, 1978) Fig. 5.6. If the salinity of fluorite of 24.8 of NaCl that was estimated from the saturated solution temperature of NaCl is considered to be the maximum salinity of the saline brine that deposited fluorite, this will indicate the presence of other salts apart from NaCl. The room temperature eutectic of pure NaCl solution is only at -20.8°C with 23.2 wt % NaCl (Potter et al, 1978). Thus with 24.8 equivalent weight percent dissolved salts, the presence of divalent metal cations is possible.

Barite

Fluid inclusions in post ore barite are aqueous 2 phase (L + V) types. Primary and pseudosecondary inclusions range in size between 5 to 10 µm averaging 6 µm. They are spherical or negative crystal shapes with a degree of filling approximately 95%. Secondary inclusions are generally large, with sizes ranging from 8-22 µm. They frequently have evidence of necking down.

Homogenization experiments were performed on 21 primary inclusions. Temperatures of homogenization range between 135 to 144°C with a mean at 137.7 ± 2°C one standard deviation (Fig. 5.7). The homogenization temperatures of the obvious secondary inclusions in barite are considerably higher. Homogenization temperatures on 3 secondary inclusions are 160, 161°C and 163°C respectively. These suggest that the secondary inclusions

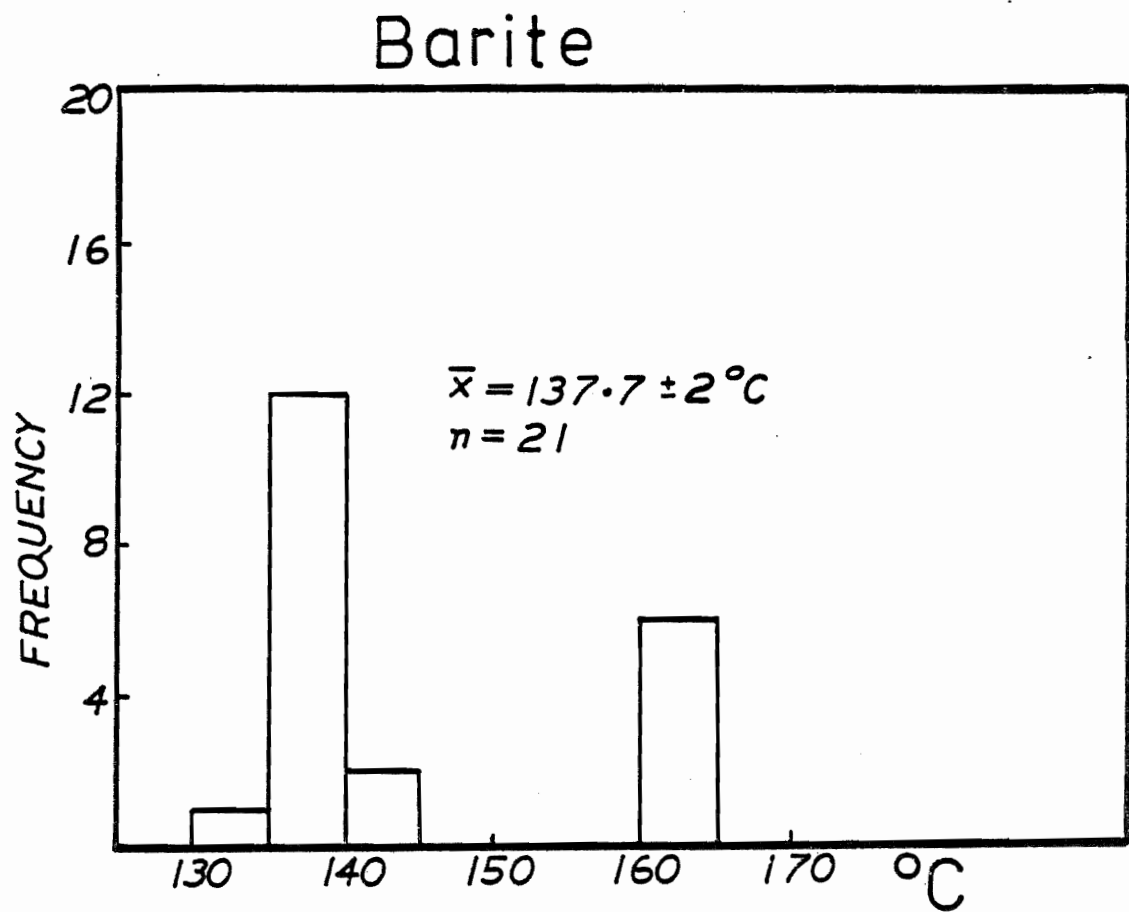


Figure 5.7 Histogram for the frequency distribution of barite fluid inclusion temperature.

have trapped a hotter fluid in another period.

Quartz in the metasedimentary basement

Aqueous primary and secondary inclusions were identified in the vein quartz fillings in the metasedimentary basement. The primary inclusions are isolated spherical or ovoid forms with an average diameter of 6 μm . They are generally 2 phase (L + V) with a degree of fill of approximately 91%. The secondary inclusions in the quartz veins are confined to fracture networks. They are generally irregular in shape and have an average size of 8.5 μm across and a higher degree of fill of approximately 95%. Homogenization experiments were performed both on the primary and secondary inclusions. Homogenization temperatures for the primary inclusions range from 250-306°C and occur in 2 distinct groups. Group one (P) 300-306°C; Group two (P) 250-265°C (Fig. 5.8). Secondary inclusions homogenize at temperatures of 220-227°C.

The T_h of primary inclusions are different from the mineralization event in the carbonate host and probably represent a different thermal event. The grouping of the secondary inclusions within a narrower range of temperatures suggest that the inclusions were bathed by a different hydrothermal fluid regime. Primary inclusion temperatures are similar to those reported by Graves (1976) from gold bearing quartz veins in the metasedimentary basement in nearby gold districts. The secondary inclusions temperature of homogenization are quite similar to T_h for sphalerite inclusions at a maximum of 219°C. The 8° difference between these two groups of inclusions (maximum T_h of quartz (S) - maximum T_h of sphalerite) indicate that the hydrothermal fluid was probably slightly hotter in the basement. This close relationship suggests that the hydrothermal fluids that were responsible for the main period of lead and zinc

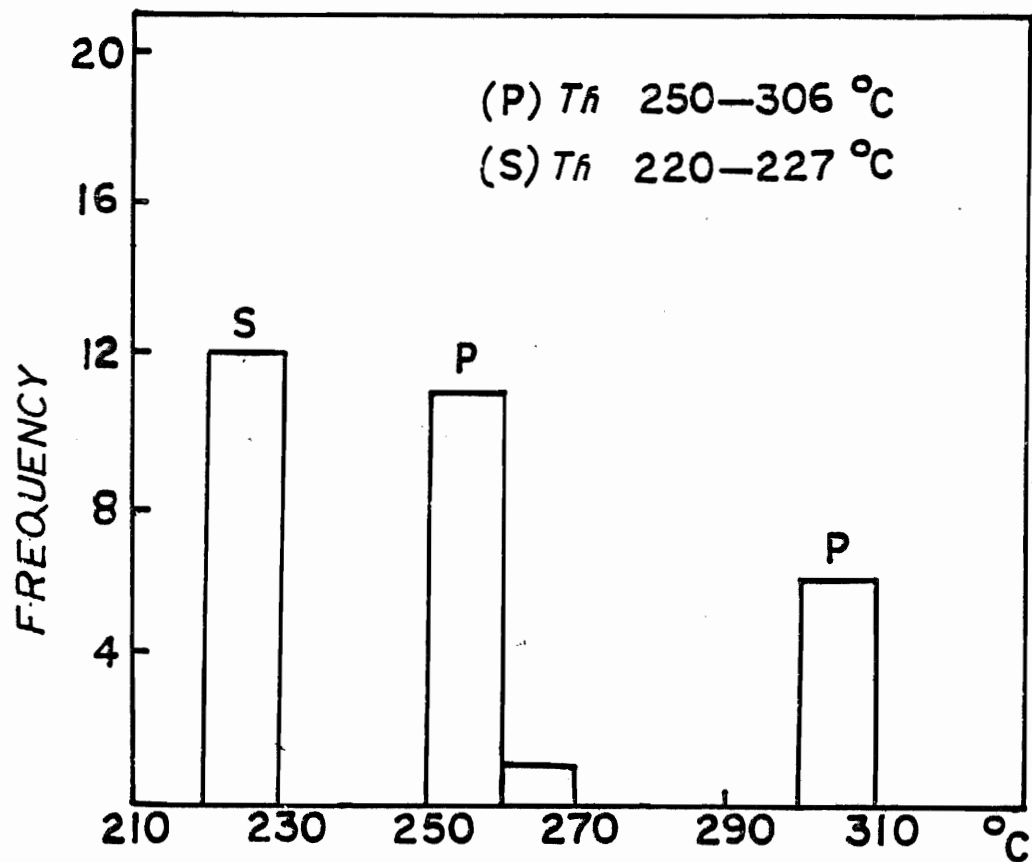


Figure 5.8 Histogram for the frequency distribution of quartz fluid inclusion temperature in quartz veins from the quartz meta-wacke basement, Gays River mine.

mineralization probably bathed the older quartz veins in the basement to form secondary inclusions within the fracture networks in quartz.

f. Freezing Experiments

The depression of the freezing point of the fluid, depends upon the salt concentration i.e. total dissolved salts (TDS). The higher the salt content, the lower the freezing point of the fluid. This above rule has to be applied with caution because of the obvious uncertainty in estimating the salinity of the fluid from the depression of freezing point for mixed salt solution. Although NaCl is frequently the dominant salt in Mississippi Valley type deposits, several details of the freezing data have proved the presence of at least some other salts other than just NaCl. This is related to the fact that pure NaCl can only lower the freezing point to -20.8°C but many inclusions have lower freezing temperatures (Roedder, 1962; 1976).

g. Method

The freezing experiments were performed by freezing the fluid inclusions solid during continuous supercooling and the inclusions were later gradually warmed up. Two to three runs were performed on the usable inclusions to enhance precision. Freezing was achieved by passing a jet of compressed gas into a heating stage mounted on the microscope. The compressed gas was cooled as it passed through a piping system immersed in liquid Nitrogen. Because of the failure of the inclusions to freeze at a reasonable temperature close to their true freezing point, gross supercooling was carried out to a temperature as low as -95°C . Some of the inclusions freeze into a solid mass of ice and become opaque during the freezing runs.

The initial melting temperature occurs when the first of the solid components melt. As the warming process continues, more solid ice melted. The freezing temperature is taken as that temperature at which the last ice crystal melts. In theory, this freezing temperature should actually be the temperature at which the first solid crystal appears. This has been found to be untrue for Mississippi Valley Type deposits and indeed gross supercooling is needed to achieve a homogeneous frozen ice. Such behaviour has been associated with the complete freedom of the solid nuclei in suspension during freezing (Roedder, 1976). Roedder pointed out that daughter crystals of NaCl and other phases in the inclusions of the Mississippi Valley Type deposits do not act as nuclei for ice.

h. Observations and Results

After continuous gross supercooling down to temperatures of -95°C no nucleation of ice was observed in the inclusions within sphalerite and ore stage calcite after several trials. In one instance, a vapour bubble in the sphalerite inclusions exhibited "brownian movement" for a short period of time and it adhered to the inclusion wall during the initial stage of cooling. No other movement or changes was seen during cooling and subsequent warming. This type of metastability was interpreted as a characteristic of inclusions formed from dense saline brines (Roedder, 1976). Aqueous inclusions in the post ore calcite and fluorite indicate considerable changes during the freezing experiments. These inclusions become completely frozen on cooling at a temperature of -75°C and are opaque. The inclusion walls in the post ore calcite become quite distinct and the relief increases with gradual cooling. Darkening from the walls into the interior of the inclusion can be observed until the

inclusion becomes completely opaque at -75°C (Fig. 5.9). Increase in the relief of the inclusion is noticeable in the aqueous inclusions in fluorite. As the temperature increases, melting starts from the interior of the inclusions towards the walls and the vapour bubble is often dislodged. The ice crystals collapse and are suspended in the melt. The melting of the last ice crystal is recorded as the freezing temperature. Since this took place within a narrow range from the initial melting of ice and the final melting, these 2 temperatures are recorded.

Freezing temperatures recorded for the post ore calcite range from -16°C to -19°C with a mean value of -17.4°C . This corresponds to an approximate value of 20.7 equivalent weight percent total dissolved salts which is believed to be NaCl (Fig. 5.10). Aqueous inclusions in post ore fluorite freeze at -17°C corresponding to 20.4 equivalent weight percent total dissolved salts. If the major proportion of the total dissolved salts is NaCl in the fluorite and post ore calcite, the estimated salinity in accord with the degree of filling will correspond to an approximate density of 1.1 gm/cm^3 for the 2 minerals (Rankin, 1978) Fig. 5.11.

Attempts to freeze the hydrocarbon inclusions in fluorite was met with difficulty as no distinct freezing behaviour was seen in cooling to -95°C . Touray and Balier (1974) and Burrus (1981) indicated the considerable difficulty encountered in freezing hydrocarbon inclusions even at temperatures as low as -140°C . Indeed Roedder (1963) reported that most hydrocarbon inclusions rarely show distinct freezing behaviour even on cooling to -180°C . Burrus (1981) indicated that the non freezing characteristic can be used to distinguish hydrocarbon inclusions from the aqueous inclusions apart from their fluorescent property.

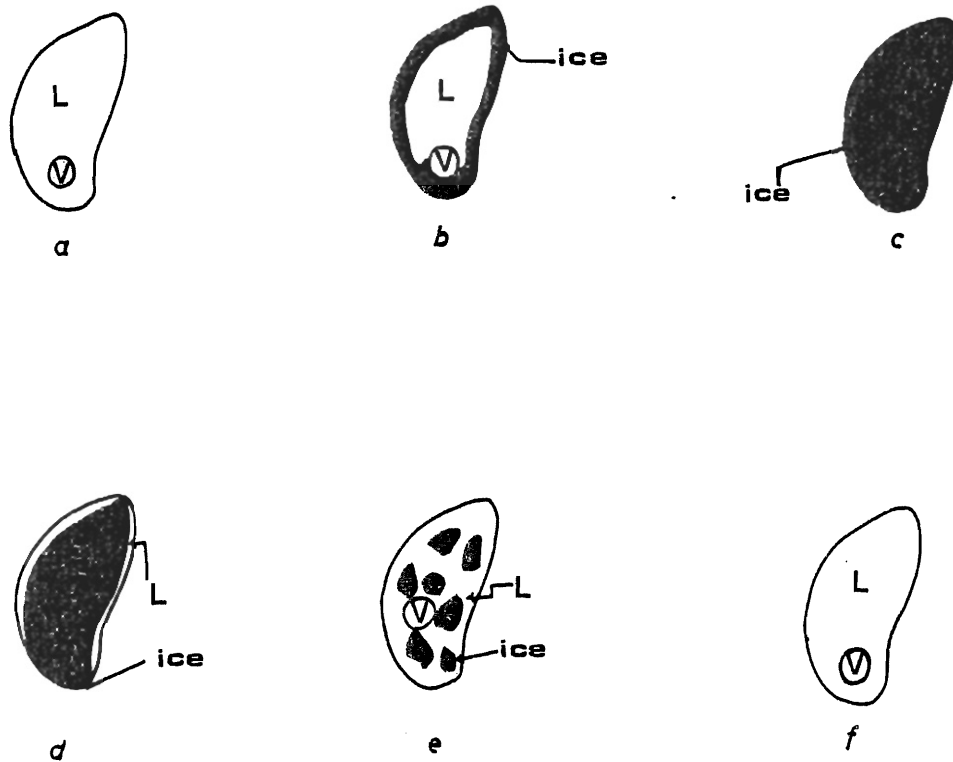


Figure 5.9 Diagrammatic representation of the freezing behaviour of post ore calcite.

- a. initial appearance before freezing run
- b. first appearance of ice on the walls of inclusion
- c. complete freezing of inclusion, note the dark appearance
- d. first appearance of liquid on warming
- e. appearance of ice blocks dislodged in the liquid phase
- f. final melting of ice, recorded as the freezing temperature.

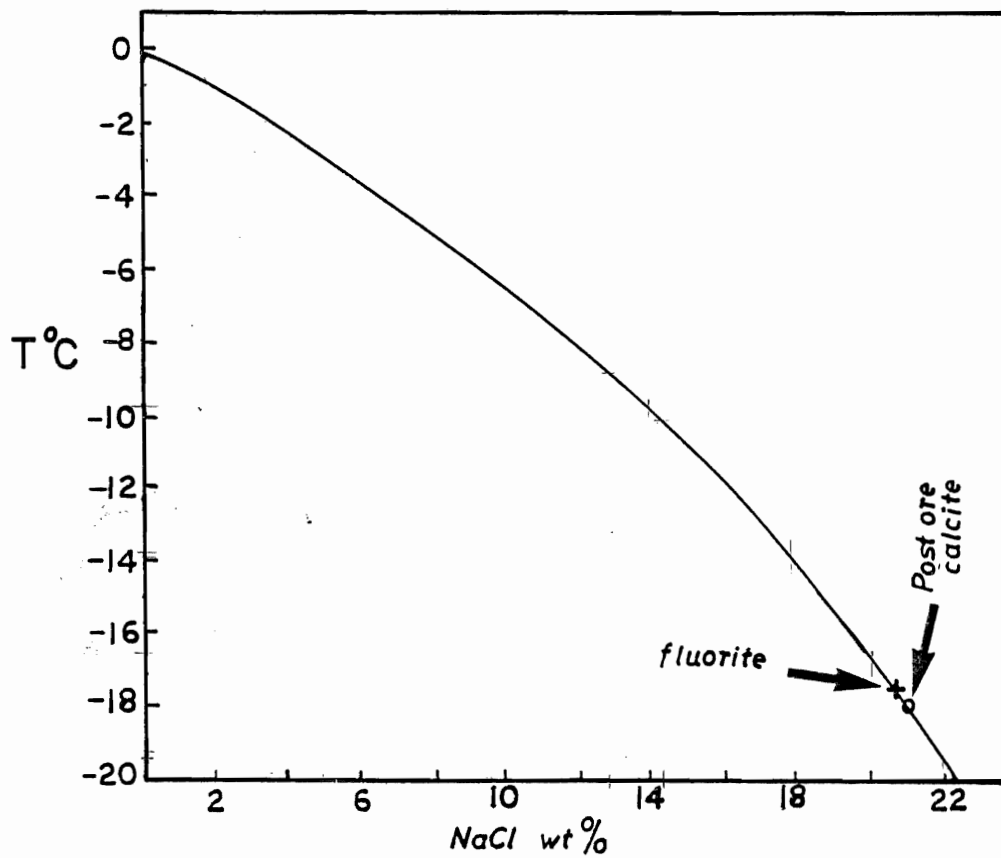


Figure 5.10 Plot of the concentrative properties of aqueous NaCl solution. (Adapted from Wolf and Brown 1966).

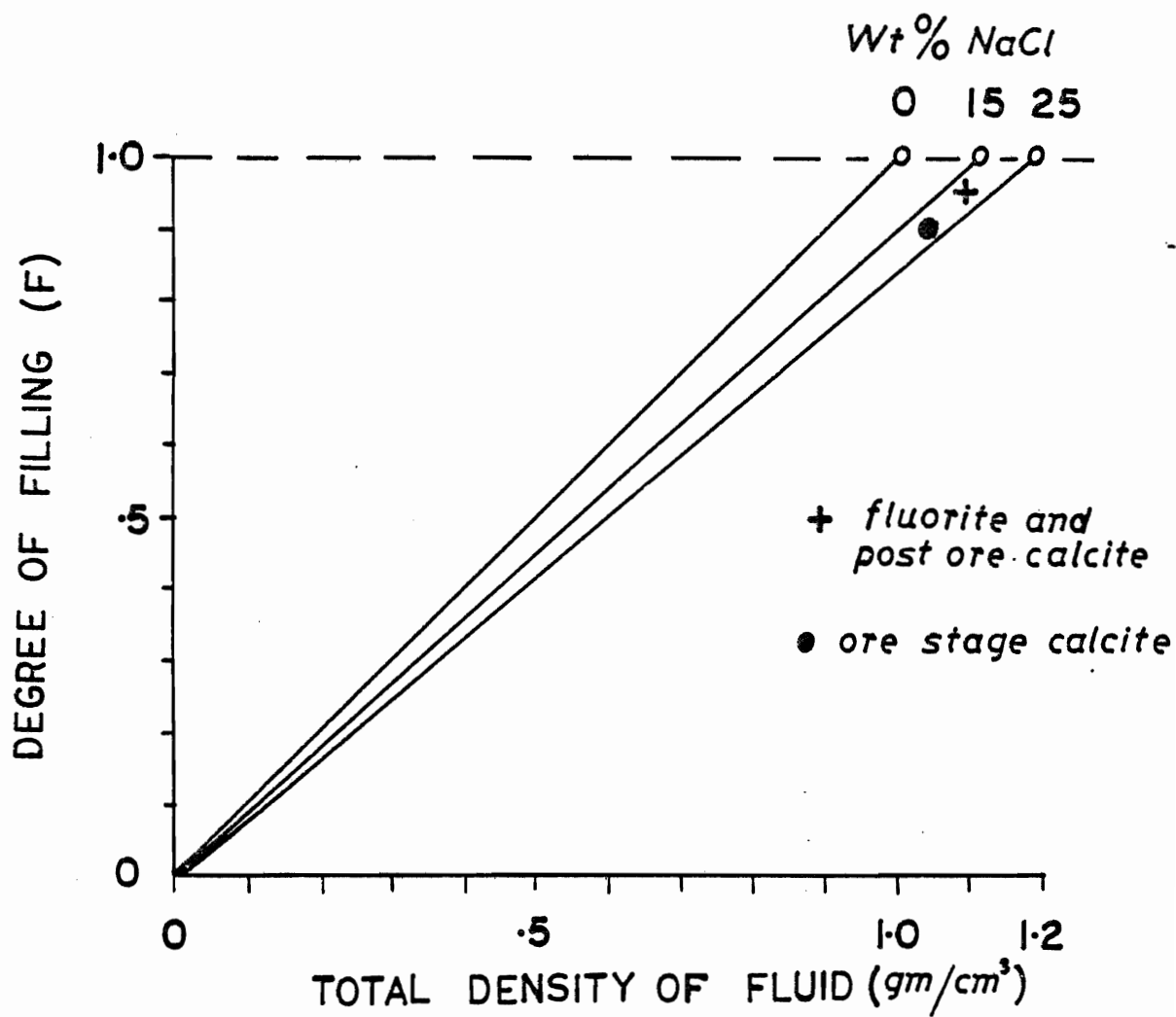


Figure 5.11 Relationship between the degree of filling at 25°C and the total density of the inclusion for different NaCl brines. After Rankin (1978).

5.5 Pressure Corrections

The adjustment of the homogenization temperatures for the pressure existing at the time of the formation of the inclusions is of considerable importance in fluid inclusion geothermometry. The homogenization temperature represents the minimum temperature of formation in a non-boiling environment. In order to obtain the temperature of formation from the homogenization temperature of a primary inclusion, an adjustment for the difference between the vapour pressure of the solution and the total pressure must be made. Klevtsov and Lemmlin (1959) showed that the pressure correction also depends on the salinity of the hydrothermal fluid from which the inclusion grew. A confining pressure at the time of the formation of the inclusion normally decreases the size of the vapour phase and this will considerably reduce the homogenization temperature. Indeed, the pressure correction involves the estimation of the stratigraphic thicknesses or cover at the time of mineralization.

The Gays River lead-zinc mineralization is hosted in a carbonate build up of Lower Carboniferous (Windsor) age within the Maritime Carboniferous basin. If the Gays River lead-zinc mineralization was deposited simultaneously with the carbonate host (i.e. syngenetic) no pressure correction is needed for the temperatures of homogenization of the fluid inclusions studied. However, in this instance, there would have been evidence of boiling. No evidence of boiling was seen in the inclusions studied. Boiling in another situation may be prevented by the hydrostatic head (hydrostatic pressure) that prevailed at the time of formation of the inclusions (Haas, 1971). In this instance, it is estimated that a minimum depth of 170 metres (17 bars) will prevent the Gays River ore solutions from boiling and a minimum depth of 20 metres (2 bars) will prevent

the Gays River post ore fluorite and calcite solutions from boiling on the basis of their salinities and homogenization temperatures (Haas, 1971) Fig. 5.12. At this minimum depth however, it is doubtful whether algal stromatolites will thrive. But high grade lead-zinc sulfide mineralization are commonly contained in the intra pore and inter pore spaces of the algal stromatolites and within well grown bioclasts associated with the stromatolites at Gays River. In general, the crosscutting relationship and the nature of the high grade vein sulfide ores, the presence of block relics of the host carbonate within the massive sulfide vein ores and the present fluid inclusion homogenization temperatures in a non-boiling environment suggest that the main mineralization event post-dated the host carbonate deposition. Galena and sphalerite veinlets interfinger into gypsum and anhydrite and also replace them in few localities in the 119 drift area. This also suggests that the sulfide deposition was later than the evaporite sequence overlying the Gays River carbonate.

If the lead-zinc mineralization occurred after all the Carboniferous sequences have been deposited, a lithostatic pressure correction will have to be applied to the homogenization temperatures. At present only about 35-60 metres of glacial overburden overlies the Carboniferous sequence at Gays River. Hacquebard (1970) determined a vitrinite reflectance of .84% Ro and .96% Ro for the coaly particles (bark vitrains) in the Lower Carboniferous Horton group in the Gore district (approximately 24 kilometres N.W. of Gays River). Since organic metamorphism could reflect the depth of burial if the effective time of cooking is known, this high reflectance of vitrinite requires a thick cover over a considerable length of time or in another instance a high heat flow (high geothermal gradient) over a short time period. On the assumption that the high reflectance was

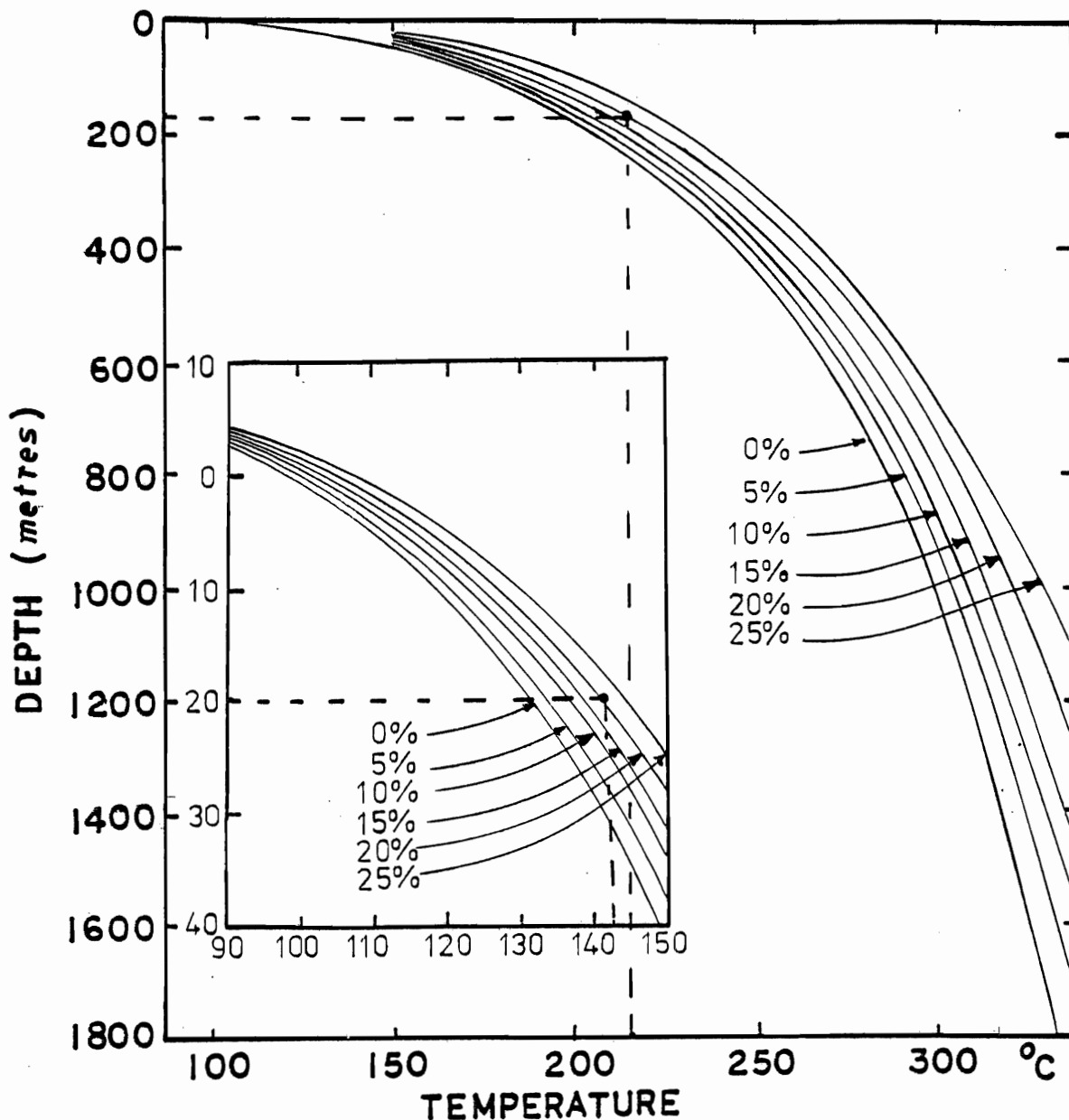


Figure 5.12 Boiling-point curves for H_2O liquid (0 wt %) and for brine of constant composition given in wt % NaCl. Relations between 100°C and 150°C is enclosed in the inset. The temperature at 0 metres of each curve is the boiling point for the liquid at 1.0 atmosphere. Load pressure \equiv atmospheric pressure at sea level. Uncertainty is contained in the width of the lines. Adapted from Haas (1971).

caused by a depth of burial over a considerable time (Carboniferous to Triassic) Hacquebard (1970) extrapolated a thickness of at least 3.6 kilometres of Upper Carboniferous sequence on the Lower Carboniferous Horton group in this area. If such a thickness of strata overlies Gays River at the time of mineralization, an approximate lithostatic pressure of 900 bars will have to be applied as pressure correction. This will correct the homogenization temperatures of sphalerite from 215°C to 305°C , ore stage calcite from $172 \pm 2^{\circ}\text{C}$ to $262 \pm 2^{\circ}\text{C}$, post ore calcite from $143 \pm 2^{\circ}\text{C}$ to $233 \pm 2^{\circ}\text{C}$, post ore fluorite from $142 \pm 2^{\circ}\text{C}$ to $232 \pm 2^{\circ}\text{C}$ and post ore barite from $137 \pm 2^{\circ}\text{C}$ to $227 \pm 2^{\circ}\text{C}$ on the basis of the inclusion salinity, homogenization temperature and pressure (Fig. 5.13). These corrections appear unreasonably high and not compatible with the simple mineralogy of the deposit e.g. the low ratios of copper, and the absence of sulfosalts and precious metals. These high temperatures are not typical of "Mississippi Valley Type deposits".

Eaton (1980) reported homogenization temperatures of $142 \pm 8^{\circ}\text{C}$ for the Gays River fluorite and $172 \pm 2^{\circ}\text{C}$ for the calcite. Eaton corrected these temperatures from $142 \pm 8^{\circ}\text{C}$ to $157 \pm 8^{\circ}\text{C}$ and $172 \pm 2^{\circ}\text{C}$ to $185 \pm 2^{\circ}\text{C}$ on the basis of 350 bars hydrostatic pressure. A hydrostatic pressure is less acceptable for the pressure correction needed if the geometry of the vein mineralization in fractures and faults are considered. If hydraulic fracturing through fluid overpressures created the normal faults and fractures in the carbonate rocks then the hydrostatic pressure during the vein formation will be equal to the lithostatic pressure. Hence, the lithostatic pressure will represent the appropriate correction needed. In another instance, if the mineralization event closely succeeded the deposition and diagenesis of the carbonate host and evaporite within a

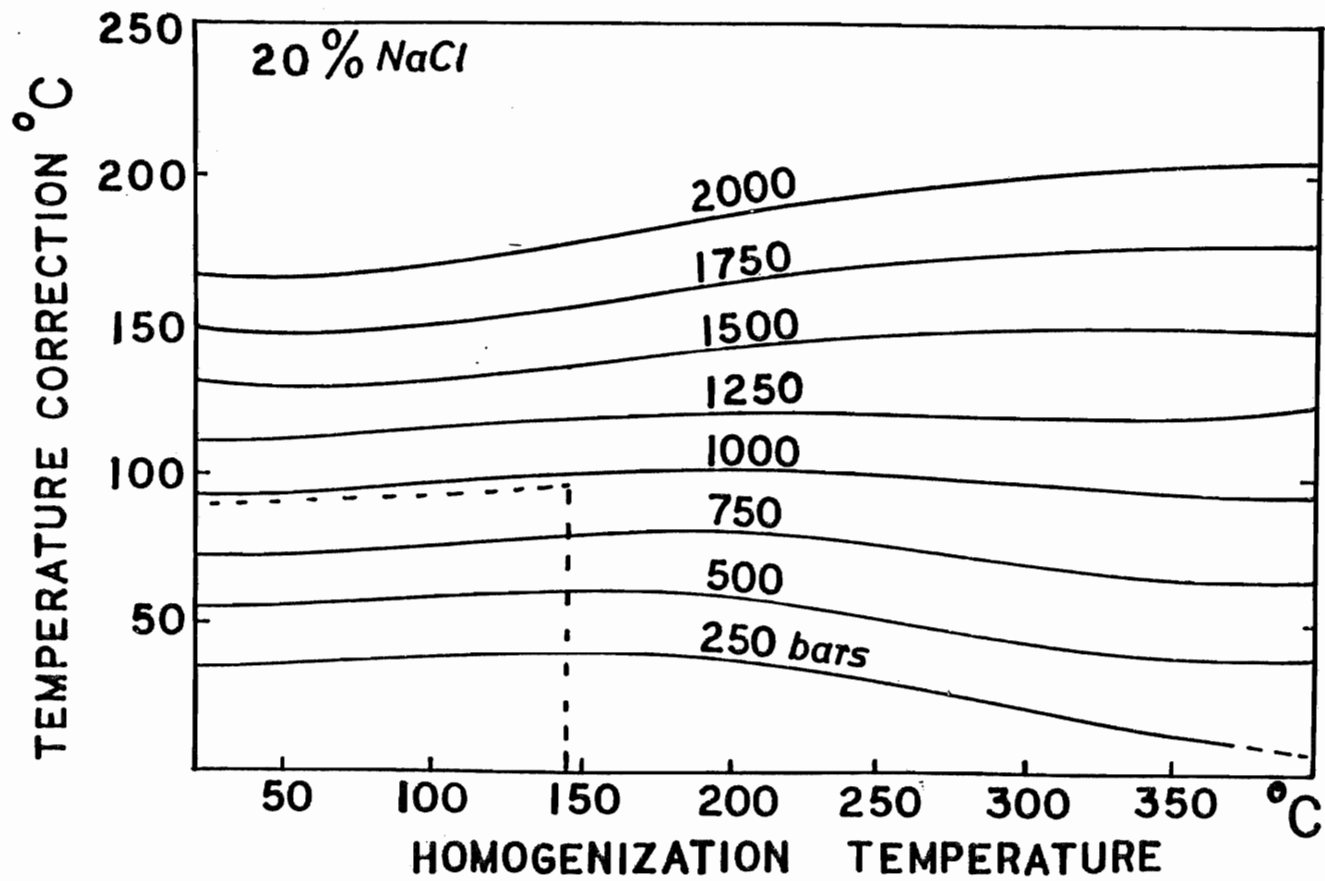


Figure 5.13 Temperature correction for a 20% NaCl solution as a function of the homogenization temperature and pressure. Modified after Potter (1977).

short time interval, a pressure correction for the homogenization temperature may not be needed. Beales et al. (1974) reported a similar remanent magnetization for the ore and host in the Newfoundland zinc deposit. These authors concluded that the emplacement of the ores seems close in a geological time sense. If the sulfide mineralization at Gays River closely succeeded the deposition and diagenesis of the carbonate host, the present homogenization temperature of 214°C for sphalerite, 172°C for ore stage calcite, 142°C for post ore calcite, 143°C for fluorite and 137°C for barite will be representative of the trapping temperatures. Analysis of bitumen and illite associated with the massive vein sphalerite indicate the presence of 2 m muscovite (a polymorph of illite). This suggests a temperature of 215°C to 230°C which is compatible with the homogenization temperatures in the vein sphalerite. Boiling was probably prevented by a minimum depth of 170 metres. If the hydrostatic pressure equals lithostatic pressure at this period, normal faulting, through hydraulic fracturing might have resulted from fluid overpressures generated during the dewatering of the Gays River evaporite.

5.6 Discussion

The Gays River sphalerite, calcite, fluorite and barite appear to have been deposited in the range of temperatures from 214°C to 137°C. Primary inclusions in sphalerite homogenize at 214°C, ore stage calcite at 172°C, post ore calcite at 142°C, fluorite at 143°C and barite at 137°C (Fig. 5.14). Although these homogenization temperatures can be theoret-

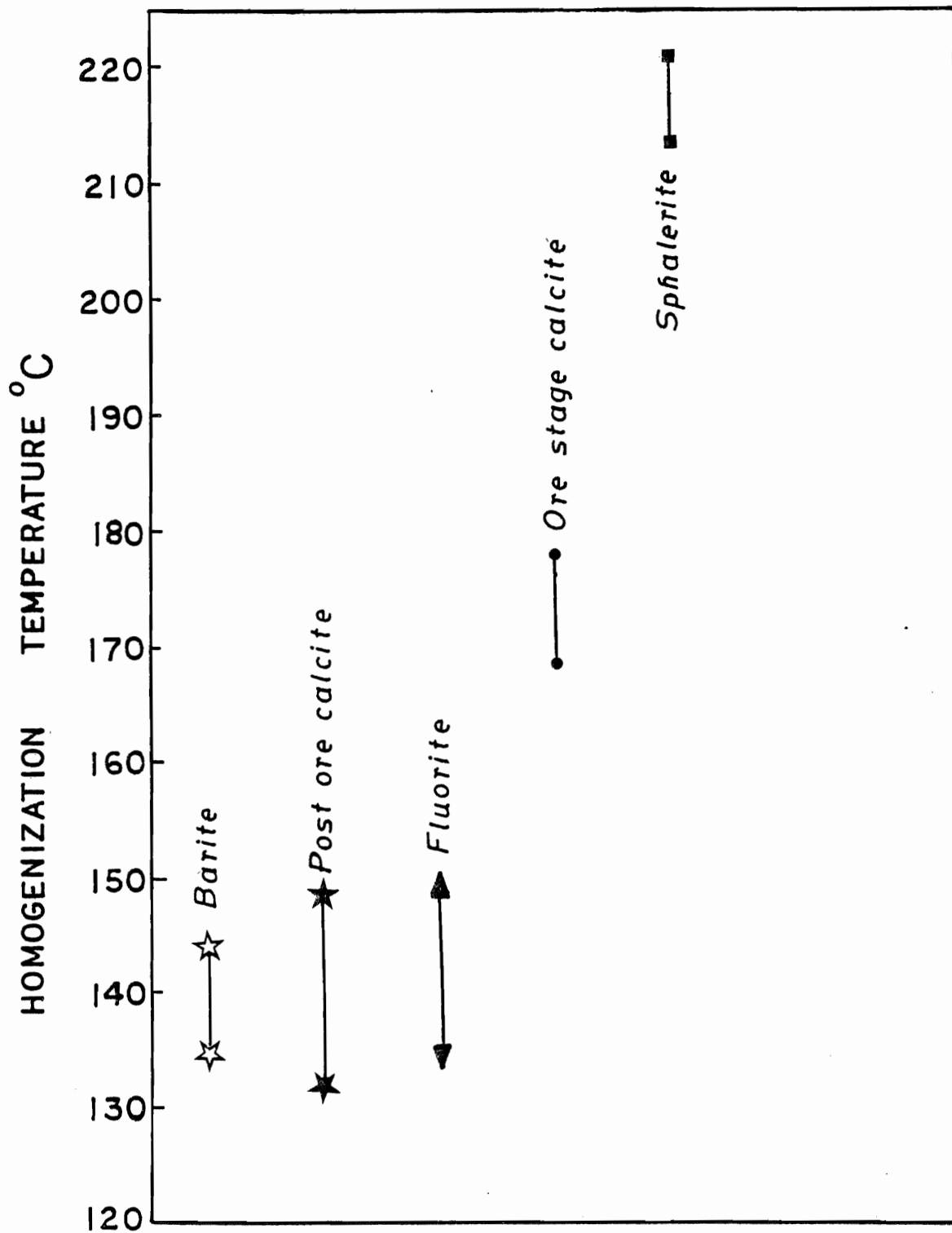


Figure 5.14 Summary comparison of homogenization temperatures in sphalerite, calcite, fluorite and barite; Gays River mine.

ically considered as the minimum temperature of formation, they appear to be representative of the trapping temperatures for the inclusions. The salinity of the hydrothermal solution that was determined from the ice melting temperatures of the post ore calcite and fluorite is approximately 20.5 equivalent weight percent NaCl. This warrants a minimum depth of 170 metres to prevent boiling during sphalerite precipitation.

The estimated temperatures of the hydrothermal solutions that was responsible for the Gays River lead-zinc mineralization put great constraints on any genetic model that may be applicable to this deposit. Macleod (1975) concluded that the lead-zinc mineralization closely followed evaporite deposition and dolomitization of the carbonate build up. Macleod indicated that the mineralization must have been derived from metal rich connate brines supplied by the evaporites within a temperature range of 0-70°C in the realm of diagenesis.

The present fluid inclusion temperatures illustrate that the Gays River sphalerite, galena, calcite, fluorite, and barite were not deposited by low temperature diagenetic brines but from highly saline hydrothermal brines. The implication of this suggestion with regards to the genesis of the deposit is further discussed in the subsequent chapter.

CHAPTER 6

STABLE ISOTOPE GEOCHEMISTRY

6.1 Introduction

One of the major aims of mineral deposits research is to identify the source or sources of the different components of the mineralizing solutions from which the ore and the gangue minerals were formed. The interpretation of isotopic and geochemical data combined with geological information on Mississippi Valley Type ore deposits have placed significant constraints on the several possible hypotheses of ore formation.

Isotopic investigations of sulfur, lead, oxygen and carbon of Mississippi Valley Type ores are different in several respects from one district to the other as shown for the south-east Missouri lead-zinc district, the Appalachian Valley zinc district in the eastern United States, and the Pine Point deposits in N.W. Territories (Heyl et al., 1974). Sulfur isotope studies by Ault and Kulp (1959), Jensen and Dessau (1967), Brown (1967), Pinckney and Rafter (1972) indicate that the bulk of the sulfur in these Mississippi Valley Type deposits is of crustal origin and each district exhibits a distinctive range in the $\delta^{34}\text{S}$ of the sulfate and sulfide minerals.

Lead in galena in all large deposits in the Mississippi Valley of the United States is appreciably enriched in radiogenic J-type anomalous lead isotopes compared to the ordinary lead of other localities (Heyl et al., 1974). The enrichment in the more radiogenic isotopes is interpreted as an indication of a shallow crustal source for the lead either from the underlying basement rocks or the associated carbonate or sandstone.

Previous investigation of the oxygen and carbon isotopic composition in the carbonate host for lead and zinc deposits have shown that the $^{18}\text{O}/^{16}\text{O}$ ratios of the carbonate hosts tend to decrease with proximity to ore in the Upper Mississippi Valley and Tri-state districts and distinct variations exist in the different carbonate stages (Hall and Friedman, 1969). At the Tynagh deposit in central Ireland, Boast et al., (1981) reported that mineralized limestone, ore stage carbonate and post-ore carbonate are significantly depleted in the heavier isotope of carbon and oxygen with respect to the unmineralized limestone. These depletions in the $\delta^{18}\text{O}$ of the host rocks are interpreted to have been caused by the hydrothermal alteration and isotopic exchange with the ore fluids.

As a part of the objective of this thesis, the isotopic composition of sulfur, lead, oxygen and carbon in the Gays River deposit are examined and interpreted in order to better understand the implications of these on the ore genesis.

6.2 Sulfur Isotopic Composition

a. Principles and Assumptions

Sulfur in the crust has four stable isotopes with the following abundance; $^{32}\text{S} = 95.02\%$, $^{33}\text{S} = 0.75\%$, $^{34}\text{S} = 4.21\%$ and $^{36}\text{S} = 0.02\%$. The sulfur isotopic composition of any mineral or compound is commonly expressed in terms of $\delta^{34}\text{S}$ where the $\delta^{34}\text{S}$ of mineral species x is defined as

$$\delta^{34}\text{S}_x(\text{‰}) = \frac{\left(\frac{^{34}\text{S}}{^{32}\text{S}}\right)_x - \left(\frac{^{34}\text{S}}{^{32}\text{S}}\right)_{\text{std}}}{\left(\frac{^{34}\text{S}}{^{32}\text{S}}\right)_{\text{std}}} \times 1000$$

where $^{34}\text{S}/^{32}\text{S}$ std is the sulfur isotopic composition of troilite of Canyon Diablo meteorite (CDT) in which the $^{34}\text{S}/^{32}\text{S}$ is 0.0450045 (Macnamara and Thode, 1950; Ault and Jensen, 1963). This is an appropriate standard be-

cause the isotopic composition of sulfur in mafic igneous rocks is identical to that of meteorites (Schneider, 1970). Hence the $\delta^{34}\text{S}$ of a sample is the measurement of the change that has taken place since its initial introduction into the earth crust.

Fractionation

Sulfur isotopes can be fractionated in equilibrium systems and during kinetic reactions. In systems where isotopic equilibration is approached, such quantity as the fractionation factor may become significant. The fractionation factor α between 2 mineral species A and B is defined as

$$\alpha_{A-B} = \frac{R_A}{R_B} = \frac{\delta_A + 1000}{\delta_B + 1000}$$

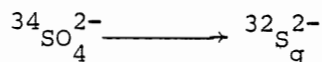
where R is the isotopic ratio $^{34}\text{S}/^{32}\text{S}$. The quantity $10^3 \ln \alpha$ is defined as the per mil fractionation. This logarithmic function has theoretical and experimental significance. For perfect gases, $\ln \alpha$ varies as $\frac{1}{T^2}$ (K) and $\frac{1}{T}$ (K) in the high and low temperature limits respectively and commonly result in linear curves. $10^3 \ln \alpha$ can be approximated by the Δ value where

$$\Delta_{A-B} = \delta_A - \delta_B \frac{\Omega}{10^3} \ln \alpha_{A-B}$$

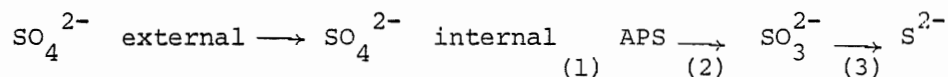
This approximation can be derived by subtracting the δ values of the mineral pairs when the δ value difference is less than or equal to 10. The linear relationship of the fractionation factor with temperature enables the construction of geologic thermometers in equilibrium systems with a reasonable degree of precision. However such geothermometers in some hydrothermal ore deposits give temperatures that are too high. Although such high temperatures can be interpreted with a quenched isotope equilibrium distribution from greater depth, the δ values commonly demonstrate disequilibrium relationships. Where isotopic equilibrium is approached,

the variations in the $^{32}\text{S}/^{34}\text{S}$ distributions among naturally occurring coexisting sulfide minerals are systematic and consistent with the estimates of the metal-sulfur bond strengths (Bachinski, 1969). On the basis of the sulfide mineral bond strengths, Bachinski (1969) predicted that the $\delta^{34}\text{S}$ values of coexisting sulfide minerals will decrease in the order pyrite > sphalerite > chalcopyrite > galena under equilibrium conditions. Hence for pairs of base metal sulfides that have been deposited simultaneously from a common hydrothermal fluid, a specific sulfur isotope thermometer can be constructed on the basis of their enrichment factors (Sakai 1968, Czamanske and Rye 1974).

Apart from the equilibrium fractionation reactions, the most important cause for the variation in sulfur isotopic composition is by kinetic reactions through the action of sulfate reducing anaerobic bacteria. These bacteria convert SO_4 to H_2S in rate-limiting steps of reduction. The H_2S liberated is enriched in ^{32}S as indicated in the reaction



Trudinger and Chambers (1973) and Rees (1973) concluded that this reaction proceeds in at least three steps as shown;



The conversion of sulfate to sulfide gas may lead to variable enrichment of ^{32}S depending on which step is rate-limiting. Rees (1973) indicated that step 1 of the reaction is only accompanied by 3 ‰ fractionation. Tudge and Thode (1950) estimated a fractionation factor $\alpha = 1.075$ at 25°C for the chemical equilibrium in the total conversion of the sulfate to sulfide. This exchange equilibrium is capable of causing an enrichment of H_2S in ^{32}S of up to 75 ‰ at 25°C relative to the sulfate. Trudinger

and Chambers (1973) indicated that such extreme fractionation can only be approached in nature by enzyme catalyzed reactions in the sulfate reducing bacteria.

The chief concern of previous sulfur isotope studies has been to investigate the variability in $\delta^{34}\text{S}$ values and their deviation from magmatic values. Ore deposits in which the sulfide minerals have $\delta^{34}\text{S}$ values near 0‰ were interpreted to have formed from magmatic fluids, while deposits with variable $\delta^{34}\text{S}$ values were interpreted as biogenic. More recent studies of Sakai 1968, Ohmoto (1972) Rye and Ohmoto (1974) have shown that the $\delta^{34}\text{S}$ values of sulfide minerals reflect not only the temperature and isotopic composition of sulfur in the fluid from which they formed but may also be controlled by pH, the fugacities of oxygen and sulfur, the total sulfur content and the ionic strength of the ore forming fluid. These factors are of immense importance with the approach of isotopic equilibrium between the mineral species and the ore forming fluid.

b. Sample Selection

Samples of sulfate and sulfide minerals were collected from specific coordinates within the Gays River decline. Sulfate samples were collected where continuous drifting for ore had exposed gypsum and anhydrite stratigraphically above the ore body. Barite samples were collected underground where they occur as intergrowths with sphalerite, and also as galena and sphalerite overgrowths in fracture related cavities. Systematic samples of sphalerite and galena were collected along the strike length and across the massive sulfide veins in drifts 104, 107, 4490 and 4470 and from the stratiform lead-zinc mineralization. Marcasite and pyrite samples with no direct contact with sphalerite and galena were

collected in geopetal cavities and fractures within the carbonate host in the drifts 119 and 201. Additional samples of gypsum, anhydrite, sphalerite and galena were collected from mineralized drill cores at the distal ends of the N-E trending ore body.

c. Sample Preparation

Separates of sulfate and sulfide minerals were selected by hand-picking the mineral grains under a binocular microscope. The samples were broken into pieces in order to facilitate the handpicking procedure. Coarse crystalline gypsum, anhydrite, barite galena and massive sphalerite were concentrated by handpicking alone. Monomineralic samples of complex sulfide intergrowths were obtained by a repetitive heavy liquid mineral separation method through the use of tetrabromoethane (S.G,2.9) and methylene iodide (S.G,3.2). The sulfide "sinks" were thoroughly washed in acetone and dried. The mineralogical purity of the sulfate and sulfide samples were tested by the use of XRD technique. Most of the samples analyzed are 100% pure.

The pure sulfate and sulfide samples were sent to the Nuclear Research Centre of the McMaster University and Geochron Laboratories, Massachusetts, for the analyses of their sulfur isotopic compositions. Analysis were made on the sulfur dioxide gas from the sulfate and sulfide samples and the sulfur isotopic composition (δS^{34}) were measured within a precision of ± 0.2 per ml. $\delta^{34}S$ values are reported relative to the internationally accepted Canyon Diablo troilite standard (CDT) where

$$\delta^{34}S (\text{‰}) = \frac{(^{34}S/^{32}S) - (^{34}S/^{32}S)_{\text{CDT}}}{(^{34}S/^{32}S)_{\text{CDT}}} \times 1000$$

d. Sulfur Isotope Ratios: Tables IV-1, IV-2, IV-3 in Appendix IV

i. Sulfate Minerals

Twelve samples of gypsum, anhydrite and barite were analyzed for their sulfur isotopic composition. The precipitation of these three sulfate minerals span the time from the pre-ore to the post-ore stages in the mineral paragenesis. Despite this time-space relationship, gypsum, anhydrite and barite at Gays River have very similar sulfur isotopic compositions with identical mean values. The range of $\delta^{34}\text{S}$ values in 5 gypsum samples fall between +13.1 to +16.1 per mil with a mean of 14.62 per mil; 5 anhydrite samples have $\delta^{34}\text{S}$ values ranging from +9.6 to 15.60 per mil with a mean of +14.00 per mil and the 2 samples of barite have exactly the same $\delta^{34}\text{S}$ values of +14.1 per mil (Table IV-1).

ii. Sulfide Minerals

The sulfur isotopic composition of the sulfide minerals show distinct groupings of $\delta^{34}\text{S}$ values which closely follow paragenesis.

Pre-ore marcasite: Three samples of pre-ore stratiform clots of diagenetic marcasite with no direct contact with sphalerite and galena have heavy values of $\delta^{34}\text{S}$ ranging from +10.7 to +13.27 per mil with a mean value of +11.72 per mil.

Ore-stage sulfides: The ore stage sulfide minerals consist of the stratiform and vein sphalerite, galena and chalcopryrite. Isotopic ratios were determined for 4 samples of microcrystalline stratiform sphalerite, 11 samples of massive fine to coarse grained vein sphalerite, 8 microcrystalline stratiform galena, 9 coarse crystalline vein galena and 1 sample of chalcopryrite. The $\delta^{34}\text{S}$ values of these ore stage sulfide minerals are similar to the values in the pre-ore marcasite. All the $\delta^{34}\text{S}$ values

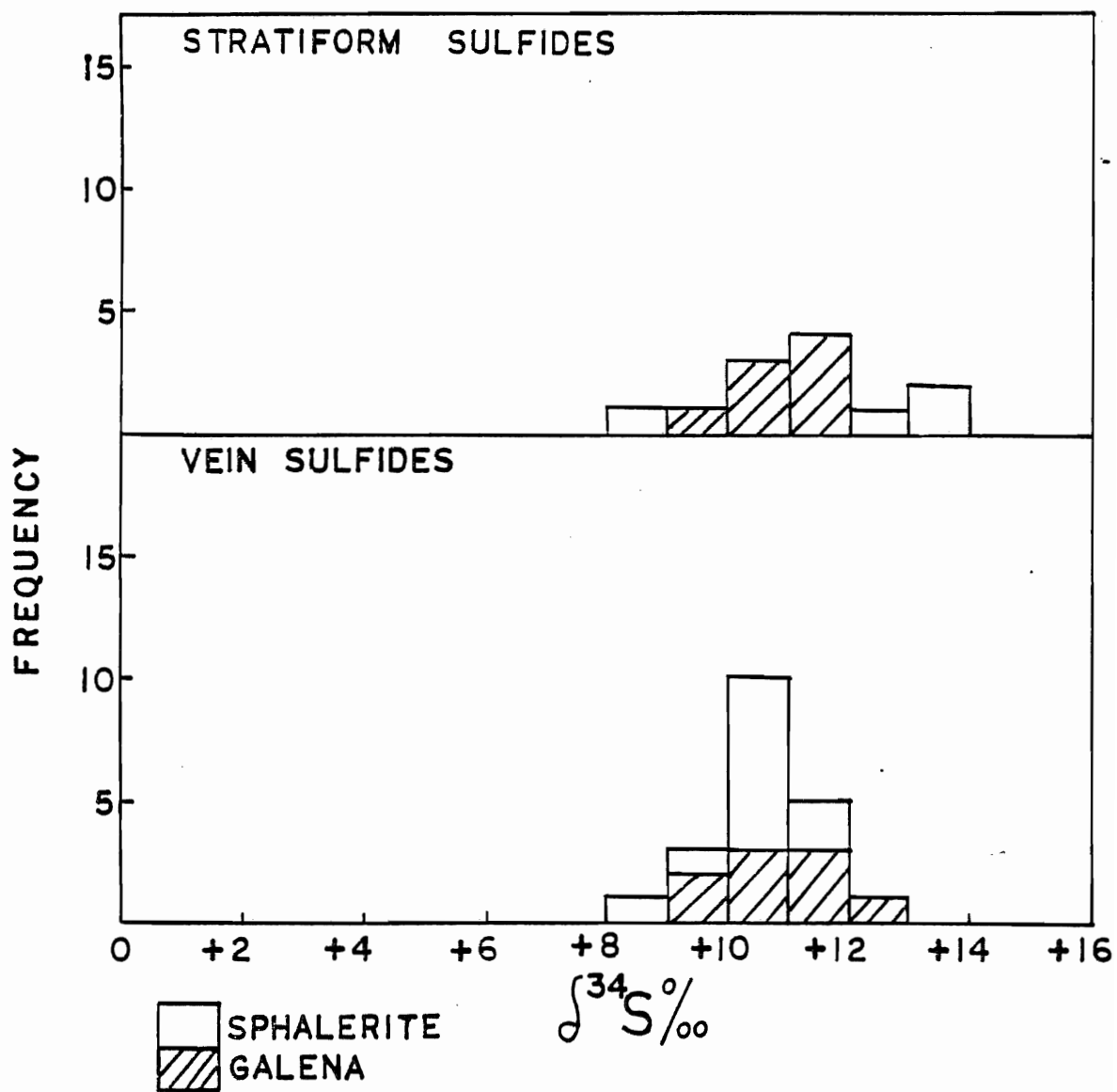
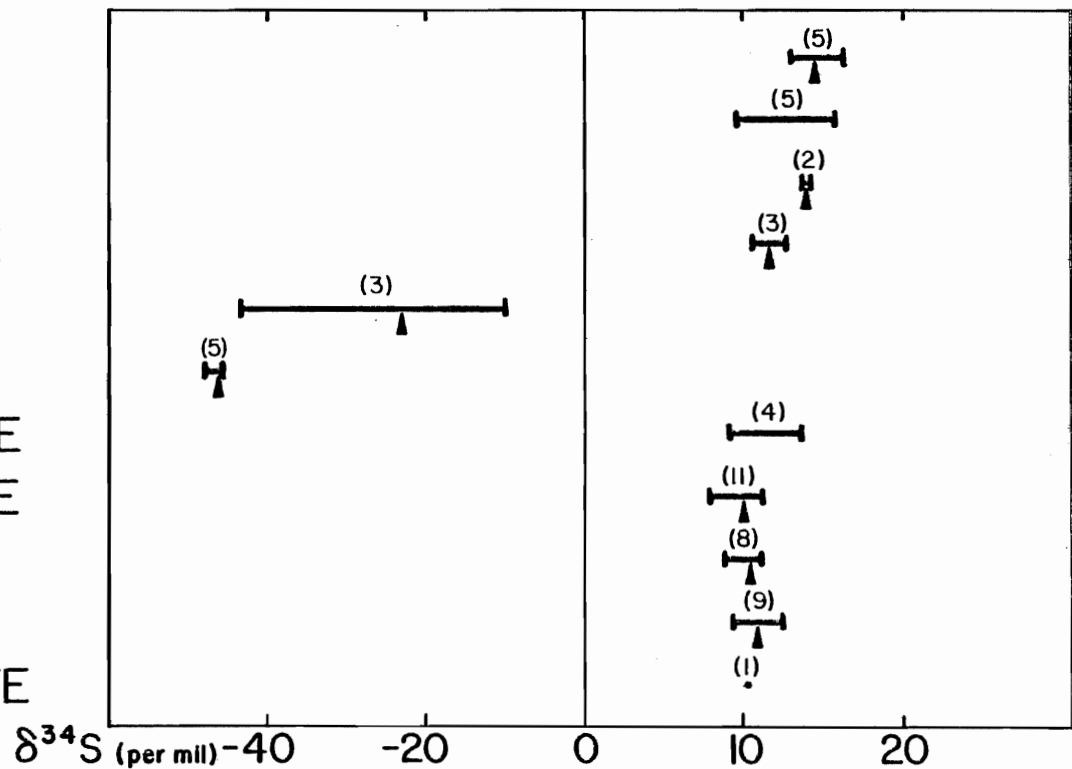


Figure 6.1 Histogram of all sulfur isotope ratios in the stratiform and vein sphalerite and galena.

GYPSUM
 ANHYDRITE
 BARITE
 E. MARCASITE
 L. MARCASITE
 L. PYRITE
 S. SPHALERITE
 V. SPHALERITE
 S. GALENA
 V. GALENA
 CHALCOPYRITE



$$\delta^{34}\text{S} \text{ is defined as } \delta^{34}\text{S} = \left[\frac{\left(\frac{^{34}\text{S}}{^{32}\text{S}}\right)_{\text{sample}} - \left(\frac{^{34}\text{S}}{^{32}\text{S}}\right)_{\text{standard}}}{\left(\frac{^{34}\text{S}}{^{32}\text{S}}\right)_{\text{standard}}} \right] \times 10^3\text{‰}$$

Figure 6.2 Sulfur isotope ratios of sulfate and sulfide minerals at Gays River. E. - early, L. - late, S. - stratiform, V. - vein.

in sphalerite, galena and chalcopyrite are heavy with a range of +8.0 to +13.65 per mil and a mean of +10.86 per mil.

$\delta^{34}\text{S}$ values in stratiform sphalerite range from +8.7 to +13.65 per mil with a mean of +12.02 per mil, vein sphalerite range from +8.0 to +11.4 per mil with a mean of +10.31 per mil, stratiform galena range from +9.4 to 11.7 per mil with a mean of +10.79 per mil, vein galena range from +9.5 to +12.1 per mil with a mean of +10.92 per mil, and chalcopyrite gave a $\delta^{34}\text{S}$ value of +10.40 per mil (Figs. 6.1, 6.2).

Post ore marcasite and pyrite: The post ore marcasite and pyrite display variable sulfur isotopic ratios that are markedly different from the ore-stage sulfide minerals. Post ore marcasite overgrowths along unmineralized fractures, exhibit a broad range of $\delta^{34}\text{S}$ from -9.7 to -42.9 per mil with a mean of -22.8 per mil. Post ore pyrite has $\delta^{34}\text{S}$ values within a narrow range of -45.2 to -46.0 per mil and a mean of -45.6 per mil.

e. Interpretation of the Sulfur Isotope Ratios

i. Sulfate Minerals

The remarkable similarities of the sulfur isotopic composition in the pre-ore anhydrite, post ore gypsum (selenite) and barite point to either an identical sulfur isotopic composition of the source sulfate or a uniform isotopic fractionation mechanism for the sulfur sources in these sulfate minerals. Mean $\delta^{34}\text{S}$ values for anhydrite is +14.00 per mil, gypsum, +14.62 per mil and barite +14.10 per mil.

The Gays River evaporite sequence is believed to represent a part of the basal anhydrite of the Mississippian Windsor Basin (Giles and Boehner 1979). If this gypsum and anhydrite sequence represents direct precipitates from the Mississippian Windsor sea, their sulfur isotopic

composition should be identical to the values of $\delta^{34}\text{S}$ of the Mississippian evaporite. Present day sea-water sulfate has a remarkably consistent isotopic composition (Rees et al, 1978) although the $\delta^{34}\text{S}$ values of sea-water sulfate has varied during geological time (Thode and Monster, 1965; Holser and Kaplan, 1966). The isotopic fractionation that is associated with sulfate species that is precipitated from sea water brine is believed to be negligible (Thode and Monster 1965). These authors indicate a fractionation factor of 1.00165 for the brine-sulfate precipitation reaction.

$$\text{i.e. } \alpha = \frac{{}^{34}\text{S}/{}^{32}\text{S}_{\text{ gypsum}}}{{}^{34}\text{S}/{}^{32}\text{S}_{\text{ brine solution}}} = 1.00165 \pm 0.00012$$

$$\text{or } \Delta^{34}\text{S} = \delta^{34}\text{S}_{\text{ gypsum}} - \delta^{34}\text{S}_{\text{ brine}} = 1.65 \pm 0.12 \text{ per mil (Thode and Monster 1965).}$$

Thode and Monster indicated that the $\delta^{34}\text{S}$ values of evaporite samples are therefore very close to that of the ancient seas from which they are derived. Mississippian marine evaporitic sulfate are believed to exhibit a range of $\delta^{34}\text{S}$ values from +13.6 to 22.6 per mil with a best value of +14.0 per mil (Thode and Monster 1965). This strongly suggests that sulfur in the Gays River gypsum and anhydrite is derived from a seawater source. Gypsum as selenite is derived from the hydration of the pre-existing anhydrite without a significant change in the primary sulfur isotopic composition.

Holser and Kaplan (1966) indicated that primary gypsum and anhydrite are commonly identical to one another isotopically and the successive alterations to anhydrite and back to gypsum do not change the sulfur-isotope composition significantly. Thus, the remarkable similarity in

the $\delta^{34}\text{S}$ values of the pre-ore anhydrite and post-ore gypsum (selenite) at Gays River confirm that the subsequent hydration of anhydrite to gypsum at later periods is not accompanied by significant change in their sulfur isotopic composition. The lowest $\delta^{34}\text{S}$ value of +9.6 in the anhydrite sample AGR 117 is quite unusual for Mississippian evaporite. Thode and Monster (1965) indicated a best value of +9.6 for the Permian evaporite. Although this one $\delta^{34}\text{S}$ value for sample AGR 117 could possibly be interpreted as caused by the effect of Permian sea water influx during the diagenesis of the Gays River anhydrite, the present author believes that this interpretation is unlikely. Instead, the light $\delta^{34}\text{S}$ value could have resulted from the fractionation effects caused by sulfate reducing bacteria in an open system. Sulfate reducing bacteria are commonly found in association with organic material and can produce significant kinetic isotope effect at low temperatures (Trudinger and Chambers, 1973). Sample AGR 117 is located at the evaporite/carbonate contact in drift 119. The carbonate host in this area contains abundant organic material in the form of algae and bioclasts. This is compatible with the active growth of sulfate reducing bacteria.

The sulfur isotopic composition of barite with a mean of $\delta^{34}\text{S} +14.1$ per mil is identical to the best value of $\delta^{34}\text{S}$ predicted by Thode and Monster (1965) for Mississippian sea water sulfate. If this barite crystal were formed from hot saline brines at temperature of 137°C during the waning stages of mineralization, the sulfate content of the brine may have been derived from trapped seawater or partly from the leaching of the Mississippian evaporite.

ii. Sulfide Minerals

Pre-Ore Marcasite

The distribution of $\delta^{34}\text{S}$ values from +10.7 to +13.27 in the pre-ore marcasite indicates a heavy source of sulfur for this group of sulfide mineral. If the mean $\delta^{34}\text{S}$ value of the Gays River gypsum, anhydrite and barite is +14.0 ‰, assuming this is the $\delta^{34}\text{S}$ of the Mississippian sea water sulfate, in this area, then the pre-ore marcasite is depleted in ^{34}S by +0.73 to 3.3 per mil with respect to the contemporaneous sea-water sulfate or associated evaporite solution. This slight depletion in ^{34}S with respect to the sulfate with a peak close to the best value for the Mississippian sea water sulfate and the fairly uniform values of $\delta^{34}\text{S}$ comparable to the sulfate minerals is interpreted as being a consequence of kinetic fractionation effect associated with biogenic reduction of sea-water sulfate.

Ore Stage Sulfides

A remarkable similarity exists in all the $\delta^{34}\text{S}$ values of the ore stage sphalerite, galena and chalcopyrite (Fig. 6.2). This similarity compares with the $\delta^{34}\text{S}$ values of pre-ore marcasite. Several samples of sphalerite and galena that were collected along the strike lengths and across the near vertically dipping massive sulfide veins display very small variations of less than 2 ‰. These uniformities in the sulfur isotopic composition (Fig. 6.3) indicate a uniform sulfur source or a uniform physical and chemical environment of deposition. Indeed, there is no correlation in the variation of the sulfur isotopic composition with the host lithology or elevation in both the stratiform and vein sphalerite and galena. Sphalerite and galena samples from mineralized drill cores at the extreme ends of the ore body gave similar $\delta^{34}\text{S}$ values comparable to the

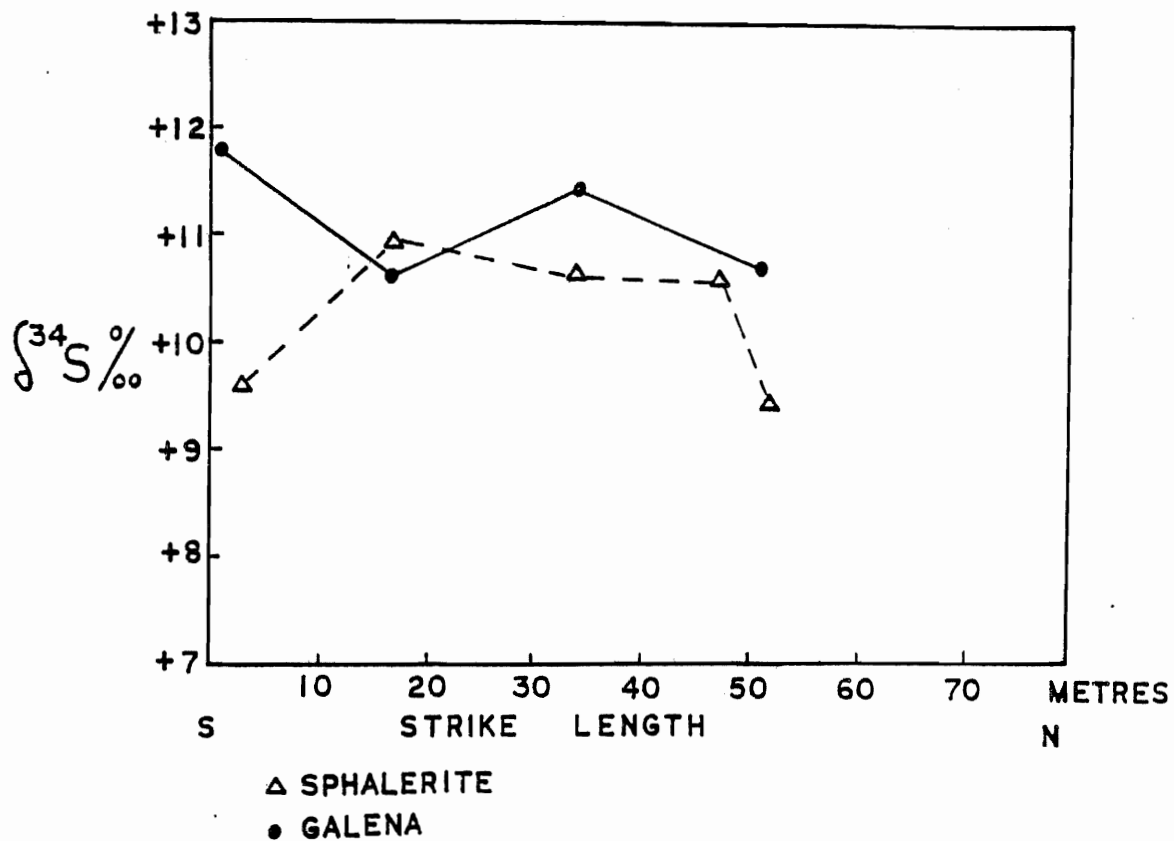


Figure 6.3a Variation in the sulfur isotopic composition of sphalerite and galena in a N/S vein. Note disequilibrium relationship in coexisting sphalerite and galena.

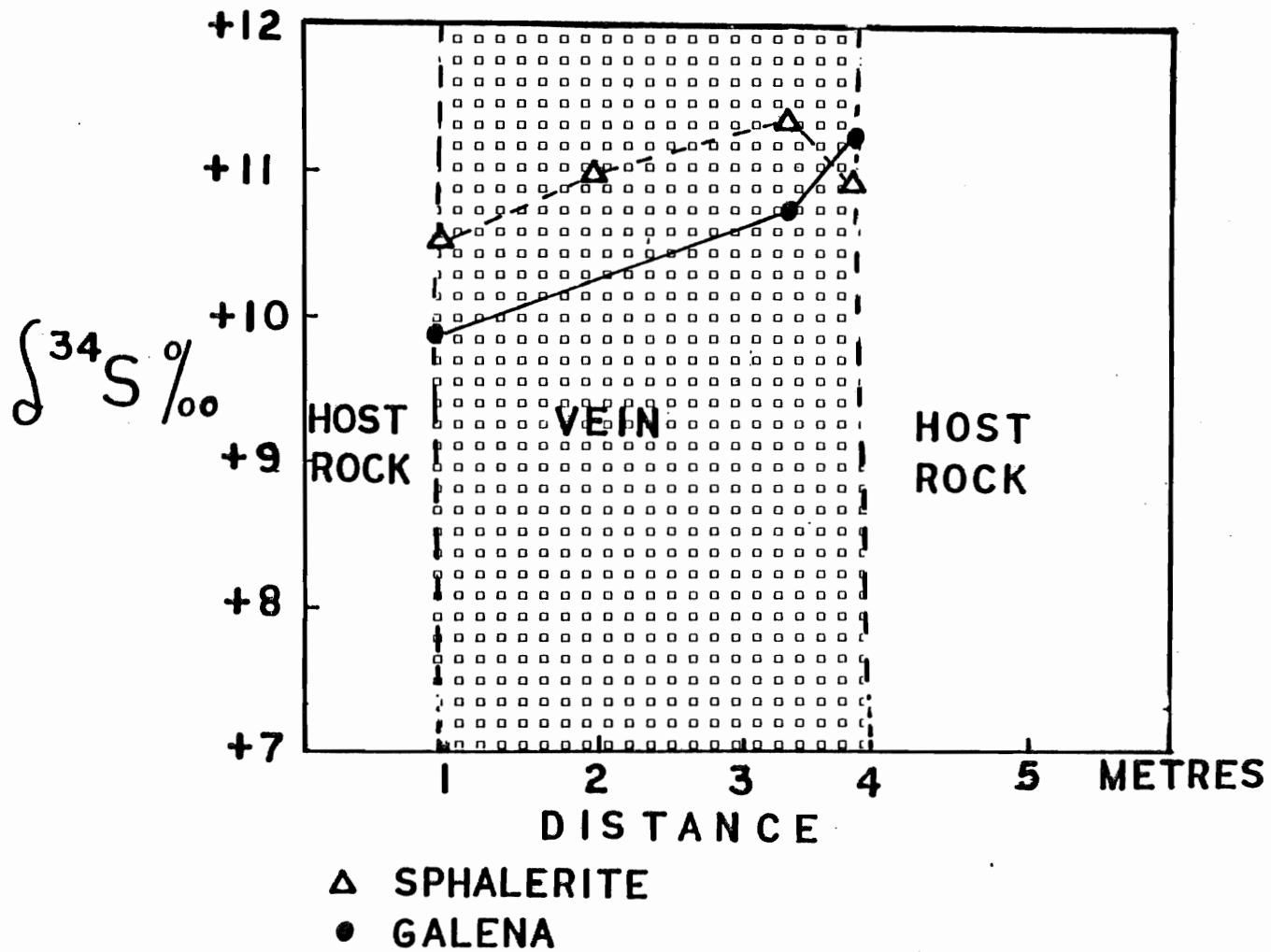


Figure 6.3b Variation in the sulfur isotopic composition of sphalerite and galena across a massive sulfide vein.

samples from the central, richer part of the ore body. This suggests that the sulfur isotopic composition of the ore stage sulfide minerals is independent of the host lithology, stratigraphic elevation and the areal extent of the lead and zinc mineralization.

Many authors indicate that the sulfur source for early diagenetic pyrite, marcasite, ore stage sulfide minerals and sulfate of some ore deposits are related. The sulfur in the ore-stage sulfide and sulfate minerals of such ore deposits are interpreted as being derived from the dissolution of the pre-ore iron sulfide minerals (William and Rye, 1974, Rickard et al., 1979). Williams and Rye (1974) indicated that the sulfur in early diagenetic pyrite, ore stage sphalerite and galena and the post ore pyrite in the McArthur lead and zinc deposit are derived from a single source under different modes of deposition. Rickard et al. (1979) indicated that the $\delta^{34}\text{S}$ for pyrite sulfur is identical to that of barite sulfur in the Laisvall sandstone hosted lead-zinc deposit. Rickard et al. concluded that the barite sulfur is therefore derived from a pyritic sulfide bearing solution due to the dissolution of the early pyrite.

The present author believes that this mechanism of sulfur extraction from the pre-ore iron sulfide minerals is unlikely for the ore-stage sulfide minerals at Gays River because there is no direct contact between the locally occurring pre-ore iron sulfide minerals and the ore minerals. The similarity between the heavy $\delta^{34}\text{S}$ values of the evaporite minerals, pre-ore marcasite and ore stage sphalerite, galena and chalcopryrite probably point to a common derivation of sulfur. If the mean $\delta^{34}\text{S}$ values of the Gays River pre-ore sulfate is taken as +14.00 per mil, then the ore-stage sulfide minerals ($\delta^{34}\text{S}$ +8 to 13.65 ‰) are depleted in ^{34}S by 0.35 to +6 per mil with respect to connate sulfate brines of seawater origin. This

range of sulfur isotope ratios could be produced by equilibrium fractionation between sulfate and sulfide at a temperature of about 800°C (Sakai, 1968). This temperature range is geologically unrealistic for this type of deposit and implies an isotopic disequilibrium between the sulfate and sulfide minerals.

If the partitioning of sulfur between oxidized and reduced species in response to changing physicochemical conditions (pH and Eh) were the main factors controlling the production of sulfide from a sulfate rich brine (Ohmoto, 1972), one would expect the variations in the $\delta^{34}\text{S}$ values of the ore stage sulfide minerals to be more systematic in distribution. However, the lack of systematic variations in the $\delta^{34}\text{S}$ values in the sphalerite and galena indicates a disequilibrium relationship between the oxidized and reduced mineral species. Partitioning of reduced sulfur between the oxidized and reduced species can proceed in the presence of adequate reductant without attainment of equilibrium.

The sphalerite-galena isotopic pairs gave temperatures of about 650°C (Table IV-2). This temperature is geologically unrealistic for this deposit and demonstrates that these two sulfide minerals were not precipitated under isotopic equilibrium. Although isotopic equilibrium can be approached between coexisting pairs of sphalerite and galena within the range 137° to 215°C shown in the fluid inclusion study, most sphalerite in the stratiform ores occupy the pre-existing pores in the carbonate host and are believed to predate galena. This relationship suggests that sphalerite and galena were not precipitated simultaneously. The paragenetic order of deposition may explain the lack of chemical and isotopic equilibrium.

The consistency of the sulfur isotopic compositions in the sphalerite, galena, chalcopyrite within a narrow range suggests that the isotopic

composition of the ore solution was homogenous during the mineralization event. Sulfide precipitation probably took place under fairly constant pH, fO_2 and fS_2 conditions. The heavy $\delta^{34}S$ values in the ore-stage sphalerite, galena and chalcopyrite compares closely with the range of δ values in the Gays River sulfate minerals. If the sulfate-sulfide fractionation mechanism was caused by sulfate-reducing bacteria interacting with an infinitely large sulfate reservoir in an open system, a very significant or large fractionation effect may have resulted. This mechanism of sulfate reduction is dominant at low temperatures of less than $50^\circ C$ (Tudge and Thode, 1950; Trudinger and Chambers, 1973). Besides, during the thermal maturation of oil in high temperature reservoirs $> 80^\circ C$ to $120^\circ C$, sulfate reduction may proceed through a non microbial inorganic reaction with negligible isotopic fractionation (Orr, 1974). This conclusion is based on the presence of heavy sulfur in mature oils which is isotopically similar to the associated sulfate. Barton (1967) indicated that the inorganic sulfate reduction in the presence of organic compounds such as methane may similarly result in sulfate-sulfide fractionation at temperatures of about $100^\circ C$.

The present author prefers the interpretation that the inorganic sulfate reduction mechanisms in the presence of petroleum hydrocarbons best explains the sulfate-sulfide fractionating mechanism for the Gays River ore-stage sphalerite, galena and chalcopyrite. The presence of intergrown petroleum hydrocarbons in the form of pyrobitumen in the sulfide minerals suggest that the ore solution consists of significant quantities of organic compounds. These might have participated in the reduction of the sulfate contained in the ore solution.

Post Ore Marcasite and Pyrite

The broad range of $\delta^{34}\text{S}$ values in the marcasite and pyrite samples indicate a low temperature of formation and disequilibrium. Sulfur in the post ore marcasite is isotopically lighter by 24 to 57 per mil with respect to the Mississippian sea water sulfate. If the marcasite sulfur was derived from the Mississippian sea water sulfate source, or solution of evaporite, the range of $\delta^{34}\text{S}$ in marcasite could be produced by equilibrium fractionation between sulfate and sulfide over a temperature range of approximately 380°C to 110°C (Sakai, 1968). This temperature range is geologically unrealistic and the fluctuations in the $\delta^{34}\text{S}$ values of the marcasite is too sporadic to be compatible with equilibrium fractionation trends. It is unlikely that the marcasite sulfur isotopic composition was derived from equilibrium fractionation processes. Similarly, the pyrite sulfur is isotopically lighter by 59 to 50 per mil with respect to the Mississippian sea water sulfate and the $\delta^{34}\text{S}$ values cannot be equilibrium values.

The broad spread and sporadic fluctuations in the sulfur isotopic composition in the marcasite and pyrite is a common feature to ore deposits that are precipitated from bacterially reduced sulfur (Kemp and Thode, 1968, Kaplan et al., 1964). Indeed, Trudinger and Chambers (1973) indicated that the most important cause for variations in the isotopic composition of sulfur in nature is by the reduction of sulfate ions by anaerobic bacteria. At 25°C Trudinger and Chambers (1973) indicated an enrichment of S^{32} up to 75% in the sulfide relative to sulfate with the cultures of Desulfovibrio desulfuricans. In natural environments, the isotopic composition of the H_2S liberated, depends on the size of the sulfate reservoir (Kaplan et al., 1963). If the reservoir is infinite, the $\delta^{34}\text{S}$ of the H_2S produced will

remain constant, assuming no change in bacteria metabolism. In a finite reservoir, the $\delta^{34}\text{S}$ of the sulfate and sulfide will be highly variable with the preferential removal of ^{32}S as H_2S .

The present author believes that the broad spread of $\delta^{34}\text{S}$ in the post ore marcasite could result via bacteria reduction processes on sulfate in the faults and fractures of the carbonate host where sulfate replenishment was adequate. Fractionation of sulfur isotopes in such a semi-restricted system would enrich the sulfate in ^{34}S , whereas the lighter isotope will be preferentially used in fixing soluble Fe^{++} as marcasite. It is interesting to note that the $\delta^{34}\text{S}$ values of marcasite are -42.9, -15.8 and -9.7 per mil. The fractionation of sulfate through the action of sulfate reducing bacteria in a partially closed system of fractures may explain the trend towards the increasing $\delta^{34}\text{S}$ content.

The fairly uniform $\delta^{34}\text{S}$ value in the late pyrite can be explained with a sulfur derivation from an infinite sulfate reservoir through a low temperature action of sulfate reducing bacteria.

Apart from the sulfate source of sulfur for the marcasite and pyrite, another possible source is the organic matter contained in the carbonate host and the Cretaceous clay and sand infill in the fault gouge. Lignite is commonly associated with marcasite and pyrite as in samples AGRP 1a, 1b, and 4490-3. However these organic materials cannot produce such light sulfur during their decay (Kaplan and Rittenberg, 1964). The present author believes that the sulfur in the post ore marcasite and pyrite are derived from a low temperature biogenic reduction of sea water sulfate through the solution of evaporites.

6.3 Lead Isotopes

Lead isotopic ratios are a powerful tool in helping to define the source material for the lead in ore deposits and in some cases in determining an estimate of the age of mineralization.

a. Principles and Assumptions

The common lead method is based upon the evolution of lead since time T , when the Earth started to act as a closed system for U, Th, and Pb to the time t when the lead was isolated from its radioactive parents (e.g. crystallized as galena in an ore deposit). The term common lead refers to a lead that developed in environments with U/Pb and Th/Pb ratios commonly found in whole rock samples, feldspars or sulfides (U/Pb: 0.05-1, Th/Pb: 1-10).

A review of calculations and parameters used in interpreting the evolution of lead isotopes is given in Doe and Stacey (1974), Köppel and Grunenfelder (1979) and Zartman and Doe (1981). A summary of the parameters and equations used in lead isotope studies is presented in Appendix IV.

The lead evolution model proposed by Houtermans (1946) and Holmes (1946, 1949) assumed that lead evolved since time T in chemically closed environments with differing U/Pb ratios. Syngenetic, stratiform or conformable massive sulfide deposits, with lead isotopic compositions which are homogeneous within a given deposit have an isotopic composition which is directly correlative with the age of ore formation. This relationship was used by Stanton and Russel (1959) to construct a growth curve for conformable ore deposits from which ages of ore formation based upon lead isotopic

composition (model ages) could be determined. These initial studies suggested that conformable ores were derived from a relatively homogeneous source which had maintained nearly constant U/Pb and Th/Pb values since the Earth formed. Such a history was referred to as a single-stage lead growth. Attention focused on making the best fit of the data to rather simple closed-system models, thereby distinguishing between ordinary and anomalous occurrences depending on their adherence to such models. Emphasis has recently shifted (Cumming and Richards, 1975; Stacey and Kramers, 1975; Doe and Zartman, 1979; Zartman and Doe, 1981) toward an effort to view isotopic composition as a consequence of environment and the complex geochemical cycles of lead, uranium and thorium.

Epigenetic ores do not have the simple isotopic characteristics of conformable deposits. Typically they have relatively variable lead isotopic compositions and model ages which are "anomalous", that is they are either "too young" or "too old". Early studies of carbonate-hosted Pb-Zn deposits focussed on the ores of the Joplin or Mississippi Valley, southeast Missouri and Tri-State districts. It was found that lead in galena in these deposits is anomalous in that it is notably enriched in the radiogenic isotopes compared to ordinary lead. Hence the designation of Joplin type or J-type anomalous lead (Houtermans, 1953). In many cases, several samples from a related group of deposits form a linear array of data points on a $^{207}\text{Pb}/^{204}\text{Pb}$ versus $^{206}\text{Pb}/^{204}\text{Pb}$ plot. The linear relationship is commonly interpreted as the result of a multistage growth history with variation in the U/Pb and Th/Pb ratios of the source material from where metals were concentrated to form the ore deposit. In the simple two-stage case, a linear array (or secondary isochron) can often be used to calculate the age of the source material if the time of ore formation is known.

Sufficient data on carbonate-hosted Pb-Zn deposits are now available (Doe and Zartman, 1979) to show that there is a continuum in $^{206}\text{Pb}/^{204}\text{Pb}$ and $^{208}\text{Pb}/^{204}\text{Pb}$ values, which runs from: 1) deposits with leads that approximate single-stage model leads (e.g. Pine Point, N.W.T.) 2) those that have leads only slightly radiogenic for their ages and 3) those that are highly radiogenic for their ages, such as the deposits of the Mississippi Valley (with "negative" or future model lead ages, such as Joplin).

Doe and Stacey (1974) and Doe (1978) more recently have called attention to the fact that major base metal deposits on a regional scale tend to have lead isotopic compositions that appear to have evolved under conditions approximating single stage conditions, which is not the case for minor deposits. Thus, this difference in lead isotopic composition may provide an isotopic tool for ore prospect evaluation. Conversely, different economic deposits within a district often have similar lead compositions. Individual ore deposits tend to have uniform or near uniform lead isotope ratios so that one analysis may be sufficient to characterize the lead isotopic composition of that prospect (Doe and Stacey 1974).

b. Procedure

Two samples of galena from the Gays River deposit were collected from drill core. The lead isotopic compositions were obtained by the surface emission (silica-gel) ionization technique on the U.S. Geological Survey mass spectrometer of Bruce R. Doe in Denver, Colorado. The analyses were performed in duplicate by M. Zentilli under the supervision of M. Delevaux. The isotopic values were normalized to absolute ratios through the NBS 981 secondary lead isotope standard. All ratios were within 0.1 percent of absolute ratios of the standard. The lead isotope compositions of the Gays River samples are given in Table 6.1.

Table 6.1 Model Age of Lead in Galenas

DEPOSIT	SAMPLE NUMBER	$^{206}\text{Pb}/^{204}\text{Pb}$	$^{207}\text{Pb}/^{204}\text{Pb}$	$^{208}\text{Pb}/^{204}\text{Pb}$	MODEL AGE*
Gays River	GR H 6	18.048	15.606	38.170	446 Ma.
Gays River	GR 114	18.063	15.622	38.189	466 Ma.
Pembroke	JD-PMBK	18.080	15.614	38.169	438 Ma.
Walton	W-704	18.161	15.644	38.325	437 Ma.

*Model age using the evolution model and equations of Stacey and Kramers (1975).

c. Results

The samples from the Gays River deposit (Table 6.1) have model ages of 446 and 466 m.y (Ordovician) for the two-stage isochron model of Stacey and Kramers (1975). In Figures 6.4 and 6.5, these data plot close to the evolution curve for average orogen of Doe and Zartman (1979). It is evident that the Gays River samples plot far from the field of the Mississippi Valley deposits and are more non-radiogenic than any other carbonate hosted deposit documented, even the Pine Point N.W.T. deposit, and Bleiberg, considered an end member (Doe and Zartman, 1979).

In comparison with other galenas hosted in the Mississippian rocks of Nova Scotia, only the Pembroke deposit in Colchester County appears almost identical (Fig. 6.5). Walton, a barite polymetallic deposit in Hants County, has a similar model age (437 m.y) but is richer in ^{207}Pb and ^{208}Pb and therefore seems to have had a larger "crustal" component. Curiously, it plots close to the fields of the massive sulfide deposits of New Brunswick.

d. Interpretations

It is beyond the scope of this thesis to attempt to interpret fully what are only preliminary lead data for the Gays River deposit. However, the data have important implications for the genetic models discussed in this thesis.

The lead in the ores is non-radiogenic compared to other carbonate-hosted Pb-Zn deposits to the extent that the model lead age (ca. 450 m.y: Ordovician) is significantly older than the Mississippian carbonate host rocks for the ore body (ca. 340 m.y). This led Zentilli *et al.* (1980) to suggest that the source of the lead in the Gays River deposit must be

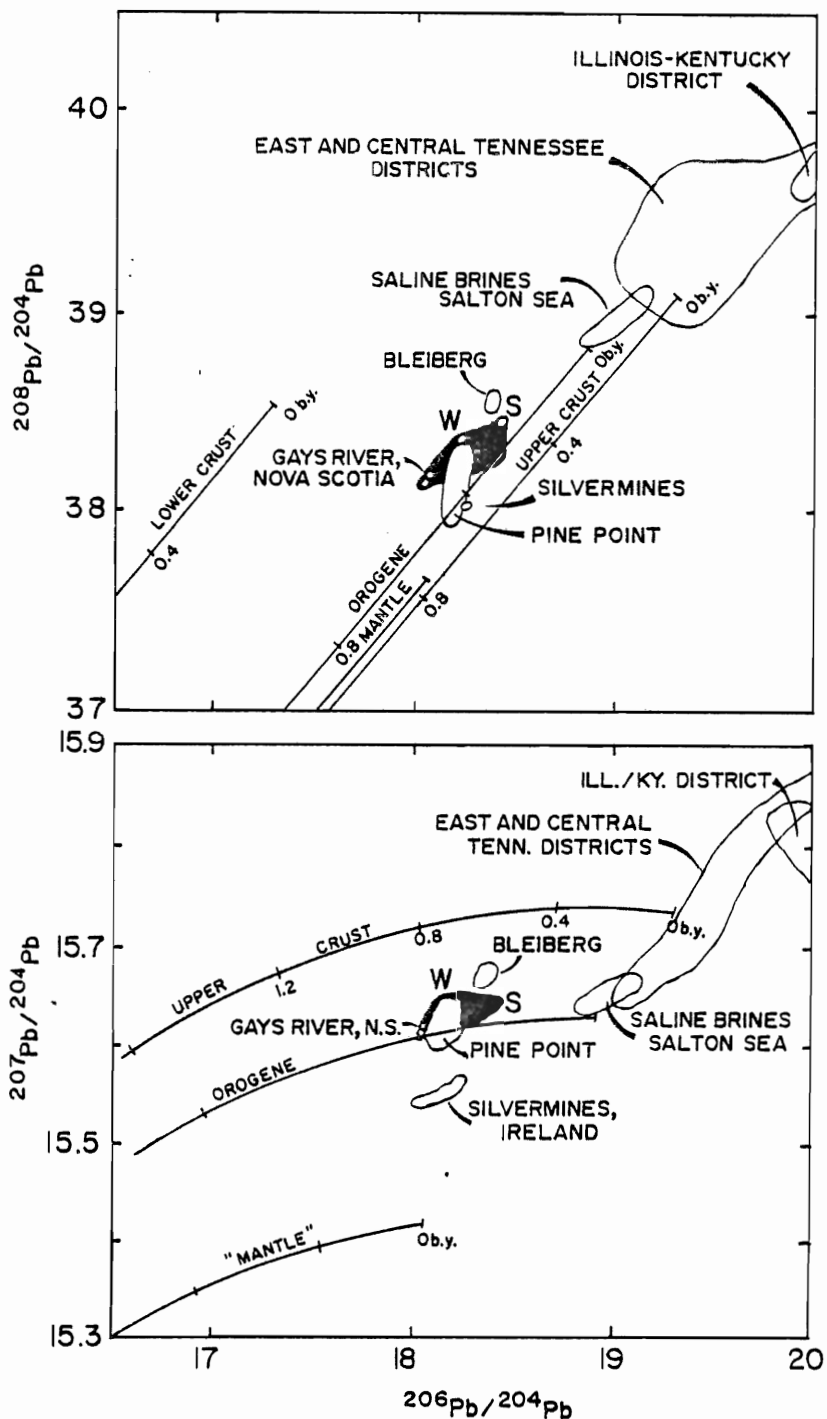


Figure 6.4 $^{207}\text{Pb}/^{204}\text{Pb}$ and $^{208}\text{Pb}/^{204}\text{Pb}$ versus $^{206}\text{Pb}/^{204}\text{Pb}$ for the Gays River, Nova Scotia deposit and other carbonate hosted deposits and selected ore environments. Data for Gays River, Walton (W), Smithfield (S) in Nova Scotia and Silvermines, Ireland from Zentilli, Doe and Delevaux (unpublished data). All others from Zartman (1979, figure 2.5). Lead evolution curves generated by "plumbo tectonics" model of Doe and Zartman (1979, figure 2.3) are given for reference.

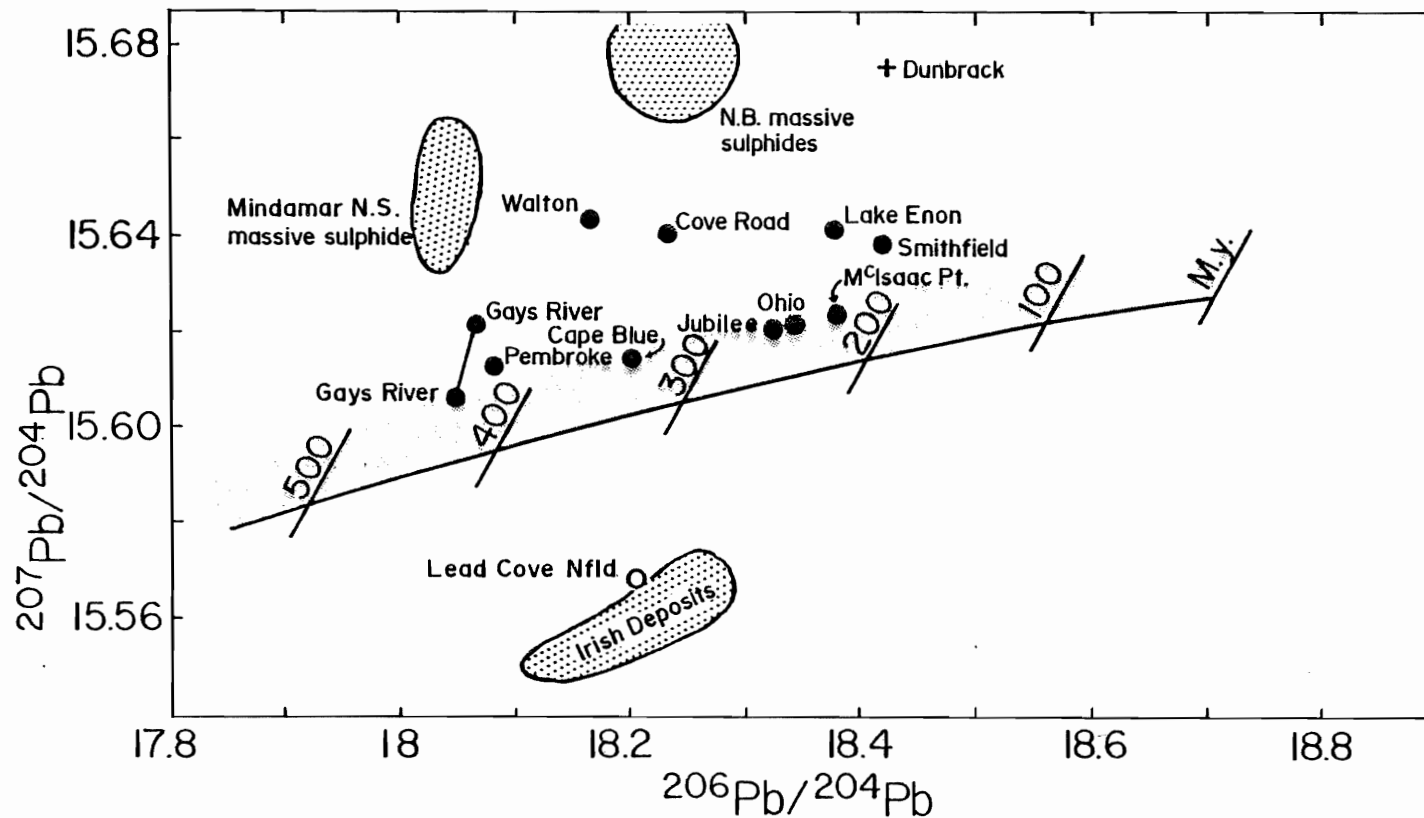


Figure 6.5. $^{207}\text{Pb}/^{204}\text{Pb}$ versus $^{206}\text{Pb}/^{204}\text{Pb}$ in galenas hosted in Lower Carboniferous sedimentary rocks in Nova Scotia (●) and Newfoundland (○). Dunbrack (+) is hosted in Devonian granite, but the alteration has been dated by K/Ar as 300 M.y. Data from Zentilli, Doe and Delevaux (unpublished data). Curve for lead evolution after Stacey and Kramers (1975) is given for reference.

sought in the Lower Paleozoic Meguma Group metasedimentary basement. The Meguma Group, a flyschoid sequence of Cambro-Ordovician age was metamorphosed to the green schist facies during the Acadian orogeny (ca. 410 m.y Reynolds and Muecke, 1978) and intruded by granitoid plutons of Devonian age (Reynolds et al., 1981).

If the lead was isolated from its radioactive parents during the sedimentation of the Meguma Group (ca. 500 m.y) or homogenized during the metamorphism of the Acadian orogeny, it is unlikely that it would have maintained its non-radiogenic character unless fixed in rocks with extremely low U/Pb and Th/Pb ratios (M. Zentilli, pers. comm.). Candidates for retention of lead could be feldspars, or another relatively lead-rich mineral phase such as sulfides. Feldspars are abundant phases in the metagreywackes of the Meguma Group, and this mineral has been strongly altered in the alteration zones below the deposit (Chapter 7). Conversely, galena occurs in association with ore shoots in many gold districts (Graves and Zentilli, 1982), and in stratabound base-metal concentrations in the Meguma Group (Jenner, 1982). Unfortunately, no reliable data on the isotopic fingerprint of these potential sources exists to date.

The lead data would seem incompatible with a source of the lead in Carboniferous or younger seawater, or in shales or clastic sediments of Carboniferous age. These settings would be expected to be richer in U and Th and thus made the lead more radiogenic in the deposit. It is premature to evaluate multistage models with the present data.

Doe (1978) suggested that the largest magmatothermal ore districts in the Western United States have the least radiogenic leads, whereas the more radiogenic leads are in uneconomic or marginally economic deposits. Doe related this relationship to the size and nature of circulating hydrothermal

cells and to the highly reactive nature of the ore fluid, which would attack lead rich, uranium poor phases (such as feldspars).

It is interesting to note that the two major mines perhaps representing two of the largest concentrations of metals in Nova Scotia (Gays River and Walton) have the least radiogenic leads. This suggests that other prospects (which have been characterized with only a few determinations) have perhaps less chance to be economic. The only exception seems to be Pembroke which although mined in the past, appears to be uneconomic. At Pembroke, veins of galena are seen cutting and filling the inter and intraparticle porosities of the highly fossiliferous Mississippian limestone. There is no evidence to suggest that the Gays River is a magmatothermal deposit, and the apparent inverse relationship between radiogenic character and size can only be conjectural. It is possible that for a given size of hydrothermal cell, with a given physicochemical character, the formation of a large deposit will depend on the availability of a concentrated source of lead. In this case, such source should have very low U/Pb and Th/Pb ratios, such as galena concentrations in the Meguma. Elsewhere, a source poorer in lead, and relatively more radiogenic would have contaminated the hydrothermal system, leading to more radiogenic lead in sub-economic deposits.

6.4 Oxygen and Carbon Isotopic Composition

a. Principles and Assumptions

Oxygen in the gaseous, liquid and solid compounds constitutes the most abundant element in the earth. It has three isotopes with the following abundances; $^{16}\text{O} = 99.763\%$, $^{17}\text{O} = 0.0375\%$, $^{18}\text{O} = 0.1995\%$ (Garlick, 1969). The oxygen isotopic composition of a substance is normally expressed as

$^{18}\text{O}/^{16}\text{O}$ ratio with reference to a standard e.g. PDB standard - a Cretaceous belemnite from the Peedee Formation or SMOW - Standard Mean Ocean Water. The PDB standard has long been exhausted and most $\delta^{18}\text{O}$ values are now expressed relative to the SMOW scale. The total carbonate of PDB has a $\delta^{18}\text{O}$ value of +30.6‰ on the SMOW scale. The absolute value for the $^{18}\text{O}/^{16}\text{O}$ ratio in the Standard Mean Ocean Water (SMOW) is 0.002005 (Baertsch 1976).

Carbon has two stable isotopes with abundance of $^{12}\text{C} = 98.89\%$, $^{13}\text{C} = 1.11\%$ (Nier, 1950, Craig 1957). The carbon isotopic composition of a compound is reported as $\delta^{13}\text{C}$ relative to the $^{13}\text{C}/^{12}\text{C}$ ratio of the Chicago PDB standard. $^{13}\text{C}/^{12}\text{C}_{\text{PDB}} = 0.0112372$ (Craig 1957). Although the Chicago PDB standard has been exhausted for several years, many laboratories have calibrated homogenous carbonate standard against the PDB and most values of $\delta^{13}\text{C}$ are commonly reported relative to the PDB standard.

Oxygen and carbon isotopic composition of the carbonate minerals is determined by the analysis of CO_2 generated from the carbonate by the reaction with 100 percent phosphoric acid (McCrea, 1950). Isotopic values of the carbonate samples are expressed as $\delta^{18}\text{O}$ and $\delta^{13}\text{C}$ respectively where

$$\delta^{18}\text{O}(\text{‰}) = \frac{^{18}\text{O}/^{16}\text{O}_{\text{sample}}}{^{18}\text{O}/^{16}\text{O}_{\text{standard}}} - 1 \times 1000 \text{ and}$$

$$\delta^{13}\text{C}(\text{‰}) = \frac{^{13}\text{C}/^{12}\text{C}_{\text{sample}}}{^{13}\text{C}/^{12}\text{C}_{\text{standard}}} - 1 \times 1000$$

Fractionation Factors:

The fractionation factor α for two coexisting mineral species A, B can be expressed as $\alpha_{\text{A-B}} = \frac{R_{\text{A}}}{R_{\text{B}}}$ where R_{A} and R_{B} represent the ratio of heavy to light isotopes in species A and B respectively.

$$\alpha_{A-B} = \frac{R_A}{R_B} = \frac{\delta_A + 1000}{\delta_B + 1000}$$

The per mil fractionation $10^3 \ln \alpha$ can be approximated by the Δ value

where $\Delta_{A-B} = \delta_A - \delta_B \approx 10^3 \ln \alpha_{A-B}$ for δ values < 10 .

Fractionation factor at 25°C for CO₂/H₂O system

$$\alpha = 1.0412 \text{ (Taylor, 1974; Friedman and O'Neil, 1977).}$$

For the H₃PO₄ generated CO₂ in carbonates, the fractionation factors are as follows:

$$\text{H}_3\text{PO}_4 \text{ liberated CO}_2/\text{CaCO}_3 \alpha = 1.01025$$

$$\text{H}_3\text{PO}_4 \text{ liberated CO}_2/\text{CaMg}(\text{CO}_3)_2 \alpha = 1.01109$$

$$\text{H}_3\text{PO}_4 \text{ liberated CO}_2 \text{ from PDB/CO}_2 \alpha = 1.00022$$

$$\delta^{18}\text{O}_{(\text{SMOW})} = 1.03086 \delta^{18}\text{O}_{(\text{PDB})} + 30.86 \text{ at } 25^\circ\text{C}$$

$$\delta^{18}\text{O}_{(\text{PDB})} = 0.97006 \delta_{(\text{SMOW})} - 29.94 \text{ (Friedman and O'Neil, 1977).}$$

The isotopic composition of carbonate rocks depends on the isotopic composition of the carbonate forming fluid, temperature of formation and various isotopic exchange reactions between the previously formed carbonate and later fluids. The carbon isotopic composition reflects in the nature of the carbon dioxide or bicarbonate that is responsible for the carbonate precipitation and the effects of temperature, pH and Eh if isotopic equilibrium is attained between the aqueous solution and the carbonate mineral (Ohmoto, 1972). When different carbonate minerals form either in isotopic equilibrium with one another or under the same conditions at different periods, the difference in the ¹⁸O content is a direct function of temperature. Thus the ¹⁸O values of carbonate minerals that presumably form under equilibrium conditions can be used to deduce the temperature of formation (Clayton and Epstein, 1958).

The oxygen isotopic composition of the hydrothermal fluid that deposited either dolomite or calcite can be calculated from the isotopic fractionation

factor for oxygen in the dolomite-water and calcite-water systems if the temperature of deposition is known. For the dolomite-water system, Northrop and Clayton (1966) gave a quantitative value of the oxygen fractionation between 300-510°C as follows:

$$1000 \ln \alpha_{\text{dol-water}} = 3.20 (10^6 T^{-2}) - 2.00 T \text{ in } ^\circ\text{K. (Northrop and Clayton, 1966)}$$

For the calcite-water system

$$1000 \ln \alpha_{\text{cal-water}} = 2.78 (10^6 T^{-2}) - 3.39 T \text{ in } ^\circ\text{K (O'Neil and Clayton, 1969).}$$

An extrapolation of these fractionations to lower temperatures appears to be valid in carbonate systems although some degree of uncertainty exists at low temperatures (Northrop and Clayton, 1966).

b. Sample Selection

Samples of the carbonate host rocks to ores and the different calcite paragenetic stages were collected underground. Samples of the carbonate rocks were collected systematically along horizontal traverses adjacent to the steeply dipping massive sulfide veins. Samples of ore stage calcite intergrowths and post ore calcite overgrowths were collected in the decline areas during mapping. Different paragenetic stages of the carbonate were carefully separated after the samples had been broken to pieces. A suite of samples of unmineralized limestone fossils of Mississippian age were kindly donated by the Nova Scotia Museum for use as unaltered standard.

Pure separates of calcite and dolomite were selected by handpicking under a binocular microscope. Where the two varieties of carbonate occurred together, calcite was separated in bromoform and dolomite was purified by leaching the calcite in dilute acetic acid. The mineralogical purity of all calcite and dolomite samples was checked by X ray

diffraction technique. Most samples analysed are 99% pure.

c. Experimental Procedure

Carbon dioxide was liberated from each aliquot (1-2 milligrams) of the pulverized samples by reaction with 100% phosphoric acid in evacuated pyrex tubes (McCrea, 1950). The CO₂ liberated was collected and purified in a liquid nitrogen cooled trap in a vacuum line. The sample was analyzed by comparison with a CO₂ reference standard (from Carrara marble or UQ2) in a mass spectrometer with a double collector attachment, following the procedure of McKinney et al. (1950). Mass ratios 45/44 and 46/44 were measured where

$$\begin{aligned} 44 &= \text{C}^{12} \text{O}^{16} \text{O}^{16} \\ 45 &= \text{C}^{13} \text{O}^{16} \text{O}^{16} \\ 46 &= \text{C}^{12} \text{O}^{16} \text{O}^{18} \end{aligned}$$

The means of duplicate measurements were made for several samples and the isotopic composition was expressed as δ notation relative to the Chicago PDB and SMOW standards. The data was corrected for the effect of ¹⁷O on $\delta^{13}\text{C}$ and of ¹³C variations on $\delta^{18}\text{O}$ by the means of the formula of Craig (1957) (Appendix IV). The precision of the measurements is approximately ± 0.1 per mil $\delta^{18}\text{O}$ and $\delta^{13}\text{C}$.

d. Oxygen and Carbon Isotope Relations

i. Unmineralized Limestone

Seven samples of unaltered brachiopod shells of Mississippian age from the Miller Brook limestone quarry were analysed for their oxygen and carbon isotopic composition. The $\delta^{18}\text{O}_{\text{SMOW}}$ values of this limestone exhibit a range from +24.49 to 26.39 per mil with a mean of $25.05 \pm .7$ per mil (Table IV-4). $\delta^{13}\text{C}_{\text{PDB}}$ values range from +3.61 to +4.55 with a mean of $+4.31 \pm .3$ per mil.

ii. Mineralized Dolomite and Limestone

All the host rock dolomite and limestone consist of heavy $\delta^{18}\text{O}$ content with a slight shift from the $\delta^{18}\text{O}$ values of the Lower Carboniferous (Mississippian) unaltered marine carbonate. The $\delta^{18}\text{O}_{\text{SMOW}}$ values in dolomite exhibit a narrow range from +22.86 to 24.82 per mil with a mean of 23.63 per mil (Table IV-5). Secondary limestone (dedolomite) have $\delta^{18}\text{O}_{\text{SMOW}}$ values ranging from +22.73 to +23.70 per mil with a mean of +23.42 per mil (Table IV-5). A larger variation occurs in the carbon composition of the dolomite and limestone. Dolomite $\delta^{13}\text{C}_{\text{PDB}}$ values range from +0.5 to +1.99 per mil with a mean of +1.2 per mil and the limestone exhibits a range of $\delta^{13}\text{C}_{\text{PDB}}$ from -2.96 to -1.34 per mil with a mean of -1.96 per mil (Table IV-5).

iii. Ore Stage Calcite

The ore stage calcite exhibits a distinct grouping of ^{18}O and ^{13}C values. The $\delta^{18}\text{O}$ values range from +13.67 to +14.24 per mil with a mean of +13.97 per mil and $\delta^{13}\text{C}$ values range from +2.22 to +3.12 per mil with a mean of +2.59 per mil (Table IV-5).

iv. Post Ore Calcite

The post ore calcite as geopetal overgrowths and encrustations exhibits the largest spread in their ^{18}O and ^{13}C values. Two distinct forms are distinguished on the basis of habit: (i) rhombohedral calcite, (ii) encrusting scalenohedra. The rhombohedral calcite have a range of $\delta^{18}\text{O}$ varying between +14.28 to +22.34 per mil with a mean of +19.00 per mil. $\delta^{13}\text{C}_{\text{PDB}}$ values vary from -5.68 to +1.58 per mil with a mean of -1.96 per mil. Two encrusting scalenohedra analysed have $\delta^{18}\text{O}_{\text{SMOW}}$ values of +24.10

and +24.31 per mil and a mean of +24.20 per mil and the $\delta^{13}\text{C}_{\text{PDB}}$ values of -0.7 and -0.29 per mil with a mean of -0.49 per mil (Table IV-5).

e. Interpretation of the Oxygen and Carbon Isotope Relations

i. Unmineralized Limestone

Variations in the ^{18}O and ^{13}C contents of marine carbonate of the same or different geological age depends on; (i) the isotopic composition of the sea water, dissolved material and food web of the local environment of deposition (ii) the isotopic fractionation by carbonate forming organisms and their relative bulk contribution to carbonate sediments and (iii) the diagenetic and subsequent isotopic exchange during the dissolution and precipitation of carbonate in sediments (Keith and Weber, 1964). Veizer and Hoefs (1976) indicated that the oxygen and carbon variations in marine carbonate are facies controlled. These authors pointed out that carbonate associated with evaporite are characterized by heavier $\delta^{13}\text{C}$ and lighter $\delta^{18}\text{O}$ contents with respect to carbonate without evaporite affiliation. Keith and Weber (1964) reported a range of $\delta^{18}\text{O}_{\text{SMOW}}$ values from +23.8 to +25.5 with a mean of +24.8 for the Carboniferous marine carbonate. A fairly consistent C^{13} content within a range of -2 to +2.0 per mil with a mean of +0.0 ‰ was reported for the Carboniferous sea water (Keith and Weber 1964). These authors suggest that the carbon content of the oceans has been fairly constant throughout the geologic time although small variations exist from one basin to the other.

The means of the $\delta^{18}\text{O}$ and the $\delta^{13}\text{C}$ values of the unmineralized limestone fossils from the Miller Brook quarry are compatible with the range of values for the oxygen and carbon isotopic composition of unaltered marine carbonate of Lower Carboniferous age (Keith and Weber, 1964; Veizer

and Hoefs, 1976). The $\delta^{18}\text{O}$ and $\delta^{13}\text{C}$ values for the 7 brachiopod shells are consistent with the $\delta^{18}\text{O}$ value of 25.9 and $\delta^{13}\text{C}$ value of +3.91 reported for an unknown brachiopod in the Mississippian Miller Brook formation (Walker, 1978). The present author believes that the heavy ^{13}C content of all the brachiopods may be peculiar to the Windsor sea, as this is slightly heavier than the values of $\delta^{13}\text{C}$ reported for the Carboniferous sea (Keith and Weber, 1964).

ii. Mineralized Dolomite and Limestone Host Rock

The range of $\delta^{18}\text{O}$ and $\delta^{13}\text{C}$ values in the mineralized host dolomite and limestone are slightly lower by at least 1-2 per mil with respect to the $\delta^{18}\text{O}$ and $\delta^{13}\text{C}$ values of the unmineralized limestone of equivalent age (Figs. 6.6, 6.7). The range of $\delta^{18}\text{O}$ values in the mineralized host rocks fall within the lower end of values displayed by other Lower Carboniferous limestone (Keith and Weber, 1964; Veizer and Hoefs, 1976). The relative depletions in the heavy isotope of carbon and oxygen in the mineralized host rocks reflects either post depositional diagenetic alterations or an isotopic exchange with hydrothermal fluids.

Systematic sampling of the host dolomite and limestone adjacent to massive sulfide veins show no clear cut pattern in the $\delta^{18}\text{O}$ and $\delta^{13}\text{C}$ values versus distance to ore. A fairly uniform $\delta^{18}\text{O}$ value was found in the areas adjacent to two sulfide veins in drift 104 (Fig. 6.8). Variations in the $\delta^{13}\text{C}$ values of dolomite and limestone are quite irregular (Fig. 6.8). Sample 4470-1 taken from about 35 meters away from the sulfide veins displayed the heaviest $\delta^{18}\text{O}$ and $\delta^{13}\text{C}$ values (Table IV-5). Although the isotopic composition of the carbonate rocks is a function of the isotopic composition of the fluid from which they formed, the temperature of formation and isotopic exchange reactions, the geological setting imposed by the carbonate

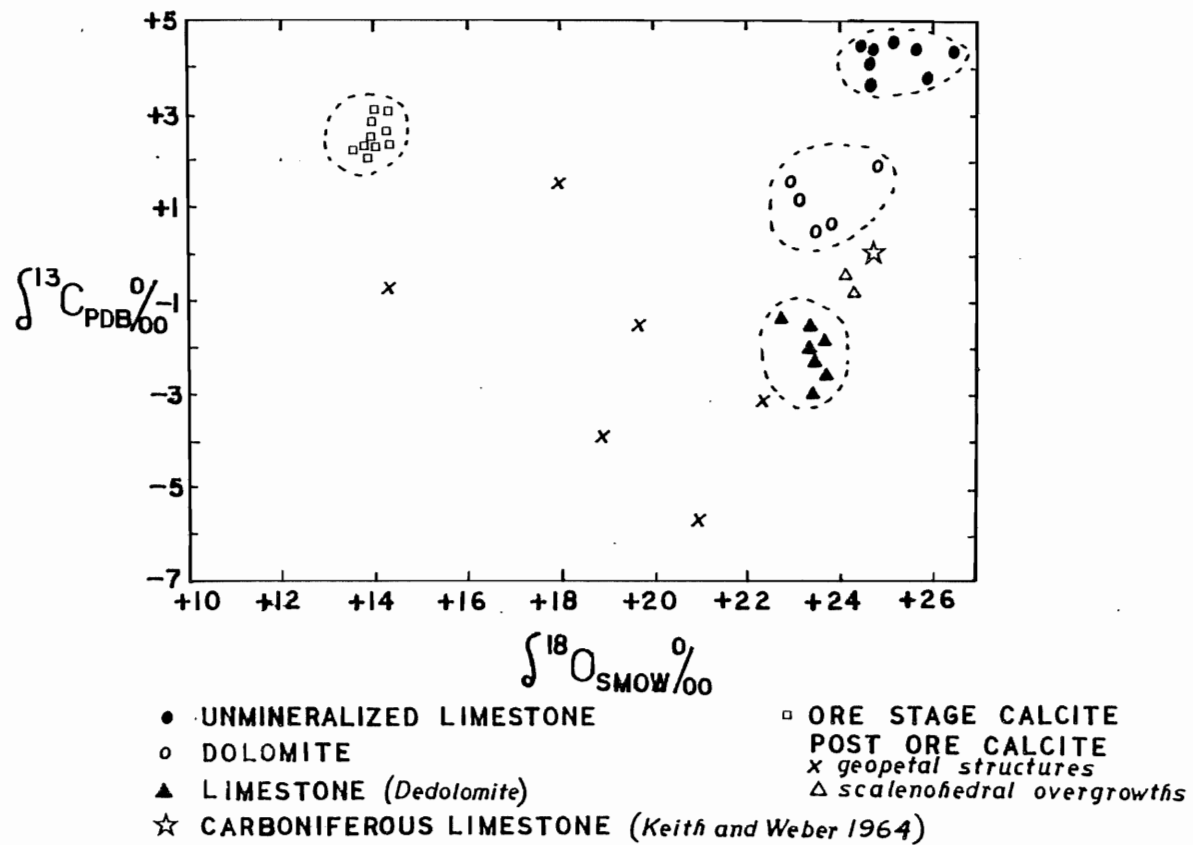


Figure 6.6 Oxygen and carbon isotopic composition of host rock to ores and carbonate gangue at Gays River.

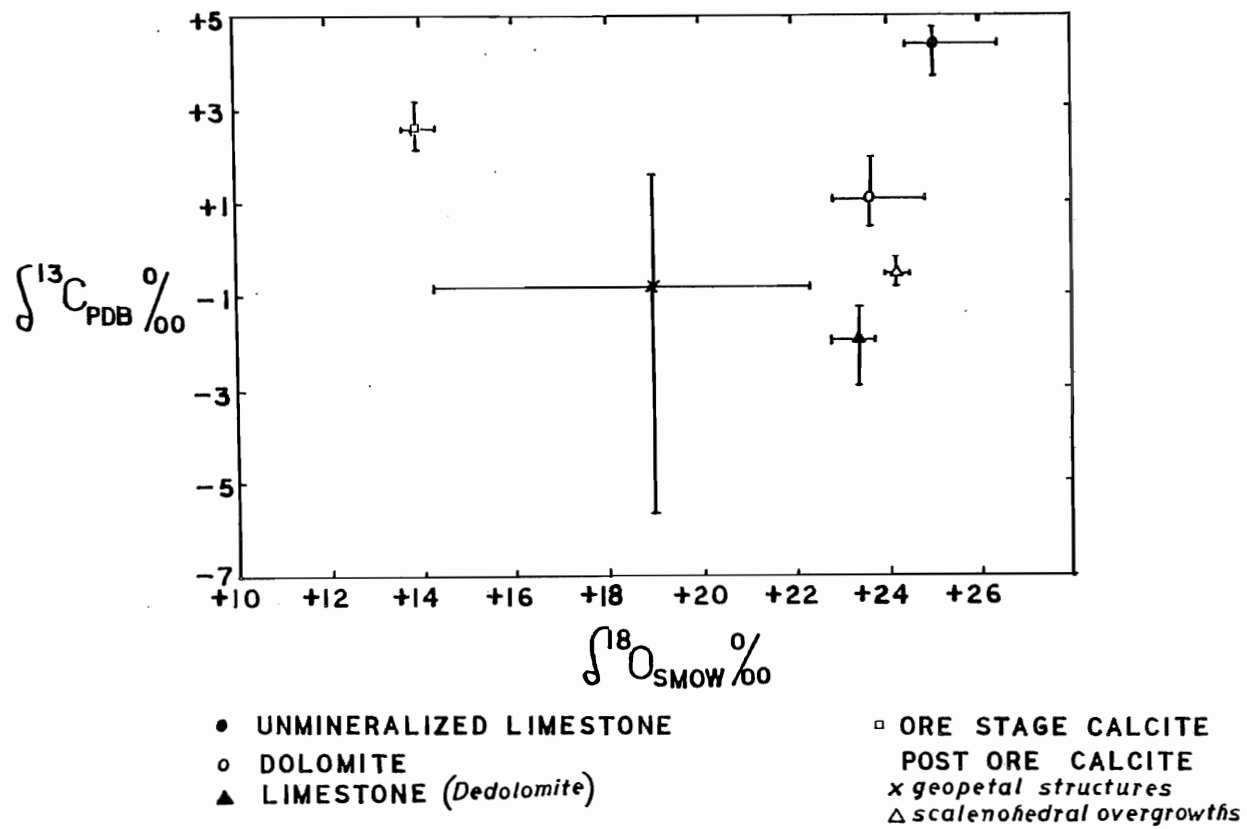


Figure 6.7 Oxygen and carbon isotopic composition of host rock to ore and carbonate gangue at Gays River; mean values and range.

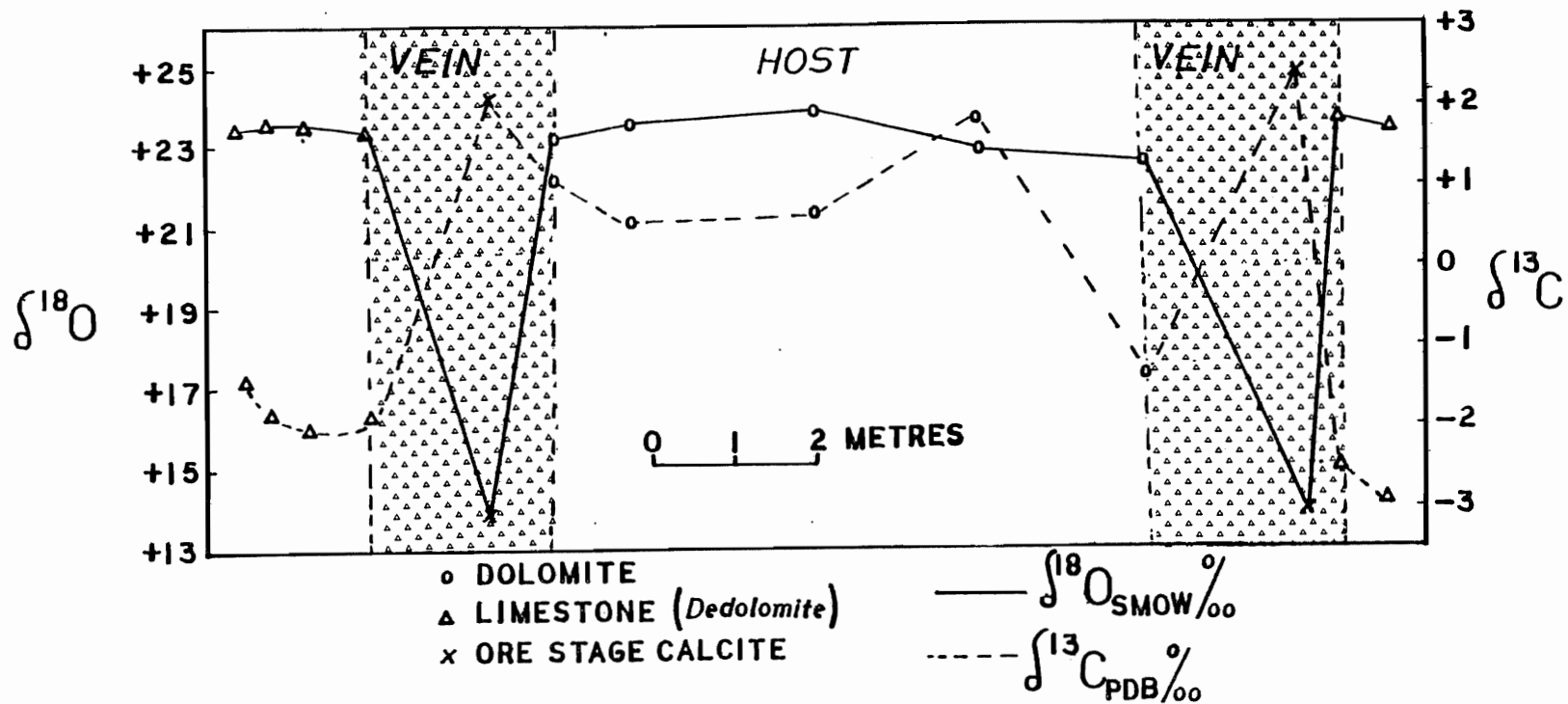


Figure 6.8 Variation in oxygen and carbon isotopic composition in the carbonate host versus distance to massive sulfide veins; drift 104, Gays River mine.

lithology may have a direct control on these factors.

Hall and Friedman (1969) indicated that the pattern of $\delta^{18}\text{O}$ values in the altered limestone host rocks to the lead-zinc deposits in the Upper Mississippi Valley and Tristate districts are the results of temperature gradient in the host rock during alteration. The depletion in the heavy ^{18}O and ^{13}C content of the host rock was caused by diminishing fractionation in the carbonate-water system at higher temperatures (Hall and Friedman, 1969).

If the relative depletion of the heavy oxygen and carbon was caused by thermal gradients on the carbonate host at Gays River, a systematic increase in the heavy isotopes should be found away from the sulfide veins. The lightest ^{18}O and ^{13}C values should therefore be at the vein. The lack of such systematic variation and the fairly uniform ^{18}O and irregular ^{13}C values adjacent to the veins suggests that a steep thermal gradient was not the only cause of depletion of the heavy isotopes in the Gays River dolomite and limestone hosts.

If the temperatures were nearly uniform within the carbonate host rock, the depletion in $\delta^{18}\text{O}$ might reflect a continuous variation in the $\delta^{18}\text{O}$ of the pore fluids as it passed through the rock. A mechanism of partial exchange of ^{18}O between hydrothermal fluids and the permeable carbonate rocks was responsible for the isotopic alteration and recrystallization of these hosts in the Hill Mine, Illinois (Pinckney and Rye, 1972). This process involves a gradual loss of the ^{16}O content of the pore fluid with increasing temperature and a gain of an equivalent amount of ^{18}O content from partial exchange with the carbonate rock. The $^{18}\text{O}/^{16}\text{O}$ content of the carbonate rock decreases and $^{18}\text{O}/^{16}\text{O}$ content of the pore water increases with time.

The present author believes that the depletion of the ^{18}O and ^{13}C content of the Gays River dolomite and limestone was caused by the isotopic exchange between these carbonates and the hydrothermal pore fluid. The fairly uniform ^{18}O values in the recrystallized dolomite and limestone indicate that a large amount of water of fairly uniform temperature and isotopic composition was transmitted through the porous carbonate.

Post ore dedolomitization and limestone formation by low temperature Ca^{++} rich meteoric water caused no significant fractionation in the ^{18}O content of the dolomite precursor. This relationship is compatible with the small or zero fractionation reported for the recent geological pairs of dolomite and calcite (Degens and Epstein 1964). These authors concluded that dolomite formation from calcite or vice versa involve the diffusion and substitution of Mg^{++} or Ca^{++} into the preexisting carbonate without oxygen isotope exchange. This suggestion is controversial because the diffusion coefficient of Mg^{++} or Ca^{++} are too low even at temperatures of 400°C to 500°C to explain the conversion of calcite to dolomite or vice versa solely by diffusion (Northrop and Clayton, 1966). It is not the intention of this thesis to consider the dolomite-calcite conversion mechanism any further.

In contrast to the dolomite ^{13}C values, the limestone gave lower ^{13}C values. This suggests that light organic carbon participated in the recrystallization and conversion of dolomite to limestone. The dark brown to almost black colour of this limestone compared to the buff brown colour of the dolomite precursor probably resulted from the addition of organic carbon.

iii. Ore stage calcite

A significant depletion in the heavy ^{18}O content with respect to the unmineralized limestone occurs in the ore stage calcite (Fig. 6.6). A distinct grouping of the $\delta^{18}\text{O}$ and $\delta^{13}\text{C}$ values of this calcite is shown by the very narrow range in the $\delta^{18}\text{O}$ and $\delta^{13}\text{C}$ values (Table IV-5). Intra-sample variation is not significant. This close grouping of the $\delta^{18}\text{O}$ and $\delta^{13}\text{C}$ values and the temperature of 172°C (this study) suggests that the ore-stage calcite is of hydrothermal origin. The extreme depletion in the heavy ^{18}O in the calcite is interpreted as due to diminishing isotopic fractionation in the $\text{CaCO}_3\text{-H}_2\text{O}$ system at the hydrothermal fluid temperature.

The $\delta^{18}\text{O}$ of the hydrothermal fluid is calculated from the calcite-water fractionation of O'Neil and Clayton (1969) from the relationship:

$$1000 \ln \alpha = 2.78 \frac{10^6}{T^2} - 3.39 \quad \text{T}^\circ\text{K.}$$

If the mean ^{18}O value of the ore stage calcite is + 13.97 ‰, and filling temperature is 172°C

$$1000 \ln \alpha = 2.78 \frac{10^6}{(445)^2} - 3.39$$

$$1000 \ln \alpha = 10.64$$

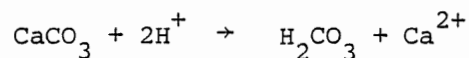
$$\delta^{18}\text{O}_{\text{H}_2\text{O}} = (13.97 - 10.64) \text{ per mil}$$

$$= 3.33 \text{ per mil.}$$

This δ value of +3.33 per mil for the ore stage calcite corresponds to very saline hydrothermal fluid. The result is compatible with the fluid inclusion salinity measurements and also confirms that the ore stage calcite was formed from highly saline brines.

The relatively constant $\delta^{13}\text{C}$ values in the ore stage calcite and a mean value of +2.59 per mil is characteristic of marine carbonate $\delta^{13}\text{C}$ values (Keith and Weber, 1964). These ^{13}C values correspond to the $^{13}\text{C}/$

^{12}C ratios found in carbonate rocks that are deposited in low temperature equilibrium with atmospheric CO_2 (Fritz, 1969). Thode *et al.* (1965) and Bottinga (1968) indicated a fractionation factor of only 1-2 per mil with the dissolution process of a carbonate rock as shown by the reaction:



No significant change occurs in the $\delta^{13}\text{C}$ values of the calcite precipitating from such dissolution reaction of carbonate host at temperatures up to 200°C (Ohmoto, 1972).

The present author suggests that the CO_2 and the HCO_3^- , which participated in the formation of the ore stage calcite were derived from marine bicarbonate dissolved out from the host primary carbonate.

iv. Post ore calcite

The post-ore calcite (rhombohedral and scalenohedral) display a broad range of $\delta^{18}\text{O}$ and $\delta^{13}\text{C}$ values which fall between those for the ore stage calcite and the mineralized host carbonate (Fig. 6.6). The post-ore rhombohedral calcite end member has a $\delta^{18}\text{O}_{\text{SMOW}}$ value of +14.28 per mil which compares with the ore stage calcite $\delta^{18}\text{O}$ values. This $\delta^{18}\text{O}$ value and the fluid inclusion homogenization temperature of 142°C for this calcite suggest that this rhombohedral calcite was formed under the influence of hydrothermal fluid. The post ore scalenohedra calcite gave $\delta^{18}\text{O}$ values averaging +24.20 per mil. This value is identical to the $\delta^{18}\text{O}$ composition of the host dolomite and limestone.

The extreme fractionation of the ^{18}O composition of the ore stage calcite at a temperature of 172°C put a boundary limit on the change in the isotopic composition of the fluid from which this calcite precipitated out. Since the oxygen isotope composition of any carbonate that is precipitated

in isotopic equilibrium from a liquid depends on the isotopic composition of the liquid and the temperature of formation, the post-ore rhombohedral calcite probably started to form as the temperature of the ore fluid decreases. This may have resulted from the mixing of the hydrothermal fluid with cooler but compositionally similar formational waters. Such temperature drop may lead to the enrichment in the $\delta^{18}\text{O}$ values in the post-ore calcite due to increasing fractionation in the $\text{CaCO}_3\text{-H}_2\text{O}$ system at low temperatures.

Assuming that the lowering of temperature was the main cause of the precipitation of the isotopically heavier post-ore calcite, an approximate temperature of formation of the post-ore scalenohedra calcite can be calculated from the fractionation factor of O'Neil and Clayton (1969) for the $\text{CaCO}_3\text{-H}_2\text{O}$ system.

If the mean of $\delta^{18}\text{O} = +24.20\text{‰}$.

and $\delta^{18}\text{O}_{\text{H}_2\text{O}}$ from ore stage calcite is $+3.33\text{‰}$ appx.

$$\alpha_{\text{Ca-H}_2\text{O}} = \frac{1,024.2}{1,003.33} = 1.0208$$

$$1000 \ln \alpha = 20.8.$$

$$\text{If } 1000 \ln \alpha = 2.78 \frac{10^6}{T^2} - 3.39 \text{ T}^\circ\text{K (O'Neil and Clayton, 1969).}$$

$$\text{Then } 20.8 = 2.78 \frac{10^6}{T^2} - 3.39$$

$$T = \sqrt{\frac{2.78 \times 10^6}{20.8} - 3.39}$$

$$= 365.5^\circ\text{K}$$

$$= 92.5^\circ\text{C}$$

This temperature can be regarded as an approximate temperature of crystallization of the post ore scalenohedra calcite assuming isotopic equilibrium with the fluid from which they precipitated. This temperature is consider-

ably lower than the temperature of approximately 142°C determined for post-ore rhombohedral calcite from the fluid inclusion studies. However, the scalenohedra commonly occur as overgrowths on the rhombohedral calcite. This suggests that the scalenohedra calcite is later than the rhombohedral type and was formed from cooler fluids. The excellent crystalline habits of the post ore calcite, their paragenetic relationships, and formation temperatures are compatible with a slow continuous precipitation of calcite with lowering temperatures during the waning stages of mineralization.

Although the ore-stage calcite has very uniform heavy ^{13}C values that are identical to marine carbonate, the post ore calcite has widely scattered ^{13}C values. The light negative ^{13}C values in the post ore rhombohedral and scalenohedral calcite indicate that a lighter source of carbon participated in the precipitation of this group of calcite. Two important sources of isotopically light carbon are deep seated sources and the organic matter in the sedimentary rocks and biosphere. Deep seated carbon has a uniform composition of -7 per mil with respect to PDB (Taylor et al., 1967). Organic carbon in sedimentary rocks is characterized by light ^{13}C values of about -25 per mil (Eckelmann et al., 1962). The lack of igneous activity in the Gays River area does not support a contribution of deep seated carbon into this geological setting. The present author believes that the participation of organic carbon probably from the biogenic decay of organic matter in the porous carbonate could result in the light ^{13}C values in the post ore calcite.

6.5 The Ore Forming Environment

The mode of transport and deposition of lead and zinc ions has been a subject of controversy. Although it is not the intention of this thesis to examine a detail analysis of metal complexing and the mechanisms of deposition of lead and zinc sulfides, a description of the possible processes which probably led to the transport and deposition of these metals at Gays River are considered here from the available field, petrological and geochemical evidence.

The ability of complexes in aqueous solutions e.g. hydroxide, carbonate, bicarbonate, sulfide, bisulfide, sulfate, bisulfate and chloride to transport Pb^{++} and Zn^{++} ions have been tested by several authors. Transportation of metal ions by colloids was rejected because of the great instability of colloids in the presence of electrolytes (Helgeson, 1964, Barnes and Czamanske, 1967). Helgeson (1964) dismissed hydroxide, bicarbonate, sulfate and bisulfate as major transporters of these metals because these radicals are not easily dissociated from their compounds.

The discovery of saline brines in fluid inclusions in sphalerite and the presence of significant quantities of metal ions in the Salton Sea and Red Sea brines lend evidence in support of the possibility that hot saline brines within a pH close to neutral are active transporters of Pb^{++} and Zn^{++} ions (Roedder 1965, Sawkins and Huebner 1965). Barnes and Czamanske (1967) suggest that the transport of metal ions of Au, Pb, Cu, Ag in bisulfide complexes could be significant in near neutral solutions at temperatures up to 300°C. Holland (1965) indicated that the addition of NaCl increases Zn^{++} solubility in the acid regions of pH if the metal is transported as a bisulfide complex.

Anderson (1973) rejected the possibility of bisulfide complexes because

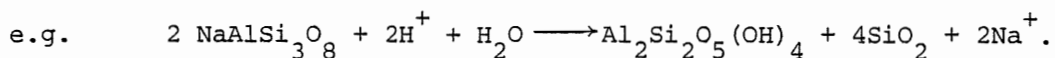
of the instability of this complex in the ore forming environment. As an alternative mode of transport, Anderson (1973) illustrated that within the acid regions of $\text{pH} \sim 5.0$, NaCl brines are capable of transporting ore quantities of lead and reduced sulfur in the same solution at a temperature of about 100°C . Under these conditions, Anderson (1973) pointed out that metal precipitation can result from cooling, neutralization and dilution. The author indicated that formational brines are not acidic enough to fulfill the requirement needed for both metal and sulfur to be carried in the same solution. In such acidic conditions calcite and dolomite are not stable (Anderson 1973, 1975, 1978). This author concluded that the presence of sulfate ions as sulfate complexes does not hinder the transportation of metal chloride ions, although a reduced sulfur source is needed to cause sulfide precipitation. Hence metal and sulfur were not transported together but the sulfur must have been supplied at the site of deposition (Anderson 1973, 1978).

Since Anderson's work, various hypotheses have emerged as to the possibility of transporting both metal and sulfur in the same solution. A study of the composition of galena at the Buick mine by Sverjensky et al (1979) indicated that both octahedral and cubic galena show different lead and sulfur isotopic compositions. Octahedral galena which is paragenetically earlier has less radiogenic lead and heavy sulfur while the later cubic galena has more radiogenic lead and is enriched in lighter sulfur. Sverjensky et al, (1979) concluded that this relationship in the lead and sulfur isotopic composition of galena suggests that both the metal and sulfur were transported together and that precipitation of galena was not a result of mixing of separate lead bearing and sulfur bearing solutions at the site of deposition. Apart from the isotopic evidence, textural

evidence and the presence of organic material intergrown with sulfides led McLimans et al. (1980) and Giordano and Barnes (1981) to suggest that both metal and sulfur for the formation of the sulfides were carried in the same solution. These authors believe that the precipitation of the sulfide minerals occurred near equilibrium conditions from slight changes in the ore fluid chemistry.

As an alternative to inorganic complexing, Giordano and Barnes (1981) indicated that the presence of organic materials with Mississippi Valley Type mineralization suggest that organometallic complexes are probably important in the transport of Mississippi Valley Type ore solutions. These authors tested the concentration levels of metal ions to which lead bisulfide and lead chloride complexes can attain at 100°C and 200°C and concluded that the values are below the minimum required for an ore deposit. Giordano and Barnes (1981) therefore concluded that neither chloride nor bisulfide complexes are sufficiently stable to have contributed significantly to lead transport in Mississippi Valley Type ore solutions but complexes of one or more aromatic carboxylate ligands like the salicylates may contribute significantly to metal transport.

The conclusions of Giordano and Barnes (1981) have several implications with regard to the metal transport and deposition of sulfide and sulfate minerals in the Gays River deposit. The heavy sulfur isotopic composition of the sulfide and sulfate suggest an evaporitic source for the sulfur in these minerals. If gypsum and anhydrite are initial primary precipitates, the solution of this evaporite will generate an initial acidic solution of pH <5 (Anderson, 1978). This solution is probably responsible for the alteration of the basement rocks along fractures and faults and the conversion of preexisting albite to kaolinite.



This footwall clay alteration suggests a pH limit within the acid regions for the sulfate rich solutions which probably became the ore solutions in the basement fractures. Within the ore zone, above the carbonate/basement unconformity, the predominant clay species is a 2 M illite. The presence of illite in the massive sulfide vein ore suggests that an alkaline pH condition was attained during the ore stage sulfide mineralization. The absence of major dissolution of the carbonate suggests that the ore solutions were saturated with respect to the carbonate host before reaching the site of ore deposition. Indeed, the overgrowths of galena on dolomite pebbles and pore filling geopetal sphalerite and galena without obvious corrosion suggest that dolomite was stable during the deposition of sphalerite and galena.

Organic hydrocarbon in the form of pyrobitumen is contained in the sulfide minerals at Gays River. This suggests that the sulfate dominated chloride brine consists of significant quantities of organic compounds. If the metal ions as organometallic complexes and sulfur were carried in the same solution in an initial acidic environment of $\text{pH} < 5$, cooling, dilution and pH change may lead to sulfide precipitation. Alternatively, the reduction of the sulfate in the brine by mixing with petroleum hydrocarbons as this migrates into the carbonate reef may cause the precipitation of sulfide minerals. The lack of chemical and isotopic equilibrium between the ore forming fluid and the coexisting sulfide minerals eliminates the possibility that pH change, cooling and dilution was the sole cause of sulfide precipitation. The present author believes that the reduction of the sulfate contained in the ore solution during the thermal degradation of petroleum may better explain the cause of sulfide precipitation.

6.6 Discussion

Several important features emerge from the survey of the sulfur, lead, oxygen and carbon isotopic composition of the mineral species in the Gays River deposit. The mean $\delta^{34}\text{S}$ value of +14.00 per mil in the Gays River gypsum, anhydrite and barite is identical to the isotopic data for the evaporite minerals of Mississippian age first determined by Thode and Monster (1965). This confirms that the sulfur in the Gays River sulfate was derived from the Mississippian sea water source (Fig. 6.9).

The heavy values of $\delta^{34}\text{S}$ in the pre-ore marcasite, ore stage stratiform and vein sphalerite, galena and chalcopyrite show a fairly narrow range of variation from +8 to +13.65 with a mean of $+10.85 \pm 0.9$ per mil in 35 samples collected over the ore body. This heavy sulfur isotopic composition over the areal extent of the ore body is quite unusual for deposits of simple magmatic origin and discounts the possibility of a magmatic source of sulfur. Such a range of $\delta^{34}\text{S}$ values might be expected in deposits of metamorphic hydrothermal origin (Jensen, 1959). In order to test this possibility, the sulfur isotopic composition of sulfide minerals in the metamorphosed basement rock below the carbonate unconformity were examined. The sulfur isotopic composition of seven sulfide samples in the metamorphosed Lower Paleozoic basement rocks of similar lithology with the Gays River basement indicate a broad range of $\delta^{34}\text{S}$ values from -0.63 to +25.03 per mil with a mean of +11.80 per mil. The sporadic distribution of the $\delta^{34}\text{S}$ values show no direct correlation with the Gays River sphalerite and galena $\delta^{34}\text{S}$ values. Hence it is unlikely that the metamorphosed basement was the main source of sulfur for the sulfide mineralization.

A comparison of the $\delta^{34}\text{S}$ values in the sulfide and sulfate minerals suggest a close relationship of the sulfur sources with the isotopically

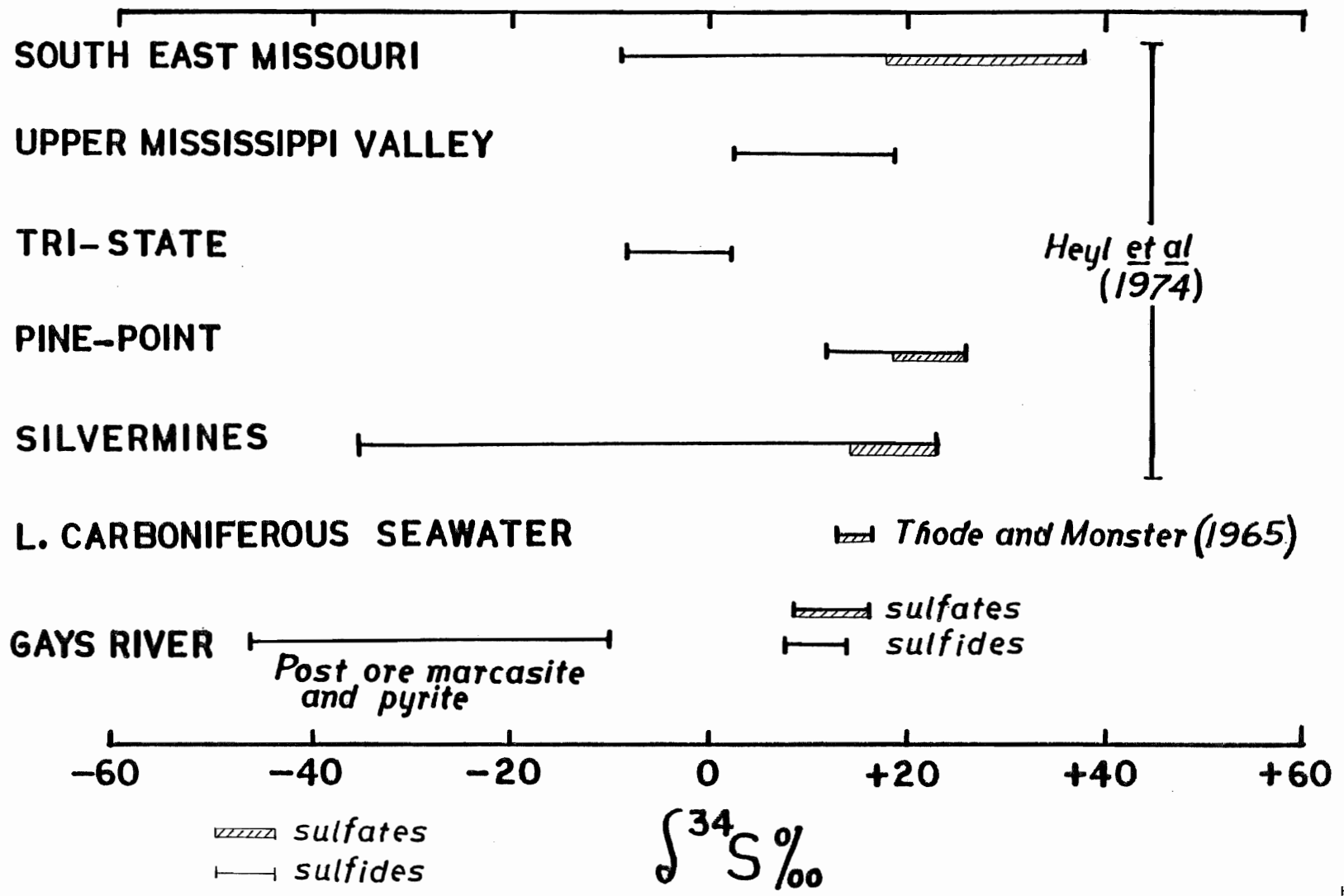


Figure 6.9 Sulfur isotope ratios at Gays River compared to selected lead-zinc deposits.

similar sea water sulfate or dissolved sulfate solution of Mississippian age. The extremely high salinities in the fluid inclusions of the Gays River calcite and fluorite indicate that the ore forming solution was derived from saline brines. It seems appropriate to expect that the sulfate contained in the ore forming brines might have supplied the large proportion of sulfur for the sulfide mineralization.

If the sulfide minerals were precipitated in chemical and isotopic equilibrium with an aqueous solution derived from evaporite at temperatures between 130°C and 215°C, the equilibrium fractionation between the $\text{SO}_4^{=}$ and S^{-2} expected within this temperature range should be between 40 to 47 per mil (Sakai, 1968). Since the maximum fractionation between the sulfate and sulfide minerals did not exceed 6.0 per mil, this suggests that isotopic equilibrium was not attained between the aqueous sulfate solution and the precipitating sulfide minerals. The sulfate/sulfide fractionation cannot be directly related to changes in temperature, pH, Eh, f_{S_2} and ionic strengths of the ore solutions as illustrated in Ohmoto (1972), Rye and Ohmoto (1974) equilibrium systems. Inorganic sulfate reduction in the presence of organic compounds and the associated kinetic isotopic effects may explain the sulfate/sulfide fractionation in the pre-ore marcasite and the ore-stage sulfide minerals in a state of disequilibrium with the ore solution. The light sulfur in the post ore marcasite and pyrite was probably supplied from the biogenic sulfate reduction processes.

Lead from the Gays River galenas are non radiogenic and are distinctly different from the J type anomalous lead reported for similar lead-zinc deposits in the Mississippi Valley of the United States. This lead gave

an Ordovician model age (Zentilli et al.,1980). The lead is probably derived from the Lower Paleozoic basement source and may represent leads remobilized from feldspars in the metagraywacke or from massive sulfide concentrations in the Ordovician Meguma Group metasedimentary basement (Zentilli et al.,1980). The present author believes that these lead isotopic ratios in the Gays River galena, are consistent with the major Gays River mineralizing event having taken place not syngenetically with the Mississippian carbonate host (ca 340 m.y) but at a later period perhaps in the Late Mississippian or Pennsylvanian time (ca. 300 ± 20 m.y).

Oxygen and carbon isotopic composition of the carbonate host to ore indicate a slight depletion of heavy ^{18}O and ^{13}C contents in this host with respect to unmineralized marine carbonate of similar age. This depletion is probably caused by the isotopic exchange between the carbonate host and the mineralizing fluid migrating through the permeable host. Significant depletion in the ^{18}O values occur in the ore-stage calcite as a result of diminishing fractionation in the $\text{CaCO}_3\text{-H}_2\text{O}$ system at the temperature of the hydrothermal fluid. The consistently heavy ^{13}C values in the ore-stage calcite are identical to those reported for marine carbonate (Keith and Weber, 1964). This suggests that the carbon in this ore-stage calcite was derived from the dissolution of the host carbonate. Post ore calcite gave widely scattered ^{18}O and ^{13}C values with the lightest values closely identical to the ore-stage calcite and the heaviest values being similar to the host carbonate. This trend of change in the ^{18}O and ^{13}C values is interpreted as resulting from increasing fractionation at low temperatures in the $\text{CaCO}_3\text{-H}_2\text{O}$ system with a gradual enrichment of the heavy oxygen isotopes with time (Figs. 6.10, 6.11). A partial influence of biogenic carbon probably supplied from cooler formational waters may be

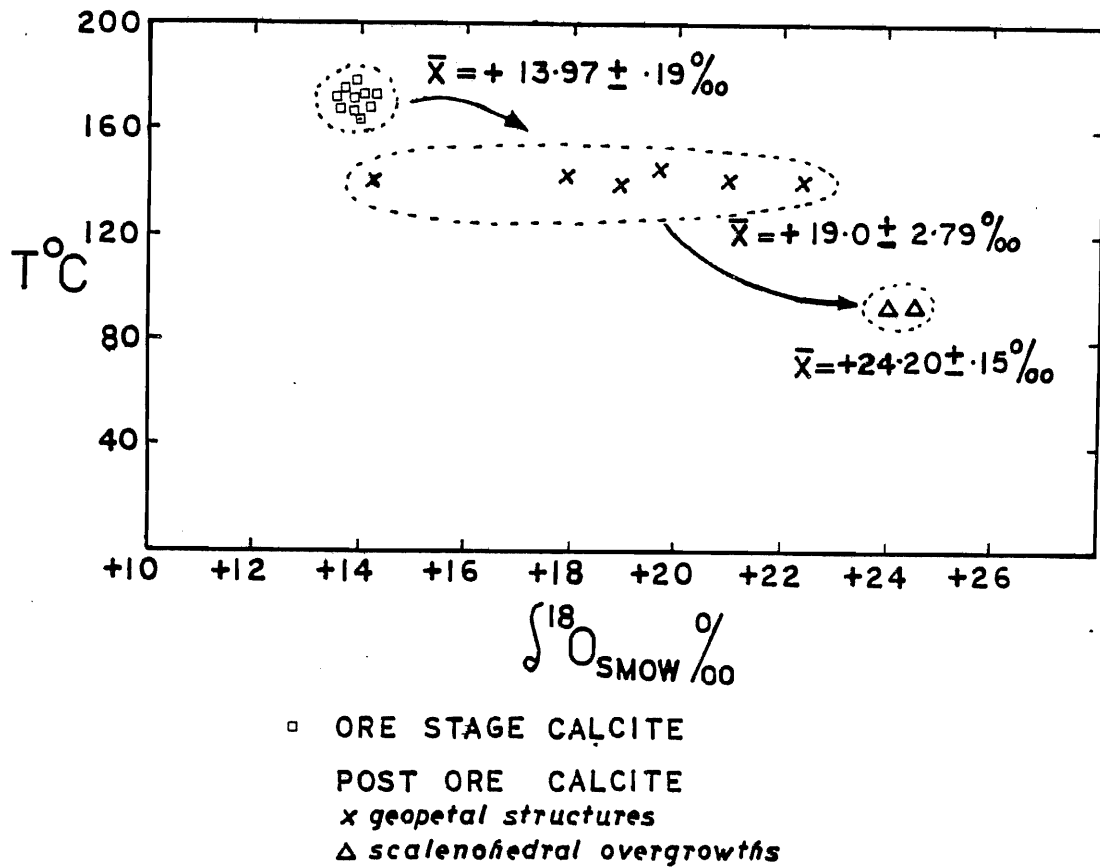


Figure 6.10 Oxygen isotopic composition and temperature relations of calcite from the Gays River mine.

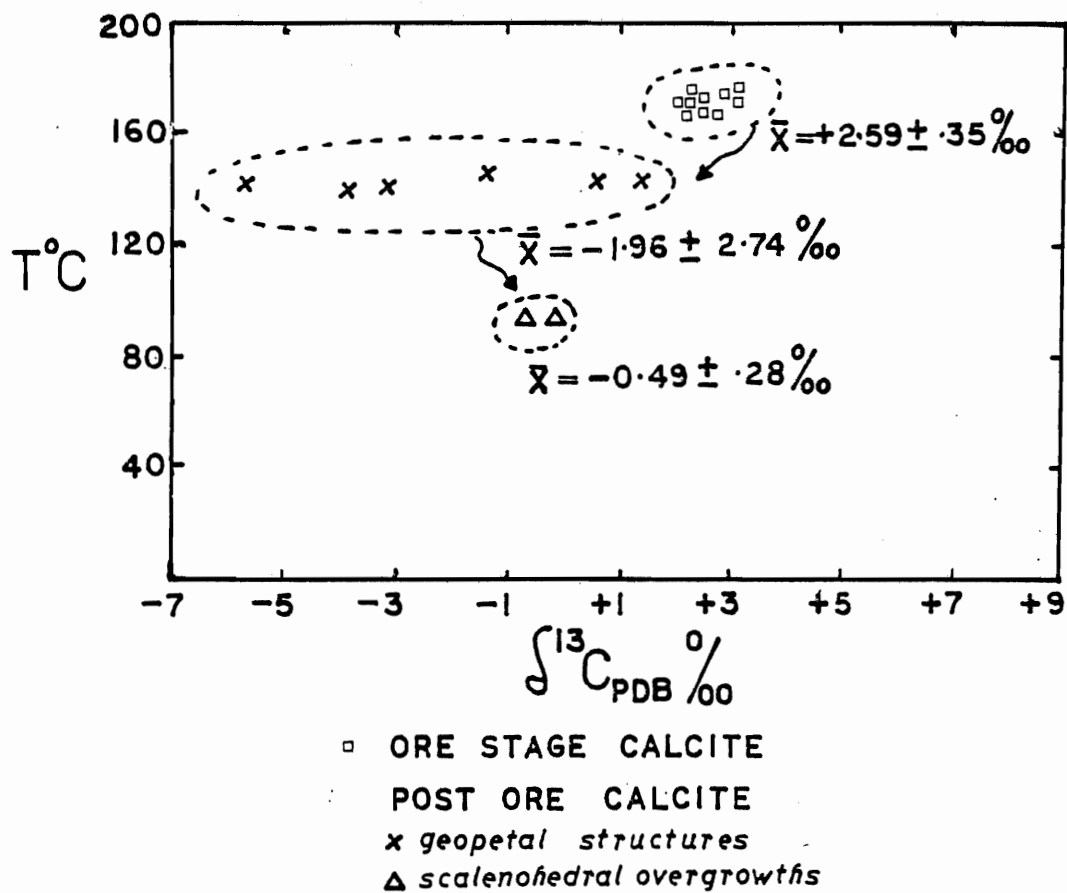


Figure 6.11 Carbon isotopic composition and temperature relations of calcite from the Gays River mine.

responsible for the lighter values of carbon in the post ore calcite and limestone host. The ^{18}O values of calcite and dolomite could not be used to determine their equilibration temperature because dolomite and calcite are not in equilibrium but belong to distinctly different paragenetic stages.

CHAPTER 7

BASEMENT ALTERATION

7.1 General Statement

The changes in the mineralogy, texture, and composition of wall rocks enclosing hydrothermal ore deposits have been identified as useful guides to ore localization. Such changes are generally believed to have resulted from the hydrothermal alteration of the wall rocks during hydrothermal activity and therefore can serve as guides to ore if the spatial and temporal relationships are known. In most hydrothermal deposits, at least some hydrothermal alteration is believed to be contemporaneous with ore deposition because hydrothermal fluids will not deposit ore if they are in chemical equilibrium with the wall rocks. Altered rocks have also become increasingly useful for the interpretation of the chemical and physical conditions of ore deposition. The alteration and recrystallization of the host carbonate rocks have been discussed in Chapter 4. The petrography and petrochemistry of the fresh and altered quartz metawacke basement rocks were studied in order to clarify the relationship of the alteration in this rock to the Gays River lead and zinc mineralization.

7.2 Occurrence

The alteration in the quartz metawacke basement rocks is confined to the faults and fractures traversing this rock in the decline areas such as the 101, 104 and 107 drifts (Appendix I). These faults extend into the overlying carbonate host for the lead-zinc mineralization. The alteration occurs generally along the borders of sulfide veins and is absent at the carbonate/basement unconformity. Alteration zones range from 20

centimetres to 15 metres in width and are commonly traversed by sulfide calcite and quartz bearing veinlets and flanked by fresh quartz metawacke.

7.3 Method of Study

Samples of fresh and altered quartz metawacke were collected underground during mapping. Systematic samples were collected in the 101 and 107 drifts adjacent to sulfide veins where continuous underground drifting have exposed the basement and the overlying carbonate. A total of 37 samples consisting of 11 fresh and 26 altered quartz metawacke were collected for study. Thin sections of the fresh and altered samples were prepared for petrographic study and a total of 35 samples were pulverised and analysed for the major and minor elements with the use of electron microprobe and atomic absorption spectrometry. Age dating was determined for two altered samples.

7.4a General Characteristics of the Quartz Metawacke

The quartz metawacke basement for the carbonate rocks at Gays River represents a part of the Cambro-Ordovician Meguma group. This rock has been folded, faulted and metamorphosed into low grade green schist metamorphic grade in the mine vicinity during the Middle Devonian Acadian orogeny (Fyson, 1966, Poole et al., 1970). Although rocks of the Meguma Group have been intruded by Devonian granite in other parts of southern mainland Nova Scotia, granitic plutons are absent in the mine vicinity. The rocks exposed underground are dominantly quartz metawacke with minor slate intercalations.

b. Petrography

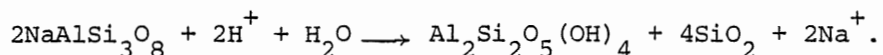
The petrography of the rocks studied will be discussed under two groupings: (i) fresh quartz metawacke and (ii) altered quartz metawacke.

(i) Fresh quartz metawacke: The fresh quartz metawacke form a thick bedded sequence directly underlying the Gays River carbonate rocks. The fresh rocks are gently dipping with dips averaging 35°. The rock consists of quartz, albite, muscovite, chlorite, biotite, epidote and pyrite in decreasing order of abundance. Quartz generally constitutes about 40% of the rock by volume, albite 30%, muscovite 15%, chlorite 10%, biotite 2%, epidote <1% and pyrite <1% approximately. In thin sections, the quartz grains are highly strained and contain abundant inclusions. Albite crystals are generally cloudy and are overgrown by muscovite. Epidote is an accessory mineral in the fresh samples and generally occurs marginal to plagioclase feldspar. Biotite and chlorite are commonly associated in the rock and the original position of biotite is almost completely occupied by light greenish chlorite. Accessory pyrite grains occur as isolated opaque bodies in thin section. The minerals are generally well sorted with respect to shape and size and well formed crystals of quartz and plagioclase feldspar are commonly distributed in a matrix of finely crystalline muscovite and chlorite.

(ii) Altered quartz metawacke: The altered quartz metawacke consists of quartz, kaolinite, muscovite, chlorite, plagioclase feldspar, epidote and opaque sulfide minerals in decreasing order of abundance. Quartz represents about 35% of the rock by volume, kaolinite 30%, muscovite 15%, chlorite 10%, albite 5% and epidote constitutes about 2% approximately. Apatite and the opaque sulfide minerals are accessories. Kaolinite, muscovite and chlorite form a finely crystalline matrix for the altered quartz metawacke and the

rock is highly friable in hand specimen. Due to the fine grained nature of the matrix, identification of the matrix material was determined by X-ray diffraction. In thin section, quartz, albite, epidote and the opaque sulfide minerals are commonly intergrown. Polished thin section examination shows that chalcopyrite, sphalerite and galena in the rock matrix contain inclusions of muscovite. Most of the albite grains are clouded and are only identifiable by the presence of ghost relics of polysynthetic twins in a mass of kaolin and muscovite. Quartz grains are generally elongated, rounded or subrounded and have strong undulose extinction due to strain.

In general, the mineralogy of the altered quartz metawacke compares well with the fresh rock. The two rocks can be distinguished by the presence of abundant kaolinite in the altered rock with a corresponding decrease in the feldspar content. Larger amounts of epidote and sulfide minerals are also present in the altered rock. The presence of kaolinite suggests that this mineral was formed from the breakdown of albite in the fresh rock. Feldspar breakdown may be accomplished during the hydrolysis of albite as shown in the reaction;



This reaction may be accompanied by volume expansion of the rock and strain (Hemley and Jones, 1964).

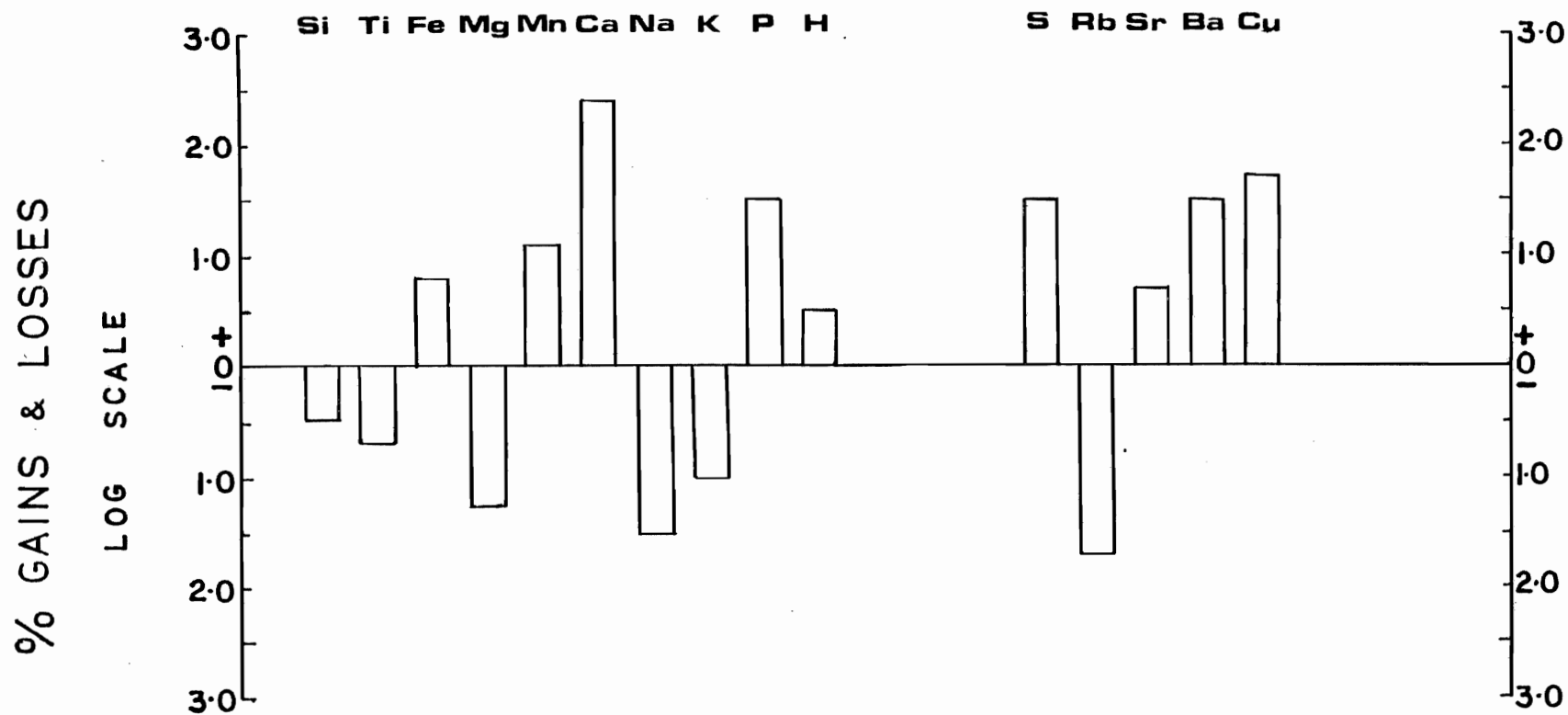
7.5 Petrochemistry

A total of 35 rock samples were analysed for their major elements and selected trace elements (Table V-1). These consist of 10 fresh and 25 altered quartz metawacke samples. The gains and losses of the individual elements in the alteration zones are calculated with respect to the

chemical composition of the fresh rock (Fig. 7.1). Details of calculations are presented in the Appendix V.

The graphical representation in Fig. 7.1 illustrates that the alteration in the quartz metawacke basement is accompanied by a percentage gain in calcium, manganese, iron, sulfur, phosphorous, strontium, barium and hydrogen, and corresponding losses in sodium, potassium, rubidium, magnesium, silicon and titanium. The trend of chemical variations in the fresh and altered suite of quartz metawacke samples indicate that this alteration involves the leaching of alkalis. The loss in Na and K probably reflects the hydrolysis of albite to kaolinite and the breakdown of biotite to chlorite. This loss in Na and K coincides with a decrease in rubidium. Rubidium is commonly incorporated in sodium and potassium bearing minerals because of the identical ionic radii, electronegativities and ionization potentials of these elements (Taylor, 1965). The small decrease in magnesium, titanium and silicon may similarly be attributed to elemental losses during feldspar hydrolysis. Hemley and Jones (1964) suggest that the process of feldspar hydrolysis may lead to the release of significant quantities of magnesium, sodium, potassium and calcium from the minerals into solution. Colloidal silica is commonly released during hydrolysis (Hemley and Jones, 1964). The present author suggests that small losses in these elements occurred during the kaolinization of albite.

The significant gain in calcium, strontium, barium and manganese suggest that these elements were introduced during the alteration process. Strontium and calcium have geochemically identical behaviour in chemical reactions because of their similar ionic radii and electronegativities (Taylor, 1965). These similarities may account for the sympathetic variations in calcium and strontium. The percentage gain in iron and sulfur



*Pb and Zn values in the fresh and altered rock are generally less than 100 ppm

Figure 7.1 Element gain and losses in the altered quartz metawacke basement, Gays River mine.

may be due to the presence of pyrite in the altered zone. The slight gain in hydrogen content in the altered rocks may be related to the hydrolysis of albite.

7.6 Discussion

The complexity of the mineralogy and geochemistry of hydrothermally altered rocks have led many authors to classify distinct facies and types of hydrothermal alteration. Burnham (1962) classified hydrothermally altered rocks into two principal facies; (i) argillic and (ii) phyllic (mica) facies. The argillic facies comprises the propylitic, montmorillonitic and kaolinitic types and the phyllic facies consists of the muscovitic and biotitic types. Meyer and Hemley (1967) expanded Burnham's classification and suggested the distinction of propylitic; intermediate argillic, advanced argillic, sericitic and potassic types also on the basis of the typical mineral assemblages. Although this terminology is applicable to the description of both hypogene or supergene alteration, a controversial problem in alteration study is to distinguish secondary (or supergene) alteration from the primary (hypogene) hydrothermal alteration.

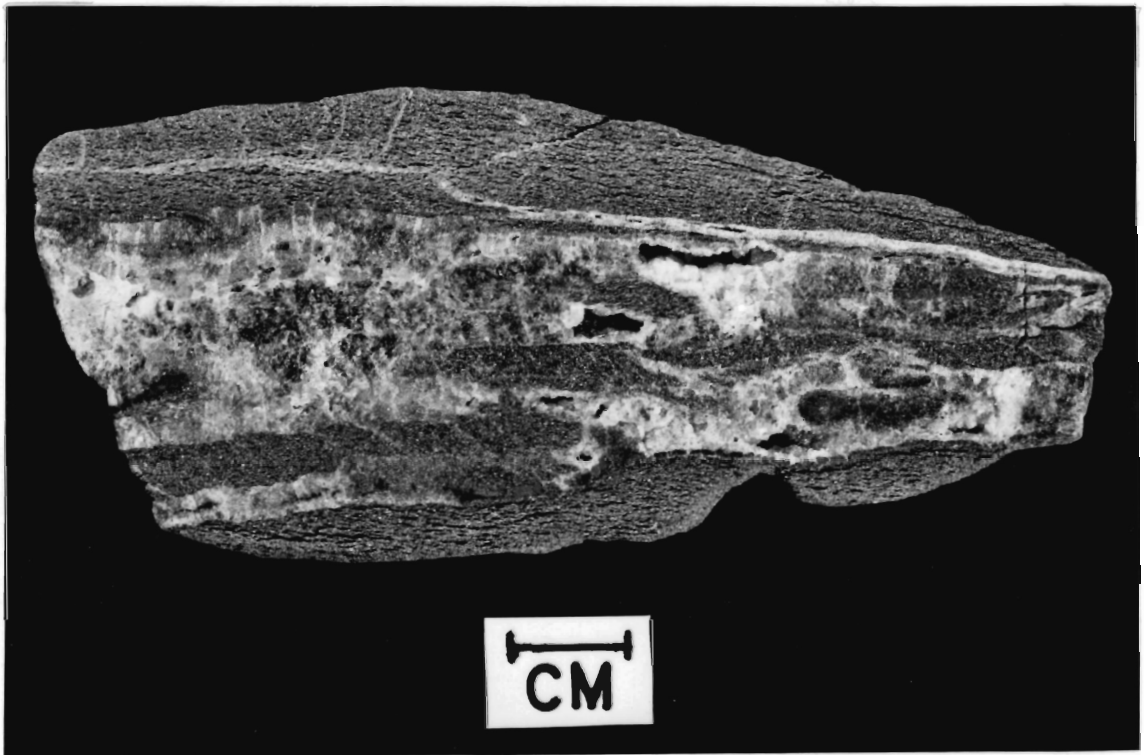
On the basis of Meyer and Hemley (1967) classification scheme, the altered quartz metawacke at Gays River can be described as an argillic alteration. This Gays River basement argillic alteration is characterized by the occurrence of kaolinite associated with muscovite, chlorite and epidote. The alteration is accompanied by appreciable leaching of sodium, potassium, rubidium, magnesium, titanium, and colloidal silica and a significant gain in calcium, strontium, barium, manganese, iron, sulfur, phosphorous and hydrogen. Although argillic alteration is a common character-

istic of hypogene alteration, experimental work of Hemley and Jones (1964) proved that it is possible to produce the argillic alteration assemblage under supergene conditions in the presence of acidic meteoric waters.

If the alteration in the quartz metawacke basement rocks were supergene in origin, as a result of interaction with near surface meteoric waters, a significant gain in aluminum and losses of calcium and potassium would be expected with increasing alteration. Although losses in sodium and potassium occur in the altered rocks, the fairly uniform content of aluminum and the significant gain in calcium content is not compatible with supergene alteration alone.

If the alteration is hydrothermal in origin, such argillic alteration could be produced under low to moderate temperatures below 300°C from a dense solution with a large proportion of highly ionized constituents and a low cation/H⁺ activity ratio (Hemley and Jones, 1964; Reed and Hemley, 1966). Detailed mapping underground reveals that the alteration zones are only confined to faults and fractures in the quartz metawacke basement and these faults commonly contain sulfide veinlets (Fig.7.2). The extensions of the fractures upwards into the carbonate coincide with the massive sulfide vein ores. In the carbonates, the veins are commonly flanked by a dedolomitized limestone. The mineral paragenesis outlined in Chapter 4 indicates that the lead and zinc sulfide mineralization is succeeded by several stages of calcite formation and a post ore dedolomitization. The enrichment of Mn, and Fe in the host carbonates, ore stage and post ore calcite and the intense dedolomitization of the areas adjacent to faults and fractures compared to a corresponding gain in Mn, Fe and Ca in the altered basement rocks, all strongly support the suggestion that the process of

Figure 7.2 Sulfide bearing calcite veinlet in the quartz metawacke basement. This sample is approximately 5 metres below the carbonate/basement unconformity in the 107 drift.



multistage calcite formation, and basement alteration are genetically related.

Whole rock K-Ar ages on 2 samples (107-13 and 107 Sub 1) from the alteration zone gave values of 382 ± 14 Ma and 418.0 ± 12 Ma respectively. These Devonian ages are significantly older than the mineralization event. This suggests that the muscovite is probably older than the mineralization event and that the ore forming fluid was not accompanied by mica formation or mica recrystallization in the basement to reset the argon clock. The latter possibility may be due to the moderate temperature of the ore fluid below that expected for argon loss or mica formation. The two whole rock ages in the alteration zone are comparable with the pre-intrusive gold forming metallogenic event of 410 Ma in southern mainland Nova Scotia (Zentilli and Graves, 1977; Reynolds *et al*, 1981). If this alteration is older than the lead and zinc mineralization, the spatial association of the sulfide minerals and faults suggests that the preexisting structures served mainly as channelways for the ore forming solutions. This however, does not rule out the possibility of alteration during or after mineralization.

Although the relationship between the lead and zinc mineralization and basement alteration is difficult to prove, the present author suggests that the significant enrichment of manganese, iron, calcium, strontium and barium in the basement alteration zone point to a genetic link between the alteration and mineralization.

CHAPTER 8
GENETIC MODELS

8.1 Introduction

The genesis of carbonate hosted lead-zinc deposits has been a subject of considerable interest and great controversy among ore deposit geologists. The carbonate hosted lead-zinc deposits or Mississippi Valley Type represents, a distinct group of the world's greatest sources of these two metals. Although they have been generally considered together with ores in sedimentary basins e.g. the red bed copper ± cobalt deposits, shale hosted lead-zinc and sandstone hosted lead, many obvious similarities and differences still remain. It is however, widely accepted that the genesis of carbonate hosted lead-zinc mineralization is related to a part of a sedimentary basin evolution.

Several genetic concepts have been put forward to explain the source, transportation, deposition and preservation of the lead-zinc ore bodies in carbonate hosts. Some of the concepts have considered the role of sediment compaction, structural deformation, topography, heat flow, hydrostatic gradients in sedimentary basins to explain the evolution of their associated lead and zinc mineralization. While opinions differ in several respects, and many questions are still unanswered, the present concept on the genesis of carbonate hosted lead-zinc deposits can be classified into three: i) synsedimentary ii) diagenetic and iii) epigenetic (Gustafson and Williams 1981; Bjorlykke and Sangster 1981). These authors demonstrate that the hypotheses involving epigenetic diagenetic and synsedimentary processes are all "alive" in sedimentary ore deposits. Although certain genetic factors are reasonably clear and obvious for a deposit type, the place of the hypo-

theses in relation to one another and to the overall process of basin evolution is still unclear (Anderson and Macqueen 1982).

An evaluation of each of the three hypotheses of sedimentary ore genesis as presented by several authors is here attempted. The objective is to integrate the salient geologic, mineralogic and geochemical features of the Gays River deposit to formulate a model which can best explain the relationships.

8.2 Jackson and Beales' Hypothesis

The classic model of shale-basin dewatering during compaction and Mississippi Valley Type mineralization originates from the detailed study of the Pine Point deposit (North West Territories) by the two authors. On the basis of the relationship of the lead-zinc ore bodies and the host carbonate in the Pine Point area, Beales and Jackson (1966 ; Jackson and Beales, 1967) concluded that the lead-zinc mineralization forms a part of a normal basin evolution. The authors argue that sulfide mineralization occurs where metal rich fluids squeezed out of shale into a fluid-escape route, intermingles with the H_2S liberated from formational waters or reefs (Fig. 8.1). Jackson and Beales (1967) emphasized that the basinal fluids acquire their metals through brine leaching. These metals are transported as chloride or organic complexes and are precipitated as sulfides where H_2S is encountered. The H_2S is believed to have been derived from the nearby evaporites through the action of sulfate reducing bacteria in the presence of petroleum. Jackson and Beales (1967) argued convincingly that the ore deposits are not of syngenetic origin and are not likely to be of juvenile hydrothermal origin. Evidence against syngeneses listed by the authors include 1) the prevalence of open space fillings and colloform

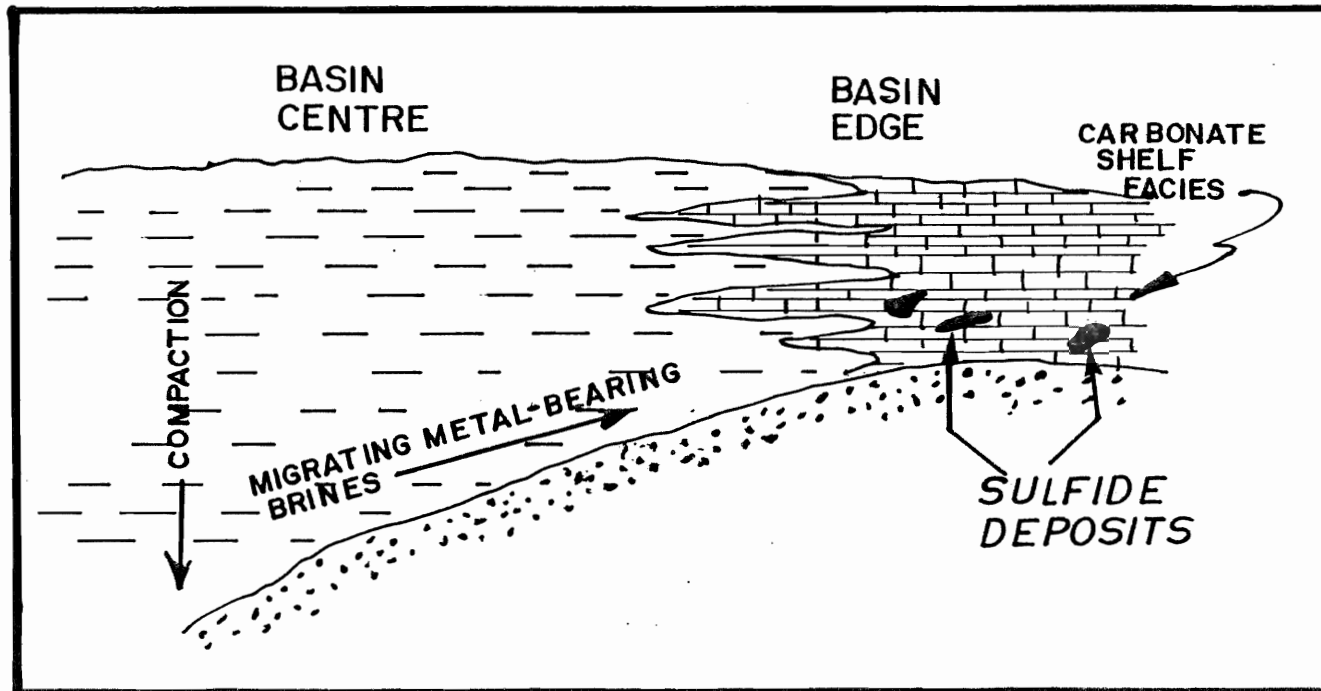


Figure 8.1 Brine release from the compaction of shale and the Mississippi Valley Type deposits; schematic representation. Modified after Jackson and Beales (1967).

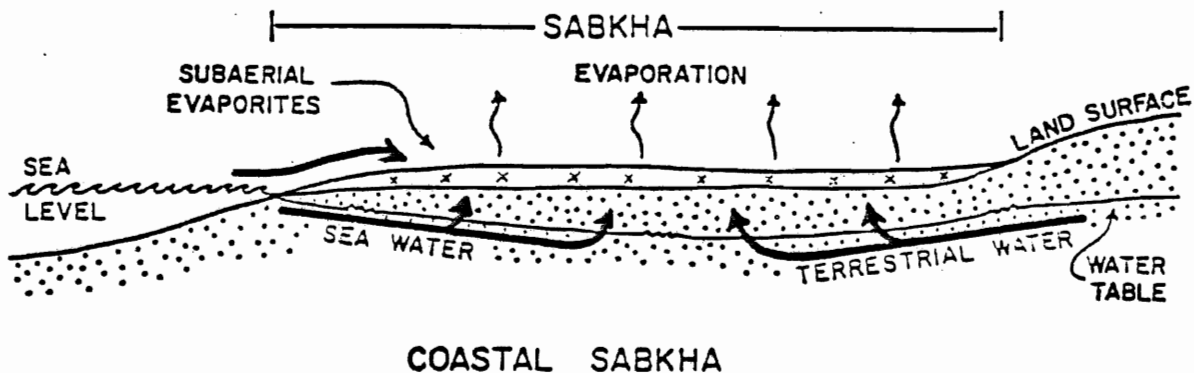
textures which suggests growths on cavity walls and breccia fragments, 2) breccia moldic porosity occupied by bituminous residues prior to ore formation, 3) narrow range of sulfur isotopic composition in the ore bodies compared with the syngenetic or early diagenetic sulfides from host rock 4) fluid inclusion salinities in sphalerite which indicate that the ore fluid was much more concentrated than sea water (Beales and Jackson, 1968). The lack of igneous affiliation with the geological setting at Pine Point and the simple mineralogy of the ores discount the possibility that the Pine Point mineralization is of juvenile hydrothermal origin (Beales and Jackson, 1967).

Although the Jackson and Beales' model is appealing to carbonate hosted lead-zinc mineralization and has reasonably well explained the Pine Point ore genesis, the derivation of the metal ions solely from shale may not be valid for all carbonate hosted lead-zinc deposits. While the model connotes a shale basin source for the metal ions, the present author believes that the derivation of metals in a basin without any proximal shale needs an alternative explanation. The mixing model of metal ions with H_2S contained in formational waters has been another area of controversy. This point has been discussed in more detail in Chapter 6. It is noted at least for the Buick mine in south east Missouri ore district, that lead and sulfur were probably transported together in the same solution (Sverjensky et al., 1979). This is supported by lead and sulfur isotope data. While Jackson and Beales' model may be suitable for the Pine Point lead-zinc mineralization, the applicability of the model to other carbonate hosted deposits may certainly need some modifications depending on the geologic, mineralogic and geochemical factors prevailing at that site.

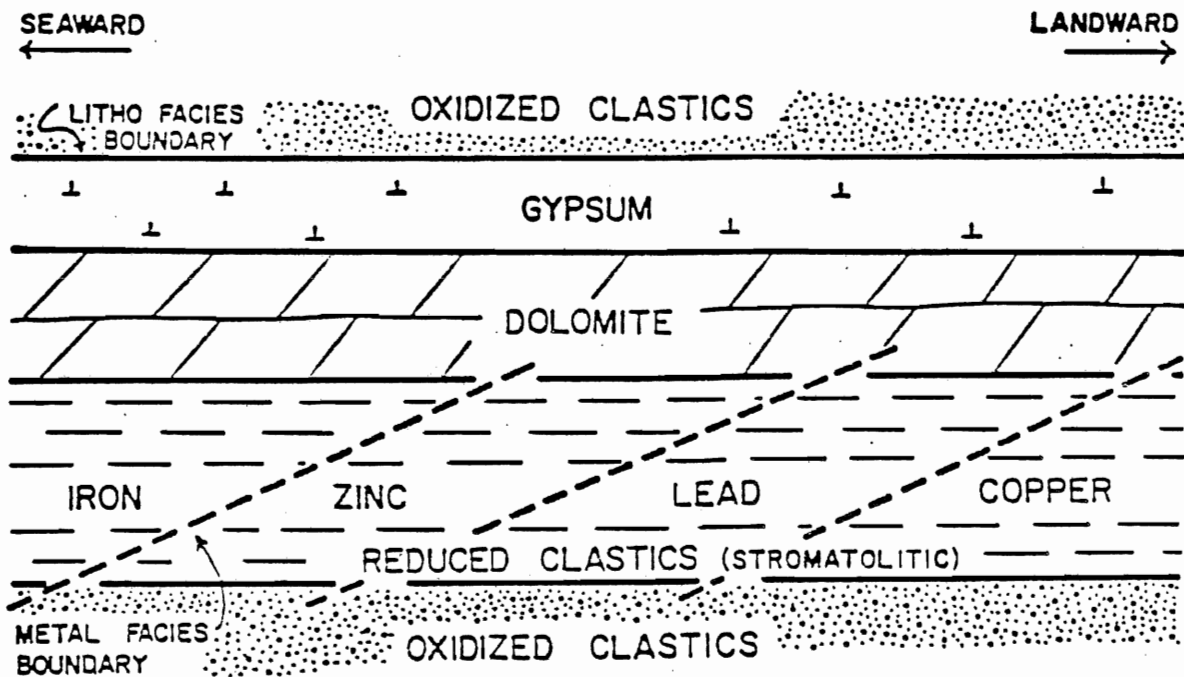
8.3 The Sabkha Model

A model involving the syngenetic and diagenetic processes of coastal sabkhas was proposed by Renfro (1974) to explain the genesis of evaporite-associated stratiform metalliferous deposits. Such deposits are commonly underlain by continental red beds or oxidized strata and overlain by evaporites. A sabkha can be described as a barren, arid, uninhabited evaporite flat bordering partially landlocked seas (coastal sabkha) and covering a number of continental depressions (continental sabkha) (Kinsman, 1969). Their positions permit a continuous loss of groundwater to the atmosphere by upward transpiration and evaporation thereby causing groundwater solutes to be deposited at or near the sabkha surface (Kinsman 1969). Coastal sabkhas are commonly bordered on the seaward end by intertidal mudflats and lagoons that are carpeted by leather-like mats of sediment binding blue green algae. The unique position of coastal sabkha permit the subsurface flow of landward migrating low Eh-high pH sea water and the seaward migrating high Eh-low pH terrestrial water (Renfro 1974) (Fig. 8.2). Renfro indicated that the seaward migrating terrestrial formation water with a low pH and high Eh can mobilize trace amounts of copper, silver, lead and zinc.

As the metal charged solution passes through the hydrogen sulfide charged algal mat, its load of metal ions is reduced and precipitated as sulfides (Renfro, 1974). This author emphasized that the regional conformable persistence of the stratiform metalliferous deposits illustrate the geometry of the hydrogen sulfide bearing host strata. Metal zonation in the deposit depends on the relative solubilities of the metal ions in the groundwater solution. The most soluble metal is commonly found in the



a — Flow regime in the sabkha environment.



b — Metal zonation in a sabkha related deposit.

Figure 8.2 The sabkha model; after Renfro (1974).

seaward end. Renfro (1974) added that the grade and size of the deposits are dependent on 1) the quantity of the available reductant, 2) duration of the sabkha process and 3) the quantity and chemistry of the metal bearing terrestrial water. Renfro concluded this process to be of syndiagenetic origin. Garlick (1981) in his study of the Mufulira copper deposit in Zambia suggests that the copper and iron sulfide precipitation was contemporaneous to sedimentation and not syndiagenetic as proposed by Renfro (1974). This author argues that the deposition of sulfides by the metal charged low pH, high Eh terrestrial water occurs after a period of mixing of the buoyant terrestrial water with saline groundwater in the anoxic alga-rich lagoons. The sulfide mineralization is terminated by sabkha regression (Garlick, 1981). This is in contrast to Renfro's model of copper precipitation from terrestrial waters, ascending through decaying algal mats under sabkha evaporites (Garlick, 1981).

Renfro and Garlick's low temperature sabkha model appears to explain the stratiform nature and consistent stratigraphic relationship of such metalliferous deposits as the Kupferschiefer of Germany and the Roan of Zambia. While such a model may apply to several low temperature syngenetic metalliferous deposits, as the copper bearing shales, it may be inadequate to explain the relatively high temperatures of approximately 150°C in carbonate hosted lead-zinc deposits. Indeed the high salinity of approximately ten times sea water in carbonate hosted lead-zinc deposits discounts the possibility of transporting the lead and zinc ions in groundwater.

8.4 Downward Excavating Hydrothermal Cells

A model involving downward excavating convection cells (mainly seawater) was put forward by Russell (1978, 1981) to explain the genesis of the

stratiform Irish type lead-zinc ± copper deposits. This author demonstrated that the Irish ore deposits and sediment hosted exhalative zinc/lead deposits e.g. Mt. Isa and McArthur River are characterized by features which can be accounted for by deriving the ore solution from the subsurface convective circulation of modified high saline sea water. This is supported by their stratiform morphology and association with submarine debris flows and iron formations in a boiling environment. The downward penetrating fluids first leach and transport zinc and lead in the basement rocks but as the cells migrate to deeper horizons, they become bigger and hotter and are able to leach and transport copper. The driving force for the convective cells is believed to be associated with the high geothermal gradient accompanying continental rifting. The resulting sulfide ores are syngenetic stratiform bodies localized near the base of fault related depressions on the sea floor (Fig. 8.3).

Russell et al. (1981) indicated that the sediment hosted deposits are of relatively high temperatures and are early in the basin evolution. This distinguishes them from the carbonate hosted lead-zinc deposit of Mississippi Valley Type. Another important feature which distinguishes the sediment hosted lead-zinc deposit is the boiling environment of deposition. The carbonate hosted lead-zinc deposit of Mississippi Valley Type are generally deposited in a non boiling environment. The lead-zinc-copper deposits at Tynagh, Navan and Silvermines, Ireland and Walton, Nova Scotia were cited as examples for the downward excavating convective cell model (Russell, 1981). This author concluded that these are coeval deposits separated by a predrift 20° of the the earth's circumference.

Although Russell's model appears to explain the genesis of sediment hosted stratiform ore deposits in these districts, the hypothesis does not

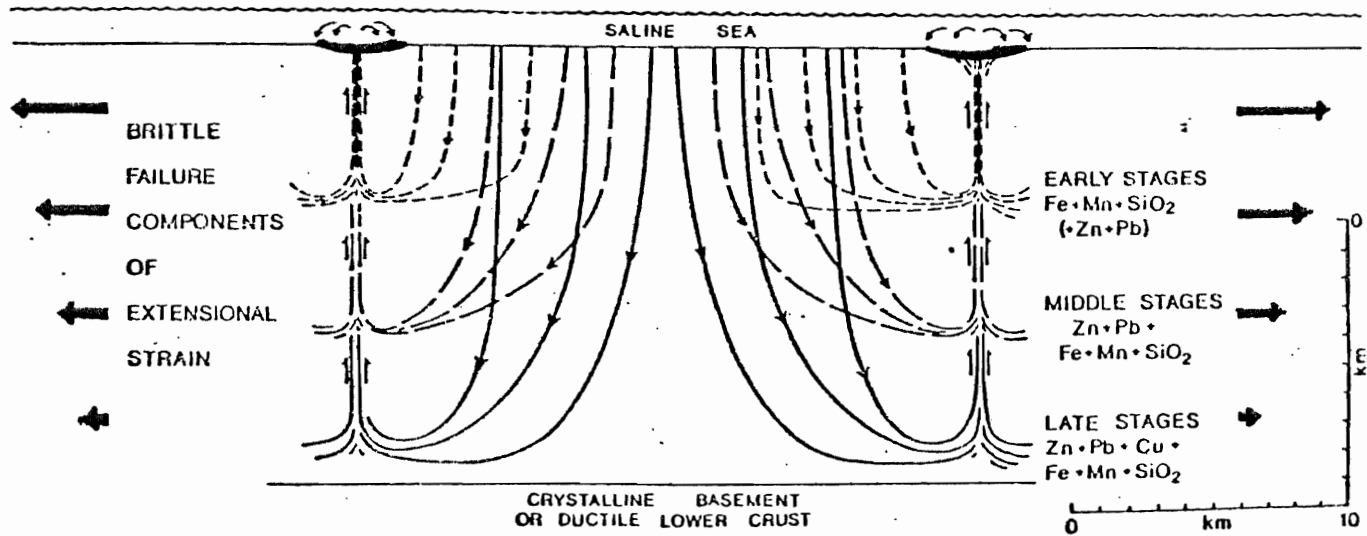


Figure 8.3 Downward excavating hydrothermal convective cell system. After Russell (1981).

explain the epigenetic vein ores that are commonly associated with the stratiform ores. Examples of such crosscutting vein ores are noted at Tynagh, Silvermines and Mount Isa. Perkins (1981), on structural grounds, considers the crosscutting copper ore bodies at Mount Isa as epigenetic and genetically independent of the sedimentary lead-zinc ores. In contrast to this inference Stanton (1963), Finlow Bates and Stumpfl (1979) in Russell et al. (1981) have argued in support of contemporaneous epigenetic copper and syngenetic lead-zinc mineralization.

The present author favours the last suggestion because epigenetic sulfide bodies may be contemporaneous with stratiform mineralization if the metal bearing convective cells fail to reach the sea floor before forming sulfide minerals in dilatant fractures within the initially deposited sediments. This may not invalidate the convective circulating hypothesis because the ability of the cells to bring mineralizing solution to the sea floor may depend on the permeability, temperature, pressure, viscosity and their ultimate size.

8.5 Boyle's Epigenetic Model

A study of the barite, manganese, lead, zinc, copper, silver deposits of the Walton Cheverie area, N.S., led R.W. Boyle to propose an epigenetic model involving deep circulating brines for the barite and the associated base metal sulfides. This is supported by the spatial association of the deposit with deep seated faults cutting through the Lower Carboniferous fluviatile and lacustrine sediments of the Horton group and the upper marine sequence of limestone and evaporites. Boyle (1976) concluded that deep circulation brines derived from the evaporite sequence, pervaded and leached metal ions as Ba, Sr, Ca, Mn, S, As, Cu, Pb, Zn, Ag from the Horton Group shales and sandstones (Fig. 8.4). The brines were driven by high geo-

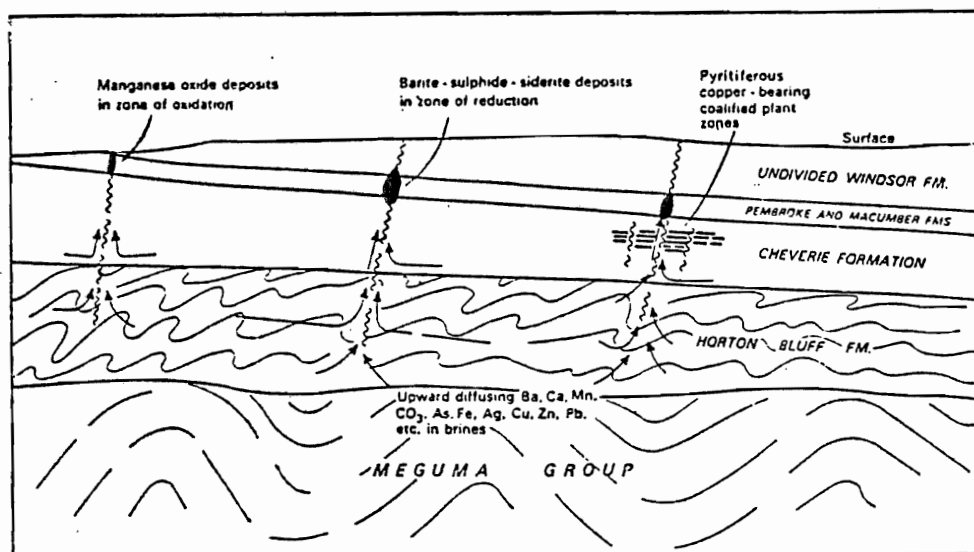


Figure 8.4 Schematic mode of emplacement of the barite, manganese, lead, zinc, copper, silver deposits of the Walton-Cheverie area, Nova Scotia. After Boyle *et al.* (1976).

thermal gradient accompanying the intrusion of diabase sill during the Triassic period (Boyle, 1976). This author concluded that the large massive cryptocrystalline barite body in the Magnet Cove deposit originated mainly by replacement of bedded gypsum and anhydrite (Ba^{2+} for Ca^{2+}). This is supported by the similarities in the isotopic composition of the sulfate in the evaporite and the resultant barite. Coarse crystalline barite veins, sulfides and sulfosalts were deposited from the deeply circulating brines in the hypogene zone of reduction (Boyle, 1976).

Although the genesis of the Walton barite, lead, zinc, copper deposit appears controversial with the more recent interpretation of Russell (1978, 1981) which suggest a synsedimentary genesis, it is difficult at this stage to discredit any model of genesis until more detail analysis of the geologic and fluid inclusion studies of the Walton deposit can be carried out. While the deposit has important geologic features which compare with the geology of the stratiform Irish lead, zinc, copper deposits (Russell, 1981), distinct epigenetic features such as discordant barite and sulfide veins in fault systems are also present (Boyle, 1976). The underlying Horton group sediments contain anomalous amounts of chalcophile elements including zinc, copper, lead, silver, gold, arsenic, antimony, tin, molybdenum and cobalt (Boyle, 1976). If deep circulating brines were responsible for the leaching, transport and deposition of the base metal sulfide ores and barite at the Magnet Cove deposit, then the process of metal derivation could be similar to the mechanism of downward excavating cells of Russell (1978, 1981) except for the timing. While Russell (1978) invoked a synsedimentary deposition probably early in the basin history, Boyle (1976) indicated a similar process at a much later time assuming the brine is dominantly of sea water composition. Indeed the time of emplacement of ore deposits has been a major problem in ore genesis. As Heyl (1968) indicated for Mississippi Valley Type deposits

"the age of the deposits cannot be definitely determined from any known relations in the Mississippi Valley" (Heyl 1968, p. 442). Similarly, while the source, transport mechanism and mode of emplacement of sulfide ore deposit may be generally acceptable to several authors, the timing of mineralization may still remain controversial until a better method of dating ore deposits is established.

8.6 Gays River Model

a. General

With the full awareness of the syngenetic and epigenetic schools of thought, a model is here proposed to explain the salient geologic, mineralogic, fluid inclusion and isotopic data that have been examined in this thesis. The consideration of the different genetic models shows that no one model may adequately explain all the salient characteristics of Gays River mineralization because of the distinct similarities and differences between this deposit and the examples made by others to formulate their models.

The Jackson and Beales model for the Pine Point deposit favours the dewatering of shales to generate brines which later mingle with the H_2S in formation water to precipitate the lead and zinc sulfide ores. Although the present author favours the suggestion that the lead and zinc mineralization at Gays River could be a part of normal basin evolution, there is no shale sequence to dewater in the Gays River area (Giles et al, 1979). Also the transport of metal and H_2S in separate solutions as required by Jackson and Beales (1967, 1975) is a controversial problem beyond the scope of the present thesis. Hence the Jackson and Beales' model may not entirely explain the Gays River genesis.

Renfro's sabkha model, for the genesis of evaporite related metalliferous deposits involves groundwater circulation of low pH and high Eh. While this process applies to evaporite associated stratiform copper shales, the groundwater process of metal leaching is not compatible with the temperature and salinity measurements in the Gays River minerals. Discordant vein systems recognized in the Gays River deposit are not in accordance with the stratiform morphology of the evaporite associated metalliferous deposits of Renfro (1974).

The work of Russell (1978, 1981) emphasized the importance of downward excavating convection cells in the genesis of the sediment hosted lead, zinc, copper deposits of Irish type, Mount Isa and McArthur River in Australia and Walton in Nova Scotia. This genesis, he believed to be a synsedimentary process in a boiling environment (Russell 1978; 1981). The resulting ore deposits are generally stratiform and commonly associated with iron formations. While the mechanism of base metal leaching by downward excavating saline brines may appeal to the Gays River genesis, certain geologic features in the Gays River deposit are not compatible with the characteristics of the sediment hosted ores.

Both stratiform and vein ores are present at Gays River. The ores were emplaced in a non-boiling environment and are not associated with iron formations. A minimum depth of 170 metres (17 bars) is estimated to have prevented the Gays River ore solution from boiling (this study). Since the high grade lead-zinc mineralization is commonly contained in intrapore and interpore spaces of algal stromatolites and within well grown bioclasts associated with the algal stromatolites, it is doubtful that this ecology was thriving at this depth at the time of mineralization. Indeed, the cross-cutting relationship of the high grade vein ores and the block relics of the

host carbonate within the massive sulfide ores suggest that the main period of ore formation post dated the host carbonate deposition. The present author believes that the epigenetic hypotheses of ore deposition proposed by Boyle (1976) invoke a similar mechanism of metal derivation as in Russell's model but at a much later period of basin evolution from brines of similar sources.

The main characteristics of the Gays River deposit from the present study are summarized in order to show how the salient features fit into a genetic model.

1. The Gays River deposit consists of stratiform and discordant vein type lead-zinc ores in a carbonate host underlain by the Lower Paleozoic quartz metawacke basement of the Meguma group and overlain by gypsum and anhydrite of Lower Carboniferous age.
2. The discordant vein systems are fault controlled, form the highest grade ores in the mine and areas adjacent to them have significant stratiform mineralization.
3. The mineralogy in the stratiform and vein lead-zinc ores are dominantly sphalerite and galena, with calcite, barite, fluorite, pyrite, marcasite, chalcopyrite and bitumen as the associated gangue minerals. A remarkable similarity exists in the mineralogy and chemical composition of the stratiform and vein ores.
4. Fluid inclusions homogenize at the following temperatures: sphalerite 215°C, ore stage calcite 173°C, post ore calcite 142°C and barite 137°C. Salinity measurements indicate that the ore fluid was much more concentrated than sea water.
5. Sulfur isotope values of the gypsum and anhydrite stratigraphically above

the ore body and barite within the ore are compatible with the Lower Carboniferous sea water derivation. Sulfur isotope values from the ore body are heavy, have a narrow range of δS values and different from late diagenetic sulfides in the host rock.

6. Oxygen and carbon isotopic composition of the host rock and calcite gangue indicate that the isotopic composition in the carbonate host was lowered during mineralization so that ore stage calcite is extremely depleted in heavy oxygen.

7. Lead isotopic composition in galena is compatible with a derivation of lead from the Lower Paleozoic Meguma basement.

8. Petroleum hydrocarbons in form of bitumen proximal to the sulfide ores suggest that the ore solution carried significant quantity of organic material and the thermal degradation of petroleum may have played a significant role in metal deposition.

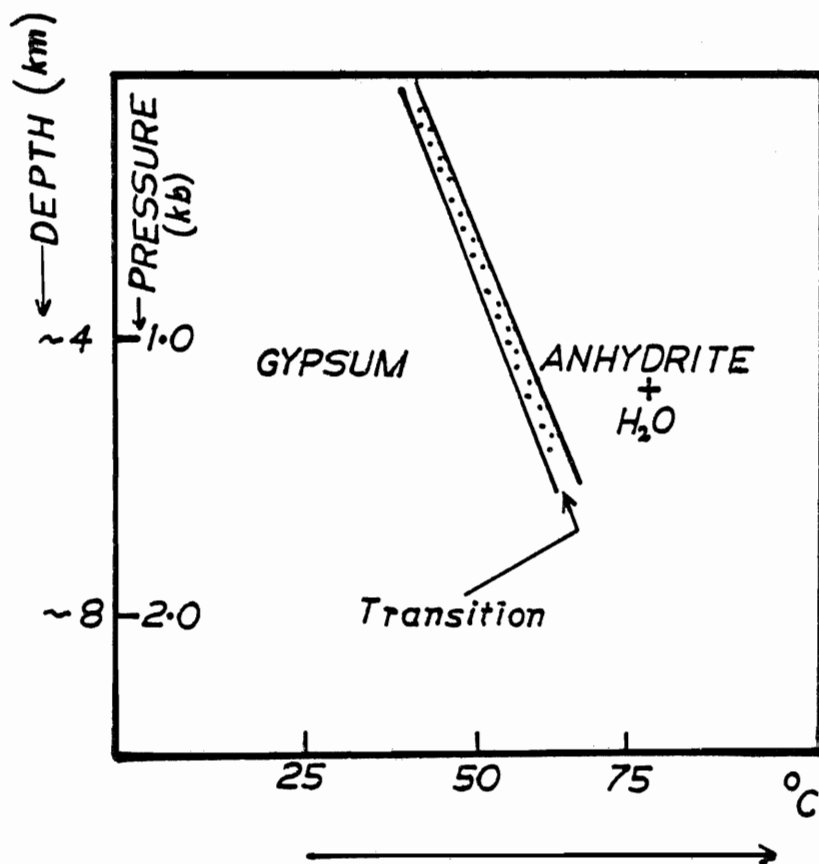
This summary of the geologic, fluid inclusion and stable isotopic characteristics of the Gays River deposit supports a model for epigenetic emplacement of lead and zinc sulfide ores with the following sequence of events.

b. Dewatering and Brine Release

As previously discussed, the carbonate rocks and the overlying evaporite in the Gays River area, form a part of the Lower Carboniferous sediments that were deposited in a portion of the large rift valley system termed the Fundy Basin (Bell, 1958; Belt, 1965; Howie and Cumming 1963; Schenk, 1969). The deposit lies specifically between two small structural basins; the Shubenacadie basin to the north west and the Musquodoboit basin to the south east.

The succession of Middle to Late Visean-Namurian Windsor Group in the Shubenacadie and Musquodoboit Basins comprises between 45 and 70% evaporites, including stratified halite and anhydrite (Boehner, 1981). If a large proportion of the evaporite was initially deposited as gypsum, a possible source of brine generation involves the conversion of gypsum to anhydrite with increasing temperature, pressure and salinity (Macdonald, 1953; Zen, 1965; Hardie, 1967; Butler, 1969; Thiede et al., 1978). Butler (1969) indicated that anhydrite is the stable form of calcium sulfate at a temperature of $> 42^{\circ}\text{C}$ and salinities > 145 parts per thousand. Although the gypsum-anhydrite conversion, volume changes and the volume of water released in the process have been a subject of controversy, Borchert and Muir (1964) proposed that the gypsum anhydrite conversion must generate enormous volumes of water in the order of 0.486 cubic meter per cubic meter of gypsum replaced. More recently, Fyfe, Price and Thompson (1978) indicated that at temperatures as low as 40°C and a confining pressure of 300 bars, gypsum releases 48.5 percent of its volume as it converts to anhydrite (Fig. 8.5).

The present author believes that this conversion of gypsum to anhydrite at the onset of replacement and during subsequent compaction of the evaporite in the Shubenacadie basin must have generated significant quantity of overpressured saline brines. The process of gypsum conversion could have been more intense in the deeper and hotter parts of the basin with appreciable contribution of sulfate and chloride into the resulting brine. The initially deposited gypsum reverts to anhydrite as a result of dewatering, compaction and volume shrinkage. This process of fluid release during gypsum-anhydrite conversion may lead to fluid overpressure as the hydrostatic



modified after Fyfe et al (1978)

CONVERSION AT 40°C ONWARDS

AT ~ 1.25 Km, 300 bars

VOLUME OF H_2O RELEASED $\sim 48.5\%$

Figure 8.5 Pressure-temperature conditions for gypsum-anhydrite conversion.

After Fyfe et al, (1978).

pressure approaches the lithostatic values. The fluids which cannot escape upwards through the impervious evaporite leave the basin laterally following the contours of the basin until they meet the porous and permeable carbonate rocks at the reef overlying the basement high. This may result in the shattering and hydrofracturing of the carbonate rocks and a contemporaneous reactivation of the preexisting fractures in the quartz metawacke basement (Fig. 8.6).

c. Mineralization

As the saline fluids pervaded the carbonate and basement rocks along faults and fractured channels, their temperature must have increased to a maximum of approximately 215°C at basement depths where metal ions were leached. Organic substances within the carbonate sequence were trapped in the saline brines and may have matured into methane and bitumen at the temperature of the hot brines. The total salt content of the original brine could have been in the order of 170,000 to 204,000 ppm according to the freezing temperature of fluid inclusions in calcite and fluorite. This saline brine may have contained significant amounts of sodium, calcium, chloride, sulfate and petroleum hydrocarbons apart from its metal load. Migration of the deeply circulating metal rich brine probably took place along the basement unconformity or deeper, through faults and fractures and surfaced through the carbonate reef.

If significant quantity of sulfate is carried in the metal bearing solution, deposition of the sulfide minerals in veins and stratiform pores could have occurred as a result of pH change, cooling, dilution and/or non biogenic reduction of sulfate to sulfide by petroleum hydrocarbons. Occurr-

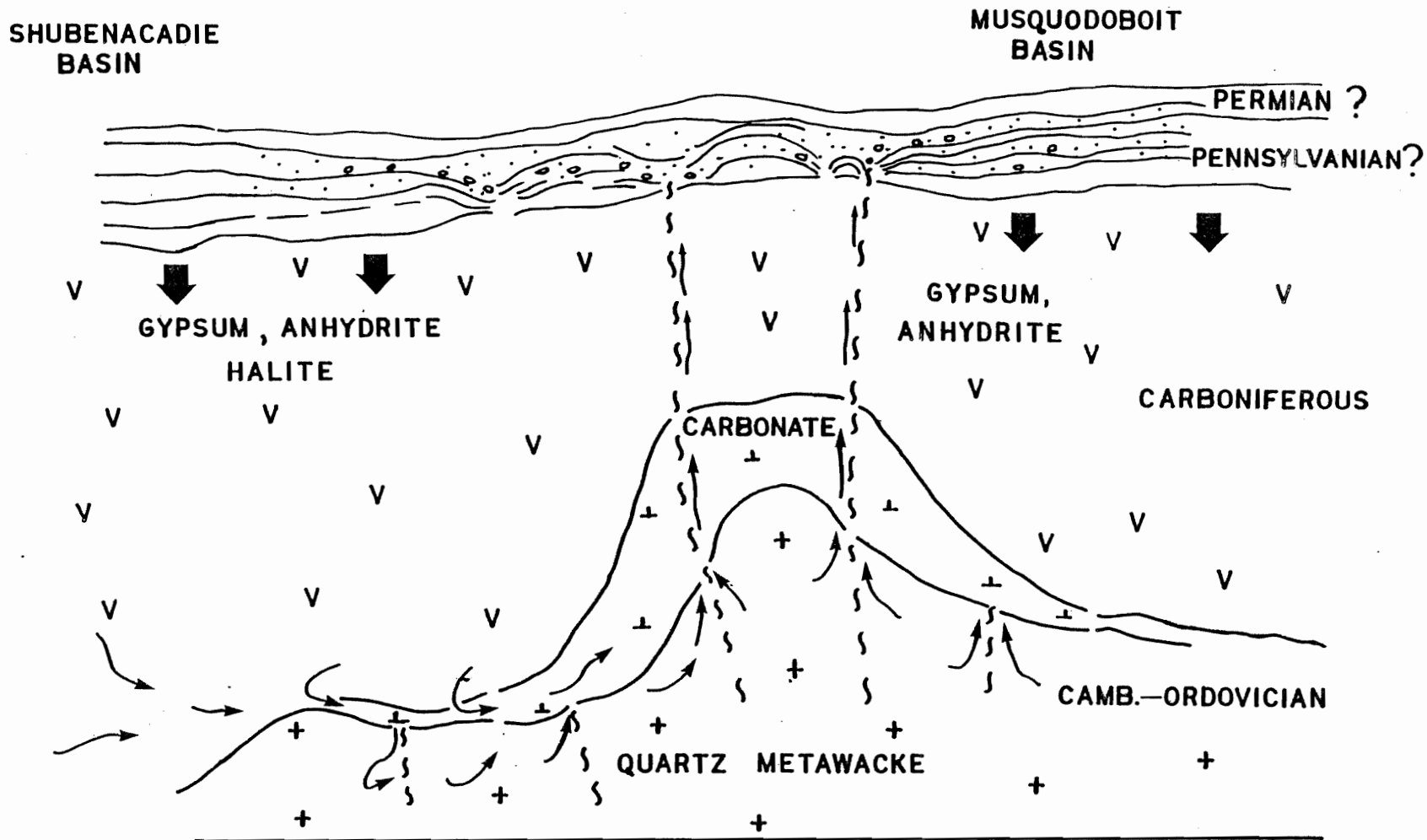


Figure 8.6 The Gays River genetic model; evaporite dewatering and the release of saline brines.

ence of high grade massive sphalerite and galena veins within the carbonate and the association of significant stratiform ores adjacent to the veins suggest that the vein systems represent the main channelways for the ore solutions and could have served as feeders for the stratiform sphalerite and galena mineralization. The mineralization event was accompanied by hydrothermal alteration and lowering of the oxygen isotopic values of the carbonate hosts. A change in pH and Eh of the ore solution during neutralization and mixing with cooler interstitial formation water in the carbonate reef probably led to the precipitation of calcite, fluorite and barite.

The age of the deposit has been another area of controversy. Fluid inclusion and isotopic data of Dickie (1977) Zentilli *et al.* (1980) have shown that the lead-zinc-silver deposit in the Dunbrack ore body (50 km southwest of Gays River) despite its position in a Devonian adamellite has affinities with mineralization found in the Carboniferous rocks of Nova Scotia. These authors concluded that the Dunbrack deposit was probably formed during a Pennsylvanian hydrothermal episode as a result of an increasing geothermal gradient at a time of tectonic disturbance (Maritime Disturbance) and possible magmatism (Reynolds *et al.*, 1981). Indeed, the increasing geothermal gradient which drove the saline fluid precursor for the ore solution into basement depths to form the Gays River deposit may have accompanied the Late Carboniferous (Pennsylvanian) tectonic disturbance.

d. Preservation

The period of mineralization was followed by uplift and erosion events of which there is little record, culminating with the influx of groundwater into faults and channelways in the carbonate reef during the Cretaceous (Fig. 8.7). This led to the deposition of Cretaceous sediments in the fault re-

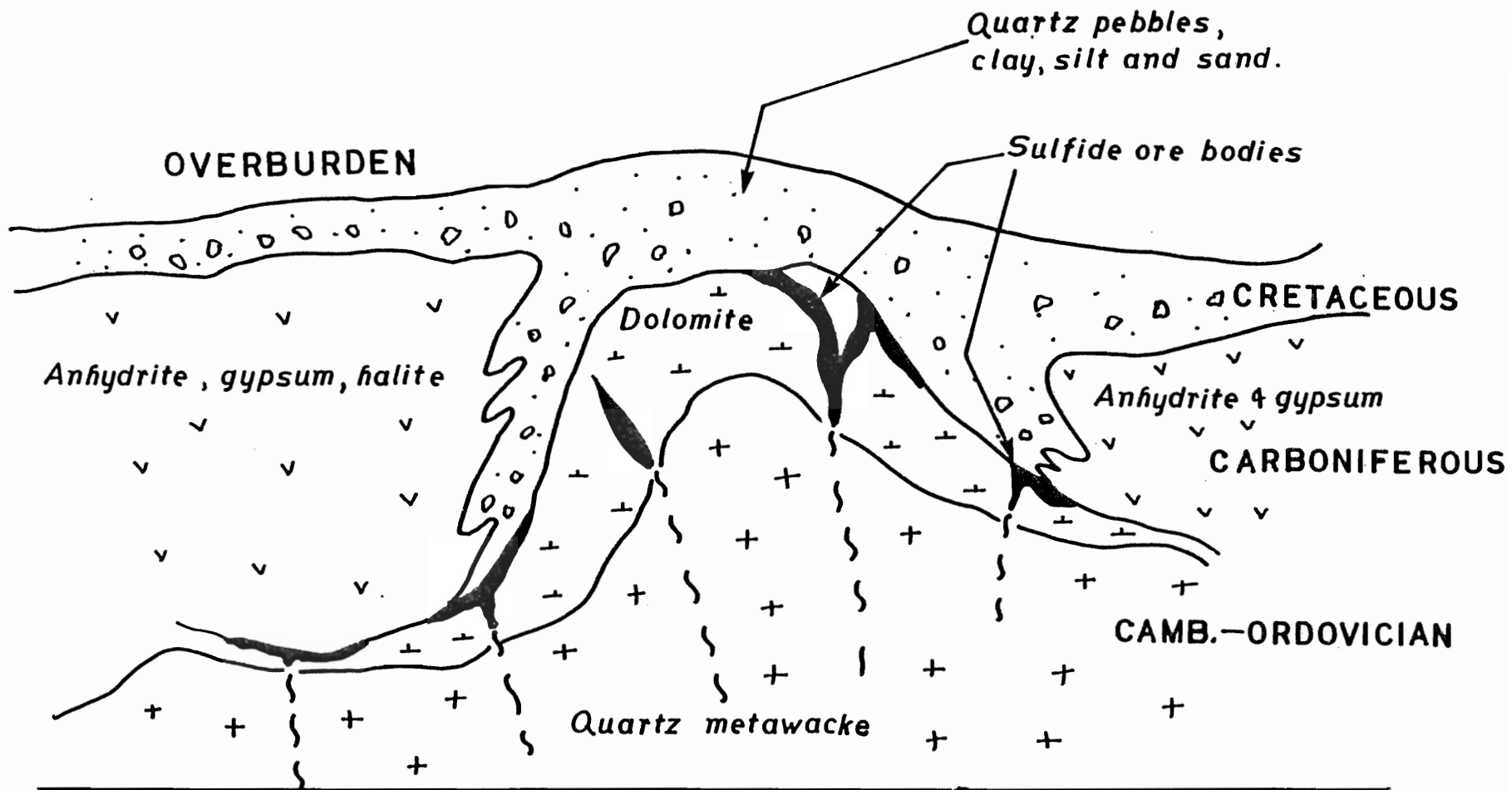


Figure 8.7 Gays River genetic model; mineralization and preservation

lated trenches and sinkholes. Marcasite and pyrite are common overgrowths on quartz pebbles, sand, silt and lignite contained in the Cretaceous sediments. The influx of groundwater resulted in continuous hydration of the anhydrite to gypsum and this process must have been accompanied by an increase in volume of the evaporite (Shearman et al, 1972). The volume increase was probably responsible for shearing and slickensiding at the evaporite/carbonate contact. Extension perpendicular to the carbonate bedding planes created channels that were later filled by concordant gypsum veins.

8.7 Evidence on the Type of Deposit

Snyder (1967) indicated that the proponents of syngenetic hypotheses of ore formation commonly base their interpretations on the widespread uniform mineralization within a restricted stratigraphic interval and a consistent relationship of mineralization to sedimentary features. On the other hand, the proponents of epigenetic hypotheses, based their interpretation on the mineralization of post depositional structures, changes in extent and grade of ore, open space fillings and district wide lack of control by sedimentary features, and the relation of ore to tectonic structures (Snyder, 1967). On the basis of the evaluation of the characteristics of syngenetic, diagenetic and epigenetic stratiform deposits, Snyder (1967) defined a list of criteria which may distinguish these deposits. A summary of the criteria are listed as follows:

a. Evidence for syngenetic origin

1. Uniform mineralization at a given stratigraphic position or within a restricted range.
2. Close relationship between mineralization and particular sedimentary facies and features.

b. Evidence for diagenetic origin

1. Mineralization within a restricted stratigraphic interval.
2. Close relationship between mineralization and sedimentary lithologies and facies.
3. Mineralization related to diagenetic features and structures.

c. Evidence for epigenetic origin

1. Mineralization of post lithification structures.
2. Marked changes in height, width, and tenor of ore that cannot be related to sedimentary or diagenetic features or environments.
3. Extensive open space fillings, vein, breccia or bedding replacements.
4. Distribution of mineralization relative to tectonic structures, fractured sediments not normally mineralized carried ore.
5. District wide lack of close control of mineralization by specific sedimentary environment.
6. Presence of J-type lead.

Observations at the Gays River deposit

1. Significant sphalerite and galena in crosscutting veins, fractures and stylolites.
2. Changes in the grade and width of stratiform ores with proximity to massive sulfide veins.
3. Extensive open space fillings of sphalerite and galena in the porous dolostone and as bedding replacements. Mineralized breccia are common adjacent to sulfide veins.
4. Sphalerite, galena, calcite, fluorite are common in faults and fine fractures in the dolomite host with no lithologic preference.
5. Mineralization is not confined to a specific sedimentary environment. It occurs in a variety of lithologies and may be related to increasing porosity and fracture development.

6. Lead in galena is of Ordovician model age.
7. No evidence of boiling of the ore solution.
8. Sulfur isotope values in the ore body are heavy and show very narrow variations, significantly different from sulfur of biogenic derivation.

From this listing it is obvious that the Gays River lead-zinc mineralization satisfy most of the criteria for epigenetic origin. This conclusion is compatible with most of the characteristics of carbonate hosted Mississippi Valley Type deposits.

CHAPTER 9

COMPARISON OF THE GAYS RIVER DEPOSIT WITH
SELECTED SEDIMENT HOSTED AND MISSISSIPPI
VALLEY TYPE LEAD-ZINC ± COPPER MINERALIZATION

9.1 General Statement

Lead, zinc ± copper deposits are known in both siliclastics and carbonate sediments throughout the world. Important deposits occur in rocks of every age from Pre Cambrian to Cretaceous although carbonate hosted deposits are absent in the Silurian and Proterozoic (Stanton 1972, Sangster 1976). Three ore districts for example; 1) the Irish type ore deposits, 2) the Pine Point district and 3) south east Missouri district, have appropriate synsedimentary and epigenetic features of relevance to the mode of ore emplacement. The objective in developing such a comparison is to broaden the scale of observation at the Gays River deposit and to see how the marked similarities and differences observed elsewhere and their interpretations lend evidence to the present genetic model.

9.2a Irish Base Metal Deposit: The Tynagh Example

The Tynagh base metal deposit containing lead, zinc, copper, silver and barite is one of the major stratabound ore occurrences within the gently folded Lower Carboniferous (Mississippian) platform carbonate sequence of the central plain of Ireland (Fig. 9.1). The ore body was discovered in 1961 by soil and hydrogeochemistry (Donovan et al., 1966). Reserves at the end of 1970 were estimated at 6 million tonnes of ore with 5.37% Pb, 4.51 % Zn, 0.37% Cu and 60 g./tonne Ag plus indicated reserves of nearly 3 million tonnes of lower grade ore (Schultz, 1971). A detailed description of the

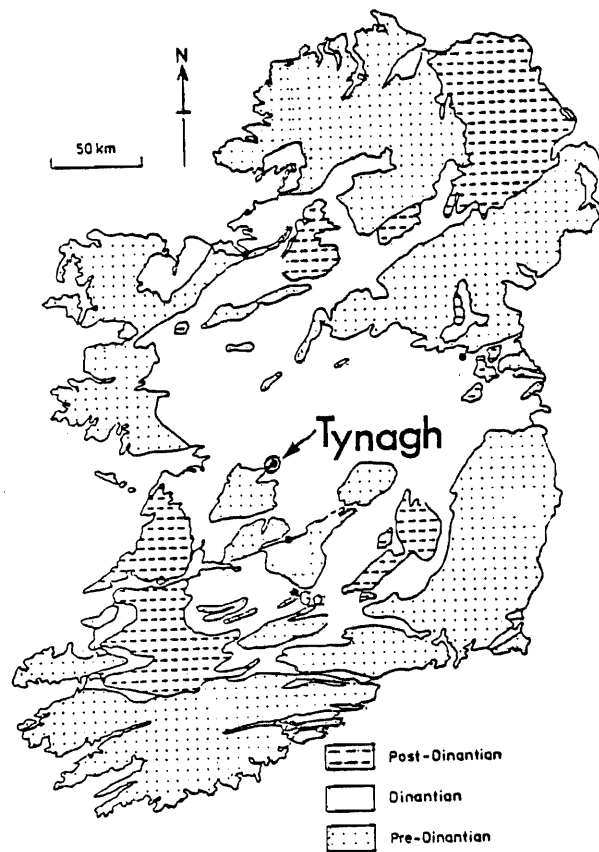


Figure 9.1 Location map of the Tynagh deposit, central Ireland.
From Boast et al. (1981).

geologic setting of the ore bodies and thoughts on genesis are discussed in the Appendix VI.

b. The Pine Point Lead-Zinc District

The Pine Point lead-zinc district is located on the south shore of the Great Slave Lake in the North West Territories (Fig. 9.2). The district consists of about 40 lead-zinc ore bodies in a Middle Devonian carbonate barrier complex (Fig. 9.3). Total production of the district to the end of 1979 is 47.8 million tonnes of ore averaging 6.7% zinc and 3.27% lead. The present official ore reserves are 38.0 million tons of ore grading 5.0% zinc and 1.9% lead (Pine Point Mines Limited, Annual Report 1979). Detailed descriptions of the geological setting of the Pine Point ore bodies and thoughts on genesis are presented in the appendix.

c. South East Missouri District: Buick Mine

The south east Missouri lead district lies on the north east margin of the Ozark uplift which occupies a position near the southern edge of the central stable region of the North American craton (Fig. 9.4). The district is situated on the flanks of the Pre Cambrian St. Francois mountains and the western flank of this Pre Cambrian ridge consists of the Virburnum Trend (Fig. 9.5). The Buick mine is located in the central part of the Virburnum Trend in the western Iron county, 6 kilometers south of Bixby, Missouri. Ore reserves at the initiation of mining was estimated at 50 million tons of 8% lead, 2% zinc (Roger and Davis, 1977). The reader is referred to the appendix for a description of the geologic setting of the ore bodies and thoughts on genesis.

The salient features of the four deposits, Tynagh, Pine Point, Buick, and Gays River are tabulated in Table 9.1 for summary comparison.

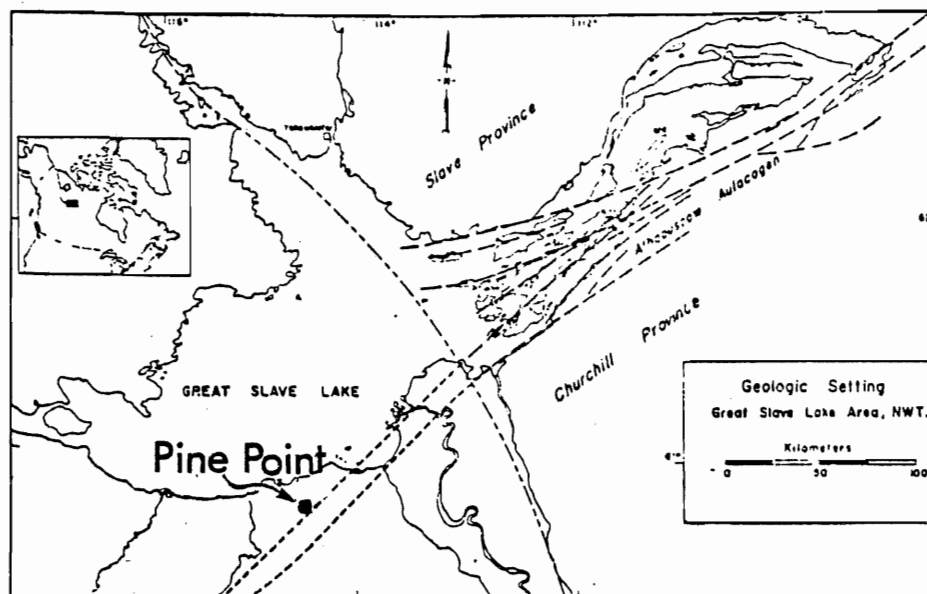


Figure 9.2 Location map of the Pine Point lead-zinc district and the geologic setting of the Great Slave Lake region, N.W. Territories. From Kyle, (1981).

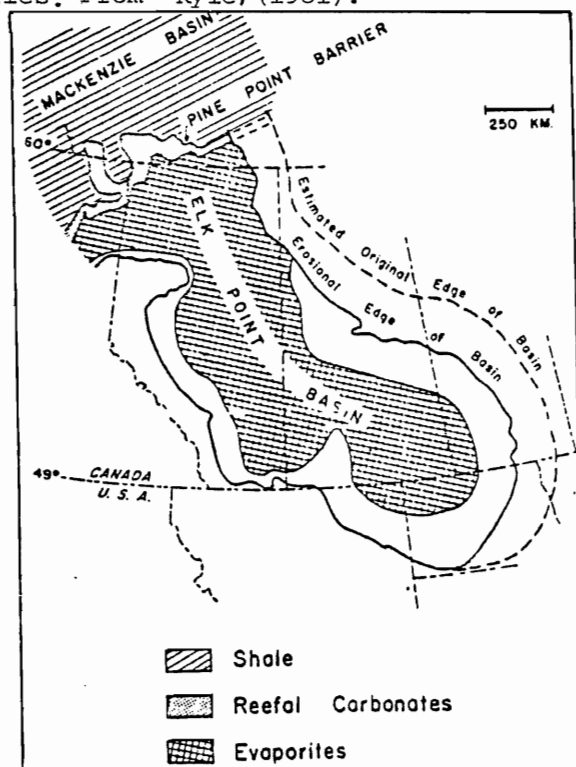


Figure 9.3 Location map of the Pine Point barrier complex. From Kyle, (1981).

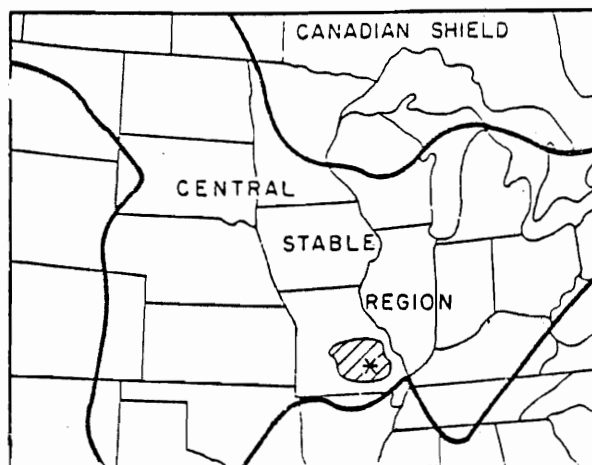


Figure 9.4 Location map of the south east Missouri lead district.

From Thacker and Anderson (1977).

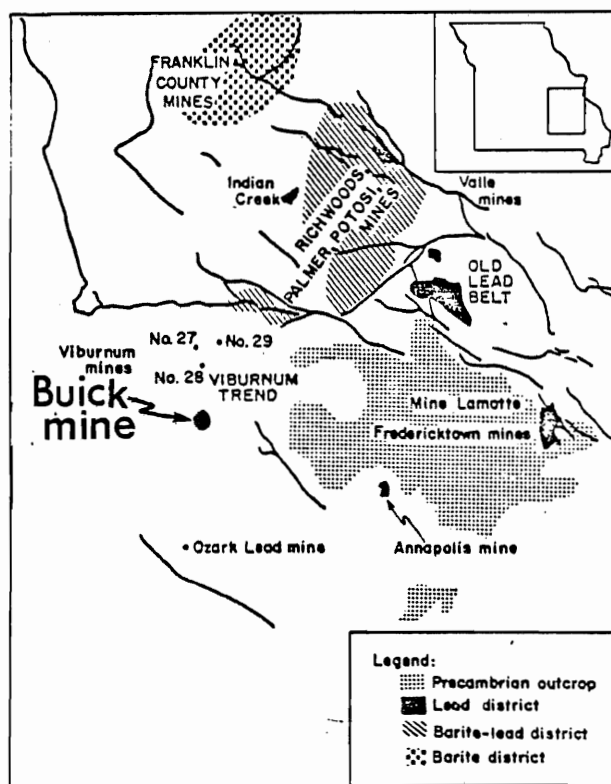


Figure 9.5 Location map of the Buick mine and major subdistricts and mines within the south east Missouri district. From Thacker and Anderson (1977).

Table 9-1 Summary Comparison of the Geological Features of Gays River, Tynagh, Pine Point and Buick Mine

FEATURES	TYNAGH DEPOSIT	PINE POINT	BUICK MINE	GAYS RIVER
1. Tonnage and grade	6 million tonnes of ore with 5.37% Pb, 4.51% Zn, 0.37% Cu and 60 g/tonne AG. 3 million tonnes of low grade ore (Schultz, 1971).	Present official ore reserve are 38.0 million tonnes of ore grading 5.0% zinc, 1.9% lead (Pine Point Mines Limited Annual Report 1979).	Ore reserve at initiation of mining estimated at 50 million tonnes of 8% Pb and 2% Zn (Roger and Davis 1977).	Ore reserve at the initiation of mining estimated at 12 million tonnes 7% combined Pb + Zn (Mac Eachern and Hannon 1974).
2. Host rock and age	Micrites and biomicrites of Lower Carboniferous (U. Tournaisian-L.Visean) Waulsortian mud banks.	Reef dolostones of Middle Devonian (Givetian) age.	Bonnetterre dolomitized limestone of Upper Cambrian age.	Dolomite and limestone of Lower Carboniferous (Visean) age.
3. Structural setting	Deposit lies in the hanging wall of a major E-W normal fault. Rocks are folded about a N/S axes and downthrow to the north at a maximum of 600 metres.	District is located at the margin of Elk Point Basin and Mackenzie Basin near the flank of Pre Cambrian Shield. N65°E hinge zone control sedimentation and the build up of a barrier complex.	Situated on the western flank of a Pre Cambrian ridge system (the St. Francois Mountains).	Located on the north west flank of a Lower Paleozoic basement anticlinal ridge between 2 sub-basins. N/S fault system occur in the central part of the ore body.
4. Diagenetic modification	Dolomitization with the associated formation of pyrite, marcasite and arsenopyrite (Morrisey <u>et al</u> ,1971)	Dolomitization and Karstification. Ore bodies are confined to fine crystalline and coarse crystalline dolostones.	Dolomitization, Karstification and development of solution collapse breccia.	Dolomitization and Post ore dedolomitization. Limited occurrence of solution collapse breccia.
5. Styles of Mineralization	Primary ore are massive, stratiform and finely banded. Irregular replacements, breccia and veins are common adjacent to faults. Linings and fillings of solution cavities.	Generally open space fillings in dolostone porosity. Collapse breccias and fault infillings. Massive tabular ore bodies depict replacement textures. Colliform textures are common. No associated veins (Kyle 1981).	Mineralization is dominantly of solution collapse breccia type with minor blanket ore. Open space fillings of sulfide minerals are important.	Both stratiform and discordant fault controlled vein systems are present. The stratiform ore are generally open space fillings and replacement types. Geopetal structures, stromatactis and stylolites have sulfide minerals. Mineralized breccia are common near faults.

Table 9-1 Continued

FEATURES	TYNAGH DEPOSIT	PINE POINT	BUICK MINE	GAYS RIVER
6. Controls of Mineralization	Both primary and secondary ore bodies are localized by the hanging wall of the E-W, Tynagh fault. Vein ore and mineralized breccia are localized in areas adjacent to faults and stratiform ores are conformable to sedimentary bedding.	Mineralization is localized within a carbonate barrier complex. Faults, collapse breccia and porosity types locally control the sulfide distribution.	Porosity and solution collapse breccia in the Bonnettere dolostone favour sulfide distribution.	Faults, fractures and the tremendous porosity in the host dolomite control the localization of the sulfide minerals at Gays River.
7. Ore mineralogy	Sphalerite, galena, tennantite, chalcopyrite, bornite form the major sulfide minerals. Minor sulfide include enargite, bournonite, geochronite, jordanite, siegenite and millerite. Gangue include pyrite, marcasite, barite, calcite, dolomite and bitumen.	The common minerals are sphalerite, galena, marcasite, pyrite, dolomite and calcite. Others include pyrrhotite, celestite, gypsum, anhydrite, thorite, sulfur, and bitumen.	Ore minerals include galena, sphalerite and chalcopyrite. Other sulfides are pyrite, marcasite, siegenite, polydynite, bravoite, vaesite and traces of bornite and arsenopyrite. Gangue minerals include dolomite, calcite, quartz, kaolinite and dickite.	Ore minerals are dominantly sphalerite and galena. Other sulfide minerals include marcasite, pyrite, chalcopyrite. Gangue minerals include calcite, dolomite, fluorite, barite, celestite, gypsum, anhydrite and bitumen.
8. Mineralizing fluid character	Ore minerals were precipitated from heated saline brines. Oxygen isotope fractionation temperature of approximately 200°C for the mineralizing fluid (Boast et al, 1981).	Homogenization temperature ranged from 50-100°C. Brine salinity 20 wt% total dissolved salts in sphalerite. Lower salinity in post ore calcite.	Fluid inclusion temperature range from 105-141°C in sphalerite. Salinity measurements indicate 4 to 5 molal chloride ion in ore solution	Temperature of the mineralizing fluid range from 95 to 215°C. Salinity measurements range from 17 to 20.4 wt% total dissolved salts in post ore calcite and fluorite.
9. Chemical constituents of ore	Major elements include Zn, Pb, Fe, Cu, Mn, Ba, As. Minor elements include Fe, Ag, Cd. Lead in galena is normal and not the "J" type radiogenic lead. Broad range in sulfur isotopic composition in the sulfides reflect biogenic and magmatic components. Sulfur in barite is from the Lower Carboniferous seawater source (Boast et al, 1981)	Major elements include Zn, Pb, Fe, Ca, Mg, S, C. Minor elements in principal minerals are Fe, Pb, Cu, Mn and Cd in sphalerite, Zn, Cu and Fe in galena. Cu in pyrite and marcasite. Lead in galena is normal, non radiogenic. Average of $^{206}\text{Pb}/^{204}\text{Pb}$ is +18.2. Sulfur isotope values in sulfides are heavy and identical to Middle Devonian seawater.	Major elements include variable amounts of Pb, Zn, Fe and Cu. Minor elements include Fe, Ag, Cd, Ni, As. Lead in galena is radiogenic "J" type. The sulfur isotopic composition of sulfide minerals are heavy within a broad range.	Major elements in ore include Zn, and Pb. Minor elements include Cd, Cu, Ag, Sn, V. Cu is contained in the late marcasite and pyrite. Lead in galena is non radiogenic averaging +18.4 for the $^{206}\text{Pb}/^{204}\text{Pb}$ ratio. Sulfur isotopic composition of the sulfides are heavy, occur within a narrow range and identical to the Lower Carboniferous seawater composition.

Table 9-1 Continued

FEATURES	TYNAGH DEPOSIT	PINE POINT	BUICK MINE	GAYS RIVER
10. Thoughts on genesis	Exhalative synsedimentary processes accompanying downward excavating hydrothermal convective cells (Russell, 1978, 1981). Epigenetic origin for discordant veins remain controversial.	Epigenetic emplacement of ore from basinal brines during the dewatering of shales (Jackson and Beales 1967, Kyle 1981).	Epigenetic ore emplacement subsequent to development of the dolostone porosity and solution collapse brecciation (Rogers and Davis 1977).	Epigenetic ore emplacement by deeply circulating brines subsequent to hydrofracturing and shattering of the carbonate build up (this study).

9.3 Summation

The consideration of the geology of lead-zinc sulfide ore bodies in the Tynagh deposit, Ireland, Pine Point district, Canada, Buick mine, south east Missouri, show that each of these areas have sulfide mineralization in carbonate hosts. Although controversy still remains with regard to syngenetic or epigenetic origin of these carbonate hosted lead-zinc sulfide ore bodies, each district has peculiar characteristics which may lead to an independent genetic interpretation. While similarities exist between districts, contrasting differences at local mine scales does not permit a unique genetical model for all deposits. Indeed, the more recent synsedimentary genesis for the Tynagh deposit appear to have gained more acceptance because of the available evidence. This contrasts with the epigenetic mode of ore emplacement which appears compatible with the evidence at Pine Point, Buick mine and the Gays River deposits.

CHAPTER 10

CONCLUSIONS

Consideration of the geologic, mineralogic and geochemical features of the Gays River lead-zinc ore body and the host rocks have led to the following conclusions.

1. Both stratiform (low grade) and vein (high grade) lead-zinc ores are present in the Gays River ore body. The stratiform ores are concordant open space fillings of sulfide minerals distributed in highly porous carbonates deposited on structurally controlled erosional channels separating the knobs and ridges of the Cambro-Ordovician quartz metawacke basement. Massive stratiform ore occurs locally along the evaporite-dolomite contact. Porosity types hosting sulfide minerals in the dolomite includes intraparticle, interparticle, sheltered, moldic, fenestral, vuggy and fracture. Discordant sulfide vein systems are localized within a pattern of N/S, NNE and E/W faults and contain the largest concentrations of sulfide minerals. Localized brecciation and intense post-ore dedolomitization are spatially related to faults adjacent to veins. The styles of mineralization include; disseminated sulfides, vug infillings, geopetal structures, mineralized stylolites, veins and bedding replacements.
2. The stratiform and vein ores have identical mineralogy. This consists of sphalerite, galena as the main ore minerals and marcasite, pyrite, chalcopyrite, barite and calcite as gangue. The major chemical constituents of the ore are Zn and Pb while Mn, Cd, Fe, Cu, Ag, Ba, Ni, V, Co and Sn are generally low.
3. The present study suggests 3 main stages of development of the host, the sulfide minerals and gangue: 1) a pre-ore evaporite deposition, per-

vasive reef dolomitization and growth of marcasite, 2) precipitation of ore sphalerite, galena, chalcopyrite and calcite, 3) post ore deposition of calcite, fluorite, barite, marcasite, pyrite and selenite.

4. The mineralizing fluids are hot saline brines with temperatures never less than 92°C (calculated) for post ore scalenohedral calcite. Other post ore calcite was precipitated at 142°C, fluorite at 143°C and barite at 137°C. This temperature rises steeply in the ore stage calcite which was precipitated at 172°C and vein sphalerite at 215°C in a non boiling environment. Salinity of the saline brines was approximately 20.4 equivalent weight percent NaCl during ore deposition.

5. Gypsum and anhydrite in the overlying evaporite and barite within the ore are enriched in heavy sulfur ($\delta^{34}\text{S} +13.1$ to $+16.5\%$); ore stage sphalerite, galena and chalcopyrite show a limited spread of $\delta^{34}\text{S}$ ($+8.0$ to $+13.65$ per mil) whereas post ore marcasite and pyrite give widely scattered light $\delta^{34}\text{S}$ values (-9.7 to -46.0%). The similarities of the $\delta^{34}\text{S}$ values of gypsum, anhydrite and barite with that of Mississippian sea water confirm this as the dominant sulfur source for the sulfates. The heavy sulfur of the ore stage sulfide minerals appear to have been contributed from the solution of evaporites with sulfate /sulfide fractionation being accomplished by kinetic effects or through interaction with organic compounds in a state of disequilibrium. Sulfur in the post ore marcasite and pyrite are probably biogenic in origin.

6. Oxygen and carbon isotopic composition of the dolomite host to ore show a slight depletion of heavy ^{18}O and ^{13}C with respect to unmineralized carbonate rock of similar age. Significant depletion in the ^{18}O values occurs in the ore stage calcite as a result of diminishing fractionation in the $\text{CaCO}_3\text{-H}_2\text{O}$ system at the temperature of the hydrothermal fluid. ^{13}C values

in the ore stage calcite are heavy, comparable to that of marine carbonate and suggests that the carbon in this calcite was derived from the dissolution of marine carbonate. Post ore calcite gave widely scattered O^{18} and C^{13} values with the lightest values closely identical to the ore stage calcite and the heavier values being identical to the dolomite host. This is interpreted as resulting from increasing fractionation at low temperatures in the $CaCO_3-H_2O$ system with the gradual enrichment in the heavier isotopes with increasing time. A partial influence of biogenic carbon from cooler formational waters was probably responsible for the lighter C^{13} values in post ore calcite and dedolomite.

7. Lead in the Gays River galena is non-radiogenic and is distinctly different from the "J" type anomalous lead reported for similar lead-zinc deposits in the Mississippi Valley of the mid continent. The lead gave an Ordovician model age and is probably of basement origin; it may represent lead remobilized from sulfide concentrations in the Ordovician Meguma meta-sedimentary basement.

8. The present study eliminates the possibility that the lead-zinc sulfide ore body at Gays River is an early low temperature diagenetic cement of the dolomitic reef as previously thought. Contact relationships and remarkable similarities between the stratiform and vein sulfide ores and the present interpretations of the mineralogic, fluid inclusion and stable isotopic data suggest that the discordant veins acted as feeders for the epigenetic conformable mineralization. The data is compatible with a genesis involving deeply circulating brines released during gypsum dehydration.

REFERENCES

- Ami, H.M., 1900, Notes on some of the formations belonging to the Carboniferous system in Eastern Canada: Canadian Rec. Sci. vol. 8, pp. 149-163.
- Anderson, G.M., 1973, The hydrothermal transport and deposition of galena and sphalerite near 100°C: Econ. Geol. vol. 68, pp. 480-492.
- , 1975, Precipitation of Mississippi Valley type ores: Econ. Geol. vol. 70, pp. 937-942.
- , 1978, Basinal brines and Mississippi Valley type ore deposits: Episodes, no. 2, pp. 15-19.
- and Macqueen, R.W., 1982, Ore deposits models, Mississippi Valley type lead-zinc deposits: Geoscience Canada, vol. 9, pp. 108-117.
- Ault, W.V. and Jensen, M.L., 1963, Summary of sulfur isotope standards, in Biogeochemistry of sulfur isotopes: M.L. Jensen ed. National Sci. Found. Symposium Proceedings, Yale University, pp. 16-29.
- and Kulp, J.L., 1959, Isotopic geochemistry of sulfur: Geoch. et. Cosmoch. Acta, vol. 16, pp. 201-235.
- Bachinski, D.J., 1969, Bond strength and sulfur isotopic fractionation in coexisting sulfides: Econ. Geol. vol. 64, pp. 56-65.
- Barnes, H.L. and Czamanske, G.K., 1967, Solubility and transport of ore minerals: in Barnes, H.L. ed. Geochemistry of hydrothermal ore deposits: New York, Holt, Rinehart and Winston Inc., pp. 334-381.
- Bathurst, R.G.C., 1975, Carbonate sediments and their diagenesis: Elsevier Scientific Publishing Co., Amsterdam, Oxford, New York, 658 p.

- Barton, P.L. and Bethke, P.M., 1963, Equilibrium in ore deposits: Mine. Soc. America, special paper no. 1, pp. 171-185.
- and Toulmin, P., 1961, Some mechanisms for cooling hydrothermal fluids, U.S.G.S. Prof. paper 424-D, pp. 348-352.
- Barton, P.B. Jr., 1967, Possible role of organic matter in the precipitation of the Mississippi Valley ores in Brown, J.S. ed., Genesis of stratiform lead-zinc-barite-fluorite deposits in carbonate rocks: Econ. Geol. Mon. 3, pp. 371-377.
- Beales, F.W., 1975, Precipitation mechanisms for Mississippi Valley type ore deposits: Econ. Geol. vol. 70, pp. 943-948.
- , Carracedo, J.C. and Strangway, D.W., 1974, Paleomagnetism and the origin of Mississippi Valley type ore deposits: Can. Journ. Earth Science, vol. 11, pp. 211-285.
- and Jackson, S.A., 1966, Precipitation of lead-zinc ores in carbonate reservoirs as illustrated by the Pine Point ore field, Canada: I.M.M. Trans. Sec. B., vol. 75, pp. B278-285.
- Bell, W.A., 1929, Horton-Windsor district Nova Scotia: Geol. Surv. Can. Mem. 155, 268 p.
- , 1958, Possibilities for occurrence of petroleum reservoirs in Nova Scotia: Nova Scotia Dept. of Mines report, 227 p.
- , 1960, Mississippian Horton Group, Windsor-Horton district, Nova Scotia, Geol. Surv. Canada Mem. 314, 17 p.
- Belt, E.A., 1965, Revision of Nova Scotia, Middle Carboniferous units. Amer. Journ. Science, vol. 262, pp. 653-673.
- Bethke, P.M. and Barton, P.B., 1959, Trace element distribution as an indicator of pressure and temperature of ore deposition: abstract, Geol. Soc. Am. Bulletin, vol. 70, pp. 1569-1570.

- _____ and _____, Distribution of some minor elements between coexisting sulfide minerals: *Econ. Geol.* vol. 66, pp. 140-163.
- Billings, G.K., Kesler, S.E. and Jackson, S.A., 1969, Relations of zinc rich formation waters, northern Alberta, to the Pine Point ore deposits: *Econ. Geol.* vol. 69, pp. 1191-1206.
- Bjorlykke, A. and Sangster, D.F., 1981, An overview of sandstone lead deposits and their relationship to red-bed copper and carbonate hosted lead-zinc deposits: in B.J. Skinner ed. *Economic Geol.* 75th Anniversary volume pp. 179-213.
- Boast, A.M., Coleman, M.L. and Halls, C., 1981, Textural and stable isotopic evidence for the Genesis of the Tynagh Base Metal deposit, Ireland: *Econ. Geol.* vol. 76, pp. 27-55.
- Boehner, R.C., 1977, The Lower Carboniferous stratigraphy of the Musquodoboit Valley, Central Nova Scotia, unpubl. M.Sc. thesis, Acadia University, 176 p.
- _____, 1981, Stratigraphy and Depositional history of marine evaporites in the Lower Carboniferous Windsor Group, Shubenacadie and Musquodoboit structural basins, Nova Scotia, Canada: Nova Scotia Dept. of Mines report O.F.R. 468, 28 p.
- _____ and Giles, P.S., 1976, Carboniferous basin study, the Lower Carboniferous stratigraphy of the Musquodoboit Valley, Nova Scotia: *Abst. Nova Scotia Dept. of Mines report no. 76-2*, pp. 99-100.
- Borchert, H. and Muir, R.O., 1964, Salt deposits, the origin, metamorphism and deformation of evaporites: Van Norstrand Co. Ltd., London, 338 p.
- Bottinga, Y., 1968, Calculation of fractionation factors for carbon and oxygen exchange in the system calcite-carbon dioxide-water: *Journ. Phys. Chemistry*, vol. 72, pp. 800-808.

- Boyle, R.W., 1976, Sulfur isotope investigation of the barite, manganese and lead-zinc-copper-silver deposits of the Walton-Cheverie area, Nova Scotia, Canada: *Econ. Geol.* vol. 71, pp. 749-762.
- Brown, J.S., 1967, Isotopic zoning of lead and sulfur in southeast Missouri: in J.S. Brown, ed. *Genesis of stratiform lead-zinc-barite-fluorite deposits - a symposium: Econ. Geol. Mon.* 3, pp. 410-425.
- Bubela, B. and Macdonald, J.A., 1969, Formation of banded sulphides - Metal ion separation and precipitation by inorganic and microbial sulphide sources: *Nature*, vol. 221, pp. 465-466.
- Burnham, C.W., 1962, Facies and types of hydrothermal alteration: *Econ. Geol.*, vol. 57, pp. 768-784.
- Buruss, R.C., 1981, Hydrocarbon fluid inclusions in the studies of sedimentary diagenesis: in Hollister and Crawford eds. *M.A.C. short course in Fluid Inclusions Application to Petrology*, pp. 139-156.
- Butler, G.P., 1969, Modern evaporite deposition and geochemistry of co-existing brines, the Sabka, Trucial coast, Arabian Gulf: *Journ. Sed. Petrology*, vol. 39, pp. 70-89.
- Chambers, L.A., Trudinger, P.A., Smith, J.W. and Burns, M.S., 1976, A possible boundary condition in bacteria sulfur isotope fractionation: *Geoch. Cosmoch. Acta*, vol. 40, pp. 1191-1194.
- Clayton, R.N. and Epstein, S., 1958, The relationship of O^{18}/O^{16} ratios in coexisting quartz, carbonate, iron oxides from various geological deposits: *Journ. Geol.* vol. 66, pp. 352-373.
- Craig, H., 1957, Isotopic standards for carbon and oxygen and correction factors for mass-spectrometric analysis of carbon dioxide: *Geochm. et. Cosmoch. Acta*, vol. 12, pp. 133-149.

- Crawford, M.L., 1981, Phase equilibria in aqueous fluid inclusions: in Hollister, L.S and Crawford, M.L. eds., Short Course in Fluid Inclusions Applications to Petrology, GAC/MAC, Calgary '81, pp. 75-100.
- Cumming, G.L. and Richards, J.R., 1975, Ore lead isotope ratios in a continuously changing earth: Earth Planetary Sci. Lett. vol. 28, pp. 155-171.
- and Robertson, D.K., 1969, Isotopic composition of lead from the Pine Point deposit: Econ. Geol. vol. 64, pp. 731-732.
- Czamanske, G.K. and Rye, R.O., 1974, Experimentally determined sulfur isotope fractionation between sphalerite and galena in the temperature range 600°C to 275°C: Econ. Geol., vol. 69, pp. 17-25.
- Degens, E.T. and Epstein, S., 1964, Oxygen and carbon isotope ratios in coexisting calcites and dolomites from recent and ancient sediments: Geoch. et Cosmoch. Acta, vol. 28, pp. 23-47.
- Dickie, J.R., 1977, Geologic, mineralogical and fluid inclusion studies at the Dunbrack lead-silver deposit, Musquodoboit Harbour, Halifax County, Nova Scotia: unpubl. B.Sc. thesis, Dalhousie University, Halifax, Nova Scotia, 45 p.
- Dickson, J.A.D., 1966, Carbonate identification and genesis as revealed by staining: Journ. Sed. Pet., vol. 36, pp. 491-505.
- Doe, B.R., 1978, The application of lead isotopes to mineral prospect evaluation of Cretaceous-Tertiary magma to thermal ore deposits of United States: in J.R. Watterson and P.K. Theobald (eds.). Geochemical Expl., 1978, Proceed. of the 7th Int. Geoch. Expl. Symposium, Golden, Colorado, Ass. of Expl. Geochemists, pp. 227-232.

- and Delevaux, M.H., 1972, Source of lead in the Southeast Missouri galena ores: *Econ. Geol.* vol. 67, pp. 409-425.
- and Stacey, J.S., 1974, The application of lead isotopes to the problems of ore genesis and ore prospect evaluation - A review: *Econ. Geol.*, vol. 69, pp. 757-776.
- and Zartman, R.E., 1979, Plumbotectonics, the Phanerozoic: in H.L. Barnes ed., *Geochemistry of hydrothermal ore deposits*, John Wiley and Sons, pp. 22-70.
- Donovan, P.R. and James, C.H., 1966, Geochemical dispersion in glacial overburden over the Tynagh (Northgate) base metal deposit, West central Ireland: Symposium, *Geoch. prospecting*, Geol. Survey of Canada, Bull. 66-54, pp. 89-110.
- Dozy, J.J., 1970, A geological model for the genesis of the lead-zinc ores of the Mississippi Valley, U.S.A.: *Trans. Inst. Min. Metall.* Sect. B79, pp. 163-170.
- Dunham, R.J., 1962, Classification of carbonate rocks according to depositional texture, in *classification of carbonate rocks*: Amer. Assoc. Petrol. Geol. Memoir 1, pp. 108-122.
- Dunsmore, H.E., 1973, Diagenetic processes of lead-zinc emplacement in carbonates: *Inst. Min. Metall. Trans. Sec. B*, vol. 82, pp. 168-173.
- Eaton, S.R., 1980, Fluid Inclusion geothermometry in fluorite from Gays River, Nova Scotia and Boat Harbour, Newfoundland: unpubl. B.Sc. thesis, Dalhousie University, Halifax, N.S., 104 p.
- Eckelmann, W.R., Broecker, W.S., Whitlock, D.W. and Allsop, J.R., 1962, Implications of carbon isotopic composition of total organic carbon of some recent sediments and ancient oils: *Am. Assoc. Petrol. Geologists, Bull.* vol. 46, pp. 699-704.

- Embry, A.F. and Klovan, J.E., 1971, A late Devonian reef tract on north east Banks Island: N.W.T., Bull. Can. Petroleum Geol. vol. 19, pp. 730-781.
- Evans, R., 1970, Sedimentation of the Mississippian evaporites of the Maritimes: an alternative model: Can. Journ. Earth Sciences, vol. 7, pp. 1349-1352.
- Evans, T.L., Campbell, F.A. and Krouse, H.R., 1968, A reconnaissance study of some western Canadian lead-zinc deposits: Econ. Geol., vol. 63, pp. 349-359.
- Felderhof, G.W., 1978, Barite, celestite and fluorite in Nova Scotia: Nova Scotia Dept. of Mines Bulletin no. 4, 463 p.
- Friedman, G.M., 1959, Identification of carbonate minerals by staining methods: Journ. of Sed. Pet., vol. 29, pp. 87-97.
- Friedman, I. and O'Neil, J.R., 1977, Compilation of stable isotope fractionation factors of geochemical interest: in Data Geoch., 6th ed. U.S.G.S. Prof. Paper 440 KK, pp. KK1-KK12.
- Fritz, P., 1969, The oxygen and carbon isotopic composition of carbonates from the Pine Point lead-zinc ore deposits: Econ. Geol., vol. 64, pp. 733-742.
- Fyfe, W.S., Price, N.J., Thompson, A.B., 1978, Fluids in the earth crust: Developments in Geochemistry 1, Elsevier Publishing Co. 383 p.
- Fyson, W.K., 1966, Structures in the Lower Paleozoic Meguma Group, Nova Scotia: G.S.A. Bulletin, vol. 77, pp. 931-944.
- Garlick, G.D., 1969, The stable isotopes of oxygen: in K.H. Wedepohl, ed. Handbook of geochemistry, Springer Verlag, Berlin, Heilderberg, New York.

- Garlick, W.G., 1981, Sabkhas, Slumping and Compaction at Mufulira, Zambia: Econ. Geol., vol. 76, pp. 1817-1847.
- Giles, P.S., 1977, The Carboniferous basin study: Nova Scotia Dept. of Mines, Rept. 77-1, pp. 115-121.
- , Boehner, R.C. and Ryan R.J., 1979, Carbonate banks of the Gays River Formation in central Nova Scotia: Nova Scotia Mines Dept. paper 79-7, 57 p.
- and Boehner, R.C., 1979, Windsor Group stratigraphy in the Shubenacadie and Musquodoboit Basins, central Nova Scotia: Nova Scotia Dept. of Mines report in preparation.
- and Ryan, R.J., 1976, A preliminary report on the stratigraphy of the Windsor Group in the eastern Minas Sub-Basin, Nova Scotia; Nova Scotia, Dept. of Mines report, 76-2, pp. 100-105.
- Giordano, T.H. and Barnes, H.L., 1981, Lead transport in Mississippi Valley type ore solutions: Econ. Geol., vol. 76, pp. 2200-2211.
- Graves, M.C., 1976, The formation of gold bearing quartz veins in Nova Scotia - hydraulic fracturing under conditions of greenschist regional metamorphism during early stages of deformation: Unpubl. M.Sc. thesis, Dalhousie University, 166 p.
- , Zentilli, M., 1982, A review of the geology of gold in Nova Scotia: in R.W. Hodder and W. Petruk, eds. Geology of Canadian gold deposits, C.I.M. special vol. 24, pp. 233-242.
- Gustafson, L.B. and Williams, N., 1981, Sediment hosted stratiform deposits of copper, lead and zinc: in B.J. Skinner, ed. Econ. Geol. 75th Anniversary volume, pp. 139-178.

- Haas, J.L., 1971, The effect of salinity on the maximum thermal gradient of a hydrothermal system at hydrostatic pressure: *Econ. Geol.*, vol. 66, pp. 940-946.
- Hacquebard, P.A., 1964, Stratigraphy and palynology of the Upper Carboniferous coal measures in the Cumberland Basin of Nova Scotia, Canada: 5th Congress. International Stratigraphie et. Geologie Carbonifere, Paris France, vol. III, pp. 1157-1169.
- , 1973, Pre and Post deformational coalification and significance for oil and gas exploration: *Extrait Colloque Int. Petrographic de la Matiere Organique des Sediments*, Paris, France, pp. 226-241.
- and Donaldson, J.R., 1970, Coal metamorphism and hydrocarbon potential in the Upper Paleozoic of the Atlantic Provinces, Canada: *Can. Journ. Earth Sciences*, vol. 7, pp. 1139-1163.
- Hall, W.E. and Friedman, I., 1969, Oxygen and carbon isotopic composition of ore and host rock of selected Mississippi Valley type deposits: in: *Geol. Survey Research, U.S.G.S., Prof. paper*, pp. C140-C148.
- Hancock, B.J., 1982, Depositional environment of a carbonate section exposed in the Gays River decline - A Carboniferous build up in mainland Nova Scotia, unpubl. B.Sc. thesis, Dalhousie University, 71 p.
- Hanor, J.S., 1980, Dissolved methane in sedimentary brines - Potential effect on the PVT properties of fluid inclusions: *Econ. Geol.*, vol. 75, pp. 603-608.
- Hardie, L.A., 1967, The gypsum anhydrite equilibrium at one atmosphere pressure: *Amer. Mineralogist*, vol. 52, pp. 171-200.
- Hartling, A.A., 1977, Paleoenvironment of a small portion of the Gays River carbonate complex, Nova Scotia: Unpubl. B.Sc. thesis, Dalhousie Univ., 88 p.

- Hatt, B.L., 1978, An interpretation of the carbonate geology exposed in the decline at Gays River: Unpubl. M.Sc. thesis, Dalhousie University, 134 p.
- Heard, H.C. and Rubey, W.E., 1966, Tectonic implications of gypsum dehydration: G.S.A. Bull., vol. 77, pp. 741-760.
- Heckel, P.H., 1974, Carbonate build ups in the geologic record, a review: in Reefs in time and space, L.E. Laporte, ed. Soc. Econ. Paleont. and Mineral. spec. pub., vol. 16, pp. 90-154.
- Helgeson, H.C., 1964, Complexing and hydrothermal ore deposition: Pergamon Press, Oxford, London, 128 p.
- Hemley, J.J. and Jones, W.R., 1964, Chemical aspects of hydrogen alteration with emphasis on hydrogen metasomatism: Econ. Geol., vol. 59, pp. 538-569.
- Heyl, A.V., 1968, The Upper Mississippi Valley base metal district: in J.D. Ridge, ed. Ore deposits in the United States, vol. 1, Amer. Inst. Min. Metallurgy and Petroleum Engineers, New York, pp. 431-459.
- , Landis, G.P., Zartman, R.E., 1974, Isotopic evidence for the origin of Mississippi Valley type mineral deposits, a review: Econ. Geol., vol. 79, pp. 992-1006.
- Higgins, N.C., 1979, Theory, Methods and Application of Fluid Inclusion research: G.A.C., Newfoundland Section, Short Course notes, 42 p.
- Hill, G.T., 1976, Mineralization and coal petrology of the Shubenacadie clay deposit, Nova Scotia, Unpub. B.Sc. thesis, Dalhousie University, 97 p.
- Hoefs, J., 1973, Stable isotope geochemistry 2nd edition, Springer-Verlag Berlin, Heidelberg, New York, 208 p.

- Holser, W.T. and Kaplan, J.R., 1966, Isotope geochemistry of sedimentary sulfates: *Chem. Geology*, vol. 1, pp. 93-135.
- Holland, H.D., 1965, Some applications of thermochemical data to problems of ore deposits - Mineral assemblages and the composition of ore forming fluids: *Econ. Geol.*, vol. 60, pp. 1101-1166.
- Holmes, A., 1946, An estimate of the age of the Earth: *Nature (London)*, vol. 159, p. 157.
- , 1949, Lead isotopes and the age of the Earth: *Nature (London)*, vol. 163, p. 453.
- Houtermans, F.G., 1946, The isotope ratios in natural lead and the age of uranium: *Naturwissenschaften*, vol. 33, pp. 185-186.
- Howie, R.D. and Barss, M.S., 1975, Upper Paleozoic rocks of the Atlantic Provinces, Gulf of St. Lawrence and the adjacent continental shelf: in *Offshore Geology of Eastern Canada*, vol. 2, Regional Geology, G.S.C. Paper 74-30, pp. 35-50.
- and Cumming, L.M., 1963, Basement features of the Canadian Appalachians: *Geol. Survey, Canada Bull.* 89, 18 p.
- Hutchison, C.S., 1974, *Laboratory handbook of petrographic techniques*: John Wiley and Sons, London, New York, pp. 214-218.
- Jackson, S.A. and Beales, F.W., 1962, An aspect of sedimentary basin evolution, the concentration of Mississippi Valley type ores during late stages of diagenesis: *Can. Petrol. Geol. Bull.*, vol. 15, pp. 383-433.
- Jenner, K.A., 1982, A study of sulfide mineralization in the Meguma Group sediments at Gold Brook, Colchester County, Nova Scotia, unpubl. B.Sc. thesis, Dalhousie University, 60 p.

- Jensen, M.L., 1959, Sulfur isotopes and hydrothermal mineral deposits: Econ. Geol., vol. 54, pp. 374-394.
- and Dessau, G., 1967, The bearing of sulfur isotopes on the origin of Mississippi Valley type deposits: in J.S. Brown, ed. Genesis of stratiform lead-zinc barite fluorite deposits - A symposium: Econ. Geol. Mon. 3, pp. 400-408.
- Jowett, E.C., 1975, Nature of ore forming fluids of the Polaris lead-zinc deposit, Little Cornwallis Island, N.W.T.: C.I.M., Bulletin, vol. 65, pp. 124-129.
- Kajiwara, Y. and Krouse, H.R., 1971, Sulfur isotope partitioning in metallic sulfide systems: Can. Journ. Earth Science, vol. 8, pp. 1397-1408.
- Kaplan, I.R. and Rittenberg, S.C., 1964, Microbiological fractionation of sulfur isotopes: Journ. Gen. Microbiology, vol. 34, pp. 195-212.
- Keevil, N.B., 1942, Vapour pressures of aqueous solutions at high temperatures: Journ. Americ. Chem. Society, vol. 64, pp. 841-850.
- Keith, M.L. and Weber, J.N., 1964, Carbon and oxygen isotopic composition of selected limestone and fossils: Geoch. et. Cosmoch. Acta, vol. 28, pp. 1787-1816.
- Kelley, D.G., 1967, Some aspects of Carboniferous stratigraphy and depositional history in Atlantic provinces: Geol. Assoc. Can. Spec. paper, 4, pp. 213-228.
- Kemp, A.L.W. and Thode, H.G., 1968, The mechanism of bacterial reduction of sulphate and sulphide from isotopic fractionation studies: Geoch. et. Cosmoch. Acta, vol. 32, pp. 71-91.
- Kinsman, D.J.J., 1969, Modes of formation, sedimentary associations and diagnostic features of shallow water and supratidal evaporites. A.A.P.G. Bulletin, vol. 53, pp. 830-840.

- Klevstov, P.V. and Lemmlein, G.G., 1959, Pressure corrections for the Homogenization temperature of aqueous NaCl solutions (in Russian) Doklady, Akad, Nauk, U.S.S.R., vol. 128, pp. 1250-1253.
- Koppel, V. and Grunenfelder, M., 1979, Isotope geochemistry of lead, in E. Jager, and J.C. Hunziker, (eds.), Lectures in isotope geology: Springer-Verlag, Berlin, pp. 134-153.
- Konnerup-Madsen, J., 1979, Fluid inclusion associated with a metamorphosed Molybdenite mineralization in Vest-Agder, South Norway: Econ. Geol., vol. 74, pp. 1221-1230.
- Krauskopf, K.B., 1957, Separation of manganese from iron in sedimentary processes: Geochim. et. Cosmoch. Acta, vol. 12, pp. 61-84.
- , 1967, Introduction to geochemistry, McGraw Hill Book Co., New York, 617 p.
- Kvenvolden, K.A. and Roedder, E., 1971, Fluid inclusions in quartz crystals from south west Africa: Geoch. et. Cosmoch. Acta, vol. 39, pp. 649-660.
- Kyle, J.R., 1981, Geology of the Pine Point district: in K.H. Wolf, ed. Handbook of Stratabound and stratiform ore deposits, vol. 9: Regional studies and specific deposits, Amsterdam Elsevier, pp. 643-741.
- Lemmlein, G.G. and Klevstov, P.V., 1961, Relations among the principal thermodynamic parameters in a part of the system $H_2O-NaCl$, Geokhimiya, no. 2, pp. 133-142, (in Russian), translated in Geochemistry, no. 2, pp. 148-158.
- Loftus-Hills, G. and Solomon, M., 1967, Cobalt, Nickel and Selenium as indicators of ore genesis: Mineralium Deposita, vol. 2, pp. 228-242.

- Logan, B.W., Hoffman, P. and Gebelin, C.D., 1974, Algal mats, cryptalgal fabrics and structures, Hamelin Pool, Western Australia: A.A.P.G. Memoir 22, pp. 140-194.
- Love, L.G., 1962, Biogenic primary sulfide of the Permian Kupferschiefer and Marl slate: Econ. Geol., vol. 57, pp. 350-366.
- Macdonald, G.J.F., 1953, Anhydrite, gypsum, equilibrium relations: Am. Journ. Sci., vol. 51, pp. 884-898.
- MacEachern, S.B. and Hannon, P., 1974, The Gays River discovery. A Mississippi Valley type lead-zinc deposit in Nova Scotia: C.I.M.M. Bulletin, vol. 63, pp. 61-66.
- Macleod, J., 1975, Diagenesis and sulfide mineralization at Gays River, Nova Scotia, unpubl. B.Sc. thesis, Dalhousie University, 132 p.
- Macnamara, J. and Thode, H.G., 1950, Comparison of the isotopic constitution of terrestrial and meteoric sulfur: Phy. Rev., vol. 78, pp. 307-308.
- Magara, K., 1976, Water expulsion from clastic sediments during compaction-directions and volumes: Bull. Am. Assoc. Petrol. Geol., vol. 60, pp. 543-553.
- Mamet, B.L., 1970, Carbonate microfacies of the Windsor Group (Carboniferous), Nova Scotia, and New Brunswick: Geol. Surv. Can. Paper 70-21, 121 p.
- McCrea, J.M., 1950, The isotopic chemistry of carbonates and a paleotemperature scale: Journ. Chem. Physics, vol. 18, pp. 849-857.
- McKinney, C.R., McCrea, J.M., Epstein, S., Allen H.A. and Urey, H.C., 1950, Improvements in mass spectrometers for the measurements of small differences in isotope abundance ratios: Rev. Sci. Instruments, vol. 21, pp. 724-730.

- McLimans, R.K., 1975, Systematic Fluid Inclusion and Sulfur isotope studies of the Upper Mississippi Valley, Pb-Zn deposits: (Abstract) Geol. Soc. America, Abstracts with Programs, vol. 7, p. 1197.
- , Barnes, H.L. and Ohmoto, H., 1980, Sphalerite stratigraphy of the upper Mississippi Valley, lead-zinc district, South West Wisconsin: Econ. Geol., vol. 75, pp. 351-361.
- Meyer, C. and Hemley, J.J., 1967, Wall rock alteration: in H.L. Barnes, ed. Geochemistry of hydrothermal ore deposits, Holt, Rinehart and Winston, New York, pp. 166-235.
- Morrisey, C.J., Davis, G.R. and Steed, G.M., 1971, Mineralization in the L. Carboniferous of central Ireland. Trans. Inst. Min. Metall. B80, pp. 174-185.
- Murray, R.C., 1957, Hydrocarbon fluid inclusions in quartz, A.A.P.G. Bulletin 41, pp. 950-956.
- Nier, A.O., 1950, A redetermination of the relative abundances of the isotopes of carbon, nitrogen, oxygen, argon and potassium. Physc. Rev., vol. 77, p. 789.
- Northrop, D.A., Clayton, R.N., 1966, Oxygen isotope fractionation in systems containing dolomite: Journ. Geol., vol. 74, pp. 174-176.
- Ohmoto, H., 1972, Systematics of sulfur and carbon isotopes in hydrothermal ore deposits: Econ. Geol., vol. 67, pp. 551-578.
- O'Neil, J.R. and Clayton, R.N., 1969, Oxygen isotope fractionation in divalent metal carbonates: Journ. Chem. Physics, vol. 51, pp. 5547-5558.
- Orr, W.L., 1974, Changes in sulfur content and isotopic ratios of sulfur during petroleum maturation-study of Big Horn basin Paleozoic oils, A.A.P.G. Bulletin, vol., 58, pp. 2295-2318.

- Osborne, W.T., 1977, Carbonate petrography and stratigraphy of holes 96, 100 and 106, Gays River, Nova Scotia: Implications for depositional environment: Unpubl. B.Sc. thesis, Dalhousie University, 82 p.
- Perkins, W.G., 1981, Mount Isa copper ore bodies, evidence against a sedimentary origin: Baas Becking Geological Laboratory Symposium, pp. 2-4.
- Pinckney, D.M. and Rafter, T.A., 1972, Fractionation of sulfur isotopes during ore deposition in the Upper Mississippi Valley, zinc-lead district: Econ. Geol., vol. 67, pp. 315-328.
- , and Rye, R.O., 1972, Variation of O^{18}/O^{16} , C^{13}/C^{12} , Texture and Mineralogy in altered Limestone in the Hill Mine, Cave-in District, Illinois: Econ. Geol., vol. 67, no. 1, pp. 1-18.
- Playford, P.E. and Cockbain, A.E., 1976, Modern algal stromatolites at Hamelin Pool, a hypersaline barred basin in Shark Bay, Western Australia: in Stromatolites, M.R. Walter, ed. Develop. in Sedimentology 20, Elsevier Publishing Co., pp. 389-411.
- Poole, W.H., 1967, Tectonic evolution of Appalachian region of Canada, Geol. Assoc. of Canada, special paper, pp. 9-51.
- , Sanford, B.V., Williams, H. and Kelley, D.G., 1970, Geology of south eastern Canada, Geol. Survey, Canada, Econ. Geol. Rept. 1, 5th ed., pp. 228-304.
- Potter, R.W., 1977, Pressure corrections for fluid inclusion homogenization temperature based on the volumetric properties of the system $NaCl-H_2O$. U.S.G.S., Journ. Research, vol. 5, pp. 603-608.
- , Clyne, M.A. and Brown, D.L., 1978, Freezing point depression of aqueous NaCl solutions, Econ. Geol., vol. 73, pp. 284-285.

- Ramdohr, P., 1980, The ore minerals and their intergrowths: volume I and II, Pergamon Press, Oxford, London, Toronto, 1205 p.
- Ramsay, J.G. and Graham, R.H., 1970, Simple shears and tension gashes: Can. Journ. Earth. Sci., vol. 7, pp. 786-813.
- Rankin, A.H., 1975, Fluid inclusion studies in apatite from carbonatites of the Wasaki area of western Kenya: Lithos., vol. 8, pp. 123-136.
- Rees, C.E., 1973, A steady state model for sulphur isotope fractionation in bacterial reduction processes: Geoch. et. Cosmoch. Acta, vol. 37, pp. 1141-1162.
- , Jenkins, W.J. and Monster, 1978, The sulfur isotopic composition of ocean water sulfate: Geoch. et. Cosmoch. Acta, vol. 42, pp. 377-381.
- Renfro, A.R., 1974, Genesis of Evaporite associated stratiform metalliferous deposits - A sabkha process: Econ. Geol., vol. 69, pp. 33-45.
- Reynolds, P.H. and Muecke, G.K., 1978, Age studies on slates: applicability of the $^{40}\text{Ar}/^{39}\text{Ar}$ stepwise outgassing method: Earth and Planetary Science Letters, vol. 40, pp. 111-118.
- , Zentilli, M. and Muecke, G.K., 1981, K-Ar and $^{40}\text{Ar}/^{39}\text{Ar}$ geochronology of granitoid rocks from southern Nova Scotia - its bearing on the geological evolution of the Meguma zone of the Appalachians: Can. Journ. Earth Science, vol. 18, pp. 386-394.
- Rickard, D.T., Wilden, M.Y., Marinder, N.E. and Donnelly, T.H., 1979, Studies on the Genesis of the Laisvall sandstone lead-zinc deposit, Sweden: Econ. Geol., vol. 74, pp. 1255-1285.
- Riedel, D., 1980, Ore structures and genesis of the lead-zinc deposit, Tynagh, Ireland: Geol. Rundschau, vol. 69, pp. 361-383.

- Rodgers, J., 1967, Chronology of tectonic movements in the Appalachian region of eastern North America: *Amer. Journ. of Sci.*, vol. 265, pp. 408-427.
- , 1970, *The tectonics of the Appalachians*: John Wiley and Sons, New York, 271 p.
- Roedder, E., 1960, Fluid Inclusions as samples of ore forming fluids: *Int. Geol. Congress, 21st. Proceed. Sec. 16*, pp. 218-229.
- , 1962a, Studies of fluid inclusions; low temperature application of a dual purpose freezing and heating stage: *Econ. Geol.*, vol. 57, pp. 1045-1061.
- , 1962b, Ancient fluids in crystals: *Sci. American*, vol. 207, pp. 38-47.
- , 1963, Studies of fluid inclusions, freezing data and their interpretations: *Econ. Geol.*, vol. 58, pp. 167-211.
- , 1965, Evidence from fluid inclusions as to the nature of the ore forming fluids: in *Symposium on problems of post magmatic ore deposition, Prague 1963*, vol. 2, Prague, Czechoslovakia, Geol. Survey, pp. 375-384.
- , 1967a, Environment of deposition of stratiform (Mississippi Valley type) ore deposits, from studies of fluid inclusions: in J. S. Brown, ed. *Genesis of stratiform lead-zinc, barite fluorite deposits*, *Econ. Geol. Mon. 3*, pp. 326-332.
- , 1967b, Metastable superheated ice in liquid-water inclusions under high negative pressure: *Science*, vol. 155, pp. 1413-1417.
- , 1968, Temperature, salinity and origin of ore forming fluids at Pine Point, N.W. Territories, Canada from fluid inclusion studies: *Econ. Geol.*, vol. 63, pp. 439-450.

- , 1972, Composition of fluid inclusions: U.S.G.S. Prof. paper, 440JJ.
- , 1976, Fluid inclusion evidence on the genesis of ores in sedimentary and volcanic rocks: in K.H. Wolf, ed. Handbook of Stratabound and Stratiform Ore Deposits, vol. 2, pp. 67-110.
- , 1979, Fluid Inclusions as samples of ore fluids: in H.L. Barnes, ed. Geochemistry of Hydrothermal Ore Deposits, 2nd edition, Wiley and Sons, New York, Toronto, pp. 684-737.
- and Bodnar, R.J., 1980, Geologic pressure determinations from inclusion studies: Ann. Review, Earth Planetary Science, vol. 8, pp. 263-301.
- Rogers, R.K. and Davis, J.H., 1977, Geology of the Buick-Mine, Virbunum Trend, Southeast Missouri: Econ. Geol., vol. 72, pp. 372-380.
- Russell, M.J., 1971, North-south geofractures in Scotland and Ireland: Scott Journ. Geol., vol. 8, no. 1, pp. 75-84.
- , 1974, Manganese halo surrounding the Tynagh ore deposit, Ireland: a preliminary note. Trans. Inst. Min. Metall. (Sect. B. Appl. Earth Science), vol. 83, pp. B65-66.
- , 1974, Lithogeochemical environment of the Tynagh base-metal deposit, Ireland and its bearing on ore deposition: Trans. Inst. Min. Metall. B84, pp. 128-133.
- , 1976, Incipient plate separation and possible related mineralization in lands, bordering the North Atlantic: in Geol. Assoc. of Canada, special paper, no. 14, pp. 339-348.
- , 1978, Downward excavating hydrothermal cells and Irish type ore deposits; importance of an underlying thick Caledonian prism: Trans. Inst. Min. Metall. 87B, pp. 168-171.

- , 1981, Genesis of Late Tournaisian, lead + zinc ± copper ± barite deposits in Ireland and Nova Scotia: Abstract with programs. A.G.S. Conference, Fredericton, 1981, p. 8.
- , Solomon, M. and Walshe, J.L., 1981, The genesis of sediment hosted exhalative, zinc + lead deposits, Mineral. Deposita, vol. 16, pp. 113-127.
- Rye, R.O. and Ohmoto, H., 1974, Sulfur and carbon isotopes and ore genesis, a review: Econ. Geol., vol. 69, pp. 826-842.
- Sakai, H., 1957, Fractionation of sulfur isotopes in nature: Geoch. et. Cosmoch. Acta, vol. 12, pp. 150-169.
- , 1968, Isotopic properties of sulfur compounds in hydrothermal processes: Geochem. Journ., vol. 2, pp. 29-49.
- Sangster, D.F., 1968, Relative sulphur isotope abundance of ancient seas and stratabound sulphide deposits: Trans. Geol. Assoc. of Canada, vol. 19, p. 79.
- , 1976, Carbonate hosted lead-zinc deposits: in K.H. Wolf, ed. Handbook of stratabound and stratiform ore deposits, vol. 6, pp. 447-456.
- Sasaki, A. and Krouse, H.R., 1969, Sulfur isotopes and Pine Point lead-zinc mineralization: Econ. Geol., vol. 64, pp. 718-730.
- Sawkins, F.J., 1964, Lead-zinc ore deposition in the light of fluid inclusion studies, Providencia Mine, Zacatecas, Mexico: Econ. Geol., vol. 59, pp. 883-919.
- , 1968, The significance of Na/K and Cl/SO₄ ratios in fluid inclusions and subsurface waters, with respect to the genesis of Mississippi Valley-type ore deposits: Econ. Geol., vol. 63, pp. 935-942.

- , 1969, Chemical Brecciation, an Unrecognized Mechanism for Breccia Formation? *Econ. Geol.*, vol. 64, pp. 613-617.
- and Huebner, J.S., 1965, Postmagmatic ore deposition in the light of fluid inclusion studies, Providencia Mine, Zacatecas Mexico: in Symposium - Problems of post magmatic ore deposition, Prague, 1963, Czechoslovakia, *Geol. Survey*, vol. 2, pp. 424-428.
- Schenk, P.E., 1967a, The Macumber Formation of the Maritime Provinces, Canada - A Mississippian analogue to Recent strandline carbonates of the Persian Gulf: *Journ. Sed. Petrology*, vol. 37, pp. 365-376.
- , 1969, Carbonate-sulfate-redbed facies and cyclic sedimentation of the Windsorian stage (M. Carboniferous) Maritime Province: *Can. Journ. Earth Science*, vol. 6, pp. 1037-1066.
- , 1971, Southeastern Atlantic Canada, Northwestern Africa and continental drift: *Can. Journ. Earth Science*, vol. 8, pp. 1218-1251.
- , 1975, Paleozoic evolution of African Nova Scotia - polar and deep to equatorial and continental: IX th International Congress of Sedimentology, Nice 1975, pp. 181-185.
- , 1981, Carbonate-sulfate relations in the Windsor Group, central Nova Scotia, Canada: in press.
- and Hatt, B.L., 1981, Depositional environment of the Gays River mound, Nova Scotia, Canada: *Compte. Rendu, IX Internat. Congr. Carboniferous Strat.*, in press.
- Schneider, A., 1970, The sulfur isotope composition of basaltic rocks: *Contr. Mineral. Pet.*, vol. 25, pp. 95-124.
- Schopf, T.J.M., 1969, Paleoecology of ectoprocts (Bryozoans): *Journ. Paleontology*, vol. 43, pp. 234-244.

- Schultz, R.W., 1971, Mineral exploration practise in Ireland: Trans. Inst. Min. Metall. sect. B, vol. 80, B238-B258.
- Schwarcz, H.P. and Burnie, S.W., 1973, Influence of sedimentary environments on sulfur isotope ratios in clastic rocks, a review: Mineral Deposita, vol. 8, pp. 264-277.
- Shearman, D.J., Mossop, G., Dunsmore, H. and Martin, M., 1972, Origin of gypsum veins by hydraulic fracture: Trans. Inst. M. Metall. Bull., vol. 81, pp. B149-B155.
- Skall, H., 1975, The paleoenvironment of the Pine Point lead-zinc district: Econ. Geol., vol. 70, pp. 22-47.
- Skinner, B.J., 1967, Precipitation of Mississippi Valley type ore- a possible mechanism: in J.S. Brown, ed. Genesis of stratiform lead-zinc-barite-fluorite deposits in carbonate rocks, Econ. Geol. Mon. 3, pp. 363-370.
- Smith, J.W. and Croxford, N.J.W., 1973, Sulfur isotope ratios in the Mc Arthur lead, zinc, silver deposit: Nature, vol. 245, pp. 10-12.
- Snyder, F.G., 1967, Criteria for origin of stratiform ore bodies with application to southeast Missouri: in J.S. Brown, ed. Genesis of stratiform lead-zinc, fluorite, barite deposits (Mississippi Valley type deposits) - A symposium, Econ. Geol. Mon. 3, pp. 1-13.
- Solomon, M., Rafter, T.A. and Dunham, K.C., 1971, Sulfur and oxygen isotope studies in the Northern Pennines in relation to ore genesis: Inst. Min. Metall. Trans. Sect. B, vol. 80, pp. B259-B275.
- Sourirajan, S. and Kennedy, G.C., 1962, The system $H_2O-NaCl$ at elevated temperatures and pressures: Amer. Journ. of Sci., vol. 260, pp. 115-141.

- Stacey, J.S. and Kramers, J.D., 1975, Approximation of terrestrial lead isotope evolution of a two stage model: *Earth Planet. Sci. Letter*, vol. 26, pp. 207-221.
- Stanton, R.L., 1972, *Ore petrology*, McGraw-Hill, New York, N.Y., 713 p.
- and Russel, R.D., 1959, Anomalous leads and the emplacement of lead sulfide ores: *Econ. Geol.*, vol. 54, pp. 588-607.
- Sverjensky, D.A., Rye, D.M. and Doe, B.R., 1979, The lead and sulfur isotopic compositions of galena from a Mississippi Valley type deposit in the New lead belt south east Missouri: *Econ. Geol.*, vol 74, pp. 149-153.
- Taylor, S.R., 1965, Application of trace element data to problems in petrology: *Phys. Chem. Earth*, vol. 6, pp. 133-213.
- Taylor, H.P., 1974, The application of oxygen and hydrogen isotope studies to problems of hydrothermal alteration and ore deposition: *Econ. Geol.*, vol. 69, pp. 843-883.
- , Frenchen, J. and Degens, E.T., 1967, Oxygen and carbon isotope studies of carbonatites from the Laacher Sea district, West Germany and the Alno district, Sweden: *Geoch. et. Cosmoch. Acta*, vol. 31, pp. 407-430.
- Thacker, J.L. and Anderson, K.H., 1977, The geological setting of the south east Missouri lead district - Regional geologic history, structure and stratigraphy: *Econ. Geol.*, vol. 72, pp. 339-348.
- Thiede, D.S. and Cameron, E.N., 1978, Concentration of heavy metals in the Elk Point evaporite sequence, Saskatchewan: *Econ. Geol.*, vol. 73, pp. 405-415.
- Thode, H.G. and Monster, J., 1965, Sulphur isotope geochemistry of petroleum, evaporite, and ancient seas: *Am. Ass. Petrol. Geologists, Mem.* 4, pp. 367-377.

- , Shima, M., Rees, C.E. and Kroshnamurty, K.V., 1965, Carbon 13 isotope effects in systems containing carbon dioxide, bicarbonate, carbonate and metal ions: *Can. Journ. Chemistry*, vol. 43, pp. 582-595.
- Touray, J.C. and Barlier, J., 1974, Liquid and gaseous hydrocarbon inclusions in quartz microcrystals from "Terres Noires" and flysch à helminthoides (French Alps): *Fort. Mineralogy*, vol. 52, pp. 419-426.
- Trudinger, P.A. and Chambers, L.A., 1973, Reversibility of bacterial sulfate reduction and its relevance to isotopic fractionation: *Geoch. et. Cosmoch. Acta*, vol. 37, pp. 1775-1778.
- Tudge, A.P. and Thode, H.G., 1950, Thermodynamic properties of isotopic compounds of sulfur: *Can. Journ. Research*, vol. 28B, pp. 567-578.
- Veizer, J. and Hoefs, J., 1976, The nature of O^{18}/O^{16} and C^{13}/C^{12} secular trends in sedimentary carbonate rocks: *Geoch. et. Cosmoch. Acta*, vol. 40, pp. 1387-1395.
- Weeks, L.J., 1948, Londonderry and Baas River map-areas, Colchester and Hants Counties, Nova Scotia: *Can. Geol. Survey, Memoir 245*, 86 p.
- William, N. and Rye, D.M., 1974, Alternative interpretation of sulphur isotope ratios in the McArthur lead-zinc-silver deposit: *Nature*, vol. 247, pp. 535-537.
- Wolf, A.V. and Brown, G.M., 1966, Properties of Aqueous solutions: Conversion tables. in *Handbook of Chemistry and Physics*, 46th ed., Cleveland Chemical Rubber Co., p. D-174.
- Yermakov, N.P., 1965, Research on the Nature of Mineral forming solutions: *Internat. Series of Monographs in Earth Sciences*, vol. 22.

- Zartman, R.E., and Doe, B.R., 1981, Plumbotectonics - the model: in R.E. Zartman and S.R. Taylor, eds., Evolution of the upper mantle, Tectonophysics, vol. 75, pp. 135-162.
- Zen, E., 1965, Solubility measurements in the system $\text{CaSO}_4\text{-NaCl-H}_2\text{O}$ at 35°C, 50°C and 70°C and one atmosphere pressure: Journ. Petrology, vol. 6, pp. 124-164.
- Zentilli, M., Doe, B.R. and Delevaux, M.H., 1980, Isotopic compositions of lead in some Nova Scotia galenas, metallogenic implications: Abstract, GAC/MAC Abstracts with Program, vol. 5, p. 89.
- and Graves, M.C., 1977, Evolution of metallogenic domains in Nova Scotia: Can. Inst. Min. Metall. Bulletin, vol. 70, p. 69.

APPENDIX I

LOCATION OF DRIFT PLANS, AND AREAS MAPPED IN THE GAYS RIVER DECLINE

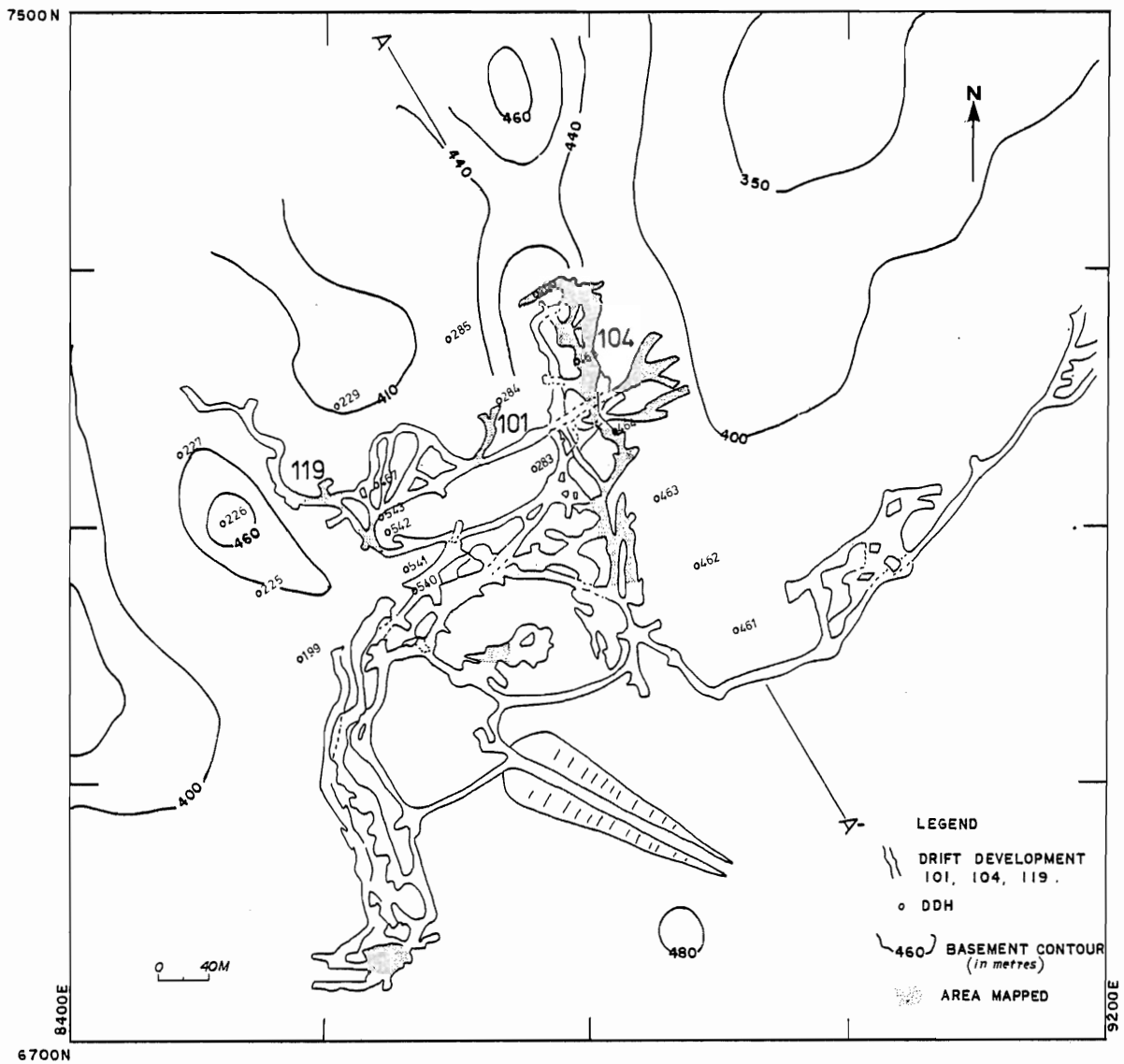


Figure I-1 Location of the drift plans, basement paleogeography and the areas mapped in the Gays River decline.

APPENDIX II
MINERALOGY AND PALYNOLOGY

A. Carbonate Staining

Aim: To Distinguish calcite from dolomite in the selected samples collected during underground mapping.

Stain Preparation

A solution of alizarin red S was prepared by dissolving about 0.1 gm of alizarin red in 100 cc of 0.2% cold hydrochloric acid. The acid was made by adding 2 cc of commercial grade (HCl) to 998 cc of water.

Procedure

Cut slabs and selected samples of carbonates were thoroughly washed in cold running water and dried. Enough quantity of the prepared alizarin red S was poured into an evaporating dish. Each sample was immersed in the alizarin red S for two to three minutes.

Results

Calcite crystals in the vugs of the samples were stained reddish pink while dolomite remains unchanged. Dedolomitized parts of the slabs appeared unaffected due to their black colour. The procedure was carried out on selected carbonate samples and it was found that the white carbonate in the cut slabs is essentially calcite.

B. Determination of the Percentage of Dolomite by X-ray Diffraction Procedure.

A diffractometer smear of each carbonate sample was made on a glass slide with acetone. The diffractometer was set at 40 Kv and 20 Ma with a $\text{CuK}\alpha$ radiation at room temperature. Scan speed was set at $1^\circ 2\theta$ per minute at a range of 1×10^3 and chart speed of 1 cm per minute.

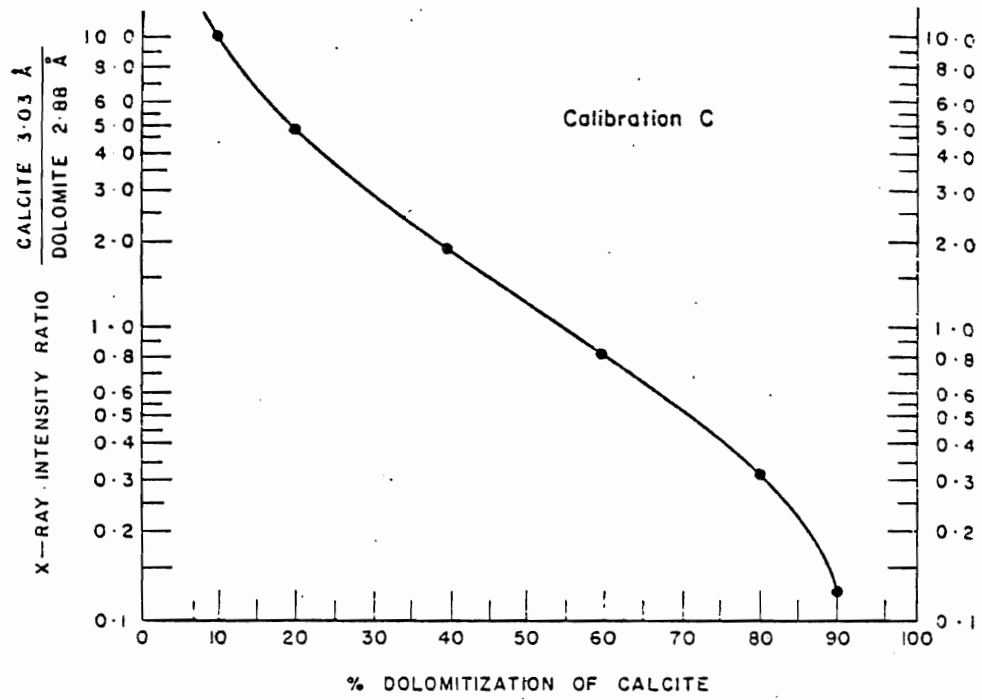


Figure II-1 Estimation of the percentage of dolomite in a carbonate sample. From Hutchison (1974).

Each carbonate smear was scanned through the region of 26° to 34° to check for interference from minerals other than calcite and dolomite. The lines of interest in this method are the 104 calcite and 104 dolomite at 29.43 and $30.98^{\circ}2\theta$ $\text{CuK}\alpha$ respectively. These lines represent the maximum intensities for calcite and dolomite. The lines have minimum interference. After establishing a suitable background, counts were made for 10 seconds on the two peaks as well as on a suitable background position at a 2θ value of about $1\ 1/2\ 2\theta$ higher than that of dolomite line and a $1\ 1/2^{\circ}\ 2\theta$ value just below the calcite line. These values were applied to derive a ratio of calcite to dolomite as follows:

$$\frac{\text{counts 10 sec calcite}_{104} \text{ peak} - \text{counts 10 sec background}}{\text{counts 10 sec dolomite}_{104} \text{ peak} - \text{counts 10 sec background}}$$

This ratio is plotted on Fig. II-1 (from Tennant and Berger 1957) and the percentage of dolomite in the sample is read off the graph. The precision of the Tennant and Berger's curve indicated by Royse *et al.* (1971) in Hutchinson (1974) is within $\pm 6\%$ at 95% confidence level.

The variations in the carbonate composition and percentage of dolomite adjacent to the massive sulfide veins were estimated from the above relationship using systematic carbonate samples in the 104 drift.

C. Vitrinite Reflectivity

Fifty reflectivity measurements were made on two coaly materials from the Gays River semi-consolidated "trench" sediments in the laboratory of Dr. P. Hacquebard at the Bedford Institute of Oceanography, Dartmouth, Nova Scotia. The measurements are presented in Table II-1 and graphed on a reflectogram in Fig. II-2.

Table II-1 Reflectance Readings (Ro) on Lignite

.46	.43	.37	.39	.40	.41	.42	.42	.45	.50	.42	.43	.41
.43	.47	.47	.49	.41	.45	.45	.47	.43	.41	.43	.46	.43
.44	.42	.49	.50	.41	.42	.46	.47	.50	.44	.42	.50	.49
.42	.43	.42	.46	.49	.45	.44	.42	.45	.46	.44		

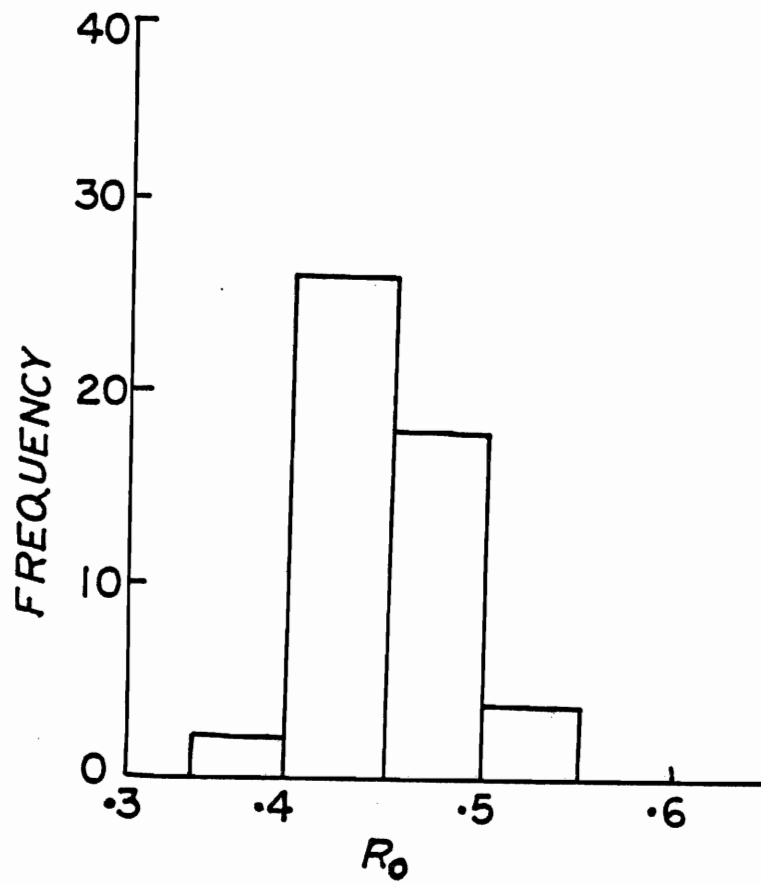


Figure II-2 Histogram of the frequency distribution of vitrinite reflectivity measurement on the coaly materials in the Gays River "trench" sediments.

D. Palynological analysis of the semi-consolidated "trench" samples
(Table II-2).

Table II-2 Palynological Analysis of the Semi-Consolidated "trench" samples, Gays River Mine.

SAMPLE NUMBER	COORDINATES	DESCRIPTION	POLLEN AND SPORES	AGE
AGR 107A	7275.5N 8809.6E	Lignite	No palynomorph, contain resinous material	Cretaceous (P. Hacquebard, pers. communication)
AGR 285-230	7245.25N 8691.98E	Semi consolidated clay, sand and pebbles.	Acquitriradites verrucosus (Cookson and Dettmann) Dettmann Cicatricosisporites crassitermatus (Hedland) Cicatricosisporites delicatus (Phillips and Felix) Cicatricosisporites exilioides (Maljavkina Bolchovitina) Cicatricosisporites venustus (Deak) Concavissimisporites punctatus (Delcourt and Sprumont) Concavissimisporites variverrucatus (Couper) Brenner Impardecispora apiverrucata (Couper) Venkatachela <u>et al.</u> Trilobosporites trioreticulatus (Cookson and Dettman)	Late Aptian-Early Albian (E. Davies written comm.) Late Aptian-Early Albian (E. Davies written comm.) Late Aptian-Early Albian (E. Davies written comm.)
DH 324	7301.5N 8860.0E	Semi consolidated clay, sand and pebbles	Todisporites major (Couper) Densoisporites microrugulatus (Brenner)	Probably mid Visean (M.S. Barrs, pers. comm.)
DH 372	7301.5N 8860.0E	Semi consolidated clay, sand and pebbles	Alisporites bilateralis (Rouse) Podocarpidites potomancensis (Brenner) Callialasporites cf. trilobatus (Balme)	Late Jurassic- Early Cretaceous (E. Davies, written comm.)

Table II-2 Continued

SAMPLE NUMBER	COORDINATES	DESCRIPTION	POLLEN AND SPORES	AGE
DH 409	7301.5N 8860.0E	Semi consolidated clay, sand and pebbles	Alisporites bilateralis Alisporites grandis (Cookson) Dettmann Cicatricosisporites delicatus Klukisporites pseudoreticulatus (Couper) Parvisaccites amplus (Brenner) Parvisaccites radiatus " Podocarpidites potomacensis Trilobosporites purverulentus (Verbitskaja) Dettman Trilobosporites trioreticulatus	Aptian (E. Davies, written comm.)
P 19715	-	Semi consolidated clay, sand and pebbles	Alisporites bilateralis Appendicisporites cristatus (Markova) Pocock Cicatricosisporites delicatus Cicatricosisporites sp. A Impardecisporites apiverrucatus Klukisporites pseudoreticulatus Parvisaccites amplus Trilobosporites purverulentus	Aptian (E. Davies, written commun.)

Table II-3 Electron Microprobe Analysis of Sphalerite and Galena. (Wt. %).

Massive vein sphalerite

Mean of 5 grains

Element						
Zn	66.45	67.16	66.31	68.52	66.92	67.07
Fe	0.05	0.09	0.40	-	0.5	0.20
S	33.58	33.70	33.50	33.82	35.22	33.96
Total	100.08	100.95	100.21	102.34	102.14	101.23
	*Fe content 0.4 mole % FeS					

Stratiform sphalerite

Mean of 5 grains

Element						
Zn	67.02	67.77	66.82	67.64	66.03	67.05
Fe	0.5	0.45	0.68	0.77	0.55	0.59
S	34.50	33.88	33.93	33.97	33.60	33.97
Total	102.02	102.1	101.43	102.38	100.18	101.61
	*Fe content 1.1 mole % FeS					

Vein galena

Mean of 2 grains

Element			
Pb	88.27	88.41	88.34
S	13.20	13.26	13.23
Total	101.47	101.67	101.57

Stratiform galena in vugs

Mean of 4 grains

Element					
Pb	88.15	88.65	88.28	88.37	88.36
S	12.98	12.70	13.22	13.10	13.00
Total	101.13	101.35	101.50	101.47	101.36

Table II-4 Electron Microprobe Analysis of Marcasite,
Pyrite and Chalcopyrite. (Wt %).

Marcasite interstratified with dolomite							Mean of 6 grains
Element							
Fe	49.52	49.97	49.47	49.81	49.84	49.84	49.67
S	50.79	51.26	51.41	51.16	50.07	51.32	51.00
Total	100.31	101.23	100.88	100.97	99.53	101.16	100.67
Marcasite intergrowths with sphalerite and dolomite							Mean of 5 grains
Element							
Fe	46.79	46.83	47.02	46.82	46.63	46.81	
S	54.24	54.36	54.35	54.04	54.10	54.21	
Total	101.03	101.19	101.37	100.86	100.73	101.02	
Marcasite inclusions in chalcopyrite							Mean of 2 grains
Element							
Fe	46.12	46.20	46.16				
S	54.22	53.86	54.04				
Cu	0.13	0.23	0.18				
Total	100.47	100.29	100.38				
Chalcopyrite intergrowths with sphalerite and galena							Mean of 4 grains
Element							
Fe	31.04	31.02	31.09	31.07	31.05		
Cu	34.61	35.26	34.84	34.82	34.88		
S	35.54	35.84	35.51	35.42	35.57		
Mn	0.09	-	-	-	0.02		
Total	101.28	102.12	101.44	101.31	101.52		

Table II-4 (Continued)

Chalcopyrite veinlet in dolomite

Mean of 5 grains

Element						
Fe	30.54	30.72	30.75	30.83	30.94	30.75
Cu	34.97	35.19	34.58	34.45	34.38	34.71
S	35.37	35.88	35.20	35.66	35.94	35.61
Total	100.88	101.79	100.53	100.94	101.26	101.07

Pyrite overgrowths on fractures

Mean of 5 grains

Element						
Fe	47.08	46.94	47.13	47.13	46.83	47.02
Zn	0.15	0.04	0.17	0.19	0.2	0.15
S	52.22	54.27	54.34	54.37	54.61	53.96
Total	99.45	101.25	101.64	101.69	101.64	101.13

Pyrite in geopetal cavity

Mean of 5 grains

Element						
Fe	46.57	47.07	47.03	47.73	47.28	47.13
Zn	0.09	0.28	0.08	0.11	0.17	0.14
S	54.32	54.20	54.27	54.03	54.13	54.19
Total	100.98	101.55	101.38	101.87	101.58	101.46

Table II-5a Minor and Trace Element Content of Sphalerite and Galena. (ppm).

SAMPLE NUMBER	DESCRIPTION	Cu	Cd	Co	Ni	Ag	Mn	V	Sn
AGR 03	Vein sphalerite	44	2390	17	<1	2	552	6.5	9
AGR 19	"	12.5	2055	14	2.5	<1	410	7	8.5
AGR 20	"	10	1935	19	3.5	<1	415	<5	18
AGR 21	"	74	1800	62	34	2	659	5	11
104 Sub 1	"	29	2000	28	17	<1	2125	6	9
AGR 134	"	61	2305	26	9	<1	3095	20	25
AGR 135	"	9	2215	18	<1	<1	597	5	8.5
AGR 136	"	112	2560	31	11	<1	1375	<5	25
AGR 146	"	6	1430	21	21	<1	350	10	9
AGR 147	"	22	1980	35	41	<1	359	6	12
AGR 26	Vein galena	23	396	7	2	3	122	<5	6
AGR 91	"	393	283	8	13	121	149	<5	18
AGR 169	"	5	165	7	3	<1	25	5	5
119-6	Stratiform galena	38	238	5	<1	13	318	<5	<2
	"	190	695	15	8	13	646	6	5

Table II-5b Minor and Trace Element Content of Marcasite and Pyrite. (ppm).

SAMPLE NUMBER	DESCRIPTION	Cu	Cd	Co	Ni	Ag	Mn	V	Sn
1091-11	Marcasite inter-grown with dolomite	583	<1	100	183	<1	2180	13	<5
201-11	Marcasite overgrowths on fractures	6	3	7	6	6	1146	14	9
201-12	"	155	<1	24	54	<1	1335	17	4
201-13	"	258	<1	16	32	<1	740	7	5
AGRP-1	Pyrite overgrowths on fractures	6	3	6	6	6	137	13	<5

Table II-6 Microprobe Analysis of Carbonates. (Wt %).

TYPE	SAMPLE NUMBER	Na	Mg	S	Cl	Ca	Mn	Fe	Zn	TOTAL
Dolomite Pellet	137-1	-	12.54	-	0.14	21.32	0.06	0.33	-	34.39
" "	140-2	-	13.04	-	0.12	22.24	0.07	0.39	-	35.86
" "	149-1	-	13.16	-	0.11	21.65	0.05	0.29	-	35.26
" "	149-3	-	12.24	-	0.10	18.12	0.05	0.21	-	30.72
Recrystallized Dolomite Micrite	38-2	.03	11.48	-	-	20.43	1.61	1.26	-	34.81
" "	38-3a	.07	12.18	.04	-	20.99	1.17	1.06	-	35.51
" "	38-3b	.08	11.56	.32	-	20.21	1.44	1.11	-	34.72
" "	38-4a	-	11.34	.22	-	20.27	1.39	1.17	-	34.39
" "	38-4b	-	10.49	.16	.06	18.93	1.41	1.25	-	32.3
" "	48-1	.06	10.73	-	-	21.05	1.50	1.65	-	34.99
" "	48-2	-	12.19	-	-	21.86	.10	.41	-	34.56
" "	94a-1	-	11.07	.08	-	20.67	1.78	1.36	-	34.96
" "	94a-2	-	11.58	.04	-	20.86	1.9	1.43	-	35.81
" "	94a-3	.05	11.41	-	-	21.31	1.91	1.35	-	36.03
" "	104b-3	.10	10.51	.06	.09	19.09	.9	1.0	-	31.75
" "	117-1	.17	9.22	-	-	19.20	2.65	2.26	-	33.5
" "	134-1	-	13.21	-	.05	21.69	.12	.37	.21	35.65
" "	134-3	-	12.05	.07	.15	20.15	.15	.35	.33	33.25

Table II-6 Continued

TYPE	SAMPLE NUMBER	Na	Mg	S	Cl	Ca	Mn	Fe	Zn	TOTAL
Recrystallized Dolomite Micrite	134-5	.14	12.5	.05	.12	21.96	.14	.37	-	35.28
" "	137-2	.08	12.15	.26	.18	20.81	.26	.59	-	34.33
" "	137-3	.06	11.68	-	.13	20.35	.66	.85	-	33.73
" "	139-1	-	12.6	-	.09	21.12	.69	.90	-	35.5
" "	139-2	.08	11.18	-	-	20.90	2.19	2.12	-	36.47
" "	139-3	-	10.83	-	-	20.99	2.09	2.10	-	36.01
" "	139-4	-	11.11	-	-	20.93	2.21	2.17	-	36.42
" "	139-5	-	10.89	-	-	20.76	2.06	1.95	-	35.66
" "	140-1	.05	13.2	.04	.11	21.77	.17	.47	-	35.9
" "	140-3	.12	13.20	.07	.19	22.75	.22	.47	-	37.02
" "	148-1	-	12.53	-	-	21.17	.71	.93	-	35.34
" "	148-2	.07	11.97	-	-	20.74	1.42	1.49	-	35.69
" "	148-3	-	12.47	-	.12	22.2	1.84	.43	-	37.07
" "	148-4	.1	11.65	-	-	20.58	1.91	1.95	-	36.19
" "	148-5	-	13.09	.11	.19	21.12	.31	.43	.20	35.45
" "	148-6	-	11.68	-	-	20.87	1.45	1.53	.26	35.79
" "	149a-2	-	13.18	.07	.19	21.12	.13	.35	.15	35.48

Table II-6 Continued

TYPE	SAMPLE NUMBER	Na	Mg	S	Cl	Ca	Mn	Fe	Zn	TOTAL
Recrystallized dolomite micrite	149a-4	.16	12.42	-	.08	18.31	.12	.32	-	32.13
" "	149a-5	.23	11.77	.03	.09	16.06	.13	.23	-	28.81
" "	149a-6	.13	10.52	-	-	16.83	1.66	1.31	-	30.45
" "	149b-4	-	12.19	-	0.13	21.62	.44	.64	.22	35.02
" "	149b-5	-	9.92	.03	-	20.66	3.01	2.64	.15	36.41
" "	149b-6	-	10.52	-	.04	20.62	2.10	2.14	-	35.42
" "	160-1	-	11.66	.04	.03	21.35	1.52	1.45	.07	36.05
" "	160-2	.13	11.39	-	.48	20.70	1.93	1.83	-	36.46
" "	160-3	-	11.35	-	-	21.03	2.22	1.75	-	36.35
" "	161a-1	-	2.17	.48	-	34.00	1.80	1.29	-	39.74
" "	161a-2	-	3.72	-	-	31.19	1.98	1.22	-	38.11
" "	161a-3	.06	11.30	-	-	21.09	1.42	1.12	-	34.99
" "	161b-2	-	5.91	-	-	29.58	1.49	.96	-	37.94
" "	161b-3	-	10.05	-	-	20.39	1.70	1.40	-	33.54
" "	161b-4	-	3.68	-	-	33.08	1.32	.75	-	38.83
" "	161b-5	-	7.72	-	-	24.26	1.78	1.33	-	35.09
" "	162-1	-	11.39	-	-	20.87	1.85	1.97	-	36.08

Table II-6 Continued

TYPE	SAMPLE NUMBER	Na	Mg	S	Cl	Ca	Mn	Fe	Zn	TOTAL
Recrystallized Dolomite Micrite	162-2	-	10.61	.1	.03	19.54	1.42	1.60	-	33.3
" "	162-3	-	11.60	-	-	21.14	1.27	1.66	-	35.67
" "	164-4	0.36	6.78	-	-	27.48	1.62	1.34	-	37.58
Dedolomite	39a-1	-	-	-	-	39.77	.73	.11	.43	41.04
"	39a-2	-	.04	.04	-	40.88	.74	.09	-	41.79
"	39b-1	-	6.12	-	-	30.75	.54	.28	-	37.69
"	39b-2	-	1.19	-	-	37.04	.86	.20	-	39.29
"	39b-3	-	.39	-	-	38.02	.76	.21	-	39.38
"	96-1	-	.5	-	-	37.43	1.29	.35	-	39.57
"	96-2	-	.14	.04	-	37.69	1.05	.46	-	39.38
"	96-3	-	.16	.10	.06	38.32	1.08	.39	-	40.09
"	97-1	-	.10	-	-	37.12	1.3	.62	-	39.14
"	97-2	-	3.4	-	-	33.78	1.31	.54	-	39.03
"	97-3	-	-	.03	-	38.91	1.11	.55	-	40.6
"	132-1	-	-	.09	-	38.53	.62	.36	-	39.6
"	132-2	.07	-	.19	-	38.95	.57	.29	-	40.07
"	132-3	-	-	.08	-	39.05	.64	.31	.73	40.81
"	133a-1	-	-	.05	-	38.95	1.16	.23	-	40.36

Table II-6 Continued

TYPE	SAMPLE NUMBER	Na	Mg	S	Cl	Ca	Mn	Fe	Zn	TOTAL
Dedolomite	133a-2	-	.07	.11	-	38.23	1.05	.35	-	39.81
"	133b-1	-	-	-	-	36.42	.68	.13	.09	37.32
"	133b-2	-	-	.13	-	39.22	.95	.21	-	40.51
"	142b-1	.08	-	.12	-	38.55	.74	.16	-	39.65
"	142b-2	.04	.08	.14	-	39.37	.88	.35	-	40.86
"	143a-1	-	-	.09	-	38.9	1.09	.41	-	40.52
"	143a-2	-	-	.11	-	39.44	1.01	.39	-	40.95
"	143b-3	-	-	.04	-	39.21	.71	.26	-	40.22
"	143b-4	-	-	-	-	39.52	.50	.18	-	40.2
"	144a-1	-	1.66	.14	-	33.24	.61	.27	.11	36.03
"	144a-3	-	-	.24	-	39.19	.57	.04	-	40.04
"	144b-1	-	-	.26	-	40.95	.70	.43	.31	42.34
"	144b-2	-	.06	.16	-	40.47	.74	.39	-	41.82
"	144b-3	-	-	.19	-	39.66	.76	.34	.06	41.01
"	144b-4	-	.1	.05	.08	32.31	.90	-	.10	33.54
"	145-2	-	-	.21	-	40.3	.58	.07	-	41.16
"	145-3	.13	-	.21	-	37.75	.54	.10	-	38.73
"	145-4	-	-	.42	-	38.44	.48	.29	-	39.63

Table II-6Continued

TYPE	SAMPLE NUMBER	Na	Mg	S	Cl	Ca	Mn	Fe	Zn	TOTAL
Dedolomite	147-1	-	-	.07	-	38.12	.75	.34	-	39.28
"	147-2	-	.12	.07	-	38.91	.69	.38	-	40.17
"	147-3	-	6.8	.17	-	28.4	1.31	1.11	.48	38.27
"	147-4	-	-	-	-	38.26	.99	.67	.60	40.52
Ore Stage Calcite	104a-1	-	-	-	-	39.53	.53	.1	-	40.16
" " "	104a-2	-	.03	-	-	39.39	.78	-	-	40.2
" " "	104a-3	-	-	-	-	39.27	.96	-	-	40.23
" " "	104a-4	-	-	-	-	39.81	.38	-	-	40.19
" " "	104a-5	-	-	-	-	39.47	.65	-	-	40.12
" " "	104a-6	-	-	-	-	39.55	.56	-	-	40.11
" " "	104a-7	-	.03	-	-	39.51	.51	.1	-	40.05
" " "	104a-8	-	-	-	-	39.09	.64	-	-	30.73
" " "	104a-9	-	-	-	-	39.32	.72	.1	-	40.14
" " "	104a-10	-	-	-	-	36.95	.59	.06	-	37.6
" " "	104a-11	-	-	-	-	39.63	.46	-	-	40.09
" " "	104a-12	-	-	-	-	38.97	1.08	.03	-	40.08
" " "	119-1	-	.05	-	-	38.3	1.45	-	-	39.8
" " "	119-2	-	-	-	-	38.24	1.99	-	-	40.23
" " "	119-3	-	.09	.03	-	38.03	1.76	-	-	39.91

Table II-6 Continued

TYPE	SAMPLE NUMBER	Na	Mg	S	Cl	Ca	Mn	Fe	Zn	TOTAL
Ore Stage Calcite	119-4	.08	-	-	-	38.26	1.55	.03	-	39.92
" " "	119-5	.07	-	-	-	38.41	1.37	.05	-	39.9
" " "	119-6	-	-	-	-	37.86	1.8	-	-	39.66
" " "	119-7	-	-	-	-	38.43	1.59	-	-	40.02
" " "	119-8	-	-	-	-	38.37	1.16	0.11	-	39.64
Post Ore Calcite	38-1	.25	.30	.08	.04	36.56	1.37	.21	.11	38.92
" " "	38-2	.04	.05	-	-	40.76	.87	.10	-	41.82
" " "	38-3	-	.33	.06	-	39.58	1.52	.29	.29	42.07
" " "	03-1	.05	-	.07	-	39.05	.86	.24	-	40.27
" " "	03-2	-	.04	.06	-	39.25	.31	.05	-	39.71
" " "	48-3	.03	.29	-	-	38.60	1.35	.24	-	40.51
" " "	48-4	.03	.28	-	-	39.2	1.19	-	-	40.7
" " "	104-4	-	.2	-	-	39.76	1.24	.24	-	41.44
" " "	104-5	-	-	.18	-	40.22	1.07	.24	-	41.71
" " "	134-1	-	-	-	-	40.24	.84	-	-	41.08
" " "	134-2	-	-	-	-	41.18	.47	-	.04	41.69
" " "	134-3	.05	.07	.05	-	41.25	.91	.05	-	42.38
" " "	143-1	-	.17	-	-	41.54	.97	.08	-	42.69
" " "	143-2	.04	-	.04	-	41.52	.59	.16	-	42.35

Table II-6 Continued

TYPE	SAMPLE NUMBER	Na	Mg	S	Cl	Ca	Mn	Fe	Zn	TOTAL
Post Ore Calcite	149-1	-	.1	-	-	38.72	.79	.5	-	40.11
" " "	149-2	-	-	.06	-	39.49	.76	.26	-	40.51
" " "	201-1	-	.06	-	-	38.6	.73	.08	-	39.47
" " "	201-2	-	.09	-	-	38.69	.83	.15	-	39.76
" " "	201-3	-	.12	-	-	39.01	.75	.21	-	40.09
" " "	201-4	-	.05	-	-	39.28	.72	.14	-	40.19
" " "	201-5	-	.09	-	-	39.48	.68	.27	-	40.52
" " "	201-6	-	.12	-	-	39.17	.77	.23	-	40.29
" " "	201-7	.06	.18	-	-	38.93	.85	.20	-	40.22
" " "	201-8	-	.09	-	-	38.81	.82	.19	-	39.91
" " "	201-9	-	.10	-	-	39.0	.75	.10	-	39.95
" " "	201-10	-	.06	-	-	39.2	.70	.15	-	40.11
" " "	201-11	-	.09	-	-	38.95	.77	.12	-	39.93
" " "	201-12	-	.17	-	-	39.13	.80	.16	-	40.26

Table II-7 Microprobe Analysis of Barite. (Wt %).

DESCRIPTION	Ba	Sr	S	TOTAL
Cryptocrystalline barite	61.22	3.8	34.35	99.37
" "	61.33	4.34	34.77	100.44
" "	61.48	3.81	34.30	99.60
" "	59.84	5.17	34.65	99.67
" "	60.71	4.35	34.31	99.38
" "	60.58	4.65	34.43	99.66
" "	60.70	4.37	34.24	99.31
" "	60.19	4.31	34.16	98.66
" "	60.41	4.44	33.99	98.83
" "	61.27	3.91	34.11	99.29

APPENDIX III

FLUID INCLUSION MICROTHERMOMETRY

A. Preparation of Doubly Polished Thin Sections

Procedure

Samples of sphalerite, calcite, fluorite, barite and quartz were sliced to an average of 6 to 4 millimeter thickness with a diamond cutting saw. One surface of each of the cut samples was ground down by using the 220, 400 and finally the 600 grade carborundum on a lapping machine. Samples of sphalerite, were ground on a glass plate because they are generally softer than the other minerals. The other surface of each of the minerals was ground to a flat surface, parallel to the first surface. Each ground sample has an average thickness of 80 μm .

The samples were thoroughly washed with deionized water. Each ground sample was mounted on a glass slide with lakeside cement with the smooth surface up. The glass slides were mounted on aluminum discs and the samples were transferred on to the "Vibromet" polishing machine with the smooth surfaces down, on a slurry of 0.5 μm aluminum oxide polish. The samples were left for four hours and the polishing lap was changed to a slurry of 0.25 μm aluminum oxide polish. A final polish was achieved after about 3 hours of polishing on the Vibromet with the 0.25 μm aluminum oxide slurry. The polishing procedure was repeated for the second side of each section. A final thickness between 40-60 μm was achieved on the polished sections.

Each of the polished sections was soaked in acetone for 30 minutes to dissolve the mounting lakeside cement and the delicate doubly-polished sections were cup up to provide small chips for the microscopic examination.

B. Table III-1 List of Samples Examined for Fluid Inclusions

i. Vein sphalerite

SAMPLE NUMBER	GRID REFERENCE	HOMOGENIZATION TEMPERATURE
AGR 24A	7274.88N 8785.02E	214°C
AGR 24B	7274.88N 8785.02E	215.5°C
104-Sub 1A	7243.8N 8814.5E	-
104-Sub 1B	7243.8N 8814.5E	-
AGR 134A	7292.4N 8786.5E	215°C
AGR 134B	7292.4N 8786.5E	218°C
AGR 136A	7292.9N 8787.7E	215°C
AGR 136B	7292.9N 8787.7E	215.5°C
AGR 141A	7288.5N 8796.3E	-
AGR 141B	7288.5N 8796.3E	-
AGR 147A	7202.5N 8803.4E	219°C
AGR 147B	7202.5N 8803.4E	-
AGR 167A	7257.56N 8804.76E	-
AGR 167B	7257.56N 8804.76E	-
AGR 168A	7257.24N 8805.68E	205°C
AGR 168B	7257.24N 8805.68E	214°C

Table III-1 (Continued)

SAMPLE NUMBER	GRID REFERENCE	HOMOGENIZATION TEMPERATURE
AGR 169A	7257.02N 8806.2E	274.5 ? (Secondary Inclusion)
AGR 169B	7257.02N 8806.2E	-
AGR 170A	7256.78N 8806.84E	-
AGR 170B	7256.78N 8806.84E	-
<hr/>		
ii. Stratiform sphalerite		
<hr/>		
1093-3A	6773.8N 8635.6E	-
1093.3B	6773.8N 8635.6E	-
715-340A	7543.00N 9607.60E	-
715-340B	7543.00N 9607.60E	-
<hr/>		
iii. Ore stage calcite		
<hr/>		
AGR 07	7274.88N 8788.02E	169°C (Average of 4 determinations)
AGR 11	7290.28N 8785.02E	176°C (Average of 4)
AGR 12	7284.64N 8786.4E	173°C (Average of 5)
AGR 13	7255.76N 8797.30E	174°C (Average of 4)
AGR 91	7240.9N 8790.24E	170°C (Average of 6)
SPA 105-2	6994.82N 8703.8E	172°C (Average of 2)
<hr/>		

Table III-1 (Continued)

iv. Post ore calcite		
SAMPLE NUMBER	GRID REFERENCE	HOMOGENIZATION TEMPERATURE
AGR 29	7006.82N 8734.8E	139.8°C (Average of 5)
AGR 109-1	6771.8N 8635.2E	142°C (Average of 4)
AGR 119-1	7178.2N 8544.6E	142.7°C (Average of 4)
AGR 119-2	7178.2N 8544.8E	140°C (Average of 6)
AGR 201-1	6998.2N 8968.4E	142°C (Average of 5)
AGR 201-2	7001.5N 8974.2E	145°C (Average of 4)
NE 105-1	6987.42N 8703.6E	-
AGR 89	7232.4N 8783.6E	-
v. Fluorite		
AGRF-1	6987.42N 8703.6E	143.7°C (Average of 30)
AGRF-2	6994.8N 8700.8E	142.9°C (Average of 11)
vi. Barite		
AGRB-1	7209.3N 8804.9E	138.1°C (Average of 9)
AGRB-2	7212.42N 8803.5E	137.25°C (Average of 6)

Table III-1 (Continued)

vii. Quartz veins in the basement

SAMPLE NUMBER	GRID REFERENCE	HOMOGENIZATION TEMPERATURE
AGRQ 201-1	6998.26N 8968.42E	250-306°C (Primary Inclusions)
AGRQ 201-2	6999.4N 8977.5E	220-227°C (Secondary Inclusions) -

C. Criteria for the Origin of Fluid Inclusions (modified from Roedder 1976).

Criteria for primary origin

1. Based on occurrence in a single crystal with or without evidence of direction of growth or growth zonation.
 - A. Occurrence as a single (or a small three-dimensional group) in an otherwise inclusion free crystal.
 - B. Large size relative to that of the enclosing crystal e.g. with a diameter >0.1 that of crystal, and particularly several of such inclusions.
 - C. Isolated occurrence, away from other inclusions, for a distance of >5 times the diameter of the inclusion.
 - D. Occurrence as part of a random, three dimensional distribution throughout the crystal.
 - E. Disturbance of otherwise regular decorated dislocations surrounding the inclusion, particularly if they appear to radiate from it.
 - F. Occurrence of daughter crystals (or accidental solid inclusion) of the same phase(s) as occur as solid inclusions in the host crystal or as contemporaneous phases.
2. Based on occurrence in a single crystal showing evidence of direction of growth.
 - A. Occurrence beyond (in the direction of growth), and sometimes immediately before extraneous solids (the same or other phases) interfering with the growth, where the host crystal fails to close completely. (Inclusion may be attached to the solid at some distance beyond, from imperfect growth.)
 - B. Occurrence beyond a healed crack in an earlier growth stage, where new crystal growth has been imperfect.

- C. Occurrence between subparallel units of a composite crystal.
 - D. Occurrence at the intersection of several growth spirals, or at the centre of a growth spiral visible on the outer surface.
 - E. Occurrence, particularly as relatively large, flat inclusions, parallel to an external crystal face, and near its centre (i.e. from "starvation" of the growth at the centre of the crystal face), e.g. much "hopper salt".
 - F. Occurrence in the core of a tubular crystal (e.g. beryl). This may be merely an extreme case of previous item.
 - G. Occurrence particularly as a row, along the edge from the intersection of two crystal faces.
3. Based on occurrence in a single crystal showing evidence of growth zonation (as determined by colour, clarity, composition, X ray darkening, trapped solid inclusion, etch zones, exsolution phases, etc.).
- A. Occurrence in random, three-dimensional distribution, with different concentrations in adjacent zones (as from a surge of sudden feathering or dendritic growth).
 - B. Occurrence as subparallel groups (outlining growth directions) particularly with different concentrations in adjacent growth zones, as in previous item.
 - C. Multiple occurrence in planar array(s) outlining a growth zone (Note that if this is also a cleavage direction, there is ambiguity).
4. Based on growth from a heterogeneous (i.e. two-phase) or a changing fluid.
- A. Planar arrays (as in 3-C), or other occurrence in growth zones in which the compositions of inclusions in adjacent zones are different (e.g. gas inclusions in one liquid in another, or oil and water).

- B. Planar arrays (as in 3-C), in which trapping of the growth medium has occurred at points where the host crystal has overgrown and surrounded adhering globules of the immiscible, dispersed phase (e.g., oil droplets or steam bubbles).
 - C. Otherwise primary-appearing inclusions of a fluid phase that is unlikely to be the mineral-forming fluid, e.g. mercury in calcite, oil in fluorite.
5. Based on occurrence in hosts other than single crystals.
- A. Occurrence on a compromise growth surface between two non parallel crystals. (These inclusions have generally leaked, and could also be secondary.)
 - B. Occurrence within polycrystalline hosts, e.g. as pores in fine grained dolomite, cavities within chalcedony-lined geodes ("enhydros"), vesicles in basalts, or as crystal-lined vugs in metal deposits or pegmatites. (These latter are among the largest "inclusions" and have almost always leaked.)
 - C. Occurrence in noncrystalline hosts (e.g., gas bubbles in amber; vesicles in pumice).
6. Based on inclusion shape or size.
- A. In a given sample, larger size and/or equant shape.
 - B. Negative crystal shape --- this is valid only on certain specific samples and is a negative criterion in others.
7. Based on occurrence in euhedral crystals, projecting into vugs (suggestive, but far from positive).

Criteria for secondary origin

- 1. Occurrence in planar groups outlining healed fractures (cleavage or otherwise) that come to the surface of the crystal (Note that

movement of inclusions with recrystallization can cause dispersion).

2. Very thin and flat; in process of necking down.
3. Primary inclusions with filling representative of secondary conditions
 - A. Located on secondary healed fracture, hence presumably refilled with later fluids.
 - B. Decrepitated and rehealed following exposure to higher temperatures or lower external pressures than at time of trapping; new refilling may have original composition but lower density.

Criteria for pseudosecondary origin.

1. Occurrence as with secondary inclusions, but with fracture visibly terminating within crystal.
2. Generally more apt to be equant and of negative crystal shape than secondary inclusions in the same sample (suggestive only).
3. Occurrence as a result of the covering of etch pits cross cutting growth zones.

APPENDIX IV
ISOTOPE CHEMISTRY

A. Sample Preparation for Sulfur Isotope Analysis.

Aim: To separate clean sulfur minerals for sulphur isotope analysis.

Procedure

About 0.5 kilogram of each sulfide containing sample was selected for crushing. The samples were crushed using hand comminution to less than 200 mesh. Each sample was classified on the 0.5 mm, 0.35 mm, 0.15 mm screens to optimize the grain sizes. Sieving was done for 15 minutes for each sample. The different sizes were then thoroughly washed with water to remove fines dispersed within them. After washing of the various sizes in acetone and subsequent drying, the powders were stored in clean vials. The most suitable size fraction for the sulfide separation is the sand size fraction (<0.35 mm and >0.15 mm).

The sand size fractions were separated into the sulfide and carbonate parts using the heavy liquid tetrabromoethene (density 2.96) and methylene iodide (density 3.32). The carbonate and other gangue minerals separated out as floats. The procedure of separation was carried out twice for adequate separation and the sulfide minerals were then filtered out and washed thoroughly with acetone. Each separate was dried completely and stored in clean vials. The purity of the sulfide separates was checked by X-ray diffraction.

B. Sample Preparation for Oxygen and Carbon Isotope Analysis.

Aim: To separate clean homogenous carbonate samples for oxygen and carbon isotope analysis.

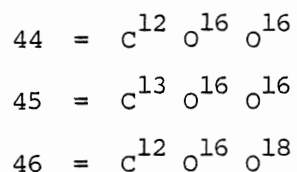
Procedure

Selected samples of dolomite and calcite were broken into pieces with a splitter. Each sample was examined with a binocular microscope. The dolomite host to sulfide mineralization was carefully examined to ascertain the degree of homogeneity. Where intergrowths of sparry calcite occur in dolomite, the calcite was carefully separated by handpicking. Most of the samples pulverised are either calcite or dolomite but not their mixtures. The samples were crushed to about less than 200 mesh using hand comminution. The crushed samples were classified on the .18 mm and .125 mm screens to optimize grain sizes. The different sizes were thoroughly washed with deionized water to remove fines dispersed within them. The most suitable size fraction for analysis is the sand size fraction (<.18 mm and >.125 mm). Where intergrowths of calcite and dolomite persist, calcite was separated in bromoform and dolomite was purified by leaching the calcite in diluted glacial acetic acid. The purity of all calcite and dolomite samples was checked by X-ray diffraction.

The clean samples were roasted at a temperature of 350°C to get rid of any organic matter contained in dolomite. About 0.9 to 1.8 milligrams of each carbonate sample was used in the mass spectrometric analysis.

C. Correction Factors for Oxygen and Carbon Isotope Analysis.

Mass ratios 45:44, and 46:44 were measured from the mass spectrometer where



Values of 45/44 and 46/44 measured from the mass spectrometer were converted

to δC^{13} and δO^{18} respectively using the correction factors of Craig (1957) as follows: $\delta C^{13} = 1.0673\delta_{45} - 0.03384$ where δC^{13} value is the measure of the carbon isotopic composition of the CO_2 with respect to the laboratory standard (δx -CM) which in this case is Carrara Marble.

Similarly,

$$\delta O^{18} = 1.001\delta_{46} - 0.0022\delta_{45} \text{ (with respect to Carrara Marble.)}$$

But
$$\delta O^{18}_{CM-PDB} = -1.19$$

$$\delta C^{13}_{CM-PDB} = +2.79$$

Therefore the values of δ relative to PDB (δ_{x-PDB}) will be

$$\delta_{x-PDB} = \delta_{x-CM} + \delta_{CM-PDB} + 10^{-3} \delta_{x-CM} \delta_{CM-PDB}$$

for the UQ2 standard.

$$\delta O^{18}_{UQ2-PDB} = -5.83$$

$$\delta C^{13}_{UQ2-PDB} = +1.91$$

D. Parameters and Equations Used in Lead Isotope Studies

If the earth is considered as a closed system for U, Th and Pb, one can describe, in a first approximation the evolution of common lead by the following equations:

$$\left(\frac{{}^{206}\text{Pb}}{{}^{204}\text{Pb}} \right)_t = \left(\frac{{}^{206}\text{Pb}}{{}^{204}\text{Pb}} \right)_o + \mu (e^{\lambda_8 T} - e^{-\lambda_8 T}) \quad (1)$$

$$\left(\frac{{}^{207}\text{Pb}}{{}^{204}\text{Pb}} \right)_t = \left(\frac{{}^{207}\text{Pb}}{{}^{204}\text{Pb}} \right)_o + \frac{\mu}{137.88} (e^{\lambda_5 T} - e^{-\lambda_5 T}) \quad (2)$$

$$\left(\frac{{}^{208}\text{Pb}}{{}^{204}\text{Pb}} \right)_t = \left(\frac{{}^{208}\text{Pb}}{{}^{204}\text{Pb}} \right)_o + W (e^{\lambda_2 T} - e^{-\lambda_2 T}) \quad (3)$$

Primordial lead isotopic ratios (Pb isotopic composition at time T) (Tatsunoto *et al.*, 1973):

$$\left(\frac{{}^{206}\text{Pb}}{{}^{204}\text{Pb}} \right)_o = 9.307 = a_o$$

$$\left(\frac{{}^{207}\text{Pb}}{{}^{204}\text{Pb}} \right)_o = 10.294 = b_o$$

$$\left(\frac{^{208}\text{Pb}}{^{204}\text{Pb}} \right)_0 = 29.476 = c_0$$

T = age of the Earth = 4.57 b.y. (Tilton, 1973)

$$\mu = \frac{^{238}\text{U}}{^{204}\text{Pb}}$$

$$W = \frac{^{232}\text{Th}}{^{204}\text{Pb}}$$

Present day $\frac{^{238}\text{U}}{^{235}\text{U}} = 137.88$ (Atomic Energy Commission, 1962).

Decay constants (Doe and Zartman, 1979)

$$\lambda_8 = 0.155125 \times 10^{-9} \text{ yr}^{-1}$$

$$\lambda_5 = 0.98485 \times 10^{-9} \text{ yr}^{-1}$$

$$\lambda_2 = 0.049475 \times 10^{-9} \text{ yr}^{-1}$$

Using equations (1) - (3) we could plot the growth of the lead isotope ratios with time for given values of μ and W . However, this procedure does not yield model ages from the measured isotopic ratio of, for instance, a galena, because we do not know the μ nor the W values in which the lead developed from time T until its separation from U and Th at time t .

Equations (1) and (2) contain as unknowns μ and t , and by dividing equation (2) by equation (1) it is possible to eliminate μ as follows:

$$\frac{^{207}\text{Pb}}{^{204}\text{Pb}}_t = b_0 + \frac{1}{137.88} \times \frac{e^{\lambda_5 T} - e^{\lambda_5 t}}{e^{\lambda_8 T} - e^{\lambda_8 t}} \times \frac{^{206}\text{Pb}}{^{204}\text{Pb}}_t - a_0$$

This equation of a straight line is the so called isochron. All the leads that evolved between T and t in reservoirs with different μ values will be on a $\frac{^{207}\text{Pb}}{^{204}\text{Pb}}$ versus $\frac{^{206}\text{Pb}}{^{204}\text{Pb}}$ plot, on a straight line passing through a_0 and b_0 .

Table IV-1 Sulfur Isotopic Composition of Sulfate and Sulfide Minerals

SAMPLE NUMBER	COORDINATES	MINERAL	DESCRIPTION	PARAGENETIC STAGE	$\delta^{34}\text{S}_{\text{CDT}} \text{‰}$
506-270	7693.40N 33626.8E	Anhydrite	Massive greyish blue anhydrite	Pre-ore	15.60
506-320	7693.40N 33636.8E	Anhydrite	Greyish blue anhydrite with relics of dolomite	Pre-ore	14.37
710-250	7743.5N 9531.0E	Anhydrite	Greyish blue anhydrite with relics of dolomite	Pre-ore	15.25
DW4-360	7123.6N 8482.8E	Anhydrite	Greyish blue anhydrite with relics of dolomite	Pre-ore	15.15
AGR 285-200	7245.25N 8691.98E	Anhydrite	Grey anhydrite	Pre-ore	9.6
DW4-405	7123.6N 8482.8E	Gypsum	Fibrous gypsum	Post-ore (hydration of pre-ore anhydrite)	15.79
AGR 117	7135.5N 8606.5E	Gypsum	Gypsum vein	Post-ore (hydration of pre-ore anhydrite)	13.3
AGR 118	7137.0N 8610.5E	Gypsum	Gypsum vein	Post-ore (hydration of pre-ore anhydrite)	14.4
AGR 119-1	7178.2N 8544.6E	Gypsum	Macrocrystalline selenite fibres in fractures	Post-ore	13.1
AGR 119-2	7178.2N 8544-8E	Gypsum	Macrocrystalline selenite fibres in fracture	Post-ore	16.5

Table IV-1 Continued

SAMPLE NUMBER	COORDINATES	MINERAL	DESCRIPTION	PARAGENETIC STAGE	$\delta^{34}\text{S}_{\text{CDT}}/\text{‰}$
AGRB-1	7209.3N 8804.9E	Barite	Platy barite crystals in fracture	Post-ore	14.1
AGRB-2	7212.42N 8803.5E	Barite	Blades of barite in fracture related cavity	Post-ore	14.1
AGR 1091-1a	6771.0N 8634.2E	Marcasite	Stratiform clots of marcasite	Pre-ore	10.7
AGR 1091-1b	6771.0N 8634.2E	Marcasite	Intergranular marcasite	Pre-ore	11.2
AGR 1091-1c	6771.0N 8634.6E	Marcasite	Stratiform marcasite	Pre-ore	13.27
AGR 69	7293.2N 8784.8E	Chalcopyrite	Chalcopyrite veinlet cross- cutting stratiform ore	Ore-stage	10.40
AGR 07	7274.88N 8788.02E	Galena	Coarse crystalline vein galena	Ore-stage	12.1
AGR 24B	7274.99N 8785.02E	Galena	Coarse crystalline vein galena	Ore-stage	10.8
AGR 38	7183.35N 8715.80E	Galena	Coarse crystalline vein galena	Ore-stage	11.5
AGR 40B	7183.4N 8716.4E	Galena	Finely crystalline galena- stratiform ore	Ore-stage	10.2
AGR 91	7240.9N 8790.24E	Galena	Coarse crystalline vein galena	Ore-stage	11.8
AGR 136B	7292.9N 8787.7E	Galena	Coarse crystalline vein galena	Ore-stage	10.7

Table IV-1 Continued

SAMPLE NUMBER	COORDINATES	MINERAL	DESCRIPTION	PARAGENETIC STAGE	$\delta^{34}\text{S}_{\text{CDT}}/\text{‰}$
AGR 167B	7257.56N 8804.76E	Galena	Coarse crystalline vein galena	Ore-stage	9.9
AGR 169B	7257.02N 8806.2E	Galena	Coarse crystalline vein galena	Ore-stage	10.7
AGR 170B	7256.78N 8806.84E	Galena	Coarse crystalline vein galena	Ore-stage	11.3
119-4	7192.4N 8546.2E	Galena	Coarse crystalline vein galena	Ore-stage	9.5
119-6	7190.0N 8546.2E	Galena	Finely crystalline stratiform galena	Ore-stage	10.6
119-7	7188.0N 8546.2E	Galena	Finely crystalline stratiform galena	Ore-stage	11.7
1090-1	6771.5N 8635.2E	Galena	Finely crystalline stratiform galena inter- bedded with dolomite	Ore-stage	10.1
1093-1	6772.5N 8635.6E	Galena	Finely crystalline stratiform galena	Ore-stage	9.4
413-342	6387.48N 7280.54E	Galena	Finely crystalline stratiform galena	Ore-stage	11.42
560-156	7494.24N 8760.59E	Galena	Finely crystalline stratiform galena	Ore-stage	11.54
AGR 24A	7274.88N 8785.02E	Sphalerite	Finely crystalline vein sphalerite	Ore-stage	10.6
104-Sub 1	7243.8N 8814.5E	Sphalerite	Finely crystalline vein sphalerite	Ore-stage	9.6

Table IV-1 Continued

SAMPLE NUMBER	COORDINATES	MINERAL	DESCRIPTION	PARAGENETIC STAGE	$\delta^{34}\text{S}_{\text{CDT}}\%$
AGR 134	7292.4N 8786.5E	Sphalerite	Finely crystalline vein sphalerite	Ore-stage	10.0
AGR 135	7292.7N 8787.0E	Sphalerite	Finely crystalline vein sphalerite	Ore-stage	8.0
AGR 136A	7292.9N 8787.7E	Sphalerite	Finely crystalline vein sphalerite	Ore-stage	10.1
AGR 141	7288.5N 8796.3E	Sphalerite	Finely crystalline vein sphalerite	Ore-stage	10.6
AGR 147	7202.5N 8803.4E	Sphalerite	Finely crystalline vein sphalerite	Ore-stage	10.7
AGR 167A	7257.56N 8804.76E	Sphalerite	Finely crystalline vein sphalerite	Ore-stage	10.5
AGR 168	7257.24N 8805.68E	Sphalerite	Finely crystalline vein sphalerite	Ore-stage	11.0
AGR 169A	7257.02N 8806.2E	Sphalerite	Finely crystalline vein sphalerite	Ore-stage	11.4
AGR 170A	7256.78N 8806.84E	Sphalerite	Finely crystalline vein sphalerite	Ore-stage	10.9
1093-3	6773.8N 8635.6E	Sphalerite	Finely crystalline pale yellow stratiform sphalerite	Ore-stage	8.7
379-498	7873.59N 33482.2E	Sphalerite	Finely crystalline stratiform sphalerite	Ore-stage	13.65
507-108	7743.60N 33527.5E	Sphalerite	Finely crystalline stratiform sphalerite	Ore-stage	12.35

Table IV-1 Continued

SAMPLE NUMBER	COORDINATES	MINERAL	DESCRIPTION	PARAGENETIC STAGE	$\delta^{34}\text{S}_{\text{CDT}}\text{‰}$
715-340	7543.00N 9607.60E	Sphalerite	Finely crystalline strati- form sphalerite	Ore-stage	13.39
AGRP-1a	7190.2N 8546.0E	Pyrite	Finely crystalline Pyrite in geopetal cavity	Post-ore	-45.9
AGRP-1b	7190.0N 8546.5E	Pyrite	Finely crystalline Strati- form pyrite lens	Post-ore	-46.0
AGRP-2a	7209.3N 8804.9E	Pyrite	Pyrite coatings on a fault plane within secondary limestone	Post-ore	-45.5
AGRP-2b	7212.42N 8803.5E	Pyrite	Finely crystalline pyrite coatings on clay gouge	Post-ore	-45.2
4490-3	7235.2N 8790.82E	Pyrite	Pyrite coatings on a clay filled fracture	Post-ore	-45.4
201-11	6998.2N 8968.4E	Marcasite	Finely crystalline over- growths on geopetal calcite	Post-ore	-42.9
201-12	7001.5N 8974.2E	Marcasite	Finely crystalline over- growths on calcite filled fracture	Post-ore	-9.7
201-13	7002.8N 8978.2E	Marcasite	Finely crystalline marcasite overgrowths on calcite filled fracture	Post-ore	-15.8

Table IV-1 Continued Sulfur Isotopic Composition of Selected Sulfide Minerals in the Lower Paleozoic Meguma Basement

SAMPLE NUMBER	LOCATION	MINERAL	DESCRIPTION	$\delta^{34}\text{S}_{\text{CDT}}/\text{‰}$
MS-1	Pyritic slate, 40 km NE of Gays River	Pyrite	Disseminated pyrite in slate	25.03
MS-2	Pyrrhotite bearing slate, 40 km NE of Gays River	Pyrrhotite	Interbedded streaks of finely crystalline pyrrhotite in slate	8.52
MS-3	Pyritic slate, 40 km NE of Gays River	Pyrite	Disseminated pyrite in slate	-0.63
MS-4	Pyritic slate, 40 km NE of Gays River	Pyrite	Disseminated pyrite in slate	19.43
MS-5	Mineralized slate, 40 km NE of Gays River	Sphalerite	Fracture filling sphalerite in slate	1.67
LHSP	Mineralized slate Lazy Head, N.S.	Sphalerite	Interbedded streaks of sphalerite in slate	16.84
LHPY	Mineralized slate Lazy Head, N.S.	Pyrite	Interbedded streaks of pyrite in slate	11.77

Table IV-2 Sulfur Isotopic Composition of Coexisting Sulfide Mineral Pairs

SAMPLE NUMBER	MINERAL	DESCRIPTION	$\delta^{34}\text{S}/\text{‰}$	$\Delta^{34}\text{S}/\text{‰}$	EQUILIBRATION* TEMPERATURE
AGR 24A	Sphalerite	Vein sphalerite	+ 10.6		
AGR 24B	Galena	Vein galena	+ 10.8	- 0.2	?
AGR 136A	Sphalerite	Vein sphalerite	+ 10.1		
AGR 136B	Galena	Vein galena	+ 10.7	- 0.6	?
AGR 167A	Sphalerite	Vein sphalerite	+ 10.5		
AGR 167B	Galena	Vein galena	+ 9.9	+ 0.6	> 650°C(?)
AGR 169A	Sphalerite	Vein sphalerite	+ 11.4		
AGR 169B	Galena	Vein galena	+ 10.7	+ 0.7	~ 650°C(?)
AGR 170A	Sphalerite	Vein sphalerite	+ 10.9		
AGR 170B	Galena	Vein galena	+ 11.3	- 0.4	?

* Equilibration temperature from Czamanske and Rye (1974).

NOTE: - The stratiform ore shows apparent textural disequilibrium and this compares with vein ore.

Table IV-3 Summary Comparison of the Sulfur Isotope Results

MINERAL	NUMBER OF SAMPLES	RANGE OF $\delta^{34}\text{S}/\text{‰}$	MEAN $\delta^{34}\text{S}/\text{‰}$	1 S.D.
Gypsum	5	+13.1 → +16.5	+ 14.62	±1.5
Anhydrite	5	+ 9.6 → +15.60	+ 14.00	±2.5
Barite	2	+14.1	+ 14.1	-
Early Marcasite	3	+10.7 → +13.27	+ 11.72	±1.36
Late Marcasite	3	- 9.7 → -42.9	- 22.8	±17.6
Late Pyrite	5	-45.2 → -46.0	- 45.6	±0.3
Stratiform Sphalerite	4	+ 8.7 → +13.65	+ 12.02	±2.3
Vein Sphalerite	11	+ 8.0 → +11.4	+ 10.31	±0.91
Stratiform Galena	8	+ 9.4 → +11.7	+ 10.79	±0.84
Vein Galena	9	+ 9.5 → +12.1	+ 10.92	±0.85

Table IV-4 Isotopic Composition of Carbon and Oxygen in the Unmineralized Limestone Fossils of
Mississippian Age.

SAMPLE NUMBER	LOCATION	DESCRIPTION	IDENTIFICATION	$\delta^{13}\text{C}_{\text{PDB}}\text{‰}$	$\delta^{18}\text{O}_{\text{SMOW}}\text{‰}$
S-001	Miller's Quarry	Brachiopod from the Miller limestone	<u>Composita windsorensis</u>	+ 3.61	+ 24.63
S-002	Miller's Quarry	Brachiopod from the Miller limestone	<u>Composita windsorensis</u>	+ 4.49	+ 24.49
S-003	Miller's Quarry	Brachiopod from the Miller limestone	<u>Dielasma davidsoni</u>	+ 4.55	+ 25.08
S-004	Miller's Quarry	Brachiopod from the Miller limestone	<u>Spirifena vernuili</u>	+ 4.20	+ 24.62
S-005	Miller's Quarry	Brachiopod from the Miller limestone	<u>Spirifena vernuili</u>	+ 4.47	+ 24.57
S-006	Miller's Quarry	Brachiopod from the Miller limestone	<u>Productus lyelli</u>	+ 4.47	+ 25.56
S-007	Miller's Quarry	Brachiopod from the Miller limestone	<u>Productus lyelli</u>	+ 4.38	+ 26.39
Range of $\delta^{18}\text{O}$		+24.49 to +26.39	Mean $\delta^{18}\text{O}_{\text{SMOW}}$	= 25.05 \pm .7 per mil	
Range of $\delta^{13}\text{C}$		+ 3.61 to + 4.55	Mean $\delta^{13}\text{C}_{\text{PDB}}$	= + 4.31 \pm .3 per mil	

Table IV-5a Isotopic Composition of Carbon and Oxygen in Host Rock, Ore Stage and Post Ore Carbonate, Gays River Mine.

SAMPLE NUMBER	COORDINATES	COMPOSITION	DESCRIPTION	PARAGENETIC STAGE	$\delta^{13}\text{C}_{\text{PDB}}\text{‰}$	$\delta^{18}\text{O}_{\text{SMOW}}\text{‰}$
AGR 137	7293.0N 8787.6E	Dolomite	Recrystallized micrite	Pre-ore	+ 1.23	+ 23.20
AGR 138	7292.4N 8788.3E	"	"	"	+ 0.5	+ 23.49
AGR 139	7287.0N 8793.0E	"	"	"	+ 1.63	+ 22.86
AGR 154	7290.2N 8791.1E	"	"	"	+ 0.69	+ 23.81
4470-1	7293.8N 8776.5E	"	"	"	+ 1.99	+ 24.82
AGR 131	7293.0N 8784.1E	Limestone	Recrystallized secondary limestone (Dedolomite)	Post-ore	- 1.34	+ 23.48
AGR 132	7293.0N 8784.5E	"	"	"	-1.78	+ 23.64
AGR 133a	7293.0N 8784.8E	"	Recrystallized limestone breccia	"	- 2.02	+ 23.5
AGR 133b	7293.0N 8785.3E	"	"	"	- 1.84	+ 23.49
AGR 140	7287.0N 8795.0E	"	Recrystallized breccia	"	- 1.34	+ 22.73
AGR 142	7287.9N 8797.2E	"	"	"	- 2.5	+ 23.70

Table IV-5a Continued

SAMPLE NUMBER	COORDINATES	COMPOSITION	DESCRIPTION	PARAGENETIC STAGE	$\delta^{13}\text{C}_{\text{PDB}}/\text{‰}$	$\delta^{18}\text{O}_{\text{SMOW}}/\text{‰}$
AGR 143	7288.8N 8797.7E	Limestone	Recrystallized breccia	Post-ore	- 2.96	+ 23.42
AGR 07	7274.88 8788.02E	Calcite	Vein calcite inter-grown with galena and sphalerite	Ore-stage	+ 2.22	+ 13.78
AGR 11	7290.28N 8785.02E	Calcite	Vein calcite inter-grown with galena	"	+ 2.24	+ 13.81
AGR 12	7284.64N 8786.4E	"	Vein calcite inter-grown with galena	"	+ 2.35	+ 14.24
AGR 13	7255.76N 8797.30E	"	Vein calcite inter-grown with galena and sphalerite	"	+ 2.96	+ 13.94
AGR 91	7240.9N 8790.24E	"	Vein calcite intergrown with galena and sphalerite	"	+ 2.40	+ 13.93
AGR 92	7235.4N 8793.2E	"	Vein calcite inter-grown with galena and sphalerite	"	+ 2.49	+ 13.96
AGR 93	7205.68N 8802.6E	"	Vein calcite inter-grown with galena and sphalerite	"	+ 2.34	+ 13.67
SPA 105-1	6987.42N 8703.6E	"	Vein calcite inter-grown with sphalerite	"	+ 3.12	+ 13.95
SPA 105-2	6994-82N 8703.8E	"	Vein calcite inter-grown with sphalerite	"	+ 2.71	+ 14.21

Table IV-5a Continued

SAMPLE NUMBER	COORDINATES	COMPOSITION	DESCRIPTION	PARAGENETIC STAGE	$^{13}\text{C}_{\text{PDB}}\text{‰}$	$^{18}\text{O}_{\text{SMOW}}\text{‰}$
SPA 105-3	6994.8N 8700.8E	Calcite	Vein calcite inter-grown with sphalerite	Ore-stage	+ 3.12	+ 14.19
AGR 29	7006.82N 8734.8E	"	Geopetal cavity filling sparry calcite	Post-ore	- 1.39	+ 19.61
AGR 109-1	6771.8N 8635.2E	"	Vein calcite not associated with sulfides	"	+ 1.58	+ 17.91
AGR 119-1	7178.2N 8544.6E	"	Vuggy calcite overgrowths on galena	"	- 3.85	+ 18.92
AGR 119-2	7178.2N 8544.8E	"	Vuggy calcite overgrowths on galena	"	+ 0.64	+ 14.28
AGR 201-1	6998.2N 8968.4E	"	Vuggy calcite in fracture related cavity	"	- 3.1	+ 22.34
AGR 201-2	7001.5N 8974.2E	"	Vuggy calcite in fracture related cavity	"	- 5.68	+ 20.99
NE 105-1	6987.42N 8703.6E	"	Encrusting scalenohedral calcite in vugs	"	- 0.29	+ 24.10
AGR 89	7232.4N 8783.6E	"	Encrusting scalenohedral calcite on dolomite pebble.	"	- 0.7	+ 24.31

Table IV-5b Summary Comparison of the $\delta^{18}\text{O}$ and $\delta^{13}\text{C}$ Values in the Host Rock, Ore Stage, Post Ore Carbonates and Unmineralized Limestone

DESCRIPTION	NUMBER OF SAMPLES	RANGE OF $\delta^{18}\text{O}$		RANGE OF $\delta^{13}\text{C}$	
		VALUES	MEAN AND 1 S.D.	VALUES	MEAN AND 1 S.D.
Recrystallized host dolomite	5	+22.86 to +24.82	$\bar{x} = 23.63 \pm .74$	+0.5 to +1.99	$\bar{x} = +1.2 \pm 0.62$
Recrystallized limestone (dedolomite)	7	+22.73 to +23.70	$\bar{x} = +23.42 \pm .32$	-2.96 to -1.34	$\bar{x} = -1.96 \pm 0.59$
Ore-stage calcite	10	+13.67 to +14.24	$\bar{x} = +13.97 \pm .19$	+2.22 to +3.12	$\bar{x} = +2.59 \pm 0.35$
Post ore rhombohedral calcite	6	+14.28 to +22.34	$\bar{x} = +19.0 \pm 2.79$	-5.68 to +1.58	$\bar{x} = -1.96 \pm 2.74$
Post ore scalenohedral calcite	2	+24.10 to +24.31	$\bar{x} = +24.20 \pm .15$	-0.7 to -0.29	$\bar{x} = -0.49 \pm .28$
Unmineralized limestone	7	+24.49 to +26.39	$\bar{x} = 25.05 \pm .7$	+3.61 to +4.55	$\bar{x} = +4.31 \pm .3$

APPENDIX V

CALCULATION OF GAINS AND LOSSES IN THE BASEMENT ALTERATION ZONES

A comparison of the whole rock chemical composition of the fresh and the altered quartz metawacke rocks was made in order to check the effect of the mineralogical changes on the chemical composition of the two groups of rocks. This comparison was based on the average of 10 whole rock analyses of the fresh quartz metawacke and 25 analyses of the altered equivalent (Table 7.1). Although a number of deductions can be made from the comparison of the weight of the oxides of the two groups of rocks with regards to gains and losses, such deductions may be inaccurate because the mass of rock remains constant. Without an independent evidence of the change in mass or volume of rock during alteration, this comparison may be difficult. As an alternative method, an assumption was made that alumina has not changed considerably during the alteration process (Krauskopf, 1979). The average analysis of the fresh and altered quartz metawacke (in atomic percent) was recalculated to 100.00 and the changes in the rock composition were based on 100 gm of fresh rock as described by Krauskopf (1979). The original value of alumina remains constant and the composition of the altered rock was normalized using the ratio of alumina values as given in Table V-1. The decrease (or increase) in each constituent was found by subtracting the normalized values from those of the fresh quartz metawacke (treating the fresh rock as grams per 100 gms rather than percent).

Table V-1 Whole Rock Analysis - Fresh Quartz Metawacke; 101-1 to 715-355
 - Altered Quartz Metawacke; 101-31 to 107 sub3

	101-1	101-3	101-4	101-5	101-30	379-510	507-327
SiO ₂	69.26	64.61	65.61	73.93	64.73	84.6	73.41
Al ₂ O ₃	16.91	18.49	17.27	12.98	18.82	8.57	13.86
TiO ₂	0.85	0.88	0.76	0.62	0.86	0.44	0.66
FeO	3.54	4.97	4.21	2.46	5.4	1.9	3.37
MgO	2.1	2.78	2.27	1.68	2.41	0.49	1.03
MnO	0.0	0.05	0.05	0.13	0.06	0.04	0.03
CaO	0.4	0.45	0.46	0.61	0.66	0.38	0.57
Na ₂ O	3.11	3.61	3.60	2.83	2.95	1.20	2.53
K ₂ O	3.81	3.55	3.45	2.59	3.59	1.17	2.66
P ₂ O ₅	0.0	0.14	0.09	0.16	0.09	-	0.05
H ₂ O ⁺	-	-	1.75	1.66	-	0.08	1.28
H ₂ O	-	-	0.27	0.29	-	0.1	0.11
S	0.15	0.23	0.16	-	0.14	0.30	0.42
TOTAL	100.13	99.76	99.95	99.94	99.71	99.99	99.98
No. of Analyses	4	5	5	5	6	4	5
Rb ppm	117	100	104.5	96.5	89.0	49	86
Sr	102	119	114.5	114.5	96	66	144
Ba	562	617	596	528	647	213	568
Cu	10	3	10	16	12	10	16
Co	22	26	26	26	17	37	38
Ni	25	30	33	31	29	15	24

Table V-1 Continued

	560-170	561-223	715-355	RHYOLITE STD	101-31	101-33	101-34
SiO ₂	70.57	72.6	76.1	76.71	65.29	60.42	65.17
Al ₂ O ₃	14.95	14.86	12.99	12.06	20.53	21.11	19.11
TiO ₂	0.54	0.55	0.58	-	0.96	1.01	0.96
FeO	3.37	3.08	2.42	1.23	5.98	6.64	5.82
MgO	1.71	0.85	0.74	-	2.21	3.01	2.46
MnO	0.09	0.03	0.02	-	0.16	0.14	0.06
CaO	0.37	0.50	0.26	0.50	2.25	1.1	2.23
Na ₂ O	2.55	2.92	2.25	3.75	-	2.11	0.05
K ₂ O	2.95	2.96	2.83	4.89	2.06	3.32	3.34
P ₂ O ₅	0.08	0.02	0.02	-	0.15	0.26	0.19
H ₂ O ⁺	1.98	1.01	0.87	-	-	-	-
H ₂ O	0.45	0.12	0.34	-	-	-	-
S	0.33	0.43	0.49	-	0.20	0.54	0.46
TOTAL	99.94	99.93	99.65	99.14	99.79	99.66	99.85
No. of Analyses	4	6	6	5	5	5	4
Rb ppm	95	79	48		62	88	81
Sr	91	116	66		28	71	39
Ba	493	532	561		477	662	594
Cu	14	22	12		10	77	24
Co	26	27	34		14	29	21
Ni	25	18	26		23	37	34

Table V-1 Continued

	101-35	107-1	107-2	107-3	107-4	107-5	107-6
SiO	64.90	69.65	69.12	78.49	74.28	77.5	71.03
Al ₂ O ₃	19.73	16.53	17.03	12.18	12.85	12.67	12.10
TiO ₂	1.02	0.72	0.7	0.34	0.58	0.53	0.56
FeO	5.49	4.20	4.1	2.65	2.83	2.3	2.87
MgO	2.48	1.46	1.75	0.82	0.82	0.62	0.84
MnO	0.08	0.01	0.04	0.03	0.09	0.03	0.11
CaO	0.92	1.28	1.14	0.90	2.29	1.33	6.34
Na ₂ O	1.24	2.56	3.04	1.84	3.41	1.82	2.72
K ₂ O	3.60	2.93	2.74	2.21	2.44	2.84	2.50
P ₂ O ₅	0.15	0.07	0.04	0.04	0.04	-	0.08
H ₂ O ⁺	-	-	-	-	-	-	-
H ₂ O	-	-	-	-	-	-	-
S	0.34	0.32	0.40	0.23	0.53	0.1	0.20
TOTAL	99.95	99.73	100.1	99.73	100.16	99.74	99.35
No. of Analyses	5	4	5	4	5	4	4
Rb	87	63.5	61	57	63	56	63
Sr	60	107.5	122.5	103	183	133	251
Ba	670	698	663	635	709	698	604
Cu	53	17	16	14	13	13	37
Co	21	23	15	14	25	16	20
Ni	36	21	19	22	22	18	21

Table V-1 Continued

	107-7	107-8	107-9	107-10	107-11	107-12	107-13
SiO	71.26	75.11	72.09	73.56	71.23	69.62	70.73
Al ₂ O ₃	14.81	12.89	14.02	13.67	15.46	16.41	15.04
TiO ₂	0.71	0.46	0.64	0.62	0.63	0.76	0.50
FeO	3.56	2.98	3.5	3.04	3.83	3.96	3.49
MgO	1.04	0.90	0.99	0.98	1.18	1.31	1.51
MnO	0.04	0.07	-	0.06	0.05	0.05	0.06
CaO	1.86	1.06	1.35	3.23	1.56	1.89	0.79
Na ₂ O	3.3	3.37	3.45	1.86	2.54	2.41	1.94
K ₂ O	2.82	2.77	2.88	2.4	2.4	2.86	3.35
P ₂ O ₅	-	-	0.17	0.02	0.03	0.12	-
H ₂ O ⁺	-	-	-	-	-	-	1.75
H ₂ O	-	-	-	-	-	-	0.31
S	0.45	0.1	0.74	0.24	0.61	0.31	0.31
TOTAL	99.85	99.72	99.83	99.68	99.52	99.69	99.78
No. of Analyses	4	4	4	4	6	5	5
Rb	64	64	60	53	59	56	76
Sr	187	195	180	96	142	103	63
Ba	649	634	615	658	655	656	653
Cu	6	5	7	5	5	3	11
Co	16	18	18	11	11	11	10
Ni	11	14	12	8	10	8	9

Table V-1 Continued

	107-14	107-15	107-16	107-17	107-18	107 Sub-1	107 Sub-2	107 Sub-3
SiO	71.1	72.38	75.09	72.54	73.15	75.43	73.97	72.08
Al ₂ O ₃	15.3	14.8	13.6	16.04	14.42	13.84	14.63	15.46
TiO ₂	0.49	0.49	0.57	0.64	0.51	0.55	0.60	0.58
FeO	3.42	3.44	3.28	3.65	3.58	2.66	3.74	3.68
MgO	1.42	1.36	1.07	1.40	1.01	1.41	1.06	1.15
MnO	0.02	0.02	0.04	0.02	0.08	0.11	0.04	0.06
CaO	1.03	0.38	0.67	0.76	1.88	2.39	2.28	2.69
Na ₂ O	1.57	2.40	2.08	1.63	1.73	1.14	0.84	0.76
K ₂ O	2.92	2.65	2.73	3.09	2.51	2.62	2.35	2.48
P ₂ O ₅	0.06	0.13	0.04	-	0.18	0.05	-	0.10
H ₂ O ⁺	1.87	1.38	-	-	-	-	-	-
H ₂ O	0.34	0.19	-	-	-	-	-	-
S	0.30	0.30	0.60	0.37	0.18	-	0.28	0.10
TOTAL	99.84	99.72	99.77	100.14	99.32	100.20	99.79	99.42
No. of Analyses	6	5	4	4	6	5	5	4
Rb	76	74	74	74	51	61	53	56
Sr	55	86	78	56	110	55	83	74
Ba	628	645	665	653	639	648	637	663
Cu	5	10	3	21	5	4	6	5
Co	11	11	19	9	12	15	19	14
Ni	11	11	11	11	10	11	11	12

Table V-2 Element Gain and Losses in the Altered Quartz Metawacke

	*Fresh Metawacke At. %	**Altered Meta- wacke At. %	Altered Metawacke Recalculated	Gains and Losses	% Gains and Losses	Log Values
Si	66.11	65.32	64.27	-1.84	-2.8	-0.45
Al	15.30	15.55	15.30	-	-	-
Ti	0.78	0.76	9.75	-0.03	-3.8	-0.58
Fe	5.25	5.68	5.59	+0.34	+6.5	+0.81
Mg	1.91	1.60	1.57	-0.34	-17.8	-1.25
Mn	0.08	0.09	0.09	+0.01	-12.5	+1.1
Ca	0.65	2.41	2.37	+1.72	+265.0	+2.4
Na	4.01	2.86	2.81	-1.20	-29.9	-1.5
K	4.83	4.44	4.37	-0.46	-9.5	-1.0
P	0.06	0.08	0.08	+0.02	+33.3	+1.5
H	0.33	0.35	0.34	+0.01	+3.03	+0.5
S	0.51	0.68	0.67	+0.16	+31.4	+1.5
Rb	0.02	0.01	0.01	-0.01	-50.0	-1.7
Sr	0.019	0.02	0.02	+0.001	+5.3	+0.7
Ba	0.09	0.12	0.12	+0.03	+33.33	+1.5
Cu	0.002	0.003	0.003	+0.001	+50.0	+1.69

* Average of 10 fresh metawacke samples

** Average of 25 altered metawacke samples

APPENDIX VI

COMPARISON OF THE GAYS RIVER DEPOSIT WITH TYNAGH, PINE POINT
AND THE BUICK MINE

A. Tynagh Deposit.

i. Geological Setting

The Tynagh ore bodies occur within the Lower Carboniferous limestone in the west of the central plain of Ireland. The older Lower Paleozoic sediments were folded during the Caledonian orogeny and were subsequently eroded and covered by the Old red sandstone sediments (Fig. VI-1). Uplifted blocks of the Lower Carboniferous sediments form paleotopographic highs in the transgressive seas of the Lower Carboniferous. The flanks of these highs were favourable for the development of carbonate mudbank complexes or Waulsortian reefs which attain a maximum thickness of about 1000 metres (Morrissey et al., 1971). The process of mud accumulation was accompanied by volcanic activity associated with submarine slumping along the flanks of the mudbanks. The Waulsortian mud banks are hosts for the significant polymetallic mineralization at Tynagh.

The most important structure in the mine area is the North Tynagh fault with an E-W strike. The fault dips 60-65°N in the centre of the mine but dips become flattened eastwards (Fig. VI-2). The North Tynagh fault was probably initiated during the pre Carboniferous times and reactivated during the Carboniferous (Derry et al., 1965). Thinning of some of the Carboniferous sediments against the fault and the presence of slump breccias in the bank limestone suggests that this fault was active during sedimentation.

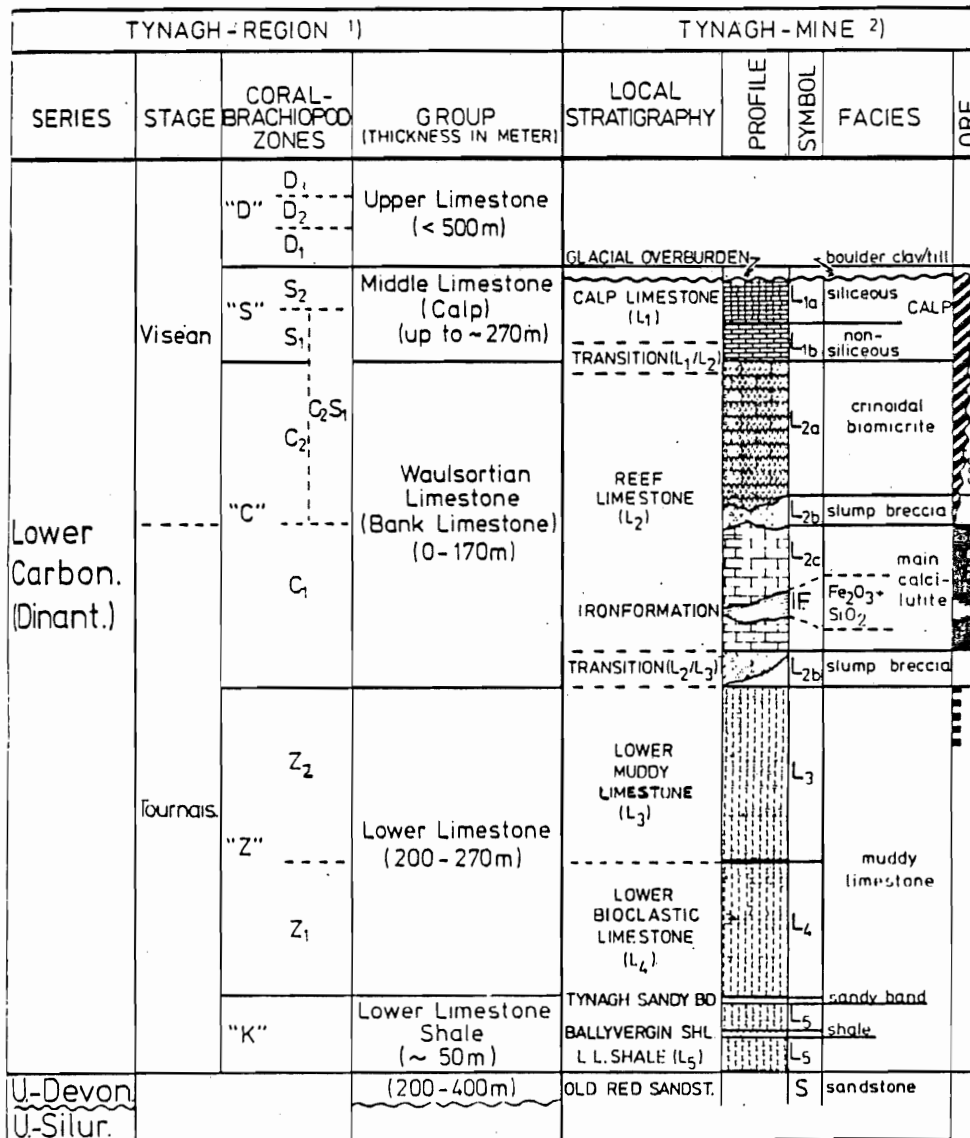


Figure VI-1 Regional and local stratigraphy at Tynagh. From Riedel (1980).

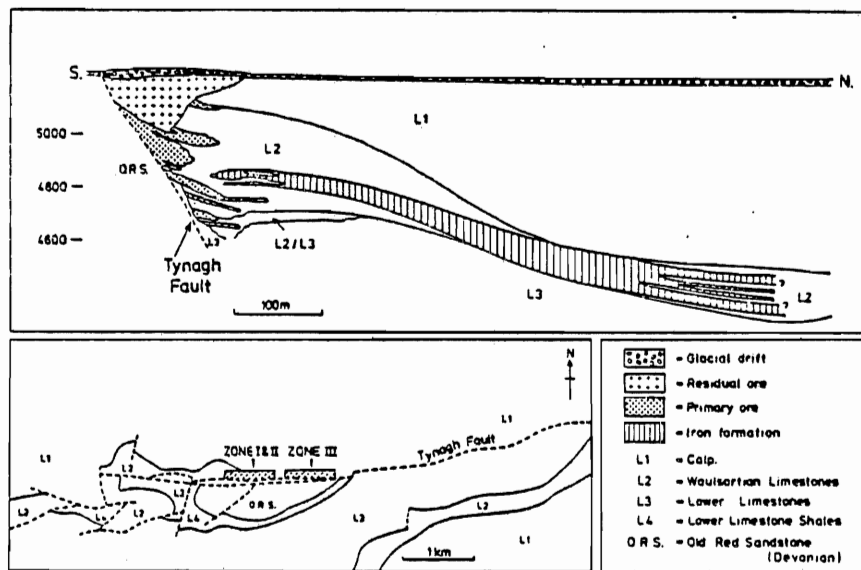


Figure VI-2 Geologic cross section of the Tynagh deposit. From Boast et al. (1981).

ii. Ore Bodies

Two main types of ores are present at Tynagh: 1) primary ore and 2) secondary ore. Both primary and secondary ores occur in the hanging wall of the Tynagh fault. The ore bodies have been subdivided into Zone I, II and III (Fig. VI-2). Zone I consists of near surface secondary ore body which passes through a transition zone into the primary zone II ore body. The zone II and zone III ore body are separated by a zone of intense dolomitization. The zone I ore body is generally irregular, have sharp contacts with wall rocks and variable grades. The zone II ore commonly occur near to the fault and are generally massive. This ore body is banded and regular with gradational boundaries with the wall rocks. Bands of mineralization in the zone II ore body commonly pass into veins and breccia matrix complex. Textures in the zone III ore body are identical to the zone II ore and the banded ore in the zone III are generally parallel to bedding. In general, the attitude of thicker mineralized bands steepens gradually towards the fault and become parallel to the fault plane. There is a concomitant increase in breccia textures adjacent to faults. Vein type barite, pyrite and copper sulphide mineralization are common adjacent to the Tynagh fault. To the north of the Tynagh fault, the Waulsortian hosts interdigitate with a sedimentary iron formation consisting essentially of finely banded hematite and chert with intercalated crinoidal limestone and thin tuffaceous beds (Derry et al, 1965; Schultz, 1966a). The minerals of main economic importance are sphalerite, galena and tennantite while barite comprises the major gangue. Marcasite, chalcopyrite, arsenopyrite and tetrahedrite are minor.

Lead isotope ratios in galena, plot close to the growth curve and are

normal (Greig et al.,1971). The sulfur isotopic ratio in the ore body exhibit a broad range indicating biogenic and deep seated components (Boast et al.,1981). The oxygen and carbon isotopic composition of the carbonate host are lowered during ore deposition (Boast et al.,1981).

iii. Thoughts on Origin

Several authors have postulated numerous theories to explain the genesis of the Tynagh ore bodies. Although the zone I secondary ore body could be regarded as products of Tertiary deep weathering, the origin of the primary ores in the zone II and III have been controversial. The association of these ores with the synsedimentary banded iron formation led Derry et al. (1965) to the conclusion that the base metal mineralization was contemporaneous with the deposition of the host Waulsortian carbonate. Schultz (1966) considered the association between the iron formation and the sulfide deposit to be coincidental and explained that the Tynagh ore body is of hydrothermal epigenetic origin. This was supported by the occurrence of the sulfide mineralization as cavity fillings, replacements and veins.

More recently, the stratiform concordant nature of the primary ore body, association with submarine debris flow and synsedimentary iron formation, in a boiling environment, elicited theories suggesting the derivation of the ore solutions from convective circulation of modified saline water (Russell 1978, 1981). This author proposed that the ore body is synsedimentary and was fed by downward excavating convective cells driven by high geothermal gradients to basement depths. A similar process was suggested for the genesis of sediment hosted exhalative zinc-lead deposits (Russell, 1981).

B. Pine Point Lead-Zinc District.

i. Geological Setting

The geology in the Pine Point area is dominated by the Pine Point and Presquile dolostones which forms a part of a carbonate barrier complex marginal to a major cratonic basin (Fig. 9.3). The Pine Point barrier reef was initiated during the early to Mid Devonian as a result of the formation of a scarp or a gentle warping of the underlying open marine Keg River platform possibly controlled by movements along basement faults (Skall 1977) (Fig. VI-3). The barrier complex developed along tectonic hinge zones separating the Elk Point evaporite to the south and the Mackenzie shale basin to the north. Several depositional environments ranging from the fore reef, reef and back reef facies developed along the Presquile barrier (Fig. VI-4).

ii. Pine Point Ore Bodies

The Pine Point ore bodies lie within the Middle Devonian Presquile and Pine Point Formations. The district consists of about 50 known lead-zinc sulfide ore bodies in an area of 100 km² (Kyle, 1981). The ore bodies vary in size, geometry, metal percentages and ratios, sulfide textures and host rock relationships. Tonnages in the separate ore bodies range from 100,000 to 15 million tons. The ore bodies are generally flat lying, stratabound and occur in several stratigraphic positions in the 200 m section of the barrier complex (Fig. VI-5). The ore consists of sphalerite, galena, pyrite and marcasite within a non metallic gangue of dolomite and calcite. Other constituents in the host rocks include minor amounts of pyrrhotite, celestite, barite, gypsum, anhydrite, fluorite, sulfur and bitumen. The majority of the ore was deposited in open cavities and vugs,

AGE	STRATIGRAPHY	FORMATION	THICKNESS (meters)	DESCRIPTION	MINERALIZATION
U. DEVONIAN (Frasnian)		HAY RIVER		Calcareous shale, minor limestone	
		SLAVE POINT	50-70	Argillaceous limestone, minor dolostone, calcareous mudstone	
M. DEVONIAN (Givellian)		WATT MOUNTAIN	15-45	Limestone and dolostone, waxy green mudstone interbeds	
		PINE POINT GROUP	75-150	Upper — Limestone of reefal and associated depositional facies; extensive coarse-crystalline dolostone (Presqu'île); transitional into calcareous shale (Buffalo River Fm.) to NW Lower — Fine-crystalline dolostones of reefal and associated depositional facies; transitional into bituminous limestone to NW and evaporites (Muskeg Fm.) to SE	
		KEG RIVER	65-75	Argillaceous dolostone and limestone	
M. DEVONIAN (Eifelian)		CHINCHAGA	90-110	Anhydrite and gypsum, minor dolostone, limestone, and mudstone	
ORDOVICIAN or older		MIRAGE POINT	60-90	Dolostone, mudstone, siltstone, anhydrite, and gypsum	
PRECAMBRIAN		OLD FORT ISLAND	0-30	Friable, fine to medium-grained sandstone	
				Micaceous quartzite and granodiorite?	

Figure VI-3 Stratigraphic column of Paleozoic Formations, southern Great Slave Lake area. From Kyle (1981).

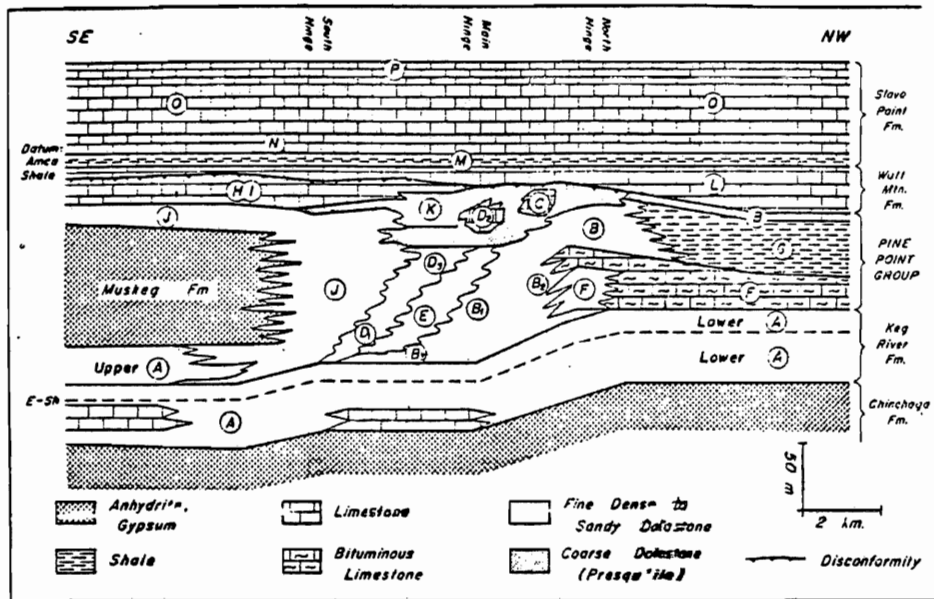


Figure VI-4 Generalized Middle Devonian stratigraphic relationships, Pine Point mining district. From Kyle (1981).

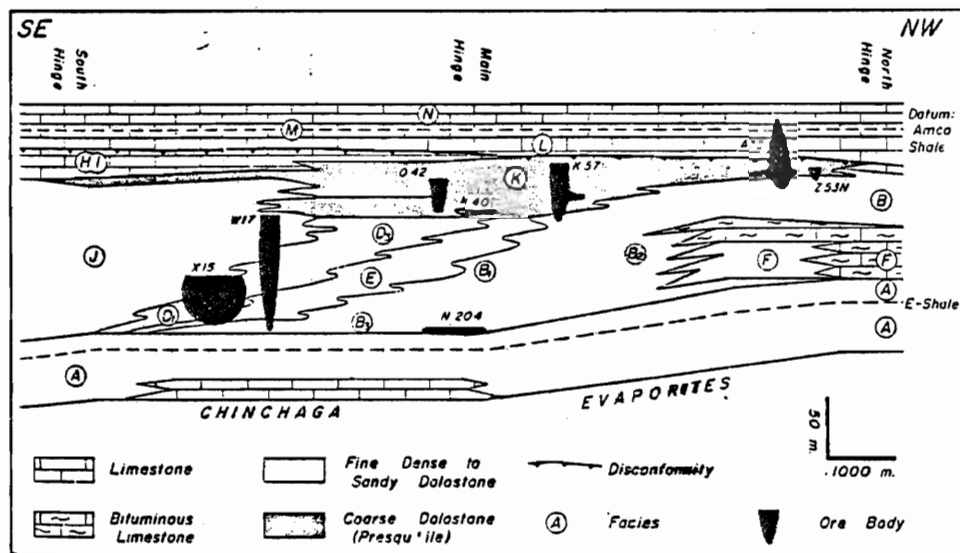


Figure VI-5 Cross-section of the Pine Point barrier complex showing stratigraphic positions of selected ore bodies. (From Kyle, 1981).

but some replacements are common. The most common sulfide mineral is sphalerite and it occurs as individual tetrahedral crystals, colloform and banded crusts, ramose and dendritic forms and as intimate intergrowths with other sulfide minerals (Kyle, 1981).

Homogenization temperatures of primary fluid inclusions in sphalerite range from 50-100°C (Roedder 1968, Kyle, 1977). The freezing temperatures indicate that the ore solutions were highly saline and range from about 15 to over 23% total dissolved salts of probably NaCl composition.

Lead in galena of the Pine Point ore are normal with an average of $^{206}\text{Pb}/^{204}\text{Pb}$ of +18.2 (Cumming and Robertson 1969). The lead is not the anomalous "J" type lead in the classic lead-zinc districts of the mid continent. Sulfur isotope values for the sulfide ore bodies are heavy, have a narrow range, with an average of +20.1 ‰. (Sasaki and Krouse 1969). This compares with the values of +19 to +20 ‰ of the Middle Devonian evaporites.

iii. Thoughts on Origin

The Pine Point lead-zinc district was originally used by Beales and Jackson (1966), Jackson and Beales (1967) for the basinal evolution model of genesis for Mississippi Valley Type deposits. This model suggests shale dewatering as the metal source and a sulfide precipitation process involving the mixing of metals released from shale with H_2S in formation waters. The model has pointed to the epigenetic nature of the deposit and has been widely applied to explain the origin of other carbonate hosted Mississippi Valley Type deposits. Kyle (1977, 1981) suggests that the prevailing association of the Pine Point ore bodies with carbonate host and evaporite and the potential of these lithologies as metal sources warrants the consider-

ation of multiple phases of metal derivation. Kyle (1981) proposed that the exhalative supply of metals to the sea floor along the N65°E hinge zones may have resulted in the metal concentration in shales, carbonates and evaporite.

C. Buick Mine

i. Geological Setting

A period of basement subsidence, uplift and erosion during the Early Cambrian to Late Cambrian in the mid continent region of North America, led to the development of major arches such as the Wisconsin Dome, Cincinnati arch and the Ozark uplift (Snyder, 1968). This was followed by periods of active deposition of the Upper Cambrian sediments. The Cambrian section includes transgressive and regressive elements comprising dominantly of carbonate and detrital facies (Howe et al., 1972). This Upper Cambrian series in the region of the St. Francois Mountains comprises six formation which in ascending order are: the Lamotte sandstone, The Bonneterre Formation, The Davis Formation and Derby Doerum Dolomite, the Potosi Dolomite and the Eminence Dolomite (Fig. VI-6). Carbonate facies dominate the lithologies above the Lamotte sandstone (Thacker and Anderson 1977).

At the Buick mine, the dominant lithology is the Upper Cambrian Bonneterre Formation. This Formation is a dolomitized limestone about 305 feet thick in the mine area. It lies unconformably on the Lamotte sandstone and it is overlain conformably by the Davis shale. The Upper third of the Bonneterre is shelf facies carbonate sand and the lower two thirds of the Bonneterre consists of three carbonate facies: 1) the fore reef, 2) the reef and 3) the back reef (Roger and Davis 1977). These facies

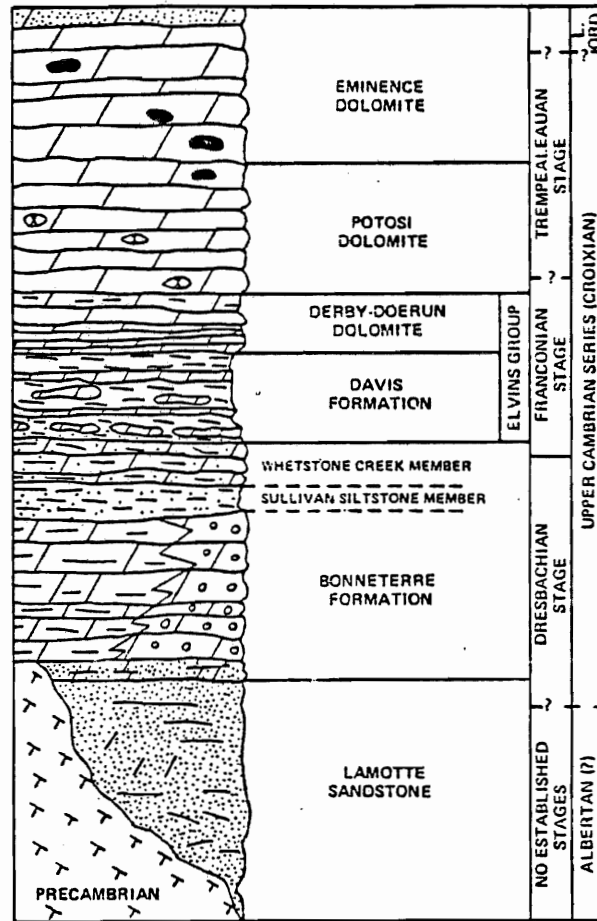


Figure VI-6 Composite stratigraphic column of Upper Cambrian in southeastern Missouri. From Thacker and Anderson, (1977).

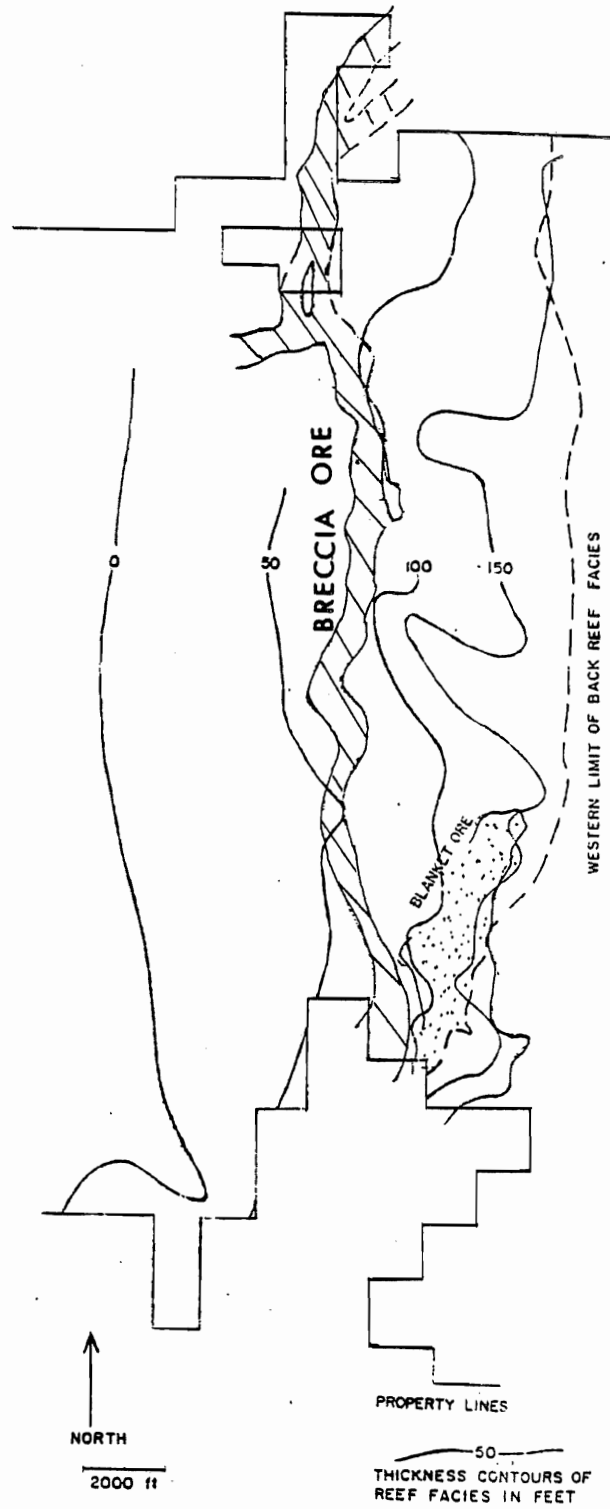


Figure VI-7 Distribution of ore bodies in the Buick deposit. (From Rogers and Davis, 1977).

rest on a north-south ridge of the Lamotte sandstone in the mine area.

ii. Ore Bodies

The ore bodies at the Buick mine occur dominantly in solution-induced collapse breccia of the Bonneterre Formation which forms a narrow sinuous continuous body in a north south orientation (Fig. VI-7). Apart from the breccia ore, a thin blanket ore body occurs in association with a buried Pre Cambrian knob in the south east corner of the Buick Property (Fig. VI-7). Open space fillings are common in the upper third of the breccia ore whereas replacements dominate the lower two thirds. The breccia ore is essentially subparallel, and fracture bounded (Fig. VI-7). Well mineralized inward dipping slump breccias are present along the boundary in some areas, although undisturbed, unmineralized beds are present elsewhere at the fracture boundary.

The ore minerals in the mine include galena, sphalerite, and chalcopyrite. Other sulfides present are pyrite, marcasite, siegenite, polydymite, bravoite, vaesite and traces of bornite and arsenopyrite. Gangue minerals in the ore zone are dolomite, calcite, quartz, kaolinite and dickite.

Fluid inclusion data in the Buick mine and the Virburnum trend in general range from 105° to 141°C with a maximum likely pressure of about 125 bars (Sverjensky 1981). Ore solutions are believed to contain about 4 to 5 molal chloride ion.

The sulfur isotopic composition of galena and sphalerite are heavy within a broad range. Interestingly, a correlation exists with isotopically lighter sulfur and more radiogenic lead in the galena. This suggests that sulfur and lead were transported together in the same solution (Sverjensky 1981).

iii. Thoughts on Origin

The genesis of the lead-zinc ore bodies in the South east Missouri district has been a subject of controversy especially with regards to the source, transportation and deposition of the sulfide minerals. Doe and Delevaux (1972) concluded from a lead isotopic study of ore and possible source rocks in the district that the Upper Cambrian Lamotte sandstone which underlie the Bonneterre dolomite could have been the source of the lead in the ore bodies. The correlation of isotopically lighter sulfur with more radiogenic lead in the late cubic galena of the Buick mine led Sverjensky et al. (1979, 1981) to conclude that the mineralization history appears too complex to be compatible with the simple model of deriving the metal solely from the Lamotte sandstone as suggested by Doe and Delevaux (1972). Sverjensky et al. (1979) argue that if both radiogenic and non-radiogenic mineral phases are present in the Lamotte sandstone, the more radiogenic lead should be leached first by the ore solution. Sverjensky (1981) proposed a reduced sulfur model to explain the precipitation of the sulphide ores. This involves the transportation of base metal from many sources and reduced sulfur in the same solution to the sites of precipitation in contrast to the mixing process involving a solution transporting lead and another carrying sulfur (Jackson and Beales 1967, Anderson 1975). The cause of sulfide precipitation was probably due to pH increase, cooling or dilution of the highly saline hydrothermal brines in the solution collapse breccia (Sverjensky, 1981).

VITA

NAME: Samuel Olusegun Akande

PLACE OF BIRTH: Lanlate, Oyo State, Nigeria

YEAR OF BIRTH: 1950

POST-SECONDARY EDUCATION AND DEGREES: University of Ibadan, Ibadan, Nigeria.
1970-1973 - B.Sc. (Hons).
University of Western Ontario, London, Ontario, Canada.
1975-1977 - M.Sc.
Dalhousie University, Halifax, Canada.
1979-1982 - Ph.D.

HONOURS AND AWARDS: Federal Republic of Nigeria, Graduate Fellowship, 1975.
Ogun State of Nigeria, Scholarship, 1979.
Federal Republic of Nigeria Scholarship, Overseas Award, 1980.

RELATED WORK EXPERIENCE: Geologist - Geological Survey of Nigeria, 1973-1975.
Assistant Lecturer - University of Ilorin, Nigeria, 1977-1979.
Geologist - Newmont Exploration of Canada Limited, 1979.
Geologist - Canada Wide Mines Limited, 1980.

PUBLICATIONS:

Akande, S.O. (1982). Mineralogy and Genesis of Three Vein Systems, Ross Mine, Holtyre, Ontario, Canada: Can. Inst. Min. Metall. special volume 24, pp. 94-97.

Akande, S.O. and Zentilli, M. (1982). The geology of the Gays River lead-zinc deposit, Nova Scotia, Canada, Conference Volume, Int. Conf. on Mississippi Valley Type deposits, Paper accepted (in press).

Akande, S.O. (1981). Stratiform and vein lead-zinc ores at Gays River, Nova Scotia, Implications on genesis: Abstracts with programs, A.G.S. Conference, Fredericton, 1981, p. 1. Paper presented at Fredericton, Canada, 1981.

Akande, S.O. and Zentilli, M. (1982). Genesis of the Gays River lead-zinc deposit reconsidered in the light of geologic and Fluid inclusion studies; G.A.C./M.A.C. Abstracts with programs, vol. 7, p. 19. Paper presented at Winnipeg, Canada 1982.

Zentilli, M. and Akande, S.O. (1982). Geologic, fluid inclusion and stable isotope evidence for the genesis of the Gays River lead-zinc deposit, Nova Scotia, Canada: Abstracts with programs, Inter. Conf. on Mississippi Valley Type lead-zinc deposits, Part 1, p. 58. Paper presented at Missouri, U.S.A., 1982.